

NASA TECHNICAL  
MEMORANDUM

NASA TM X-62,151

NASA TM X-62,151

(NASA-TM-X-62151) AERODYNAMIC  
CHARACTERISTICS OF A LARGE SCALE LIFT FAN  
TRANSPORT MODEL WITH PODDED FANS FORWARD  
AND LIFT CRUISE FANS MOUNTED J.V. Kirk, et  
al (NASA) Apr. 1972 132 p

N72-24010

Unclas  
28201

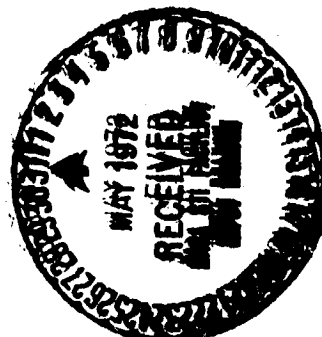
CSCS 01B G3/C2

AERODYNAMIC CHARACTERISTICS OF A LARGE SCALE LIFT FAN  
TRANSPORT MODEL WITH PODDED FANS FORWARD AND LIFT  
CRUISE FANS MOUNTED ABOVE THE WING

Jerry V. Kirk, Stanley O. Dickinson, Leo P. Hall, and Mary G. Coffman

Ames Research Center  
Moffett Field, Calif. 94035

April 1972



PRECEDING PAGE BLANK NOT FILMED

NOTATION

A	fan exit area, m <sup>2</sup> (sq ft), or wing aspect ratio
b	wing span, m (ft)
c	wing chord parallel to plane of symmetry, m (ft)
$\bar{c}$	mean aerodynamic chord, $\frac{2}{S} \int_0^{b/2} c^2 dy$ , m (ft)
C <sub>D</sub>	drag coefficient, $\frac{D}{qS}$
C <sub>l</sub>	rolling-moment coefficient, $\frac{l}{qSb}$
C <sub>L</sub>	lift coefficient, $\frac{L}{qS}$
C <sub>m</sub>	pitching-moment coefficient, $\frac{M}{qSc}$
C <sub>n</sub>	yawing-moment coefficient, $\frac{N}{qSb}$
C <sub>Y</sub>	side-force coefficient, $\frac{Y}{qS}$
D	drag, N (lb)
D <sub>e</sub>	effective diameter of the fan, m (ft)
D <sub>f</sub>	diameter of the fan, m (ft)
i <sub>t</sub>	horizontal-tail incidence angle, deg
l	rolling moment, m-N (ft-lb), or length, m (ft)
L	total lift on model, N (lb)
M	pitching moment, m-N (ft-lb)
N	yawing moment, m-N (ft-lb)
P <sub>0</sub>	standard atmospheric pressure, N/m <sup>2</sup> (lb/ft <sup>2</sup> )
P <sub>s</sub>	free-stream static pressure, N/m <sup>2</sup> (lb/ft <sup>2</sup> )

q	free-stream dynamic pressure, $N/m^2$ (lb/ft <sup>2</sup> )
RPM	corrected fan rotational speed, $\frac{\text{fan speed}}{\sqrt{\theta}}$
r	fan radius or cruise fan nacelle length, cm (in)
S	wing area, m <sup>2</sup> (ft <sup>2</sup> )
T	complete ducted thrust measured along the fan axis with $\alpha = 0^\circ$ and $\beta_v = 0^\circ$ , $\rho A v_j^2$ , N(lb)
v	air velocity, m/sec (ft/sec)
V	free-stream air velocity, m/sec (ft/sec)
$\bar{V}$	tail volume coefficient, $\frac{S_{tl} l_t}{S \bar{c}}$
Y	side force, N (lb)
X	distance from fan center line or nacelle leading edge, cm (in)
$\alpha$	angle of attack of the wing chord plane, deg
$\beta$	angle of sideslip, deg
$\beta_v$	lift-fan exit-louver deflection angle from the fan axis, deg
$\theta_v$	cruise fan exit louver deflection angle from the fan axis, deg
$\delta$	relative static pressure, $\frac{P_s}{P_o}$
$\delta_f$	trailing-edge flap deflection measured normal to the hinge line, deg
$\theta$	ratio of ambient temperature to standard temperature (519° R)
$\epsilon$	average downwash at the horizontal tail, deg
$\eta$	fraction of wing semispan, $\frac{2y}{b}$
$\mu$	tip-speed ratio, $\frac{2V}{\omega D_f}$
$\rho$	density, Kg/m <sup>3</sup> (slugs/ft <sup>3</sup> )
$\omega$	fan rotational speed, radians/sec

### Subscripts

c	corrected
j	fan exit
i	induced
s	static condition
u	uncorrected
w	wing
t	tail

AERODYNAMIC CHARACTERISTICS OF A LARGE SCALE LIFT FAN  
TRANSPORT MODEL WITH PODDED FANS FORWARD AND LIFT  
CRUISE FANS MOUNTED ABOVE THE WING

Jerry V. Kirk, Stanley O. Dickinson,  
Leo P. Hall, and Mary G. Coffman

Ames Research Center

SUMMARY

The aerodynamic characteristics of a large scale V/STOL transport model powered by tip-turbine driven lift fans were investigated in the Ames Research Center's 40- by 80-foot wind tunnel. The model had four fans; the forward fans were mounted in pods forward of the wing at mid-semispan. The aft fans were placed in cruise nacelles behind and above the wing. A cascade of variable camber exit louvers was placed behind each of the lift-cruise fans to turn the fan flow in the lift direction for hover and transition to wing supported flight. The wing of the model was mounted above the fuselage, had an aspect ratio of 5.8, sweepback of  $35^\circ$  at the quarter chord line and a taper ratio of 0.3.

Various configurations of the model were tested to explore the transition speed range. Fan performance, turning effectiveness of the variable camber exit louvers, longitudinal and lateral-directional characteristics with fan operation in crossflow are presented.

## INTRODUCTION

As a continuing program, the Ames Research Center is studying lift fan V/STOL transport configurations to assure acceptable aerodynamic characteristics throughout the speed range from hover to wing supported flight.

This study was initiated to explore the use of lift-cruise fans with axes parallel to the aircraft longitudinal axis, above and behind the wing. These fans were provided with vectoring devices to give lift at zero forward speed. The forward lift fans were located in the same position as reported in reference 1. Fan performance, longitudinal and lateral-directional characteristics are shown for various model configurations throughout the transition speed range. Wall pressure distribution and inlet total pressures were measured on the left cruise fan at several tip speed ratios.

## MODEL AND APPARATUS

Photographs of the model mounted in the Ames 40- by 80-foot wind tunnel are shown in figure 1. Figure 2(a) is a sketch of the model with pertinent dimensions.

### Model

Fuselage.- The fuselage was slab sided with rounded corners. Overall length, height, and width in meters (feet) were 13.41(44.0), 1.98(6.5), and 1.77(5.8) respectively. The fuselage used for this investigation was the same as reported in references 1 and 2.

Tail.- Horizontal tail geometry and location are given in figure 2(a). The horizontal tail pivoted about the quarter chord allowing incidence angles from  $-10$  to  $20^\circ$ . During tail off testing, only the horizontal tail was removed.

Wing.- The wing was mounted above the fuselage. Aspect ratio was 5.8, taper ratio 0.3, and sweepback at the quarter-chord line was  $35^\circ$ . An NACA 65-412 airfoil section was basic for the wing. Propulsion

system pods were mounted forward of and beneath the wing at mid-semispan. These pods housed the four gas generators and two front lift fans (figure 2(a)). Leading edge slats were mounted to the wing and extended full span except for the area containing the propulsion pods ( $\eta = 0.383$  to  $0.631$ ). The slat chord was 15 percent of the wing chord and deflection was  $20^\circ$  for the entire investigation.

A 22 percent chord trailing-edge flap extended from 15.9 percent to 37.5 percent semispan (see figure 2(b)). Deflection angles of  $0^\circ$  and  $45^\circ$  were used for this study.

#### Propulsion System

Four modified YT58 gas generators were located in pods forward of the wing (figure 2(a)) and powered the tip turbine driven X-376 lift fans. The front podded fans were in the same position as described in reference 1. The two lift-cruise fans were installed in nacelles above and near the wing trailing edge. Nacelle exit area was intended to produce a design pressure ratio of 1.1 at zero and low forward speeds. A rack of variable camber exit louvers was mounted behind each cruise fan as shown in figure 2(c). Unless otherwise stated, the rack assembly for the louvers was at a  $45^\circ$  angle to the fan exhaust. The variable camber louvers (ordinates shown in figure 2(c)) were remotely actuated from  $7^\circ$  (thrust direction) to  $82^\circ$  (lift direction). Mechanical interference did not allow deflection beyond these limits.

#### TESTING AND PROCEDURE

Longitudinal force and moment data were obtained for an angle of attack range from  $0^\circ$  to  $22^\circ$ . Lateral-directional results were obtained for a range of sideslip angles from  $-18^\circ$  to  $+2^\circ$  at  $0^\circ$  and  $8^\circ$  angle of attack. The moment center for data reduction was placed at the quarter chord of the wing MAC.

At zero angle of attack, fan RPM and wind tunnel speed were varied independently. Data were obtained at several exit vane deflection angles, two flap deflections, tail on and tail off.

When angle of attack or angle of sideslip was varied, fan RPM and wind tunnel speed were held constant. When all four fans were operating, thrust-equal-drag conditions were selected at zero angle of attack by

varying the front lift fan exit louvers and the lift-cruise fan cascade louver deflection angles at several tip-speed ratios. Angle of attack or angle of sideslip was then varied holding these settings constant. Angle of attack was also varied with exit louver deflection angles  $\pm 10^\circ$  from the trim points to provide thrust greater than drag and thrust less than drag results.

#### CORRECTIONS

Force and moment data obtained without the fans operating (power off) have been corrected for the effects of wind tunnel wall interference in the following manner:

$$\alpha = \alpha_u + 0.488 C_{L_u}$$

$$C_D = C_{D_u} + 0.0085 C_{L_u}^2$$

$$C_m = C_{m_u} + 0.0203 C_{L_u} \text{ (tail on only)}$$

Appropriate tares have been applied to the results to account for exposed strut tips.

Reference 3 gives a set of model to wind-tunnel sizing ratios that give only small wind tunnel wall effects. The subject model, according to these restraints should produce only small wall effects, therefore no wind tunnel wall corrections have been applied to the results with the fans operating.

#### RESULTS

An index to the figures is given in table 1. Fan performance, both at hover and forward speed, are shown in figures 3 through 6. Figure 3 presents the hover characteristics for 4-fan operation and lift-cruise fan operation. The static turning effectiveness of the variable camber exit louvers are presented in figure 4. The relationship between tip



speed ratio and velocity ratio are given in figure 5, while figure 6 presents the variation of fan thrust with forward speed.

Longitudinal aerodynamic characteristics at zero degrees angle of attack with fans operating are presented in figures 7 through 20. Results are shown for a representative tip speed ratio range with the forward fans operating (figure 7), all four fans operating (figures 8 through 18), and the aft lift-cruise fans operating (figures 19 and 20). Model variables included exit louver deflection angles, lift-cruise fan cascade deflection angles, wing trailing edge flap deflection, and horizontal tail off and on.

Variable angle of attack data are given in figures 21 through 30. Power off results (fans not operating) are presented in figure 21; next, results are shown with just the lift-cruise fans operating (figures 22 through 24); and finally, data with all four fans operating are presented in figures 25 through 30.

Figures 31 through 34 present lateral-directional characteristics with fans operating. Results are shown for lift-cruise fan operation (figure 31) and for all fans operating (figures 32 through 34). The exit louver and cascade angle settings were those used as trim drag points in figures 25 through 30.

Appendix A lists, in tabulated form, the inlet pressure distribution from a series of wall statics in the left cruise fan nacelle. Figure 2(c) shows the location of the static taps. Results are given for an angle of attack range from  $0^\circ$  to  $22^\circ$  at three tip speed ratios.

Inlet total pressure distributions are presented in Appendix B for the same conditions as those of Appendix A.

#### REFERENCES

1. Dickinson, Stanley O.; Hall, Leo P.; and Hodder, Brent K.:  
Aerodynamic Characteristics of a Large-Scale V/STOL Transport Model with Tandem Lift Fans Mounted at Mid-Semispan of the Wing. NASA TN D-6234, 1971.
2. Hall, Leo P.; Hickey, David H.; and Kirk, Jerry V.:  
Aerodynamic Characteristics of a Large Scale V/STOL Transport Model with Lift and Lift-Cruise Fans. NASA TN D-4092, 1967.
3. Cook, Woodrow L.; and Hickey, David H.:  
Comparison of Wind Tunnel and Flight Test Aerodynamic Data in the Transition Flight Speed Range for Five V/STOL Aircraft. NASA SP-116, 1966, pp. 447-467.
4. Kirk, Jerry V.; Hodder, Brent K.; and Hall, Leo P.:  
Large Scale Wind Tunnel Investigation of a V/STOL Transport Model with Wing Mounted Lift Fans and Fuselage Mounted Lift-Cruise Engines for Propulsion. NASA TN D-4233, 1967.

TABLE 1 INDEX OF FIGURES

FIGURE	$\alpha$ , DEG.	$\beta$ , DEG.	FANS	$U$	$\beta_v$ , DEG.	$\theta_v$ , DEG.	$i_t$ , DEG.	$\delta_f$ , DEG.	REMARKS
FAN CHARACTERISTICS									
3(a)	0	0	ALL	-	0	71	0	45	STATIC PERFORMANCE
3(b)			LIFT-CR	-	90	VAR.			
4			LIFT-CR	-	90	VAR.			
5			ALL	VAR.	0	71			TURNING EFFECTIVENESS
6			ALL	VAR.	0	71			RELATION OF $U$ TO $V/V_j$ EFFECT OF FORWARD SPEED ON FAN THRUST
LONGITUDINAL DATA AT ZERO ANGLE OF ATTACK									
7(a)(b)	0	0	LIFT	VAR.	VAR.	T	0	0	
7(c)(d)								45	
8(a)(b)	0	0	ALL	VAR.	VAR.	82	OFF	45	
8(c)(d)								0	
9(a)(b)	0	0	ALL	VAR.	VAR.	71	OFF	45	
9(c)(d)								0	
10(a)(b)	0	0	ALL	VAR.	VAR.	71	0	45	
10(c)(d)								0	
11(a)(b)	0	0	ALL	VAR.	VAR.	55	OFF	45	

TABLE 1 CONTINUED

FIGURE	$\alpha$ , DEG.	$\beta$ , DEG.	FANS	$\mu$	$\beta_V$ , DEG.	$\theta_V$ , DEG.	$i_t$ , DEG.	$\delta_f$ , DEG.	REMARKS
11(c)(d)	0	0	ALL	VAR.	VAR.	55	OFF	0	
12(a)(b)	0	0	ALL	VAR.	VAR.	55	0	45	
12(c)(d)	0	0	ALL	VAR.	VAR.	36	OFF	0	
13(a)(b)	0	0	ALL	VAR.	VAR.	36	0	45	
13(c)(d)	0	0	ALL	VAR.	VAR.	20	OFF	0	
14(a)(b)	0	0	ALL	VAR.	VAR.	20	0	45	
14(c)(d)	0	0	ALL	VAR.	VAR.	7	OFF	0	
15(a)(b)	0	0	ALL	VAR.	VAR.	7	0	45	
15(c)(d)	0	0	ALL	VAR.	VAR.	90	0	45	
16(a)(b)	0	0	ALL	VAR.	VAR.				
16(c)(d)	0	0	ALL	VAR.	VAR.				
17(a)(b)	0	0	ALL	VAR.	VAR.				
18(a)(b)	0	0	ALL	VAR.	VAR.				
18(c)(d)	0	0	LIFT-CR	VAR.	VAR.				
19(a)(b)	0	0							

TABLE 1 CONTINUED

FIGURE	$\alpha$ , DEG.	$\beta$ , DEG.	FANS	$\mu$	$\beta_v$ , DEG.	$\theta_v$ , DEG.	$\psi$ , DEG.	$\delta_f$ , DEG.	REMARKS
20 (a)(b)	0	0	ALL	VAR.	VAR.	71	OFF	0	LIFT-CRUISE FAN EXIT CARRIAGE ANGLE = 65°
20(c)(d)	↓	↓	↓	↓	↓	55	↓	↓	
20(e)(f)	↓	↓	↓	↓	↓	36	↓	↓	
LONGITUDINAL DATA WITH VARIABLE ANGLE OF ATTACK									
21	VAR	0	—	—	90	7	0	0, 45	POWER OFF
22	VAR	0	LIFT-CR	34, 50, 77	90	OFF	OFF	0	
23	VAR	0	LIFT-CR	20, 34, 50	90	OFF	OFF	45	
24 (a)	VAR	0	LIFT-CR	.12, .18	90	71, 55	0	45	
24 (b)	↓	↓	↓	.19, .25 .29, .31	↓	55, 36 20, 7	↓	↓	
25 (a)	VAR	0	ALL	.06	-5, 5 13, 21	71	0	45	
25 (b)	↓	↓	↓	↓	↓	↓	↓	↓	
25 (c)	↓	↓	↓	.11	0, 13, 23	↓	↓	↓	
25 (d)	↓	↓	↓	.19	-8, 5 13	↓	↓	↓	
26 (a)	VAR	0	ALL	.115	10, 20, 30	55	0	45	
26 (b)	↓	↓	↓	.19	10, 20, 30	↓	↓	↓	
26 (c)	↓	↓	↓	.245	-8, 5 20	↓	↓	↓	

TABLE 1 CONCLUDED

FIGURE	$\alpha$ , DEG.	$\beta$ , DEG.	FANS	U	$\beta_v$ , DEG.	$\theta_v$ , DEG.	$\psi_t$ , DEG.	$\delta f$ DEG.	REMARKS
27	VAR	0	ALL	25	15,25 35	36	0	45	
28	VAR	0	ALL	29	10,20 38	20	0	45	
29	VAR	0	ALL	30	10,28 30	7	0	45	
30	VAR	0	ALL	.11, .19 .25, .29	13,20 25,28	71,55 36,20	OFF	45	
LATERAL - DIRECTIONAL CHARACTERISTICS									
31	0	VAR.	LIFT-CR	25,34 37	90	OFF	OFF	0	
32	0	VAR.	ALL	.11, .19, .24	13,20 25,90	71,55 36,7	OFF	45	
33	0	VAR.	ALL	.11, .19, .24 .29	13,20 25,20,90	71,55 36,7	0	45	
34	0	VAR.	ALL	.11, .19	13,20	71,55	0	45	

**Appendix A**  
**Cruise fan inlet static pressure coefficients**

STATION Y/Z	80		135		225		260		350	
	OUTER	INNER	OUTER	INNER	OUTER	INNER	OUTER	INNER	OUTER	INNER
.000	-4.668		-4.790		-2.721		-2.494		-4.539	
.005	-0.150	-10.345	-0.028	-12.928	0.661	-8.733	0.694	-9.049	-0.148	-10.358
.010	0.704	-12.360	0.704	-12.678	0.911	-10.236	0.934	-9.711	0.754	-10.488
.020	0.888	-13.031	0.827	-14.556	0.849	-11.676	0.934	-11.034	0.814	-12.307
.050	0.643	-12.482	0.582	-13.554	0.160	-12.302	0.453	-11.756	0.754	-12.307
.100	0.216	-9.857	0.216	-9.985	-0.216	-9.234	0.152	-8.929	0.453	-10.942
.200	-0.089	-7.415	-0.466	-7.480	-0.717	-7.185	-0.269	-6.944	-0.158	-7.564
.300	-0.150	-6.133	-0.717	-6.102	-0.717	-5.862	-0.389	-5.621	-0.288	-6.070
.400	-0.333	-6.133							-0.353	-6.070
.500	-0.333	-0.211							-0.613	-0.288
.600	-0.333	0.643	-0.279		-0.279		-2.253	-0.329	-0.548	-0.548
.700	-0.333	0.582	-0.341	0.849	-0.341	0.754	-0.449	-0.269	-0.483	-0.418
.800	-0.333	0.460	-0.153	0.473	-0.216	0.273	-1.652	-0.209	-0.483	-0.483
.900	-0.333	0.216	-0.153		-0.279		-0.088	-0.209	-0.223	0.037
.950	-0.333	0.094	-0.216		-0.091		-0.088	0.212	-0.028	0.362

$\alpha = 0^\circ$ ,  $\phi = 11.05$ ,  $\mu = .199$ , RPM = 3360

Appendix A  
Cruise fan inlet static pressure coefficients

STATION X/Z	80		135		225		260		350	
	OUTER	INNER	OUTER	INNER	OUTER	INNER	OUTER	INNER	OUTER	INNER
.000	-4.710		-5.976		-2.336		-2.184		-3.861	
.005	-0.271	-10.972	-0.393	-13.624	0.783	-9.136	0.511	-8.204	-0.024	-9.345
.010	0.580	-12.857	0.397	-13.374	0.907	-9.695	0.631	-9.372	0.571	-9.539
.020	0.701	-14.073	0.701	-14.096	0.783	-11.441	0.691	-10.860	0.571	-11.998
.050	0.580	-12.918	0.580	-13.811	0.034	-12.252	0.152	-11.768	0.331	-12.127
.100	0.033	-9.999	0.154	-10.060	-0.340	-9.071	-0.208	-9.013	0.092	-10.380
.200	-0.211	-7.506	-0.527	-7.512	-0.777	-7.395	-0.507	-7.096	-0.158	-7.330
.300	-0.211	-6.230	-0.777	-6.078	-0.714	-6.078	-0.627	-5.718	-0.222	-5.851
.400	-0.454	-6.230							-0.287	-5.851
.500	-0.454	-0.271							-0.481	-0.158
.600	-0.454	0.519	-0.215		-0.278		-1.945	-0.567	-0.352	-0.158
.700	-0.454	0.519	-0.465	0.845	-0.402	0.571	-0.687	-0.447	-0.352	-0.158
.800	-0.454	0.337	-0.153	0.533	-0.215	0.451	-1.466	-0.447	-0.352	-0.158
.900	-0.454	0.093	-0.091		-0.153		-0.388	-0.388	-0.093	0.166
.950	-0.332	0.033	-0.153		-0.340		-0.388	-0.028	0.166	0.489

$\alpha = 4^\circ$ ,  $q = 11.90$ ,  $\mu = .199$ , RPM = 3300



Appendix A  
Cruise fan inlet static pressure coefficients

STATION Y/Z	80		135		225		260		350	
	OUTER	INNER	OUTER	INNER	OUTER	INNER	OUTER	INNER	OUTER	INNER
.000	-5.649		-6.374		-2.136		-1.636		-3.065	
.005	-0.512	-11.330	-0.572	-15.341	0.778	-8.150	0.627	-7.352	0.210	-8.196
.010	0.516	-13.204	0.395	-14.473	0.964	-9.761	0.746	-8.364	0.627	-8.261
.020	0.697	-14.533	0.758	-16.085	0.716	-11.125	0.686	-10.000	0.627	-10.833
.050	0.516	-13.204	0.637	-14.287	0.034	-12.055	0.031	-11.341	0.210	-10.833
.100	0.032	-10.121	0.153	-10.319	-0.400	-9.079	-0.266	-8.781	0.031	-9.933
.200	-0.209	-7.522	-0.462	-7.530	-0.648	-7.232	-0.564	-6.994	-0.221	-7.167
.300	-0.270	-6.132	-0.710	-6.042	-0.648	-5.982	-0.683	-5.625	-0.285	-5.752
.400	-0.512	-6.132							-0.350	-5.752
.500	-0.512	-0.270							-0.478	-0.157
.600	-0.512	0.516	-0.214		-0.214		-1.338	-0.624	-0.350	-0.028
.700	-0.512	0.516	-0.462	0.840	-0.400	0.508	-0.683	-0.445	-0.285	-0.028
.800	-0.512	0.334	-0.276	0.530	-0.214	0.567	-0.862	-0.445	-0.285	-0.028
.900	-0.512	0.093	-0.152		-0.090		-0.385	-0.385	-0.092	0.165
.950	-0.270	-0.028	-0.152		-0.400		-0.385	-0.028	0.100	0.486

$\alpha = 8^\circ$ ,  $q = 11.97$ ,  $\mu = .200$ ,  $RPM = 3300$

**Appendix A**  
**Cruise fan inlet static pressure coefficients**

STATION X/R	80		135		225		260		350	
	OUTER	INNER	OUTER	INNER	OUTER	INNER	OUTER	INNER	OUTER	INNER
.000	-5.706		-7.354		-2.157		-1.472		-2.374	
.005	-0.578	-12.604	-0.944	-16.686	0.849	-7.418	0.694	-7.245	0.393	-7.434
.010	0.460	-14.130	0.277	-15.746	0.974	-9.672	0.754	-8.508	0.633	-7.490
.020	0.704	-15.596	0.765	-17.562	0.786	-11.175	0.633	-10.012	0.633	-10.033
.050	0.521	-13.581	0.704	-15.245	0.034	-12.052	-0.088	-11.275	0.092	-10.098
.100	0.033	-10.345	0.216	-10.611	-0.279	-8.983	-0.329	-8.749	-0.028	-9.708
.200	-0.272	-7.598	-0.466	-7.668	-0.654	-7.365	-0.569	-7.005	-0.288	-7.109
.300	-0.333	-6.255	-0.654	-6.040	-0.529	-6.042	-0.630	-5.742	-0.288	-5.680
.400	-0.517	-6.255							-0.353	-5.810
.500	-0.517	-0.272							-0.483	-0.093
.600	-0.517	0.521	-0.153		-0.153		-0.930	-0.509	-0.353	0.167
.700	-0.517	0.521	-0.529	0.911	-0.404	0.513	-0.630	-0.389	-0.353	0.037
.800	-0.517	0.338	-0.216	0.661	-0.529	0.694	-0.630	-0.389	-0.353	0.167
.900	-0.517	0.033	-0.091		-0.279		-0.449	-0.389	-0.093	0.167
.950	-0.272	-0.028	-0.091		-0.529		-0.389	-0.088	0.167	0.492

$\alpha = 12^\circ$ ,  $q = 11.85$ ,  $\mu = .199$ ,  $RPM = 3300$

**Appendix A**  
**Cruise fan inlet static pressure coefficients**

STATION X/Z	80		135		225		260		350	
	OUTER	INNER	OUTER	INNER	OUTER	INNER	OUTER	INNER	OUTER	INNER
.000	-6.560		-8.331		-2.032		-1.291		-0.900	
.005	-1.005	-13.031	-1.188	-17.625	0.786	-7.731	0.814	-7.065	0.633	-6.395
.010	0.277	-14.558	0.155	-16.686	0.974	-9.046	0.814	-8.263	0.694	-7.694
.020	0.582	-16.023	0.704	-18.001	0.661	-10.862	0.694	-9.651	0.684	-9.643
.050	0.460	-13.947	0.582	-15.496	-0.091	-11.801	-0.028	-11.094	0.092	-9.643
.100	0.033	-10.467	0.094	-10.862	-0.466	-9.046	-0.269	-8.628	-0.028	-9.574
.200	-0.333	-7.720	-0.592	-7.793	-0.717	-7.305	-0.509	-6.884	-0.353	-7.109
.300	-0.517	-6.377	-0.780	-6.165	-0.529	-5.982	-0.569	-5.621	-0.353	-5.745
.400	-0.639	-6.377							-0.418	-5.410
.500	-0.639	-0.272							-0.483	-0.093
.600	-0.639	0.460	-0.153		-0.153		-0.569	-0.449	-0.288	0.297
.700	-0.639	0.399	-0.529	0.849	-0.592	0.633	-0.509	-0.329	-0.288	0.037
.800	-0.639	0.277	-0.341	0.535	-0.153	0.694	-0.389	-0.329	-0.288	0.232
.900	-0.639	-0.028	-0.153		-0.341		-0.329	-0.329	-0.028	0.232
.950	-0.517	-0.089	-0.153		-0.153		-0.329	-0.028	0.102	0.427

$\alpha = 16^\circ$ ,  $q = 11.85$ ,  $\mu = .198$ ,  $RPM = 3300$

**Appendix A**  
**Cruise fan inlet static pressure coefficients**

STATION X/P	80		135		225		260		350	
	OUTER	INNER	OUTER	INNER	OUTER	INNER	OUTER	INNER	OUTER	INNER
.000	-6.316		-7.720		-1.093		-7.185		-0.269	
.005	-1.188	-12.604	-0.883	-17.249	-0.091	-7.480	-4.500	-10.613	0.474	-5.290
.010	0.277	-14.130	0.338	-16.748	-1.155	-8.106	-2.735	-8.147	0.874	-6.590
.020	0.521	-15.962	0.827	-18.251	-0.404	-10.611	-1.171	-8.147	0.633	-8.344
.050	0.338	-14.069	0.399	-15.684	-0.529	-12.553	-0.569	-9.711	-0.148	-8.344
.100	-0.150	-10.773	-0.089	-11.300	-0.529	-8.083	-0.500	-8.268	-0.200	-9.513
.200	-0.455	-7.659	-0.780	-7.981	-0.780	-7.365	-0.530	-6.704	-0.548	-7.100
.300	-0.578	-6.438	-0.905	-6.290	-0.466	-5.922	-0.630	-6.102	-0.548	-5.810
.400	-0.761	-6.438							-0.548	-5.875
.500	-0.761	-0.272							-0.548	-0.158
.600	-0.761	0.338	-0.153		-0.153		-0.569	-0.630	-0.418	0.362
.700	-0.761	0.338	-0.592	0.661	-0.341	0.633	-0.329	-0.209	-0.418	0.037
.800	-0.761	0.155	-0.341	0.473	-0.341	0.934	-0.088	-0.209	-0.483	0.297
.900	-0.761	-0.089	-0.279		-0.216		-0.209	-0.148	-0.093	0.102
.950	-0.578	-0.150	-0.216		-0.153		-0.269	-0.028	-0.158	0.362

$\alpha = 20^\circ$ ,  $q = 11.85$ ,  $\mu = .199$ ,  $RPM = 3300$

**Appendix A**  
**Cruise fan inlet static pressure coefficients**

STATION X/Z	80		135		225		260		350	
	OUTER	INNER	OUTER	INNER	OUTER	INNER	OUTER	INNER	OUTER	INNER
.000	-6.743		-7.781		-3.911		-3.516		-0.148	
.005	-0.944	-14.313	-0.639	-17.938	-1.844	-12.866	-1.201	-11.575	1.115	-4.966
.010	0.460	-14.802	0.643	-18.314	-2.220	-15.746	-4.655	-10.733	0.934	-5.310
.020	0.704	-15.596	0.888	-18.815	-1.468	-11.425	-1.051	-8.147	0.754	-7.489
.050	0.460	-14.008	0.338	-15.871	-0.466	-11.089	-0.000	-10.252	-0.329	-9.383
.100	-0.028	-10.651	-0.211	-11.050	-0.967	-8.795	-0.509	-7.345	-0.269	-9.383
.200	-0.394	-7.781	-0.905	-7.918	-0.780	-7.185	-0.549	-6.744	-0.743	-6.980
.300	-0.455	-6.194	-1.093	-6.353	-0.842	-6.523	-0.380	-6.102	-0.678	-5.745
.400	-0.700	-6.316							-0.613	-5.875
.500	-0.700	-0.150							-0.613	-0.158
.600	-0.700	0.460	-0.216		-0.216		-0.329	-0.389	-0.483	0.297
.700	-0.700	0.399	-0.592	0.661	-0.404	0.513	-0.209	-0.088	-0.418	-0.028
.800	-0.700	0.216	-0.592	0.473	-0.404	0.994	0.032	-0.088	-0.483	0.232
.900	-0.700	0.033	-0.341		-0.341		-0.148	-0.088	-0.158	-0.028
.950	-0.517	-0.089	-0.279		-0.341		-0.148	0.032	-0.093	0.297

$\alpha = 22^\circ$ ,  $q = 11.85$ ,  $\mu = .199$ ,  $KFM = 3300$

**Appendix A**  
**Cruise fan inlet static pressure coefficients**

STATION X/ft	80		135		225		260		350	
	OUTER	INNER	OUTER	INNER	OUTER	INNER	OUTER	INNER	OUTER	INNER
.000	0.431		-0.049		0.571		0.774		0.260	
.005	0.953	-1.636	0.953	-2.941	0.893	-1.464	0.834	-1.160	0.918	-1.695
.010	0.828	-3.390	0.932	-3.284	0.700	-2.299	0.630	-2.003	0.815	-2.473
.020	0.535	-3.056	0.640	-4.398	0.400	-3.156	0.301	-2.884	0.484	-3.384
.050	-0.028	-3.996	0.055	-4.548	-0.264	-3.991	-0.254	-3.793	-0.000	-4.006
.100	-0.321	-3.202	-0.216	-3.327	-0.457	-3.006	-0.378	-2.988	-0.090	-3.530
.200	-0.404	-2.325	-0.650	-2.385	-0.714	-2.291	-0.481	-2.204	-0.384	-2.384
.300	-0.404	-1.824	-0.778	-1.828	-0.800	-1.777	-0.666	-1.695	-0.384	-1.806
.400	-0.530	-1.845							-0.384	-1.806
.500	-0.530	-0.214							-0.362	-0.273
.600	-0.530	0.285	-0.221		-0.221		1.165	-0.131	-0.294	1.127
.700	-0.446	0.243	-0.307	0.314	-0.414	0.198	-0.460	-0.255	-0.340	-0.206
.800	-0.446	0.139	-0.264	0.143	-0.328	1.329	1.144	-0.255	-0.428	1.083
.900	-0.112	0.055	-0.243		-0.393		-0.111	-0.234	-0.162	0.127
.950	-0.008	0.034	-0.221		-0.243		-0.070	0.054	0.038	0.216

$\alpha = 0^\circ, q = 34.64, \mu = .340, RPM = 3300$

**Appendix A**  
**Cruise fan inlet static pressure coefficients**

STATION X/Z	80		135		225		260		350	
	OUTER	INNER	OUTER	INNER	OUTER	INNER	OUTER	INNER	OUTER	INNER
.000	0.429		-0.341		0.676		0.914		0.730	
.005	0.991	-1.818	0.901	-3.464	0.889	-1.074	0.832	-0.725	0.914	-0.892
.010	0.908	-3.524	0.901	-3.870	0.676	-2.205	0.545	-1.627	0.709	-1.888
.020	0.617	-3.461	0.804	-5.086	0.334	-2.910	0.300	-2.611	0.382	-2.995
.050	0.013	-4.189	0.180	-4.958	-0.434	-4.041	-0.397	-3.595	-0.151	-3.504
.100	-0.257	-3.232	-0.174	-3.486	-0.562	-3.016	-0.438	-2.754	-0.131	-3.239
.200	-0.361	-2.275	-0.711	-2.440	-0.797	-2.263	-0.541	-2.099	-0.405	-2.220
.300	-0.361	-1.797	-0.775	-1.864	-0.861	-1.730	-0.684	-1.607	-0.427	-1.689
.400	-0.528	-1.797							-0.449	-1.711
.500	-0.528	-0.132							-0.272	-0.139
.600	-0.528	0.325	-0.178		-0.178		1.037	-0.069	-0.206	1.101
.700	-0.382	0.284	-0.413	0.313	-0.519	0.259	-0.356	-0.151	-0.206	-0.028
.800	-0.278	0.180	-0.263	0.164	-0.285	1.283	1.078	-0.151	-0.361	1.034
.900	-0.117	0.117	-0.285		-0.285		-0.069	-0.151	-0.117	0.171
.950	0.013	0.076	-0.220		-0.455		-0.049	0.095	0.038	0.259

$\alpha = 4^\circ$ ,  $q = 34.76$ ,  $\mu = .340$ ,  $NPR = 3300$

**Appendix A**  
**Cruise fan inlet static pressure coefficients**

STATION Y/Z	80		135		225		260		350	
	OUTER	INNER	OUTER	INNER	OUTER	INNER	OUTER	INNER	OUTER	INNER
.000	0.346		-0.820		0.634		0.997		0.936	
.005	0.971	-1.757	0.930	-4.344	0.783	-1.139	0.731	-0.664	0.854	-0.738
.010	0.930	-3.735	0.992	-4.579	0.548	-2.165	0.382	-1.341	0.484	-0.760
.020	0.638	-3.548	0.867	-5.561	0.142	-2.998	0.054	-2.347	0.177	-2.267
.050	0.013	-4.277	0.242	-5.390	-0.477	-3.916	-0.459	-3.455	-0.336	-3.308
.100	-0.299	-3.256	-0.112	-3.681	-0.648	-2.934	-0.480	-2.614	-0.254	-3.131
.200	-0.403	-2.278	-0.691	-2.464	-0.797	-2.203	-0.582	-2.019	-0.516	-2.200
.300	-0.466	-1.757	-0.840	-1.866	-0.755	-1.690	-0.623	-1.547	-0.516	-1.691
.400	-0.570	-1.778							-0.516	-1.713
.500	-0.570	-0.091							-0.294	-0.139
.600	-0.570	0.284	-0.178		-0.157		0.874	-0.028	-0.206	0.947
.700	-0.445	0.263	-0.306	0.249	-0.392	0.259	-0.234	-0.110	-0.206	-0.117
.800	-0.341	0.180	-0.285	0.142	-0.199	1.141	0.977	-0.090	-0.383	0.880
.900	-0.174	0.076	-0.306		-0.434		-0.234	-0.090	-0.161	0.149
.950	-0.174	0.055	-0.178		-0.199		-0.069	0.115	0.060	0.238

$\alpha = 8^\circ, q = 34.73, \mu = .340, \text{RPM} = 3300$



**Appendix A**  
**Cruise fan inlet static pressure coefficients**

STATION X/P	80		135		225		260		350	
	OUTER	INNER	OUTER	INNER	OUTER	INNER	OUTER	INNER	OUTER	INNER
.000	0.097		-1.176		0.763		1.020		1.020	
.005	0.973	-2.636	0.848	-5.357	0.806	-1.034	0.609	-0.316	0.650	-0.028
.010	0.931	-4.117	0.994	-5.400	0.528	-1.890	0.280	-1.077	0.239	-1.005
.020	0.681	-4.097	0.890	-6.106	0.121	-2.853	-0.008	-2.145	-0.028	-1.583
.050	0.013	-4.451	0.305	-5.550	-0.563	-3.902	-0.583	-3.194	-0.522	-3.137
.100	-0.320	-3.387	-0.091	-3.731	-0.670	-2.917	-0.563	-2.536	-0.378	-3.092
.200	-0.467	-2.344	-0.756	-2.511	-0.863	-2.207	-0.583	-1.960	-0.606	-2.226
.300	-0.487	-1.823	-0.863	-1.869	-0.649	-1.673	-0.645	-1.508	-0.606	-1.982
.400	-0.654	-1.802							-0.606	-1.760
.500	-0.654	-0.070							-0.250	-0.117
.600	-0.654	0.285	-0.157		-0.114		0.506	-0.028	-0.206	0.704
.700	-0.467	0.264	-0.521	0.271	-0.435	0.259	-0.337	-0.070	-0.184	-0.095
.800	-0.362	0.159	-0.285	0.164	-0.242	0.938	0.670	-0.070	-0.361	0.682
.900	-0.133	0.076	-0.157		-0.307		-0.152	-0.070	-0.162	0.127
.950	-0.049	0.055	-0.114		-0.499		-0.049	0.054	0.060	0.216

$\alpha = 12^\circ$ ,  $q = 34.67$ ,  $\mu = .340$ ,  $RPM = 3300$

Appendix A  
Cruise fan inlet static pressure coefficients

STATION X/Z	80		135		225		260		350	
	OUTER	INNER	OUTER	INNER	OUTER	INNER	OUTER	INNER	OUTER	INNER
.000	0.013		-1.590		0.762		1.018		0.997	
.005	0.909	-3.132	0.763	-6.117	0.719	-0.883	0.464	-0.172	0.341	0.016
.010	0.909	-4.548	1.013	-6.074	0.399	-1.673	0.136	-0.931	-0.000	-0.583
.020	0.701	-4.402	0.930	-6.480	-0.028	-2.502	-0.131	-1.916	-0.193	-1.646
.050	0.076	-4.694	0.284	-5.797	-0.691	-3.639	-0.664	-3.168	-0.623	-2.644
.100	-0.278	-3.465	-0.133	-3.831	-0.755	-2.827	-0.623	-2.491	-0.418	-2.843
.200	-0.466	-2.340	-0.819	-2.549	-0.819	-2.203	-0.623	-1.957	-0.671	-2.112
.300	-0.528	-1.799	-0.883	-1.866	-0.660	-1.649	-0.664	-1.506	-0.671	-1.646
.400	-0.674	-1.799							-0.640	-1.713
.500	-0.674	-0.049							-0.272	-0.117
.600	-0.674	0.242	-0.157		-0.114		0.238	-0.090	-0.206	0.548
.700	-0.507	0.242	-0.541	0.249	-0.306	0.218	-0.377	-0.060	-0.228	-0.073
.800	-0.403	0.159	-0.306	0.121	-0.498	0.772	0.423	-0.069	-0.383	0.526
.900	-0.195	0.076	-0.221		-0.370		-0.316	-0.069	-0.139	0.105
.950	-0.112	0.055	-0.157		-0.263		-0.234	0.013	0.038	0.193

$\alpha = 16^\circ$ ,  $q = 34.73$ ,  $\mu = .340$ , RPM = 3300

Appendix A  
Cruise fan inlet static pressure coefficients

STATION X/F	80		135		225		260		350	
	OUTER	INNER	OUTER	INNER	OUTER	INNER	OUTER	INNER	OUTER	INNER
.000	-0.776		-1.647		0.674		-0.560		0.810	
.005	0.823	-3.100	0.781	-6.181	0.057	-0.710	-0.785	-1.051	0.033	0.413
.010	0.823	-4.844	0.989	-5.990	-0.241	-1.561	-0.822	-1.552	-0.653	-0.338
.020	0.594	-4.906	0.802	-6.799	-0.667	-2.647	-0.744	-1.950	-0.662	-1.300
.050	-0.049	-4.844	0.096	-6.160	-1.306	-3.052	-0.785	-2.339	-1.010	-2.679
.100	-0.381	-3.557	-0.361	-4.010	-1.093	-2.796	-0.519	-2.600	-0.560	-2.785
.200	-0.547	-2.436	-0.880	-2.604	-1.263	-2.114	-0.642	-1.991	-0.801	-2.127
.300	-0.589	-1.917	-1.029	-1.923	-0.667	-1.664	-0.703	-1.644	-0.691	-1.707
.400	-0.796	-1.834							-0.647	-1.773
.500	-0.776	-0.070							-0.271	-0.095
.600	-0.776	0.200	-0.156		-0.092		0.033	-0.110	-0.227	0.457
.700	-0.589	0.158	-0.476	0.142	-0.390	0.217	-0.376	-0.069	-0.271	-0.073
.800	-0.568	0.075	-0.369	0.078	-0.454	0.687	0.319	-0.069	-0.382	0.457
.900	-0.298	-0.028	-0.241		-0.199		-0.212	-0.069	-0.095	-0.095
.950	-0.194	-0.049	-0.177		-0.220		-0.212	-0.008	-0.139	0.104

$\alpha = 20^\circ$ ,  $q = 34.85$ ,  $\mu = .341$ , RPM = 3300

Appendix A  
Cruise fan inlet static pressure coefficients

STATION X/F	80		135		225		260		350	
	OUTER	INNER	OUTER	INNER	OUTER	INNER	OUTER	INNER	OUTER	INNER
.000	-0.510		-1.619		-0.157		-0.812		0.796	
.005	0.809	-3.838	0.788	-6.877	-0.114	-1.767	-1.410	0.095	-0.132	0.306
.010	0.830	-5.261	0.913	-6.169	-0.522	-2.025	-0.256	-0.544	-0.709	-0.853
.020	0.537	-5.575	0.809	-7.006	-0.597	-3.313	-1.142	-1.534	-0.565	-1.320
.050	-0.091	-5.177	0.034	-6.491	-1.166	-3.635	-0.729	-2.111	-1.121	-2.456
.100	-0.405	-3.670	-0.426	-4.193	-0.780	-2.991	-0.698	-2.297	-0.729	-2.968
.200	-0.614	-2.498	-1.059	-2.755	-0.887	-2.379	-0.523	-2.214	-0.808	-2.211
.300	-0.656	-1.954	-1.231	-2.025	-0.801	-2.090	-0.565	-1.678	-0.741	-1.699
.400	-0.845	-1.954							-0.674	-1.788
.500	-0.824	-0.070							-0.385	-0.118
.600	-0.845	0.139	-0.222		-0.157		-0.070	-0.173	-0.273	0.395
.700	-0.656	0.118	-0.651	0.122	-0.350	0.054	-0.379	-0.111	-0.318	-0.073
.800	-0.594	0.013	-0.458	0.057	-0.501	0.570	0.157	-0.111	-0.452	0.395
.900	-0.363	-0.133	-0.286		-0.372		-0.255	-0.111	-0.140	-0.118
.950	-0.217	-0.154	-0.265		-0.436		-0.296	-0.193	-0.162	0.016

$\alpha = 22^\circ$ ,  $q = 34.56$ ,  $\mu = .340$ ,  $RPM = 3300$

**Appendix A**  
**Cruise fan inlet static pressure coefficients**

STATION X/F	80		135		225		260		350	
	OUTER	INNER	OUTER	INNER	OUTER	INNER	OUTER	INNER	OUTER	INNER
.000	1.007		0.723		0.981		0.915		0.890	
.005	0.697	0.023	0.800	-0.533	0.609	0.158	0.431	0.252	0.686	-0.001
.010	0.412	-0.986	0.671	-1.064	0.317	-0.374	0.150	-0.079	0.431	-0.001
.020	0.153	-0.624	0.334	-1.781	0.025	-0.931	-0.079	-0.819	0.201	-0.965
.050	-0.313	-1.660	-0.184	-2.020	-0.560	-1.728	-0.539	-1.559	-0.258	-0.965
.100	-0.494	-1.297	-0.365	-1.436	-0.533	-1.250	-0.539	-1.202	-0.207	-1.379
.200	-0.494	-0.883	-0.719	-0.905	-0.878	-0.896	-0.615	-0.870	-0.469	-0.910
.300	-0.494	-0.598	-0.799	-0.613	-0.692	-0.590	-0.692	-0.590	-0.469	-0.579
.400	-0.520	-0.598							-0.497	-0.579
.500	-0.520	-0.235							-0.276	-0.276
.600	-0.520	0.127	-0.188		-0.188		-0.334	-0.628	-0.249	0.275
.700	-0.494	0.127	-0.427	0.104	-0.400	0.074	-0.360	-0.130	-0.276	-0.166
.800	-0.494	0.101	-0.400	0.025	-0.400	0.558	-0.079	-0.130	-0.442	0.302
.900	-0.132	0.075	-0.374		-0.241		-0.105	-0.130	-0.194	0.100
.950	-0.028	0.075	-0.241		-0.347		-0.079	-0.054	-0.001	0.100

$\alpha = 0^\circ$ ,  $q = 27.93$ ,  $\mu = .504$ , RPM = 2000

**Appendix A**  
**Cruise fan inlet static pressure coefficients**

STATION X/Z	80		135		225		260		350	
	OUTER	INNER	OUTER	INNER	OUTER	INNER	OUTER	INNER	OUTER	INNER
.000	1.064		0.648		0.925		0.945		0.996	
.005	0.804	0.102	0.960	-1.149	0.585	0.265	0.228	0.535	0.510	0.055
.010	0.544	-1.121	0.882	-1.522	0.212	-0.268	-0.028	0.151	0.100	0.055
.020	0.258	-0.730	0.544	-2.189	-0.162	-0.089	-0.156	-0.592	-0.028	-0.084
.050	-0.236	-1.719	-0.002	-2.349	-0.589	-1.816	-0.618	-1.386	-0.413	-1.218
.100	-0.392	-1.329	-0.262	-1.602	-0.615	-1.282	-0.618	-1.104	-0.310	-1.246
.200	-0.418	-0.835	-0.749	-0.989	-0.855	-0.823	-0.618	-0.771	-0.499	-0.831
.300	-0.418	-0.574	-0.855	-0.615	-0.695	-0.541	-0.669	-0.515	-0.499	-0.526
.400	-0.496	-0.548							-0.499	-0.526
.500	-0.496	-0.132							-0.194	-0.167
.600	-0.496	0.154	-0.188		-0.162		-0.336	0.049	-0.167	0.276
.700	-0.496	0.154	-0.428	0.078	-0.482	0.125	-0.285	-0.028	-0.305	-0.084
.800	-0.262	0.154	-0.322	0.025	-0.375	0.535	-0.080	-0.028	-0.360	0.304
.900	-0.080	0.102	-0.348		-0.402		-0.054	-0.028	-0.111	0.165
.950	-0.002	0.102	-0.215		-0.162		-0.054	0.023	0.055	0.165

$\alpha = 4^\circ$ ,  $q = 27.81$ ,  $\mu = .503$ ,  $RPM = 2000$

**Appendix A**  
**Cruise fan inlet static pressure coefficients**

STATION X/F	80		135		225		260		350	
	OUTER	INNER	OUTER	INNER	OUTER	INNER	OUTER	INNER	OUTER	INNER
.000	1.008		0.560		0.982		0.891		0.865	
.005	0.853	-0.106	0.983	-1.624	0.477	0.344	0.150	0.610	0.099	0.551
.010	0.568	-1.298	0.957	-1.996	0.211	-0.161	-0.150	0.278	-0.182	0.551
.020	0.283	-0.936	0.646	-2.581	-0.161	-0.932	-0.258	-0.411	-0.304	-0.304
.050	-0.288	-1.869	0.075	-2.661	-0.640	-1.677	-0.667	-1.254	-0.616	-0.332
.100	-0.495	-1.376	-0.236	-1.677	-0.666	-1.198	-0.667	-1.050	-0.611	-1.104
.200	-0.495	-0.884	-0.799	-1.012	-0.879	-0.820	-0.667	-0.769	-0.580	-0.773
.300	-0.495	-0.599	-0.906	-0.640	-0.720	-0.539	-0.667	-0.516	-0.580	-0.497
.400	-0.599	-0.573							-0.580	-0.525
.500	-0.599	-0.132							-0.166	-0.111
.600	-0.599	0.153	-0.161		-0.135		-0.386	0.022	-0.139	0.220
.700	-0.599	0.153	-0.427	0.078	-0.480	0.125	-0.284	-0.003	-0.277	-0.056
.800	-0.313	0.101	-0.347	0.051	-0.587	0.457	-0.105	-0.003	-0.359	0.247
.900	-0.313	0.075	-0.294		-0.135		-0.105	-0.003	-0.139	0.137
.950	-0.054	0.049	-0.214		-0.640		-0.054	0.023	0.027	0.137

$\alpha = 6^\circ$ ,  $q = 27.90$ ,  $\mu = .503$ ,  $ReM = 2000$

Appendix A  
Cruise fan inlet static pressure coefficients

STATION X/Z	80		135		225		260		350	
	OUTER	INNER	OUTER	INNER	OUTER	INNER	OUTER	INNER	OUTER	INNER
.000	0.913		0.024		0.937		0.770		0.719	
.005	0.887	-0.342	0.992	-2.255	0.320	0.320	-0.080	0.770	-0.262	0.779
.010	0.652	-1.571	0.966	-2.497	-0.002	-0.162	-0.389	0.461	-0.518	0.751
.020	0.338	-1.336	0.756	-3.167	-0.270	-0.887	-0.466	-0.209	-0.569	-0.056
.050	-0.264	-2.042	0.155	-2.899	-0.753	-1.665	-0.827	-1.085	-0.776	-0.084
.100	-0.473	-1.493	-0.159	-1.826	-0.726	-1.182	-0.750	-0.930	-0.516	-1.002
.200	-0.499	-0.918	-0.806	-1.021	-0.780	-0.776	-0.750	-0.498	-0.664	-0.724
.300	-0.551	-0.578	-0.887	-0.645	-0.619	-0.518	-0.724	-0.466	-0.668	-0.501
.400	-0.656	-0.578							-0.641	-0.501
.500	-0.656	-0.081							-0.140	-0.084
.600	-0.656	0.155	-0.136		-0.082		-0.441	-0.003	-0.112	0.166
.700	-0.656	0.155	-0.484	0.106	-0.270	0.100	-0.328	-0.003	-0.251	-0.001
.800	-0.342	0.129	-0.377	0.025	-0.458	0.384	-0.131	-0.003	-0.362	0.194
.900	-0.159	0.076	-0.297		-0.136		-0.260	-0.003	-0.140	0.111
.950	-0.081	0.076	-0.162		-0.323		-0.080	0.023	0.055	0.139

$\alpha = 12^\circ$ ,  $q = 27.65$ ,  $\mu = .502$ , RPM = 2000



**Appendix A**  
**Cruise fan inlet static pressure coefficients**

STATION X/Z	80		135		225		260		350	
	OUTER	INNER	OUTER	INNER	OUTER	INNER	OUTER	INNER	OUTER	INNER
.000	0.830		-0.237		0.933		0.638		0.382	
.005	0.830	-0.601	0.986	-2.751	0.158	0.479	-0.362	0.818	-0.874	0.830
.010	0.674	-1.746	0.986	-2.804	-0.135	-0.028	-0.561	0.561	-1.028	0.830
.020	0.388	-1.694	0.778	-3.578	-0.482	-0.662	-0.664	-0.105	-0.900	0.110
.050	-0.158	-2.188	0.154	-3.098	-0.963	-1.616	-0.951	-1.002	-0.577	0.082
.100	-0.445	-1.564	-0.210	-1.843	-0.802	-1.149	-0.823	-0.926	-0.618	-0.970
.200	-0.523	-0.913	-0.829	-1.069	-0.936	-0.707	-0.823	-0.95	-0.721	-0.748
.300	-0.575	-0.627	-0.909	-0.616	-0.616	-0.515	-0.772	-0.438	-0.721	-0.527
.400	-0.679	-0.601							-0.683	-0.527
.500	-0.679	-0.054							-0.139	-0.111
.600	-0.679	0.128	-0.135		-0.055		-0.567	-0.028	-0.111	0.082
.700	-0.679	0.128	-0.535	0.078	-0.349	0.074	-0.336	-0.028	-0.278	-0.001
.800	-0.445	0.102	-0.269	-0.002	-0.295	0.254	-0.259	-0.028	-0.333	0.082
.900	-0.210	0.102	-0.215		-0.295		-0.310	-0.028	-0.139	0.055
.950	-0.106	0.076	-0.135		-0.375		-0.105	-0.028	-0.001	0.082

$\alpha = 16^\circ$ ,  $q = 27.80$ ,  $\mu = .502$ ,  $RPM = 2000$

Appendix A  
Cruise fan inlet static pressure coefficients

STATION Y/F	80		135		225		260		350	
	OUTER	INNER	OUTER	INNER	OUTER	INNER	OUTER	INNER	OUTER	INNER
.000	0.674		-0.367		0.692		-0.233		0.023	
.005	0.856	-0.991	0.961	-3.205	-0.429	0.692	-1.233	0.869	-1.310	0.996
.010	0.700	-2.266	0.961	-3.072	-0.375	0.132	-2.310	0.746	-1.413	0.996
.020	0.466	-2.110	0.726	-3.872	-0.909	-0.215	-1.592	0.382	-1.204	0.387
.050	-0.184	-2.527	0.050	-3.312	-1.390	-1.390	-1.336	-0.618	-1.285	0.249
.100	-0.471	-1.642	-0.393	-2.084	-1.096	-1.150	-1.079	-0.695	-0.746	-0.915
.200	-0.575	-0.965	-0.963	-1.150	-1.016	-0.797	-0.721	-0.592	-0.459	-0.665
.300	-0.653	-0.601	-1.043	-0.696	-0.883	-0.515	-0.515	-0.413	-0.721	-0.499
.400	-0.731	-0.549							-0.693	-0.582
.500	-0.731	-0.054							-0.111	-0.056
.600	-0.731	0.076	-0.108		-0.082		-0.618	-0.054	-0.111	-0.001
.700	-0.731	0.076	-0.349	0.052	-0.375	0.100	-0.182	-0.054	-0.333	-0.001
.800	-0.697	0.050	-0.295	-0.082	-0.269	0.177	-0.233	-0.054	-0.416	0.027
.900	-0.315	0.024	-0.349		-0.242		-0.285	-0.054	-0.139	0.027
.950	-0.211	0.024	-0.189		-0.189		-0.157	-0.028	-0.001	0.082

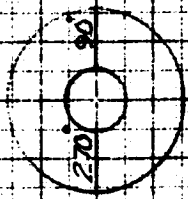
$\alpha = 20^\circ$ ,  $q = 27.79$ ,  $\mu = .503$ , RPM = 2000

**Appendix A**  
**Gauge fan inlet static pressure coefficients**

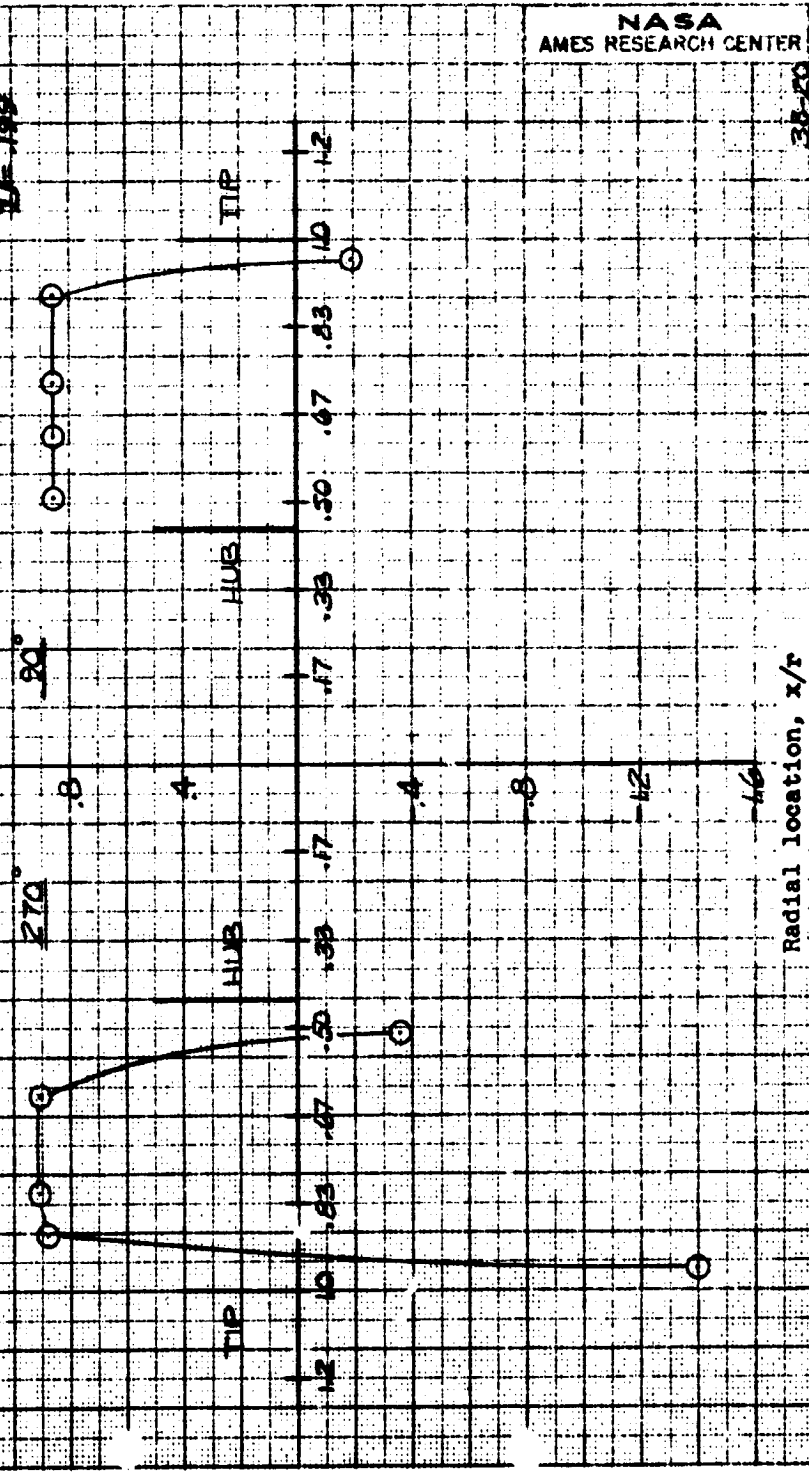
STATION X/Z	80		135		225		260		350	
	OUTER	INNER	OUTER	INNER	OUTER	INNER	OUTER	INNER	OUTER	INNER
.000	0.520		-0.290		0.374		-0.877		0.174	
.005	0.586	-1.622	0.990	-3.431	-0.645	-0.743	-2.313	-0.666	-1.521	0.917
.010	0.755	-2.640	0.964	-3.833	-1.046	-0.744	-2.979	0.461	-1.469	0.917
.020	0.442	-2.118	0.677	-4.261	-0.939	-0.645	-1.186	0.022	-1.289	0.950
.050	-0.237	-2.692	-0.028	-3.726	-1.502	-1.261	-1.135	-0.672	-1.405	0.222
.100	-0.444	-1.831	-0.472	-2.145	-1.314	-1.184	-0.723	-0.740	-0.926	-0.973
.200	-0.551	-1.021	-1.154	-1.180	-0.886	-1.032	-0.569	-0.607	-0.913	-0.723
.300	-0.681	-0.681	-1.207	-0.752	-0.725	-0.723	-0.723	-0.569	-0.695	-0.556
.400	-0.838	-0.655							-0.668	-0.584
.500	-0.812	-0.054							-0.195	-0.112
.600	-0.812	0.050	-0.136		-0.109		-0.545	-0.080	-0.167	-0.001
.700	-0.655	0.050	-0.537	-0.002	-0.296	-0.003	-0.414	-0.054	-0.390	-0.028
.800	-0.577	0.024	-0.511	-0.055	-0.511	0.126	-0.337	-0.054	-0.445	-0.001
.900	-0.342	-0.028	-0.377		-0.296		-0.208	-0.054	-0.167	-0.112
.950	-0.237	-0.054	-0.189		-0.537		-0.183	-0.080	-0.306	-0.028

$\alpha = 22^\circ$ ,  $q = 27.69$ ,  $\mu = .562$ ,  $RPM = 2000$

Appendix B  
Cruise fan inlet total pressure  
distribution

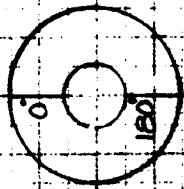


$\alpha = 0^\circ$   
8-11-65  
JL-199

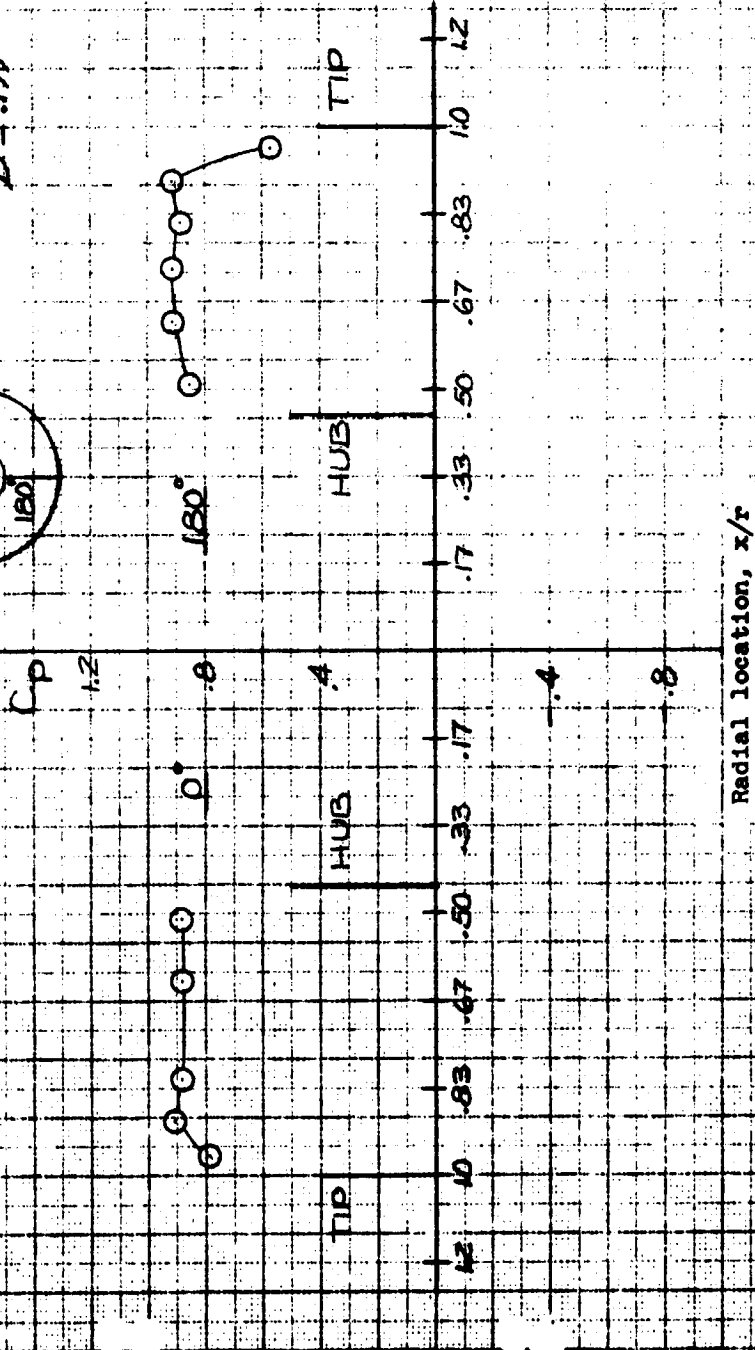


Radial location,  $x/r$

Appendix B  
Cruise fan inlet total pressure  
distribution

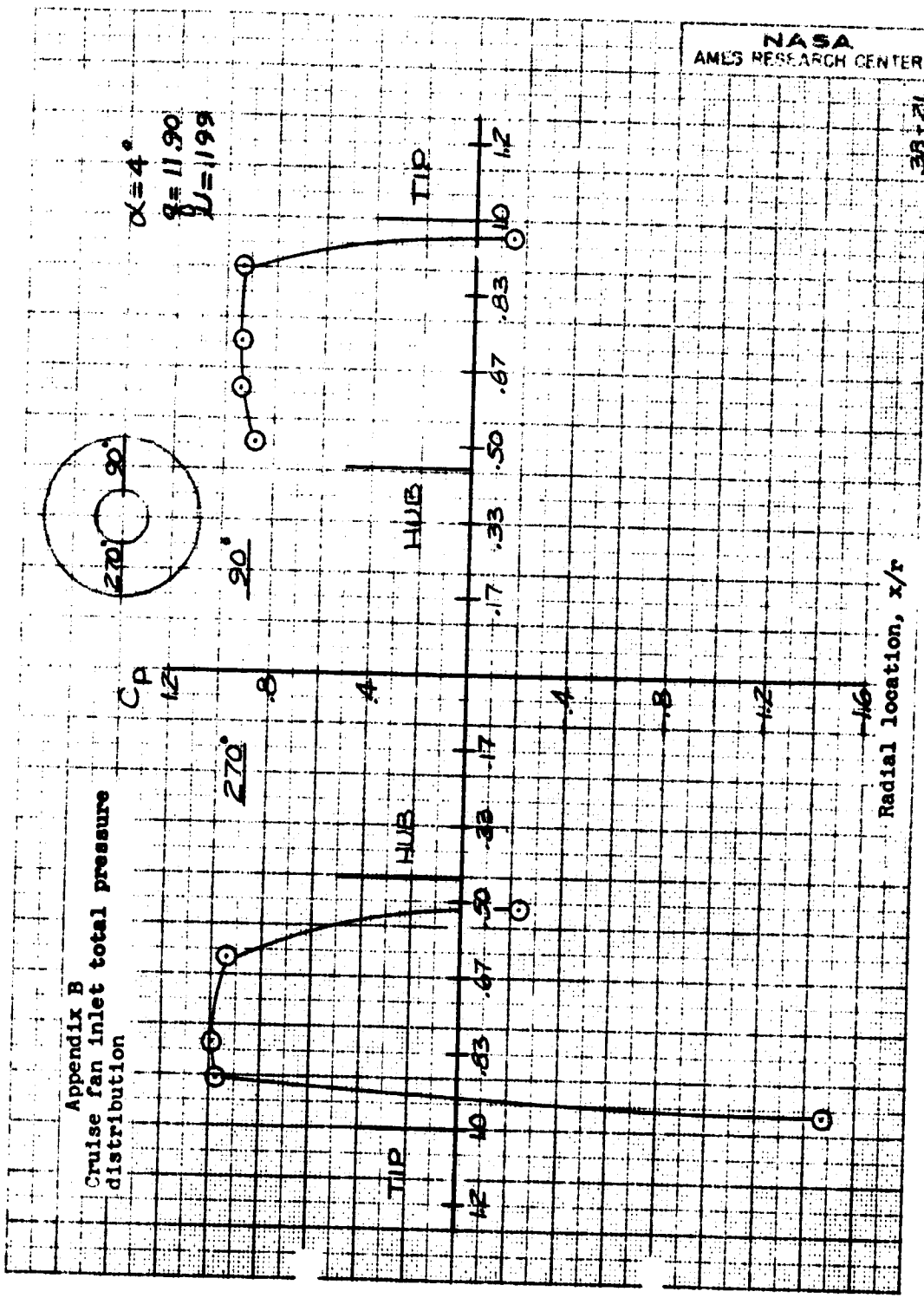


$\alpha = 0^\circ$   
 $\beta = 11.85^\circ$   
 $\Delta l = .199$

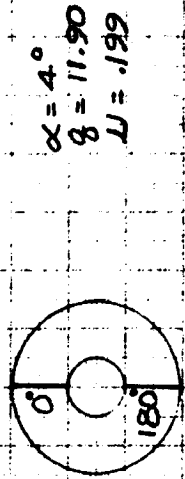


NASA  
AMES RESEARCH CENTER

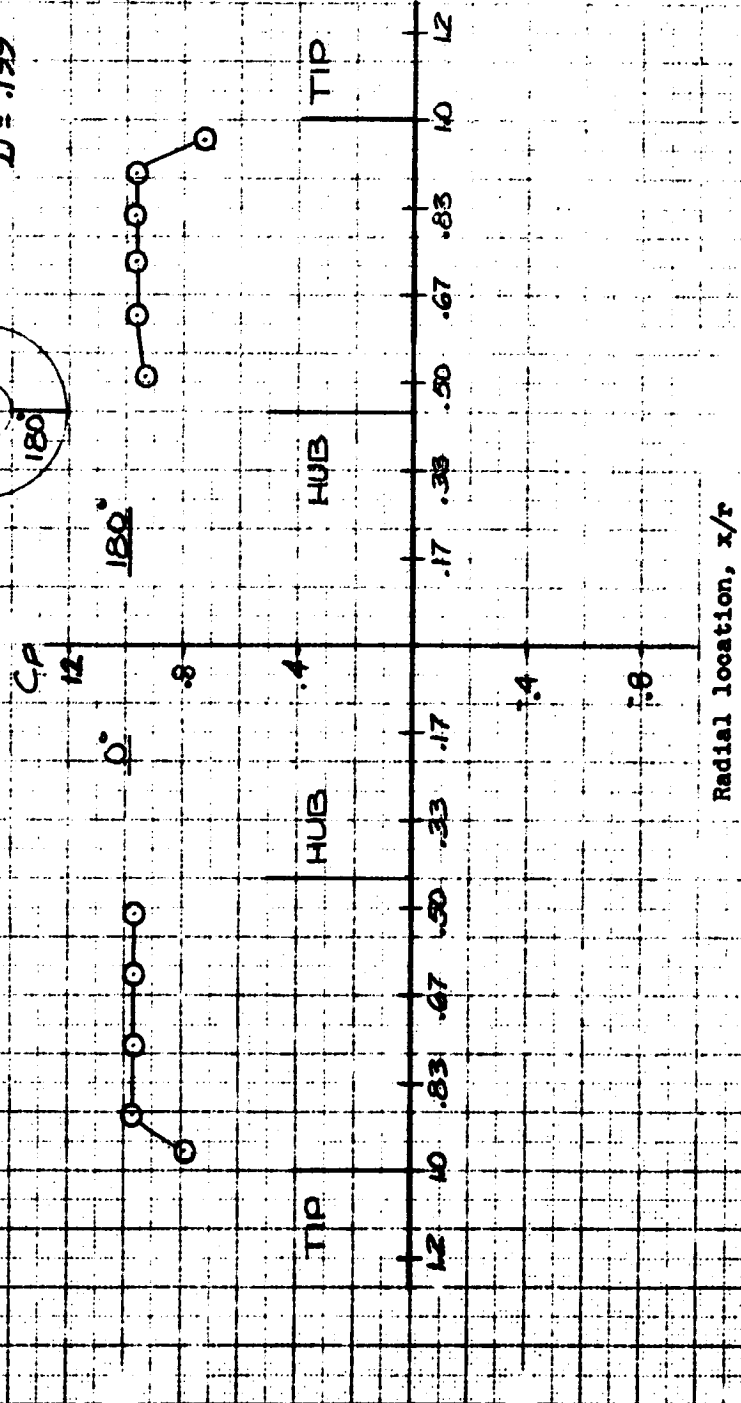
38-20



Appendix B  
Cruise fan inlet total pressure  
distribution



$\alpha = 4^\circ$   
 $\beta = 11.90$   
 $U = .199$



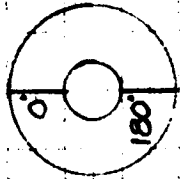
2  
P  
S  
A  
AMES RESEARCH CENTER

38-21

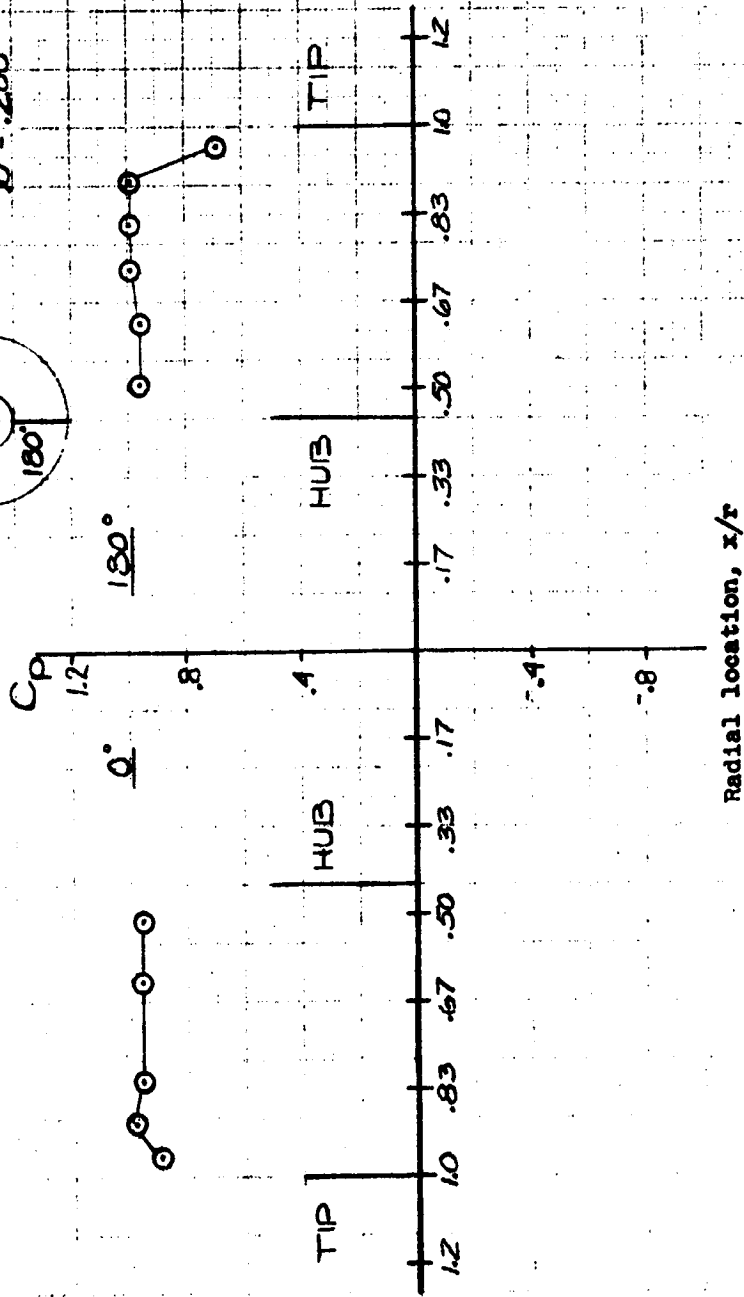




Appendix B  
Cruise fan inlet total pressure  
distribution

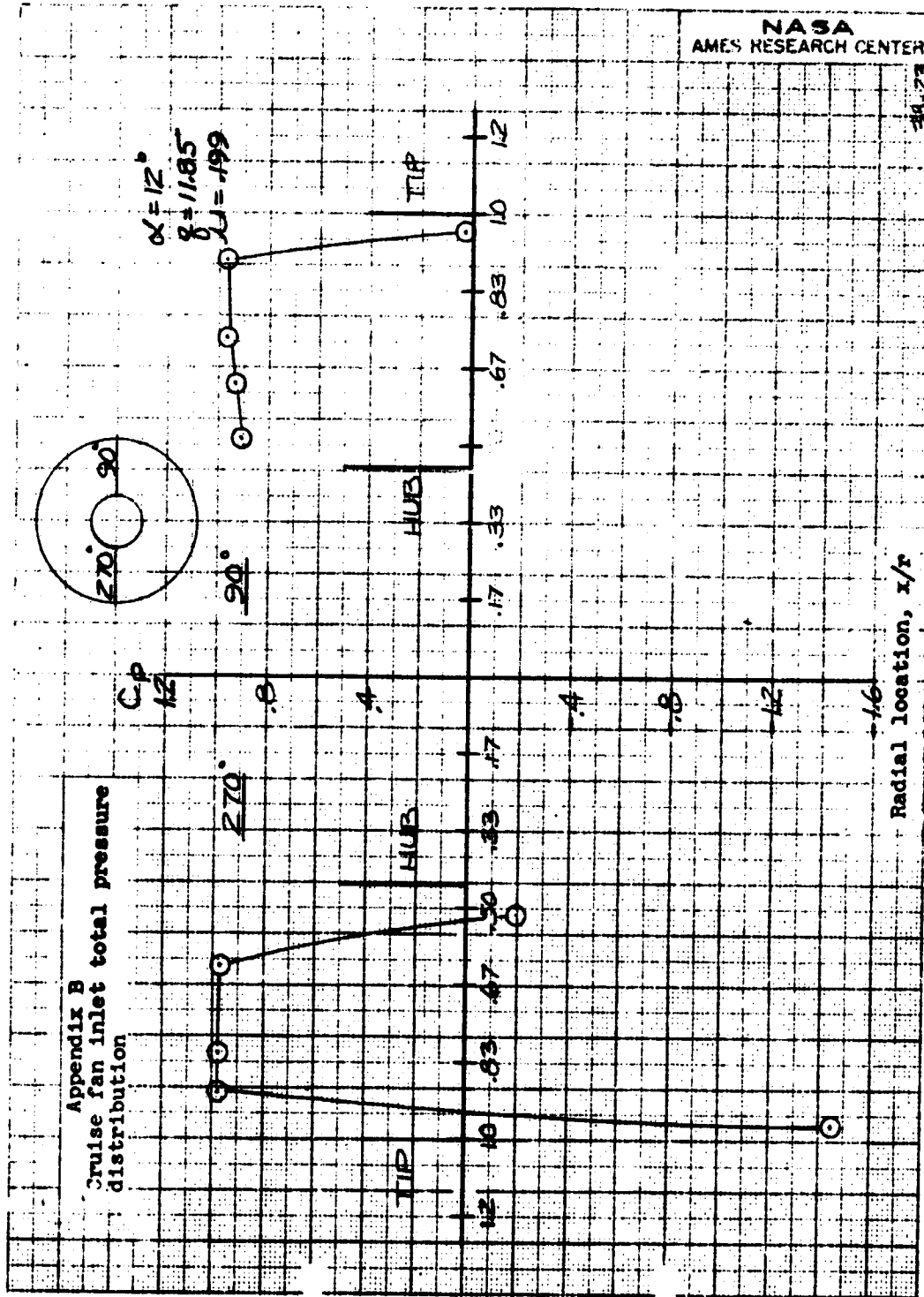


$\alpha = 8^\circ$   
 $\beta = 11.97$   
 $M = .200$

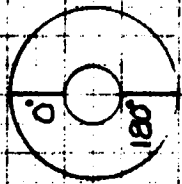


NASA  
AMES RESEARCH CENTER

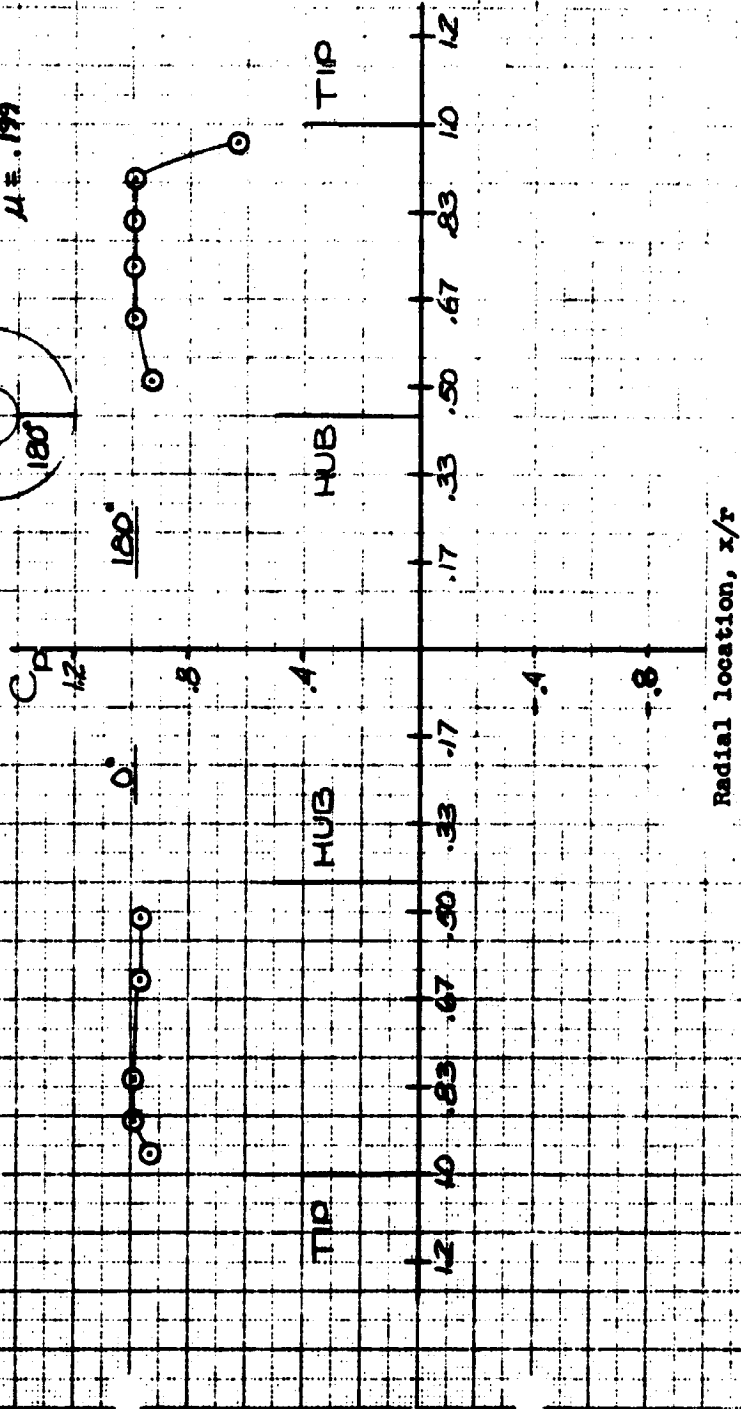
38-12



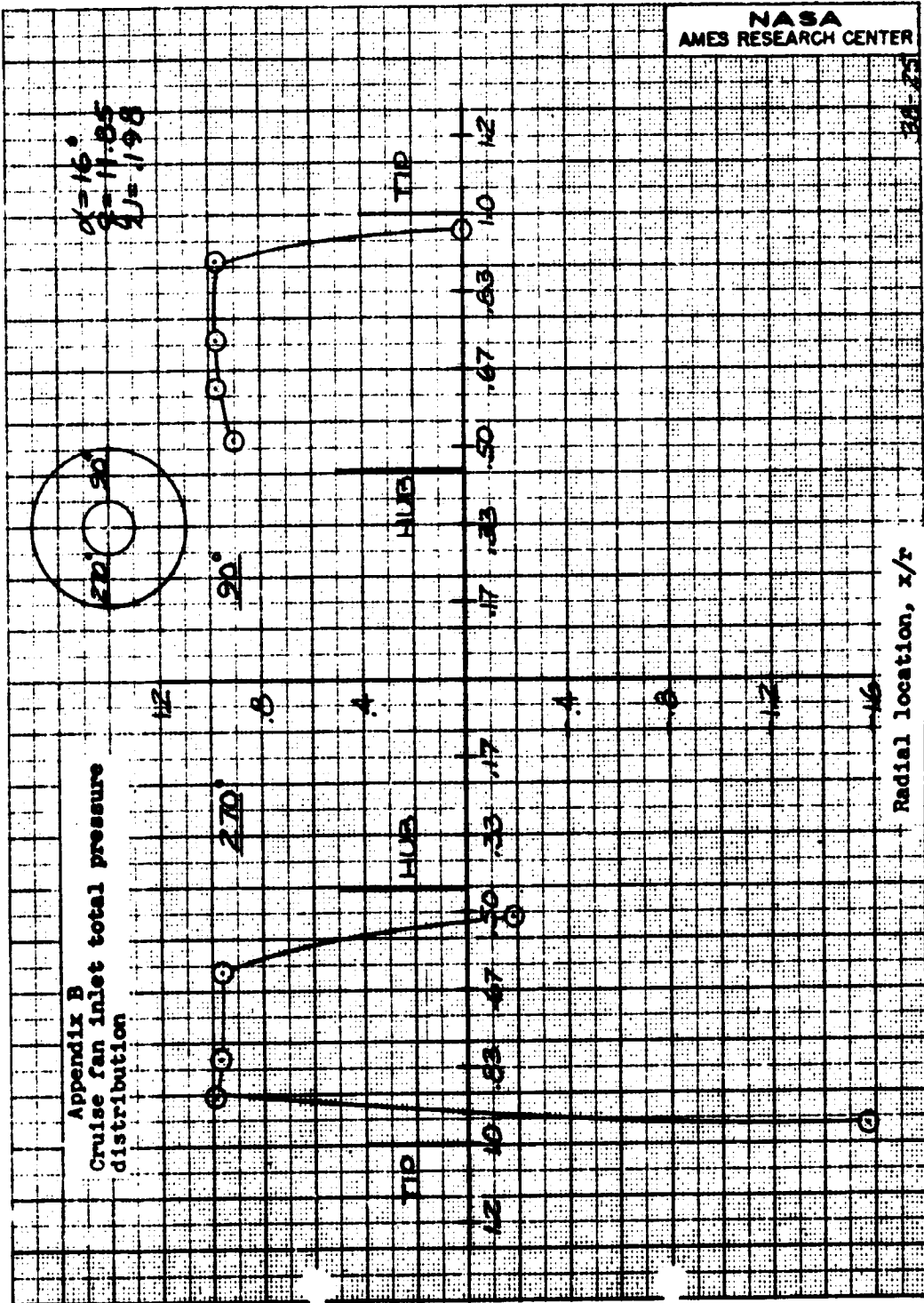
Appendix B  
Cruise fan inlet total pressure  
distribution

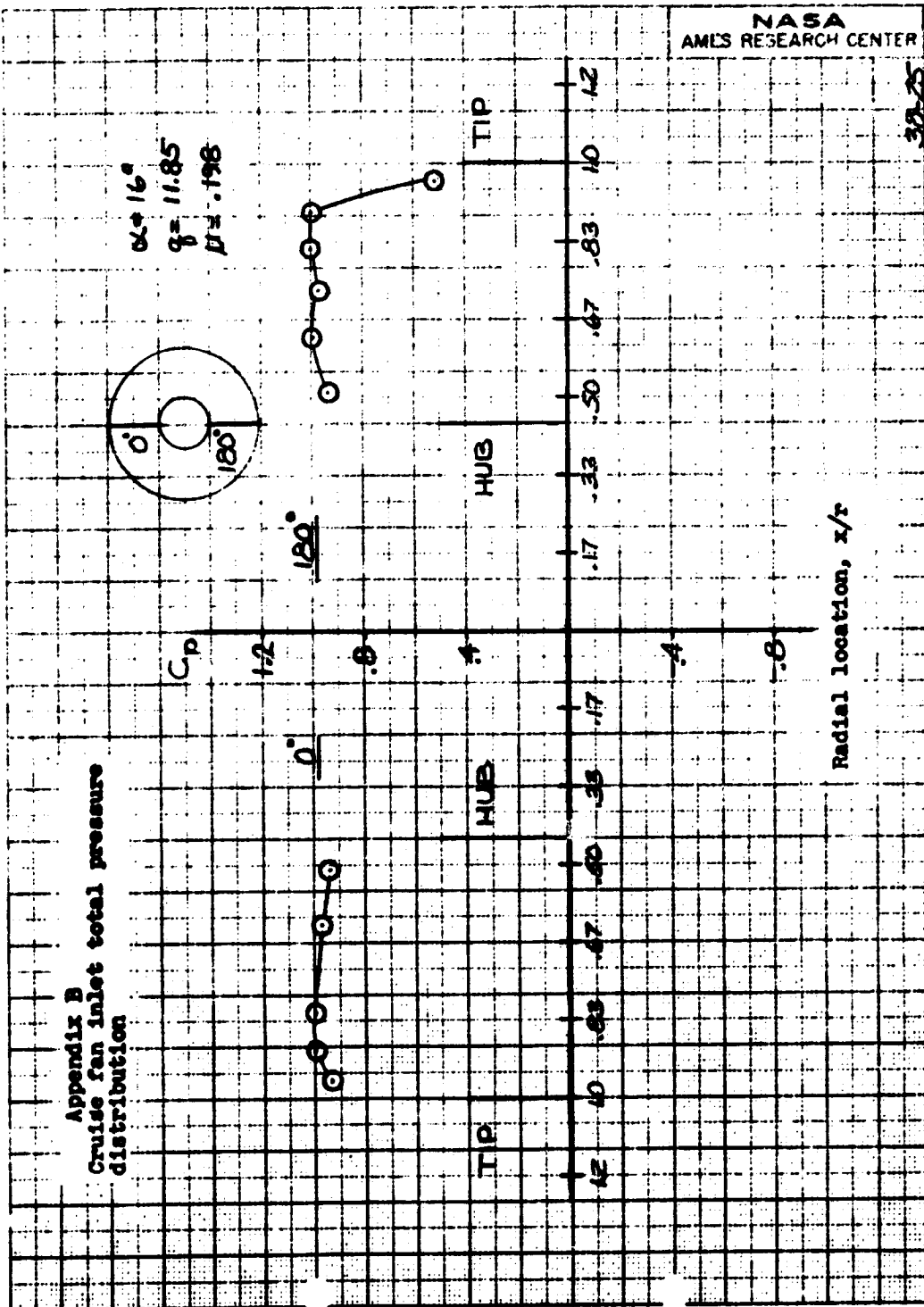


$\alpha = 12^\circ$   
 $q = 11.85$   
 $\mu = .199$

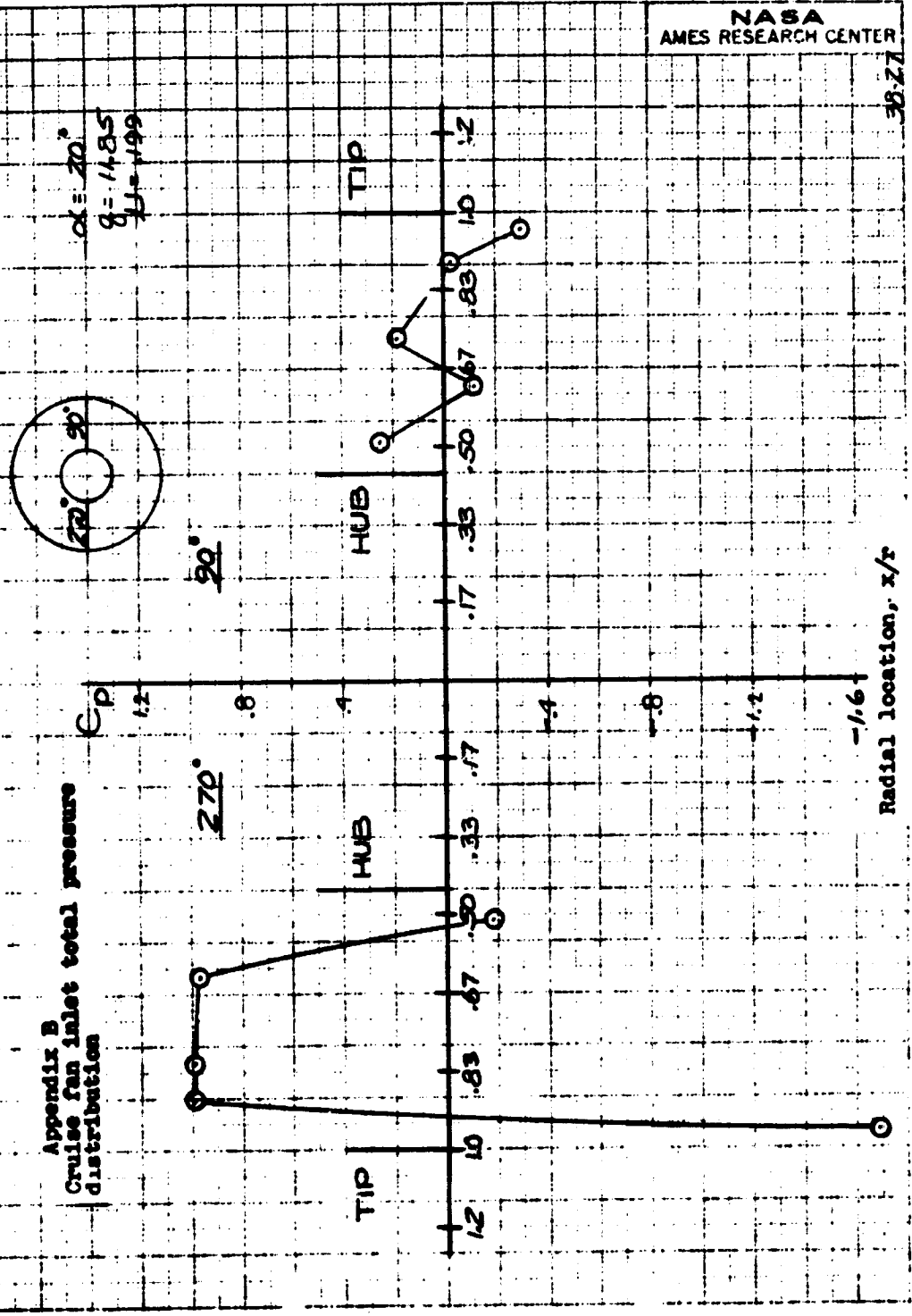


AWES 2015





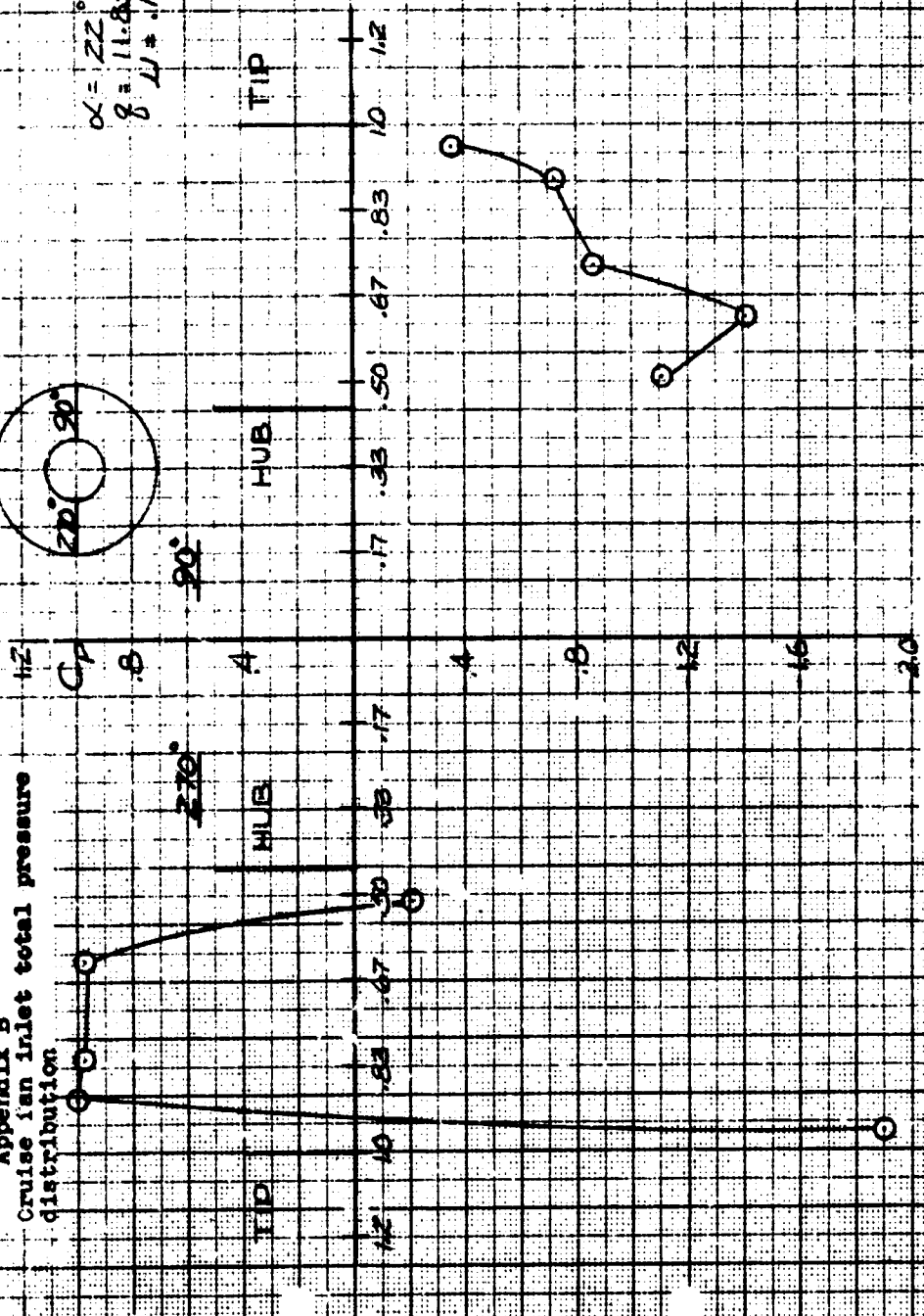
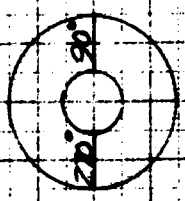
38-75





Appendix B  
Cruise fan inlet total pressure  
distribution.

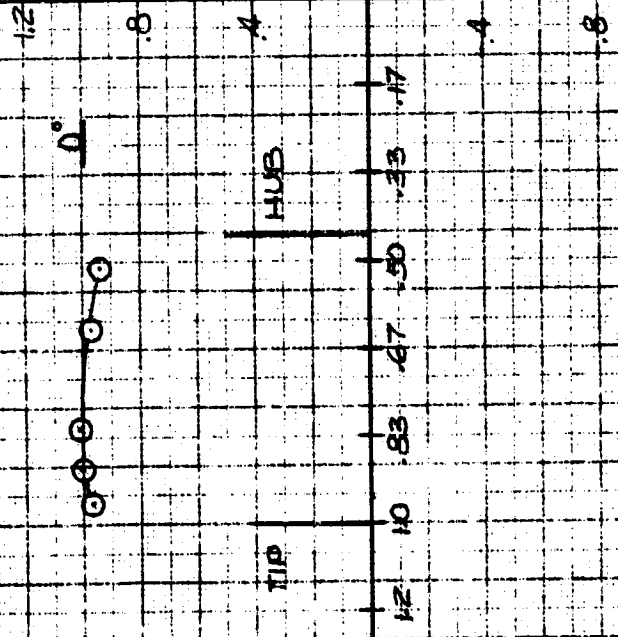
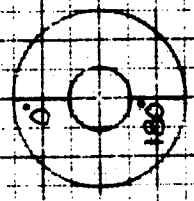
$\alpha = 22^\circ$   
 $\beta = 11.85^\circ$   
 $U = .199$



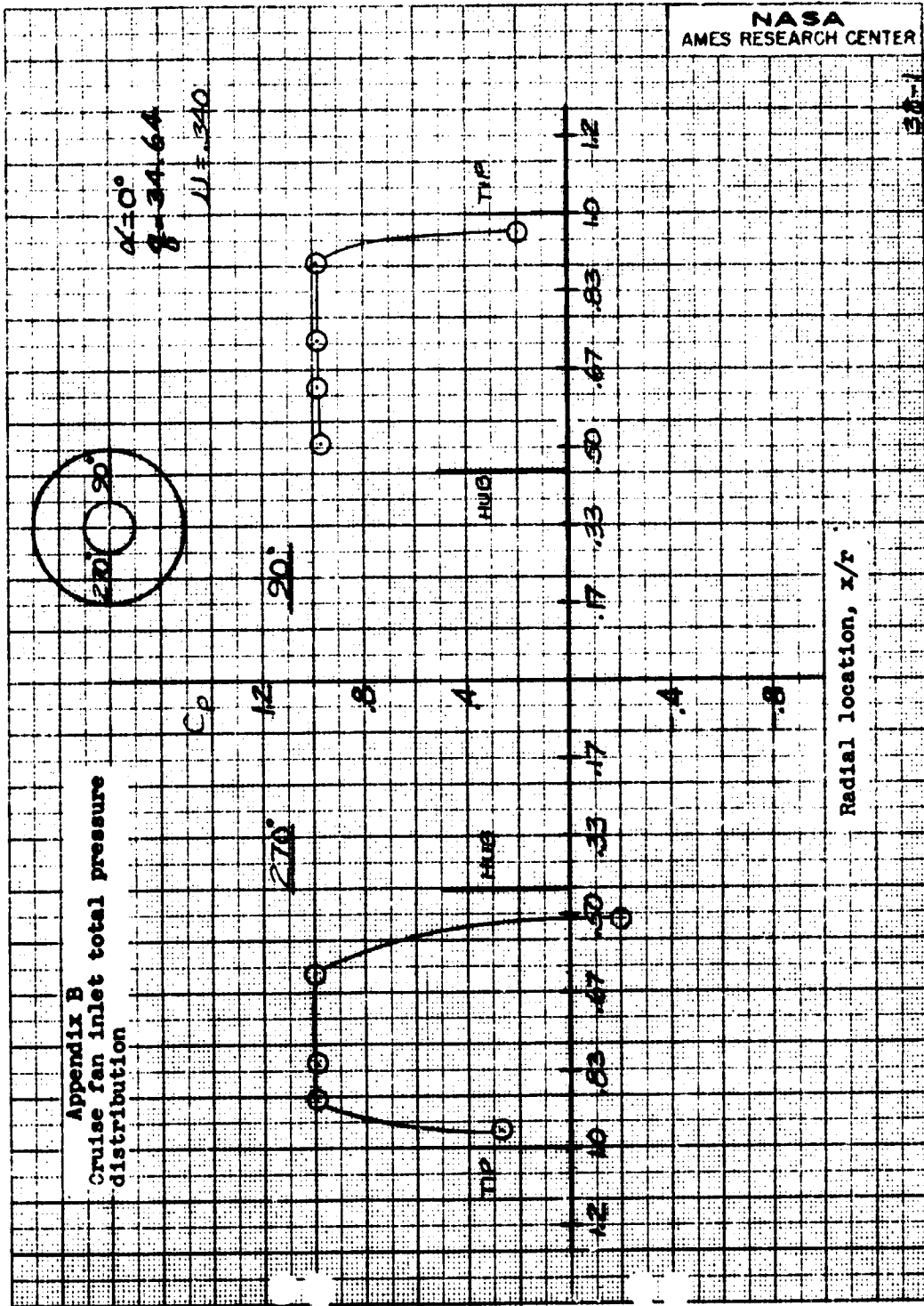


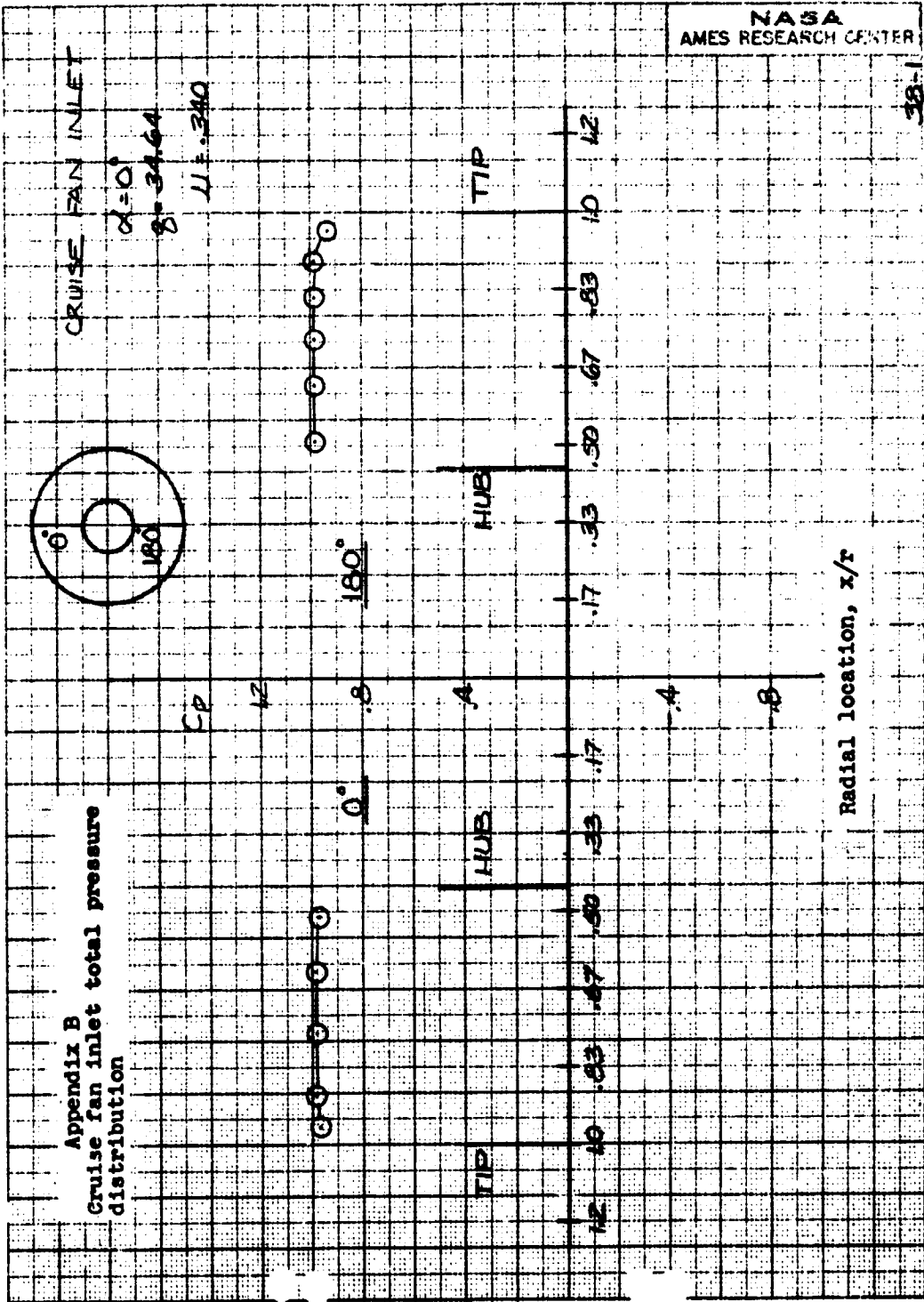
Appendix B  
Cruise fan inlet total pressure  
distribution

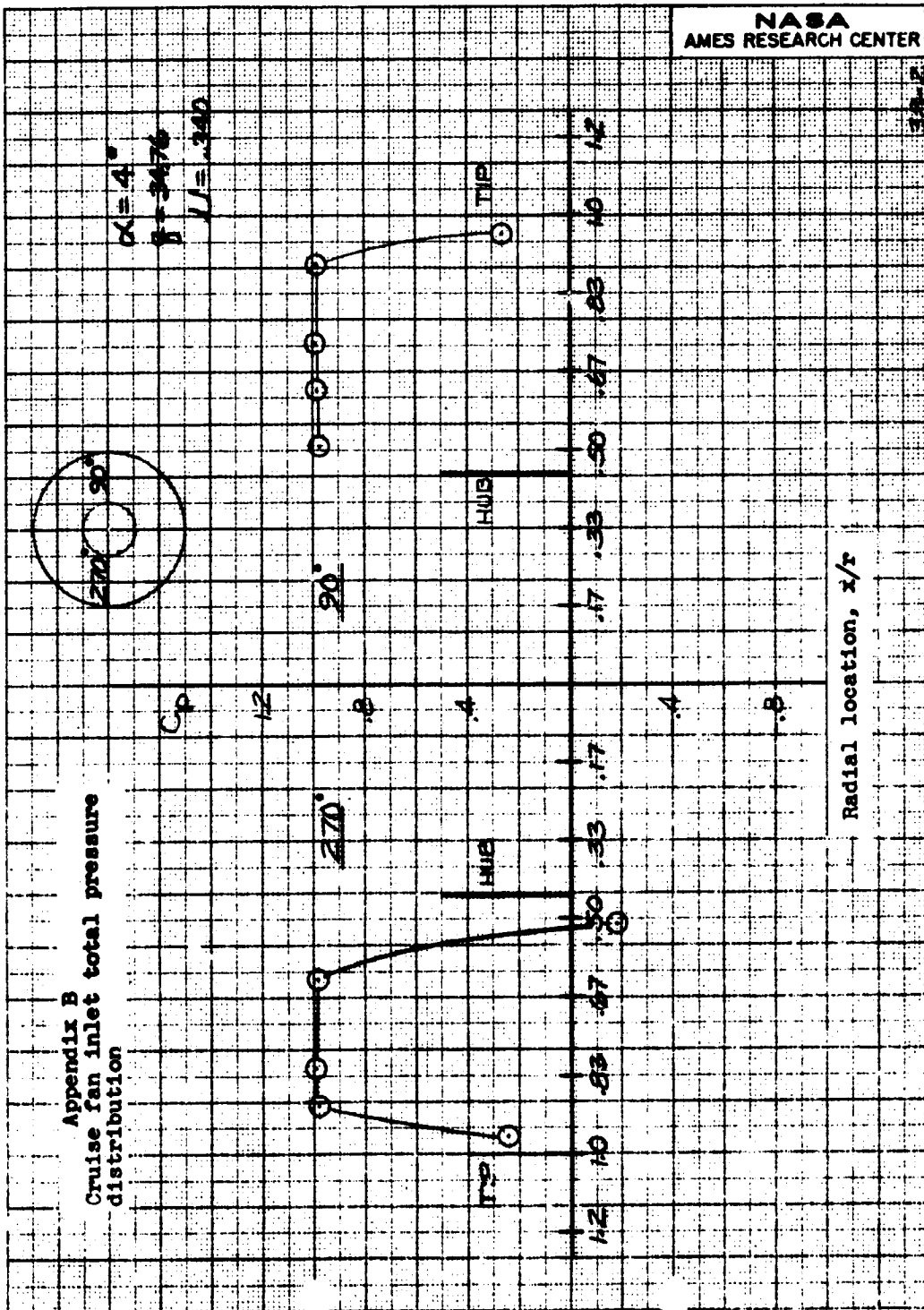
$\alpha = 22^\circ$   
 $\beta = 17.85^\circ$   
 $M = 1.99$



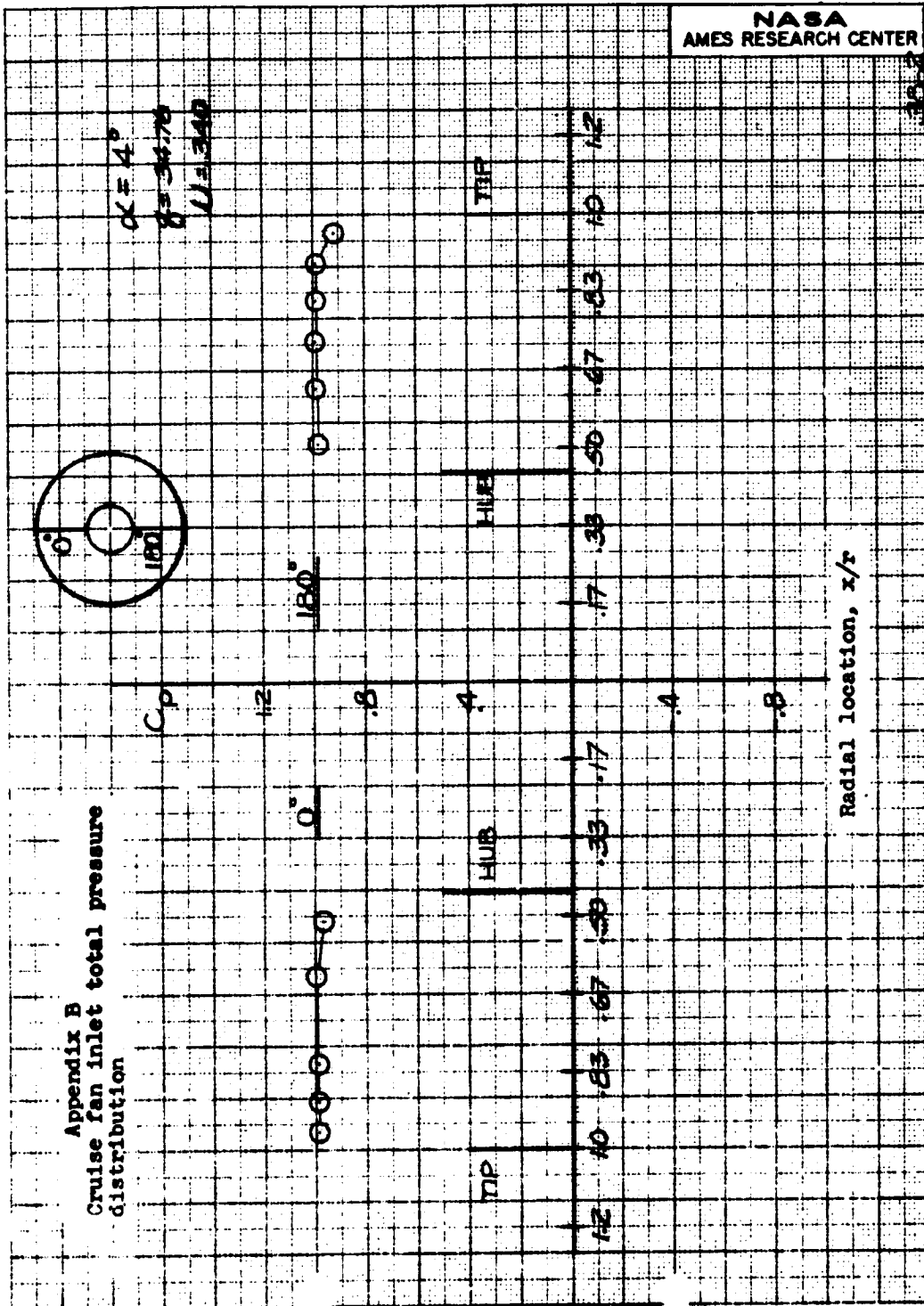
Radial location, x/r

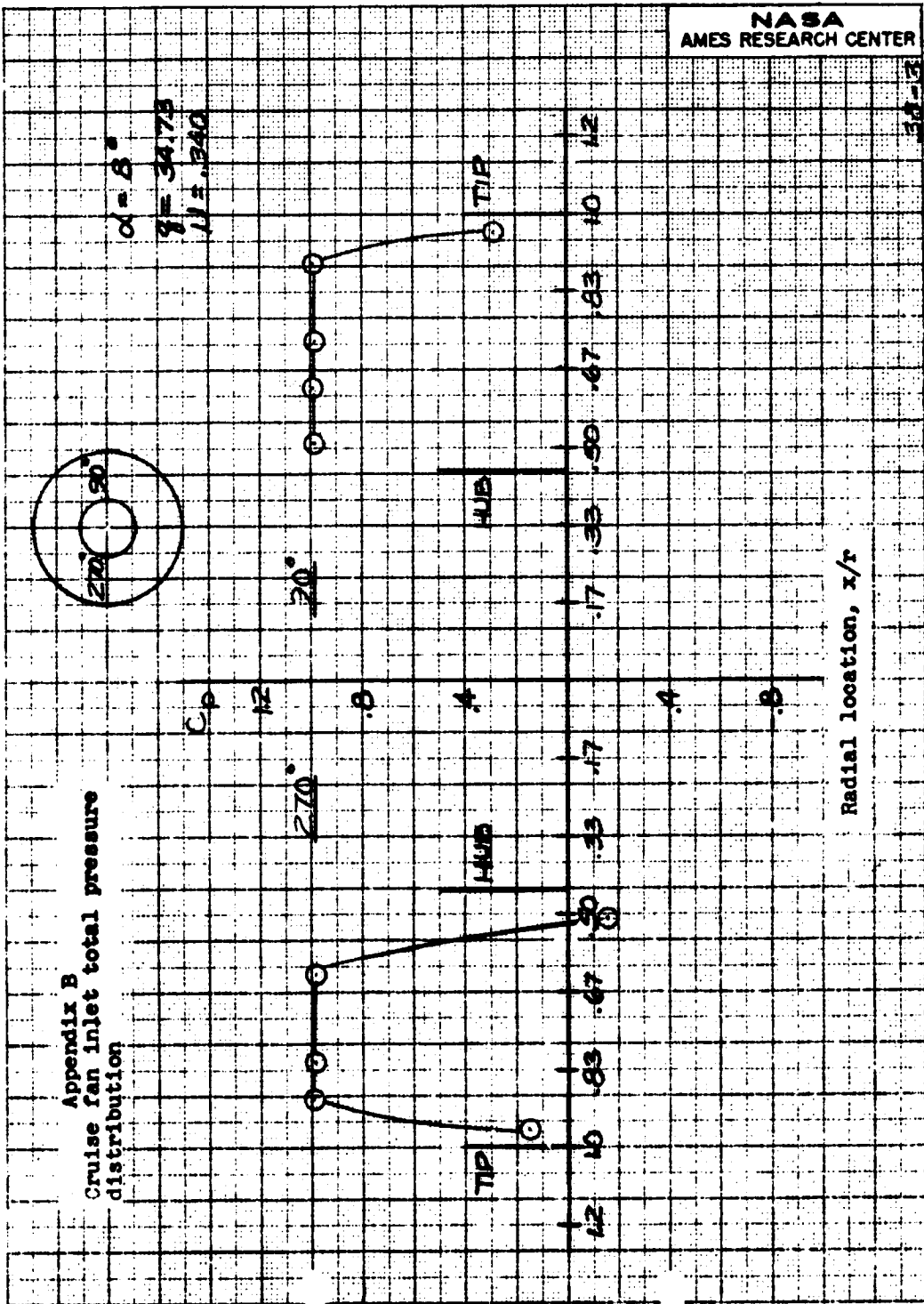




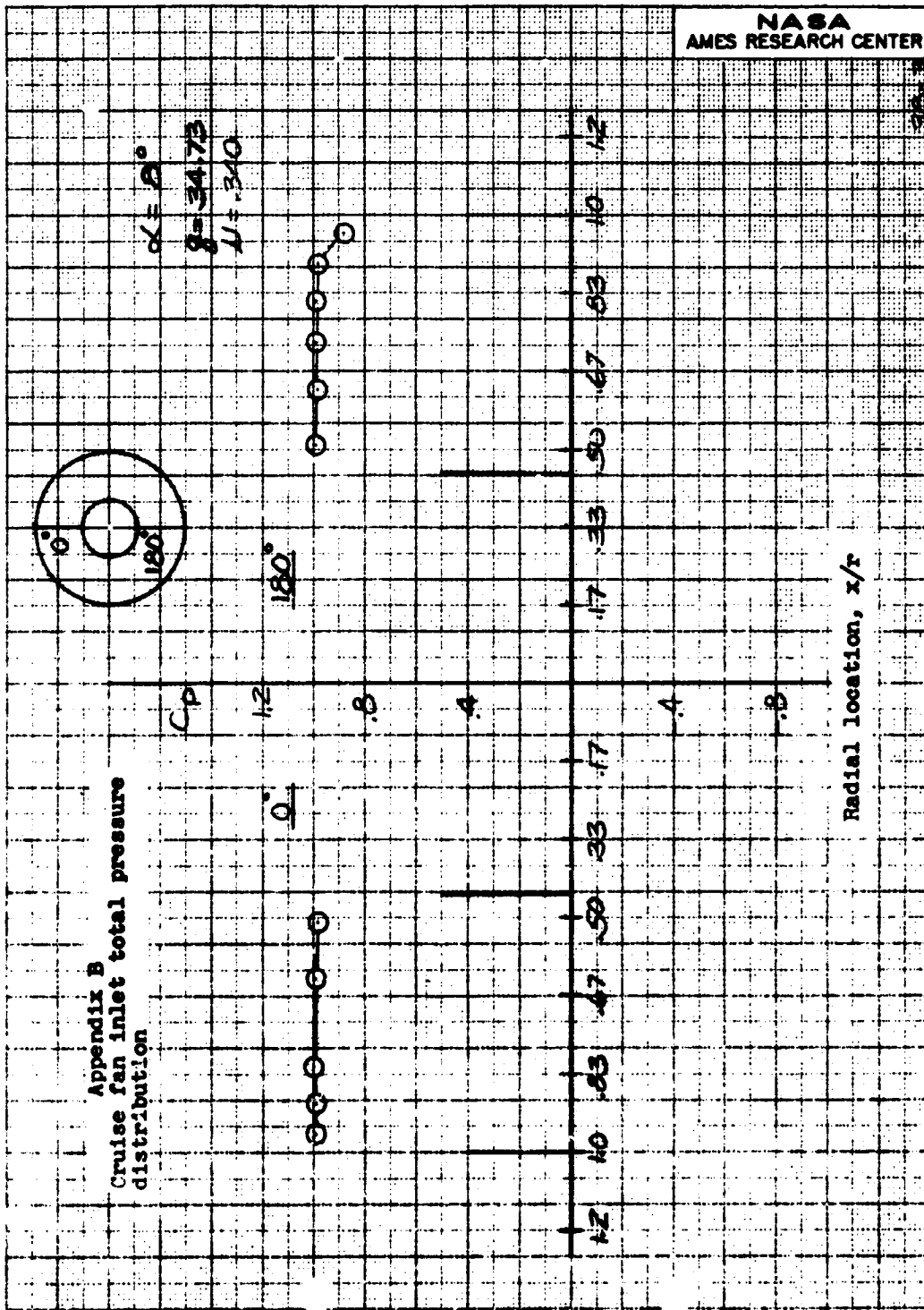


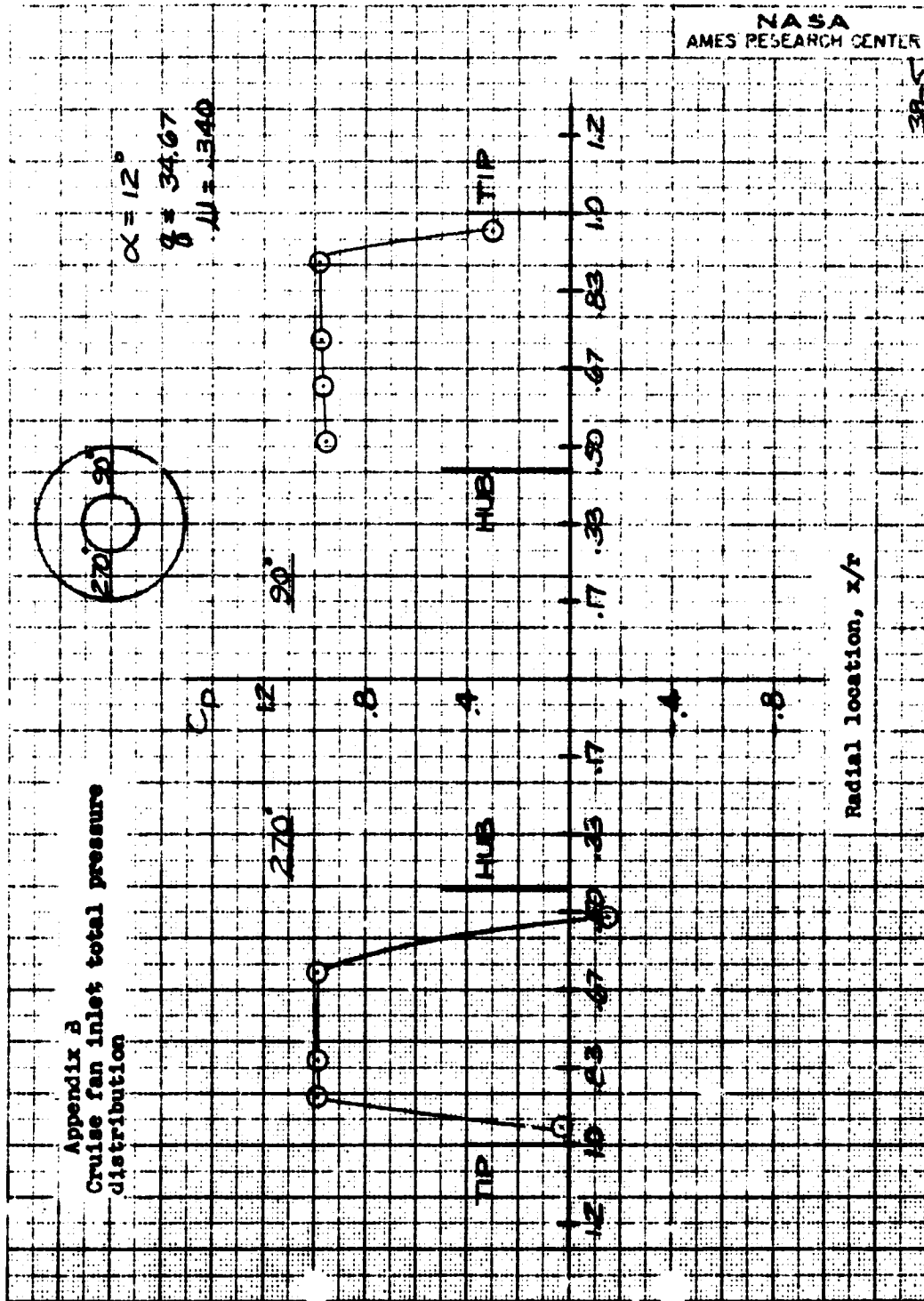
Appendix B  
Cruise fan inlet total pressure  
distribution





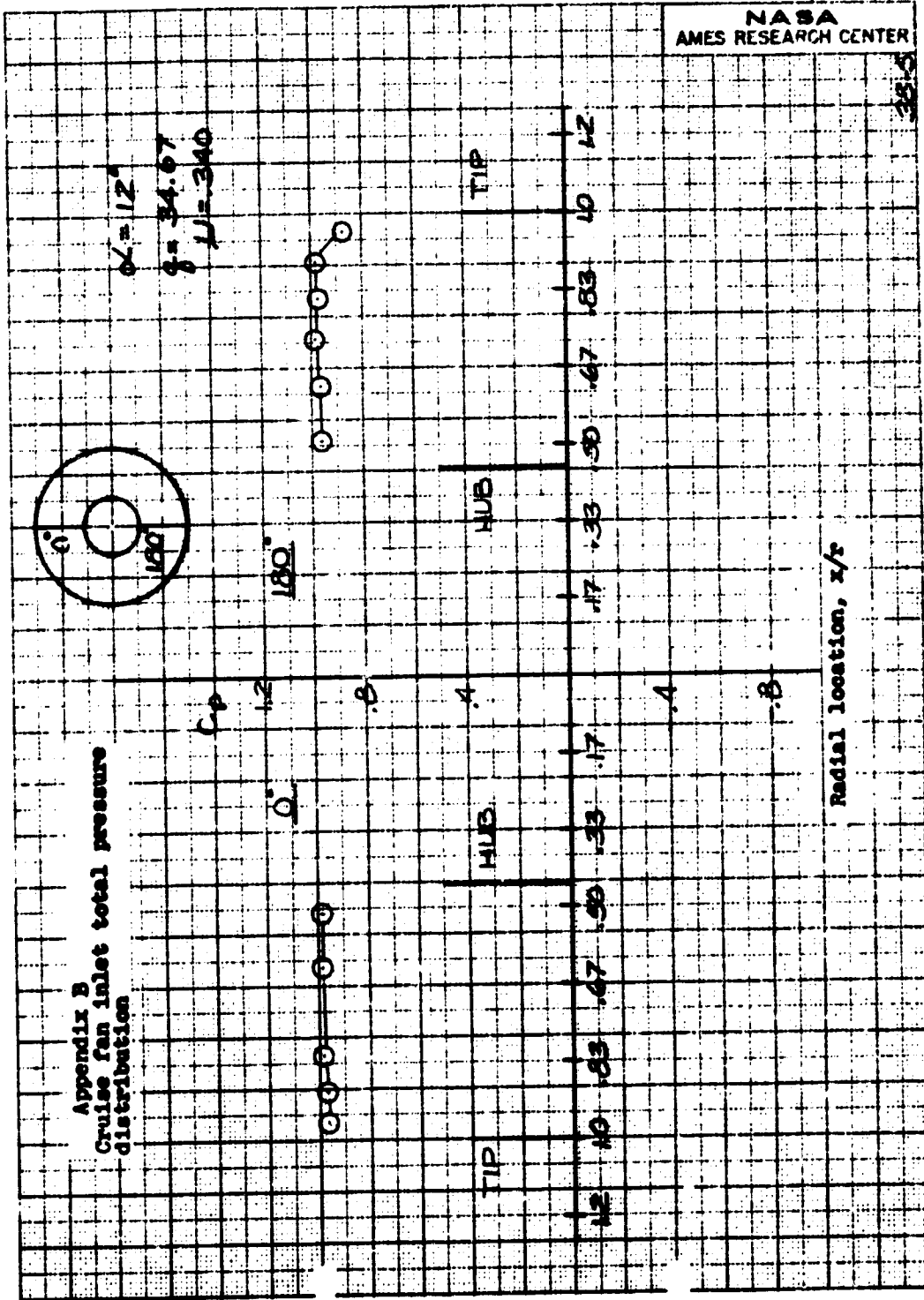
Appendix B  
Cruise fan inlet total pressure  
distribution



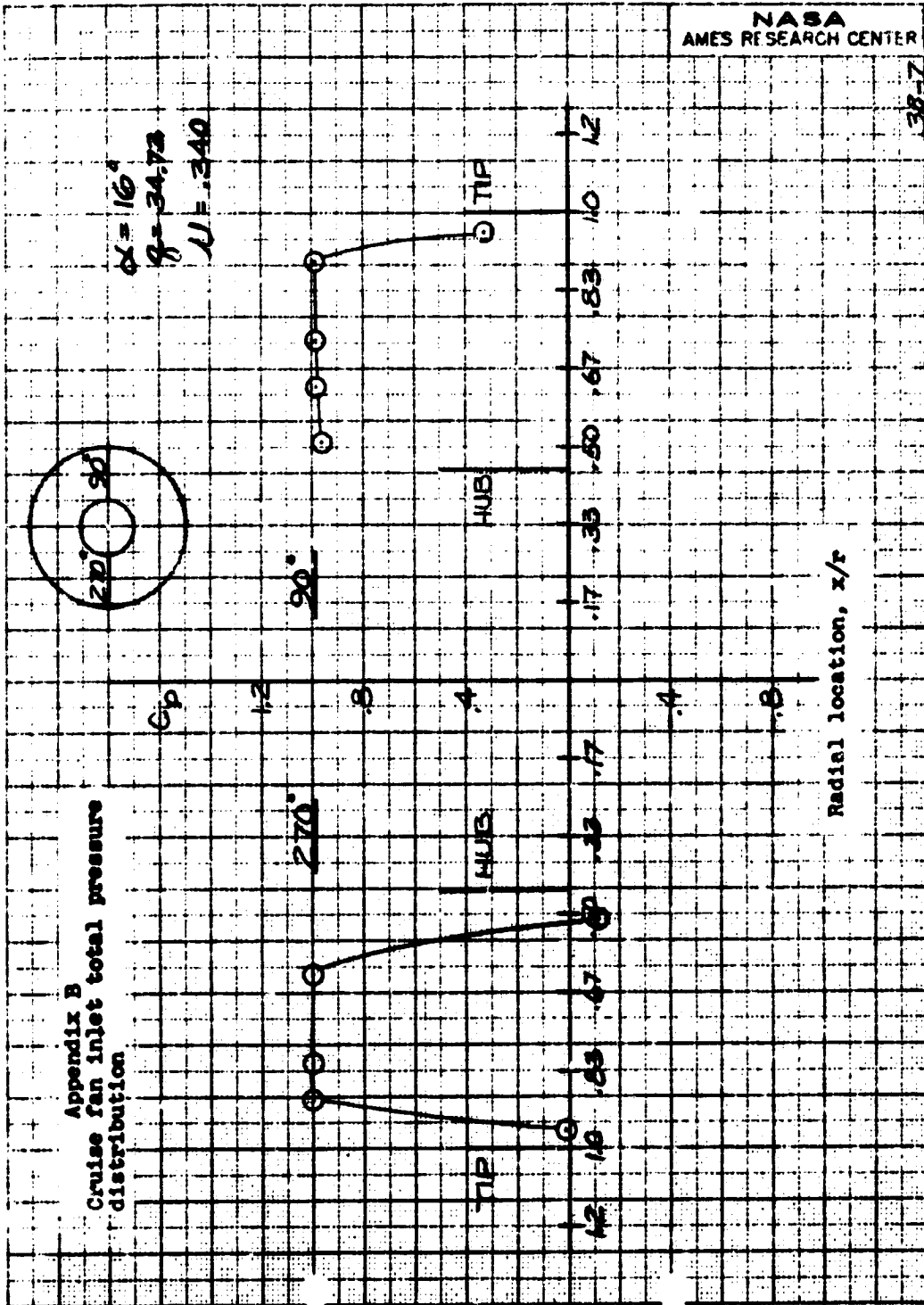




Appendix B  
Cruise fan inlet total pressure  
distribution



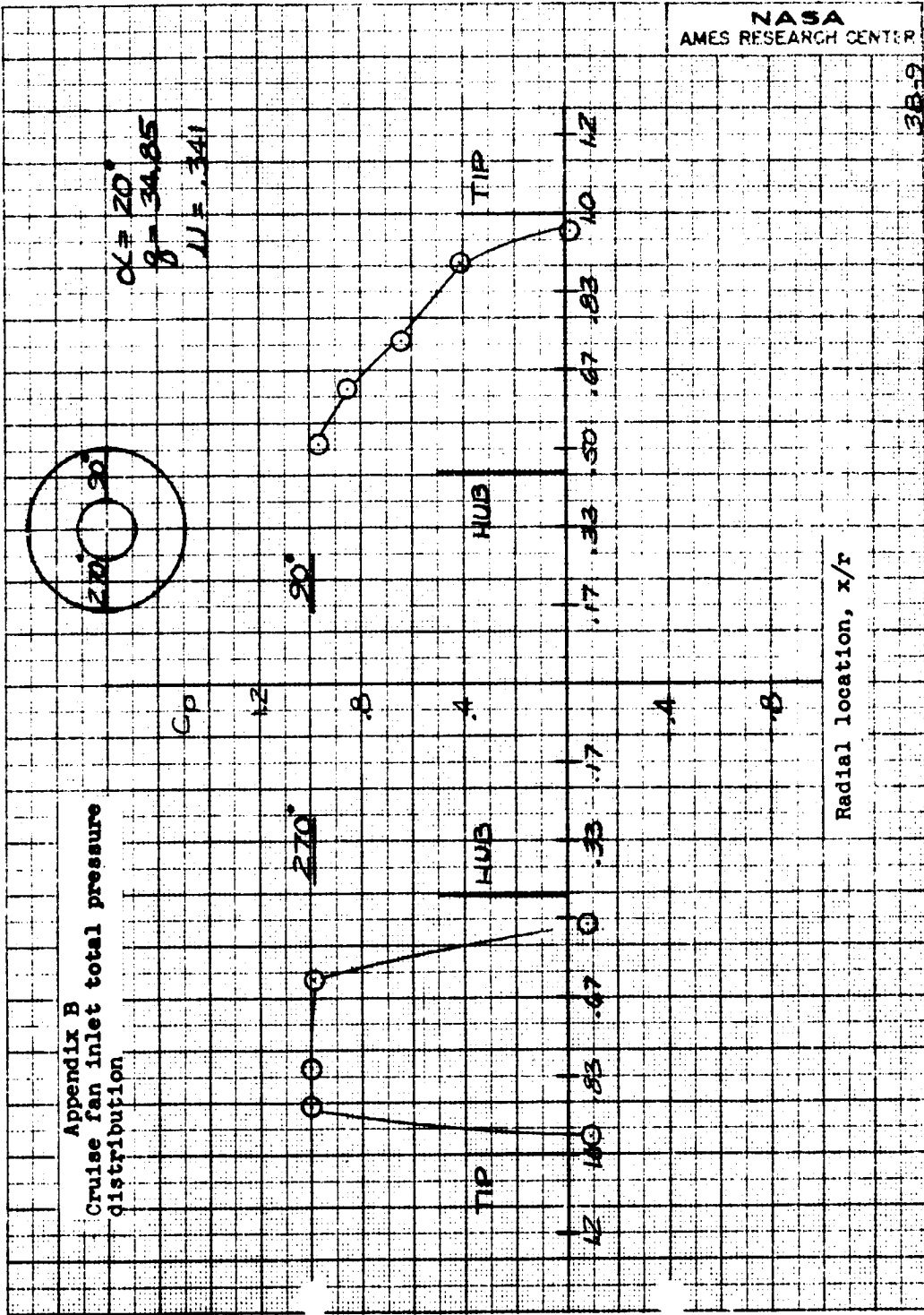
Appendix B  
Cruise fan inlet total pressure  
distribution



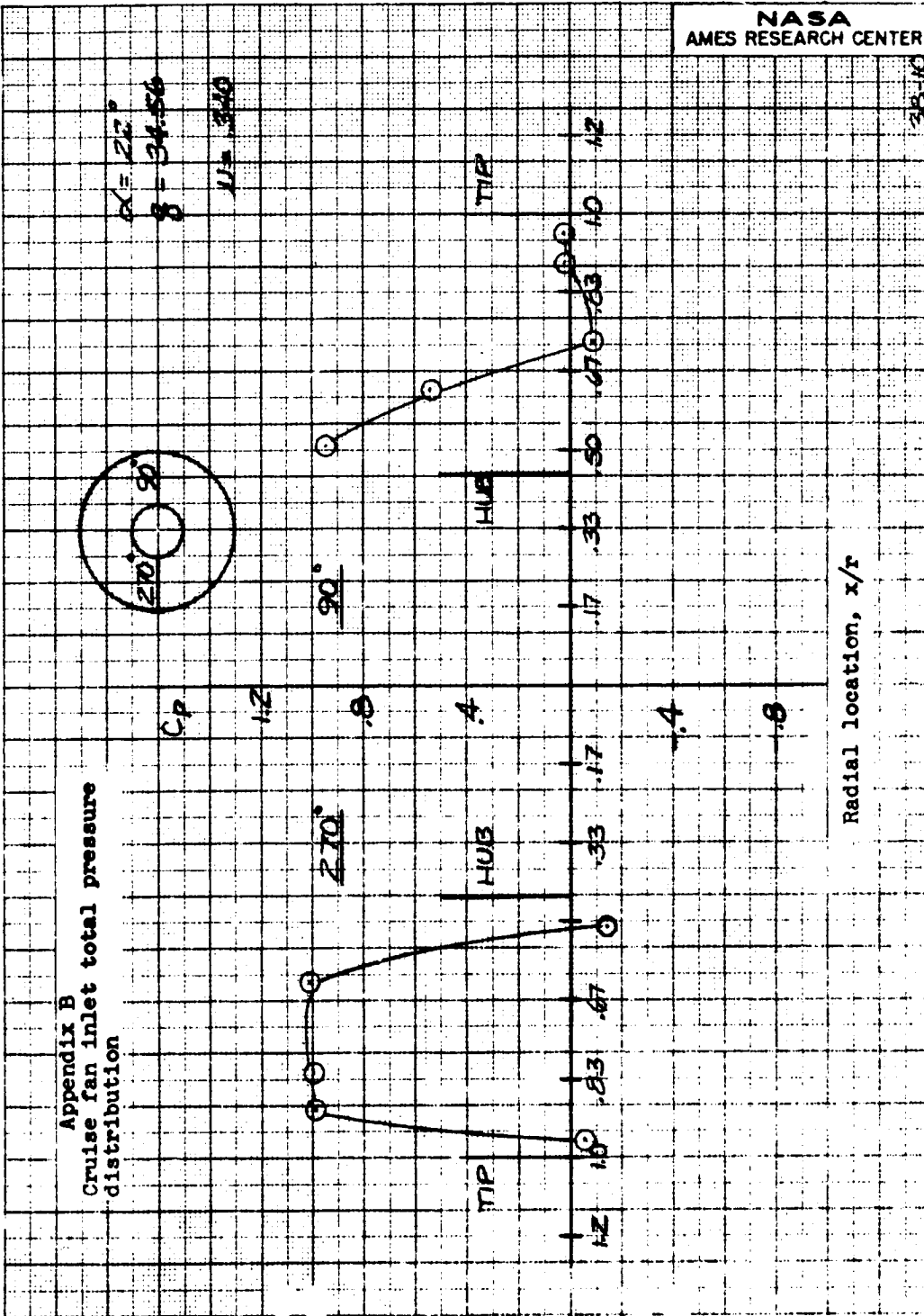
NASA  
AMES RESEARCH CENTER

38-7



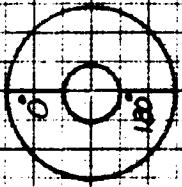






Appendix B  
Cruise fan inlet total pressure  
distribution

$\alpha = 22^\circ$   
 $\beta = 34.5^\circ$   
 $U = 340$



CP  
1/2  
.8

180°  
180°



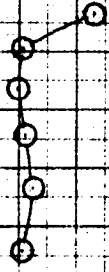
0°

TP

HUB

.4

1.2 1.0 .83 .67 .50 .33 .17



HUB

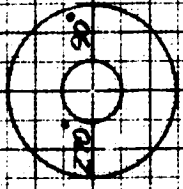
TP

.4

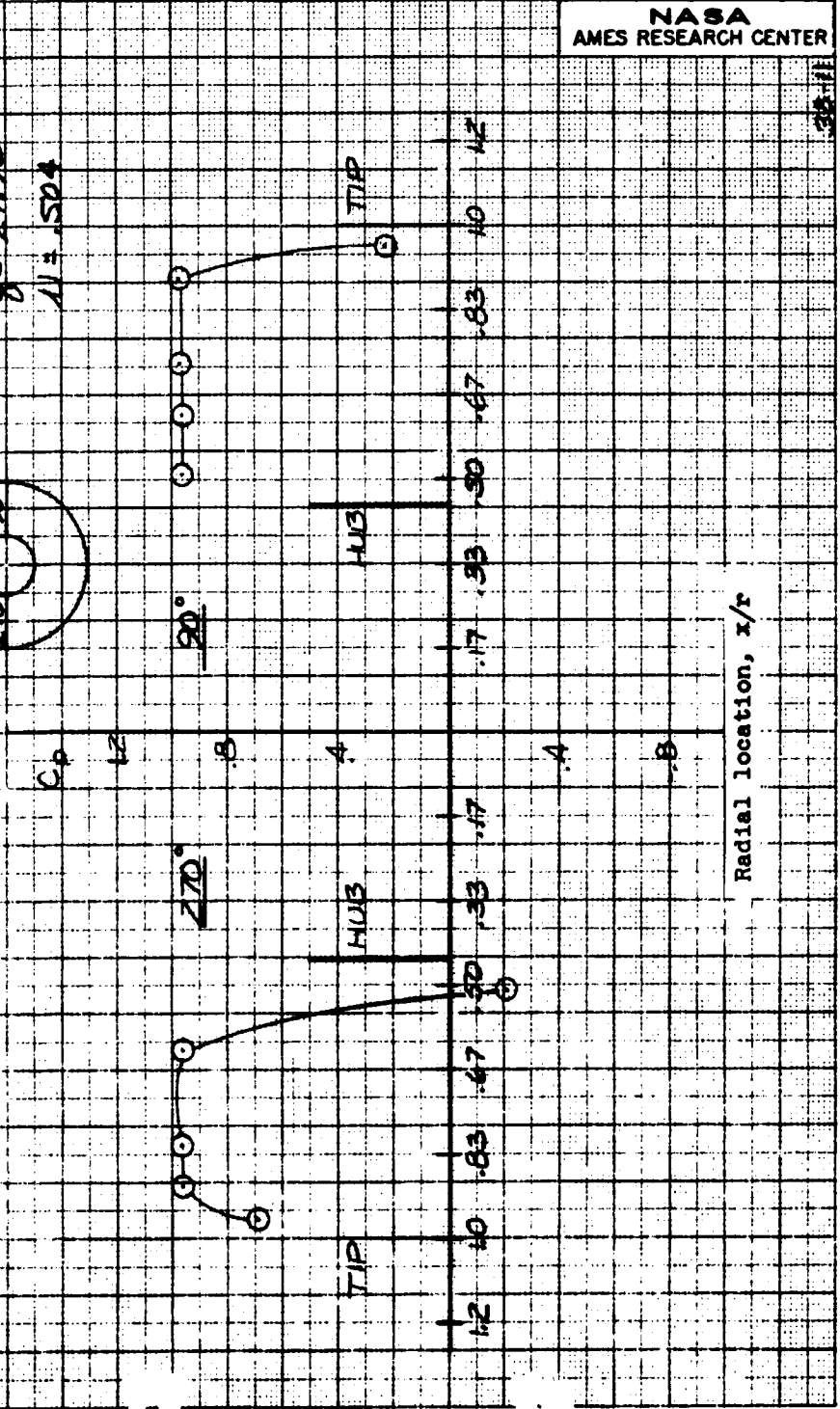
1.2 1.0 .83 .67 .50 .33 .17

Radial location, x/r

Appendix B  
Cruise fan inlet total pressure  
distribution



$\alpha = 0^\circ$   
 $g = 27.93$   
 $M = .504$



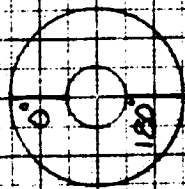
NASA  
AMES RESEARCH CENTER

38-11

Radial location, x/r



Appendix B  
Cruise fan inlet total pressure  
distribution



$\alpha = 0^\circ$   
 $\beta = 27.93$   
 $U = .504$

$C_p$

12

8

4

4

8

$0^\circ$

$180^\circ$

HUB

TIP

HUB

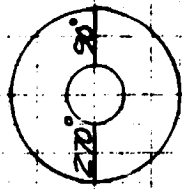
TIP

12 10 .83 .67 .50 .33 .17

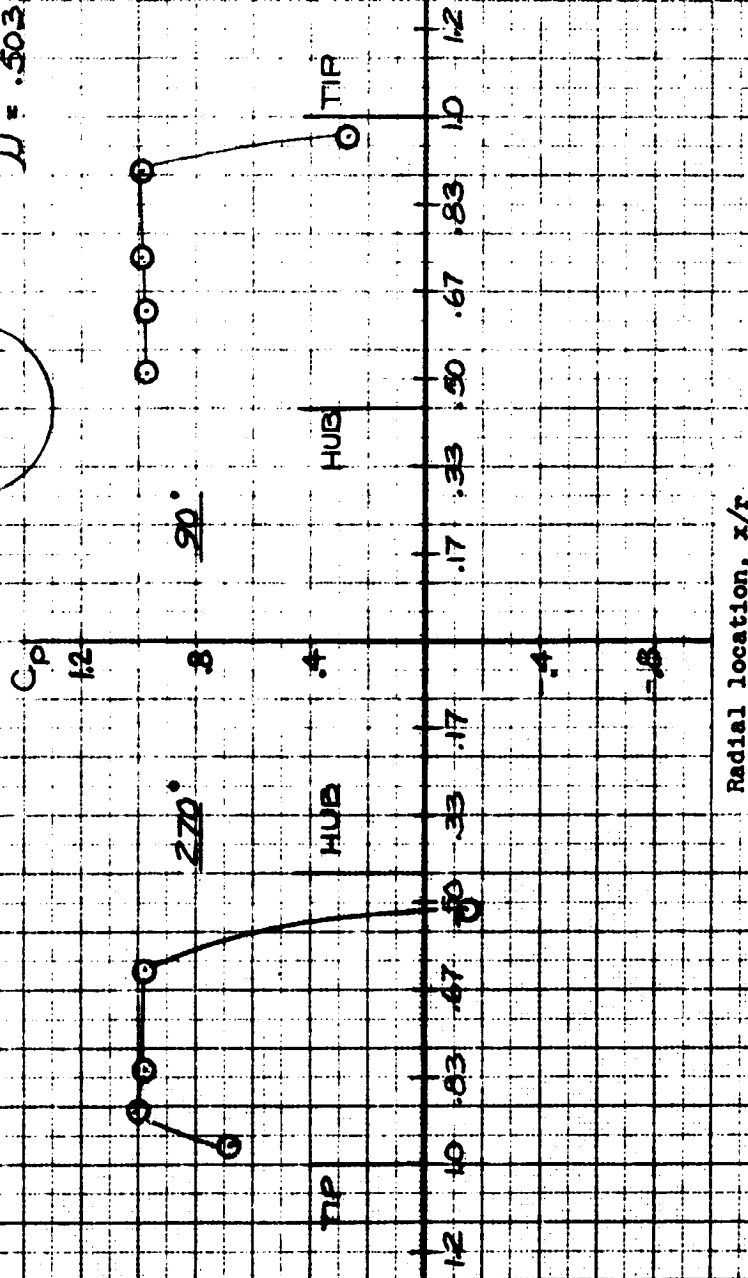
.17 .33 .50 .67 .83 1.0 1.2

Radial location, x/r

Appendix B  
Cruise fan inlet total pressure  
distribution

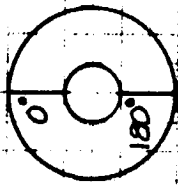


$\alpha = 4^\circ$   
 $\beta = 27.81$   
 $\mu = .503$

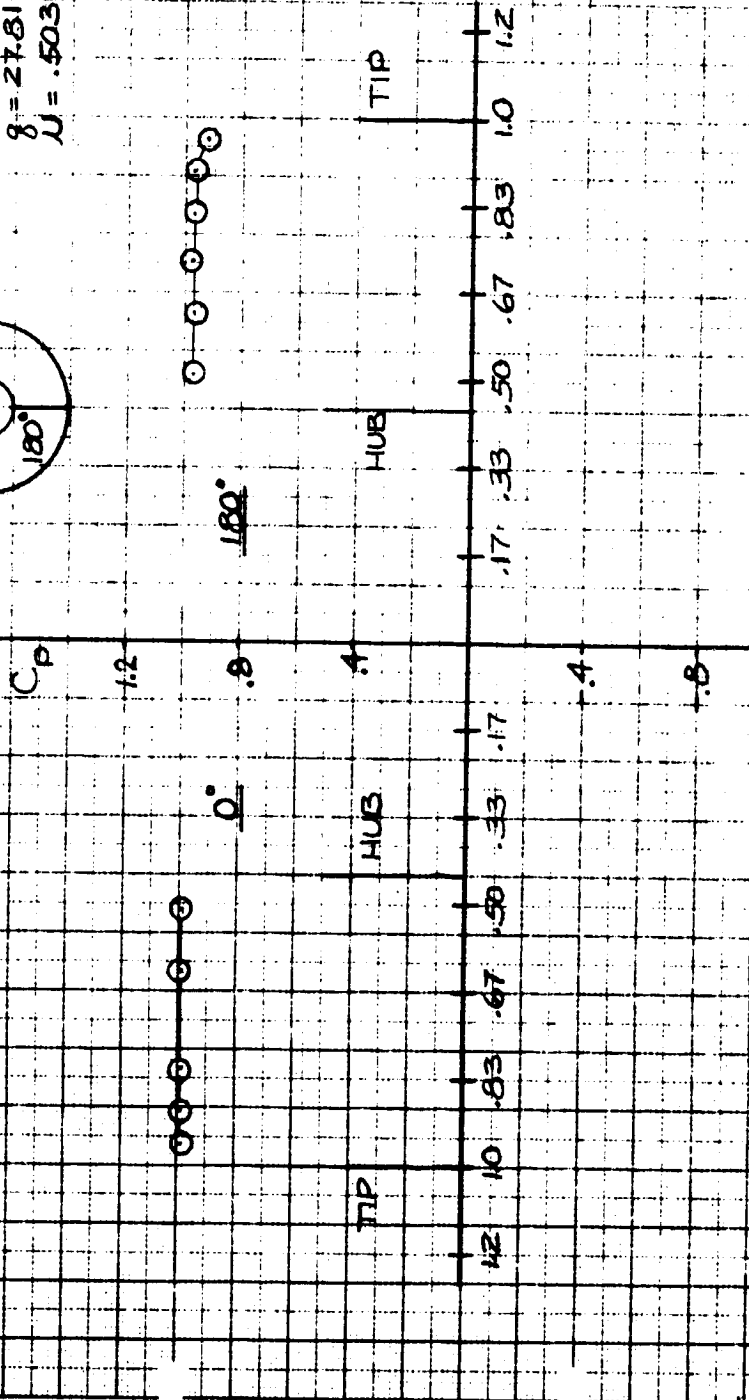


NASA  
AMES RESEARCH CENTER

Appendix B  
Cruise fan inlet total pressure  
distribution



$\alpha = 4^\circ$   
 $\beta = 27.81$   
 $U = .503$



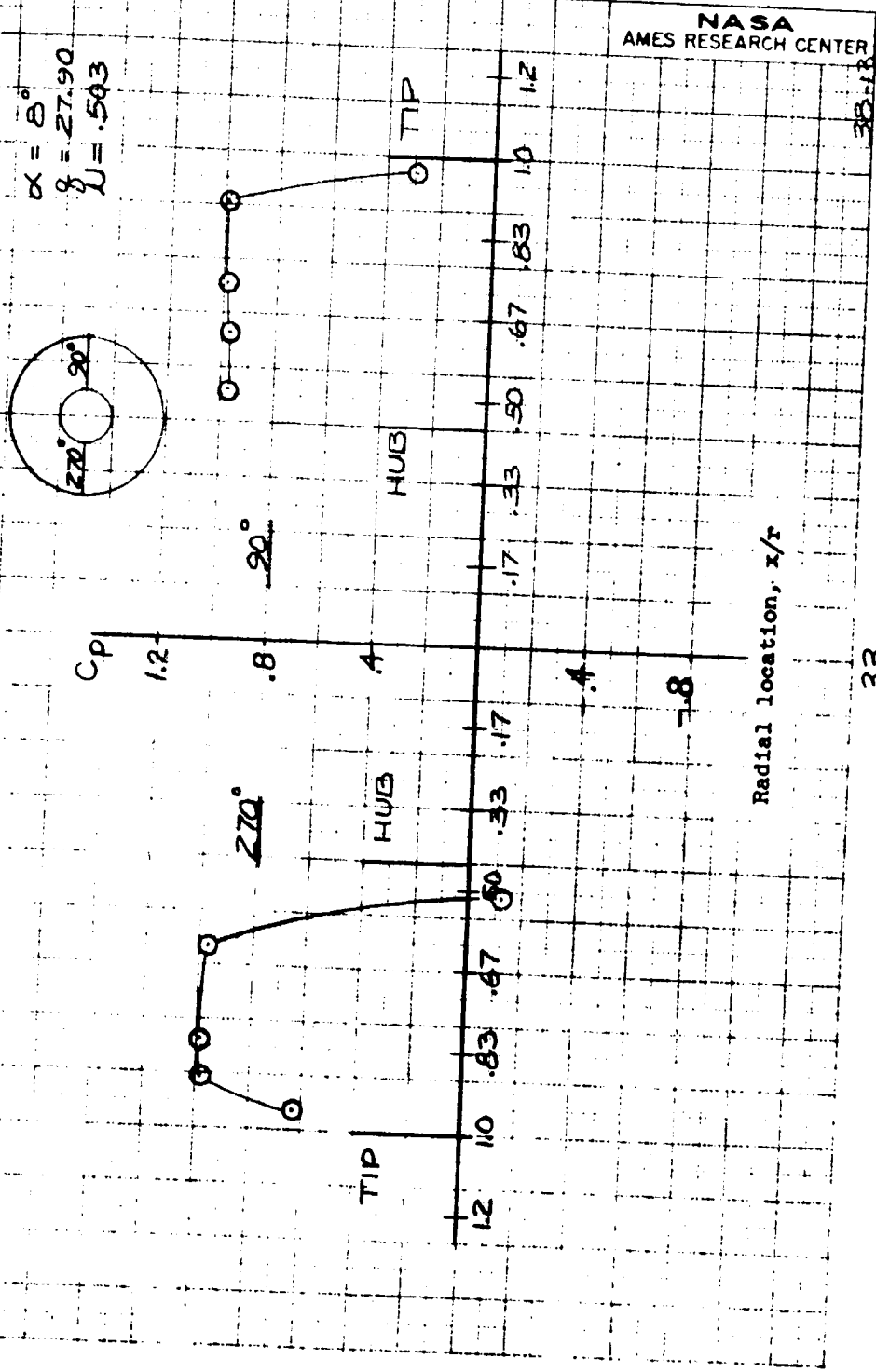
NASA  
AMES RESEARCH CENTER

Radial location,  $x/r$

38-12

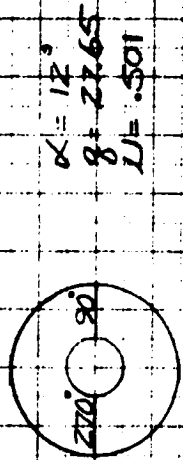
32

Appendix B  
Cruise fan inlet total pressure  
distribution

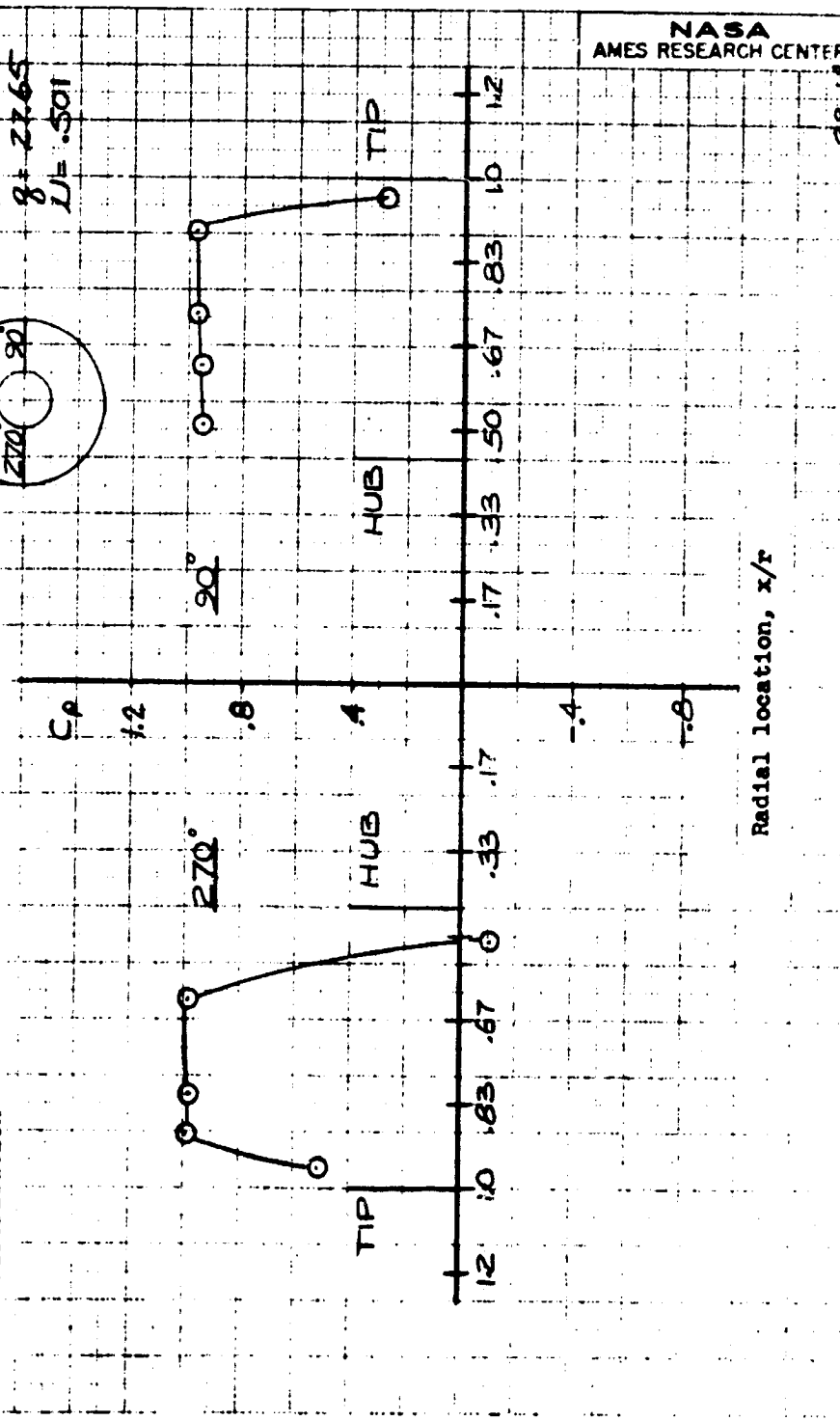




Appendix B  
Cruise fan inlet total pressure  
distribution

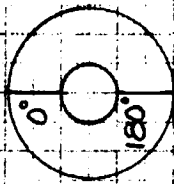


$\alpha = 12^\circ$   
 $\delta = 27.65$   
 $U = .501$

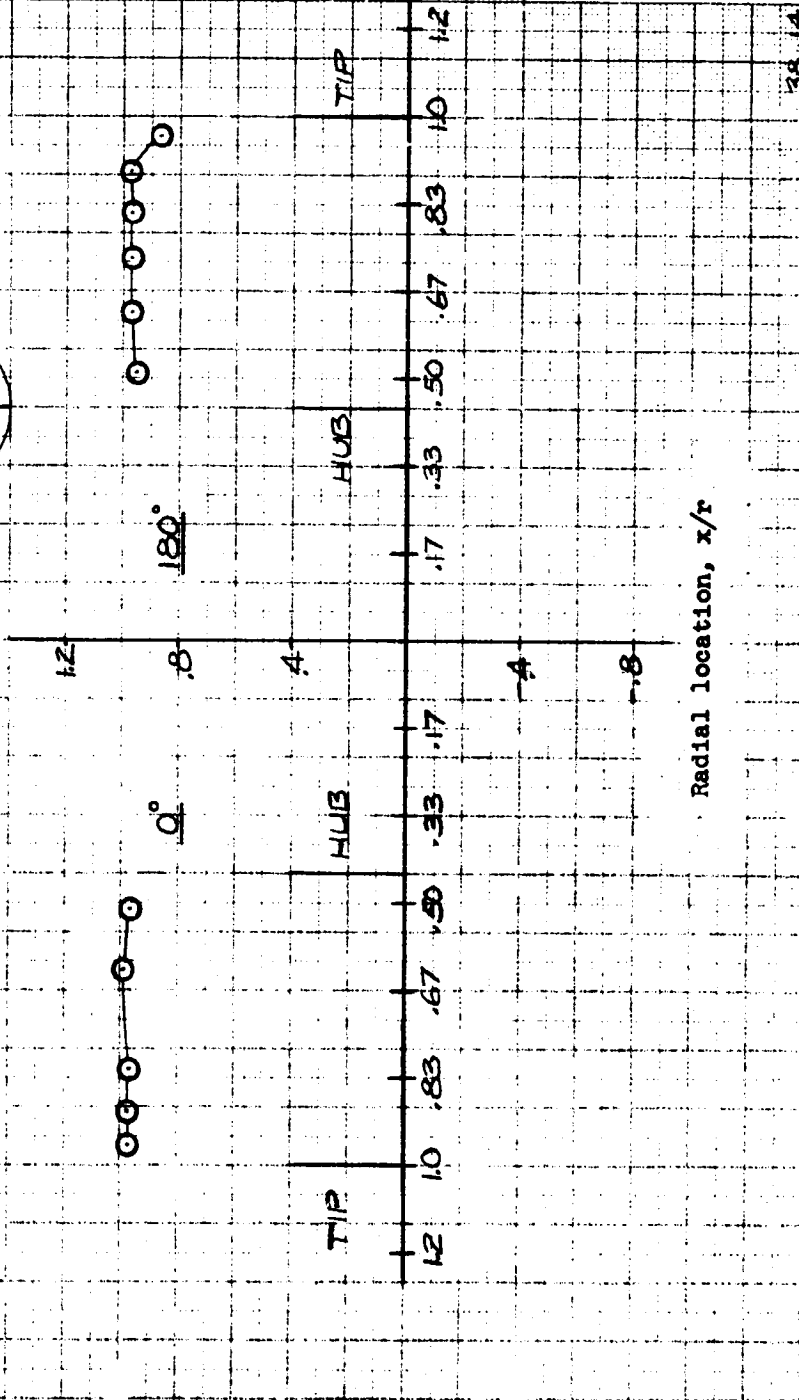


Radial location,  $x/r$

Appendix B  
Cruise fan inlet total pressure  
distribution



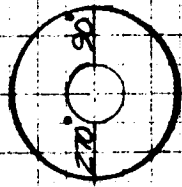
$\alpha = 12^\circ$   
 $\beta = 27.65$   
 $U = .501$



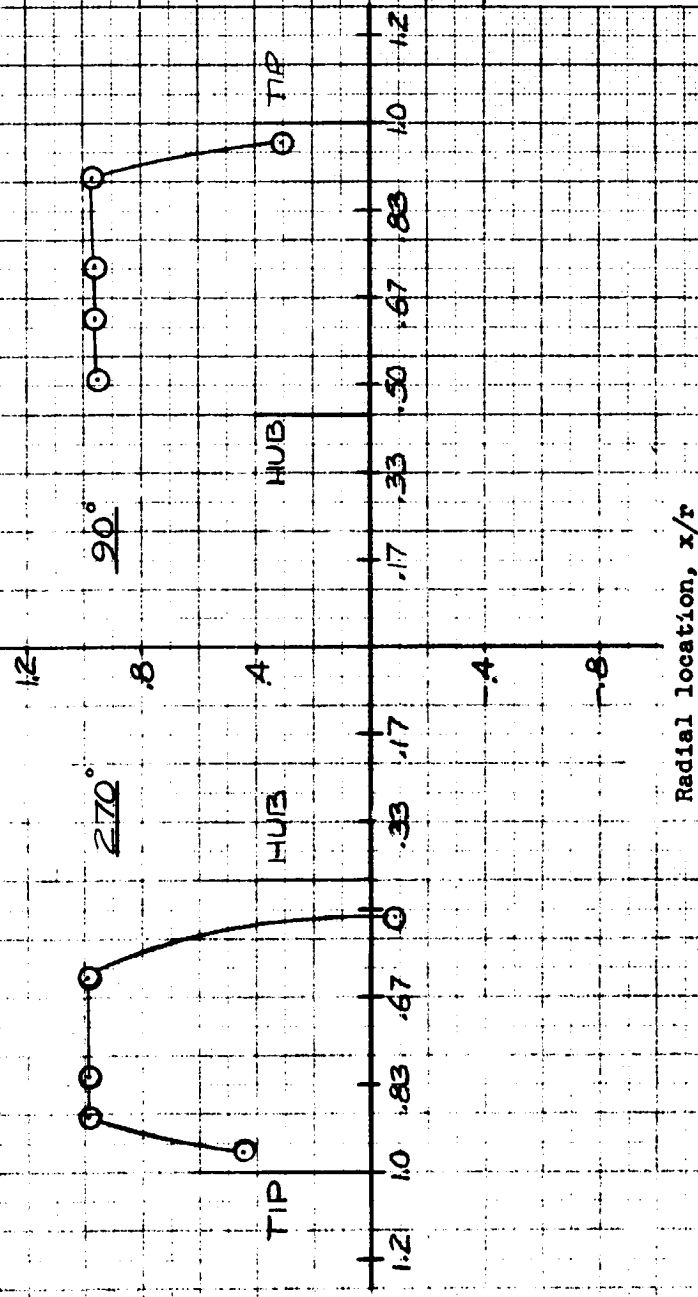
NASA  
AMES RESEARCH CENTER

38-14

Appendix B  
Cruise fan inlet total pressure  
distribution



$\alpha = 16^\circ$   
 $q = 27.80$   
 $U = .502$

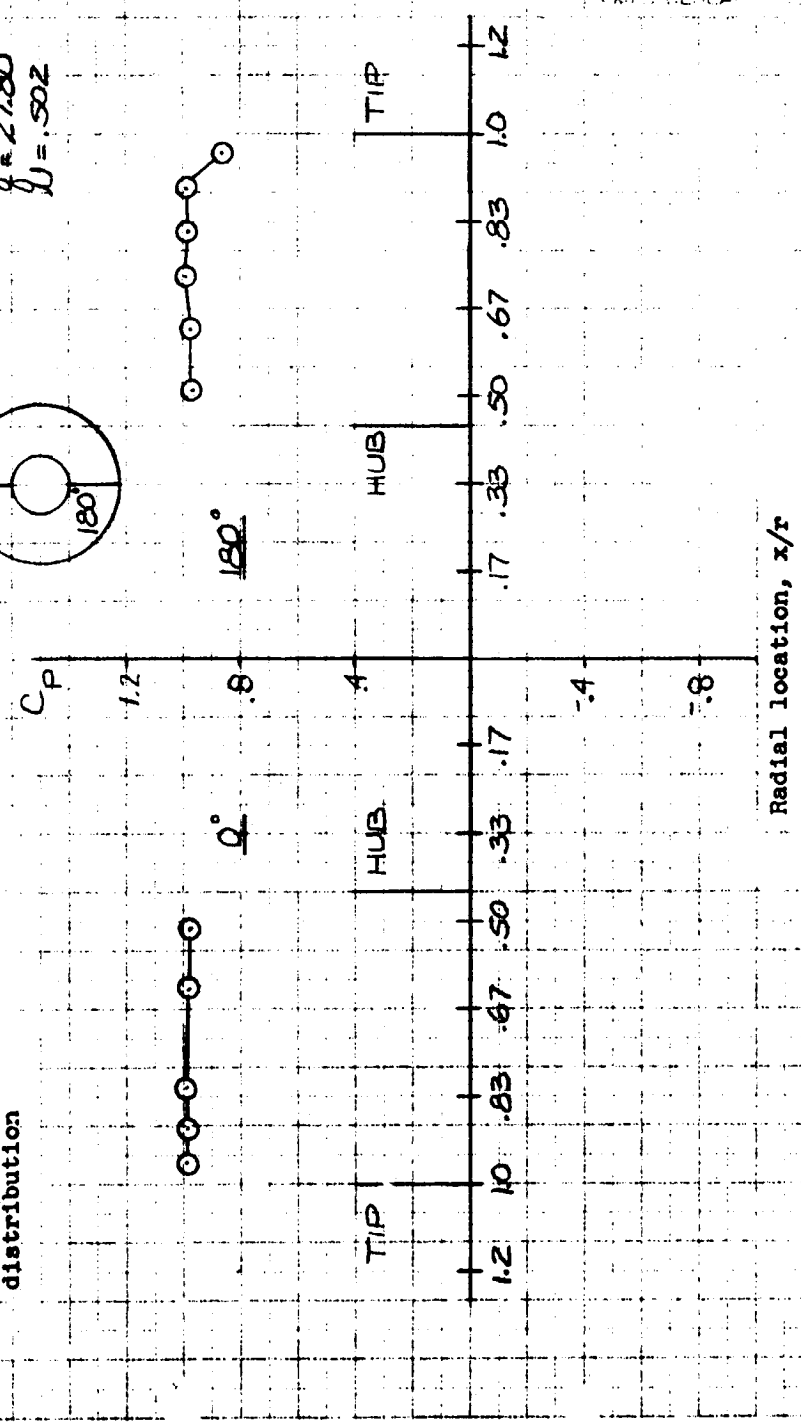
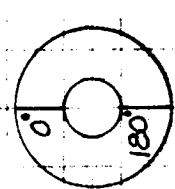


NASA  
AMES RESEARCH CENTER



Appendix B  
Cruise fan inlet total pressure  
distribution

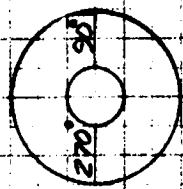
$\alpha = 16^\circ$   
 $Q = 27.80$   
 $U = 502$



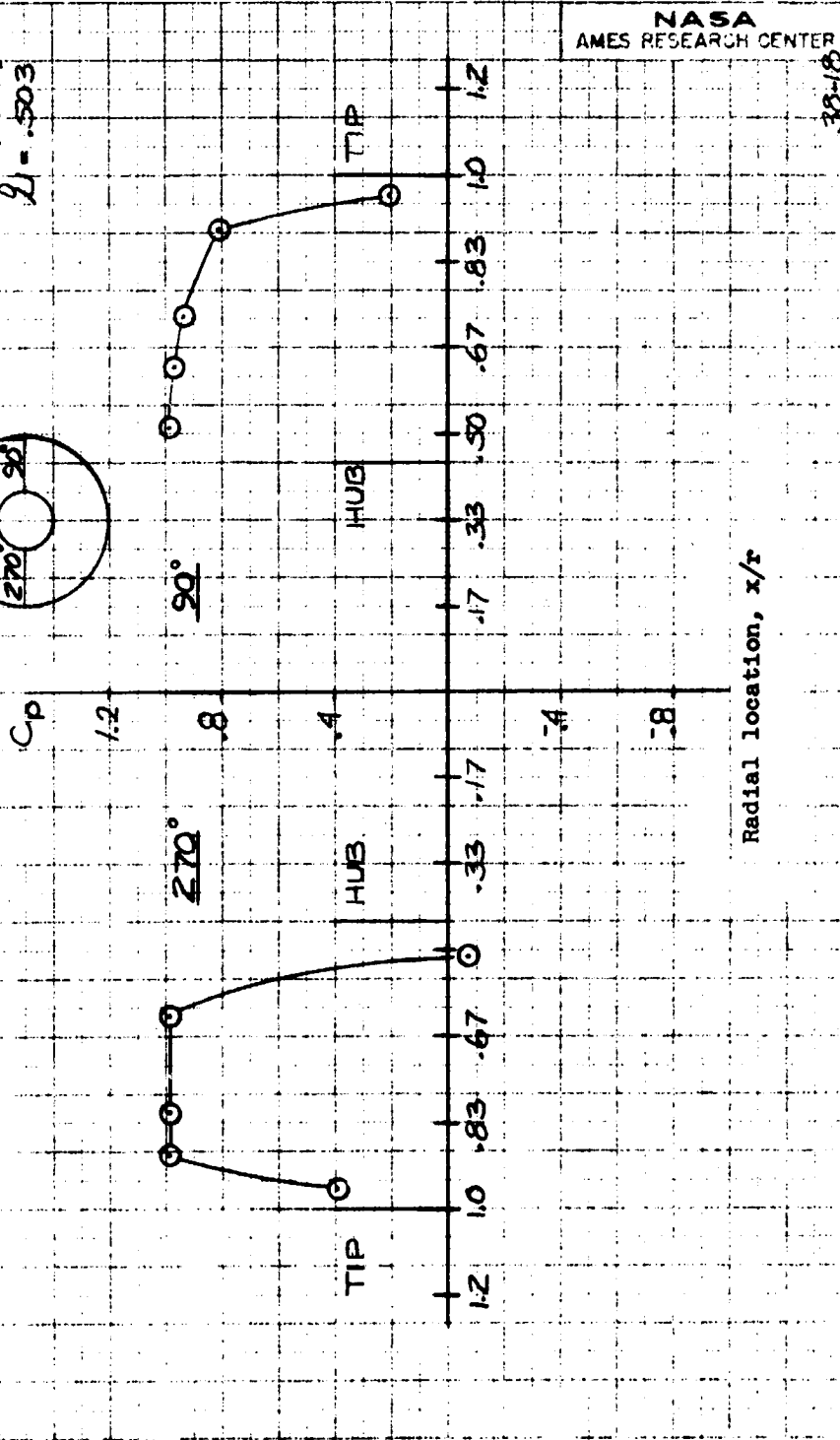
NAVY RESEARCH CENTER

38-16

Appendix B  
Cruise fan inlet total pressure  
distribution

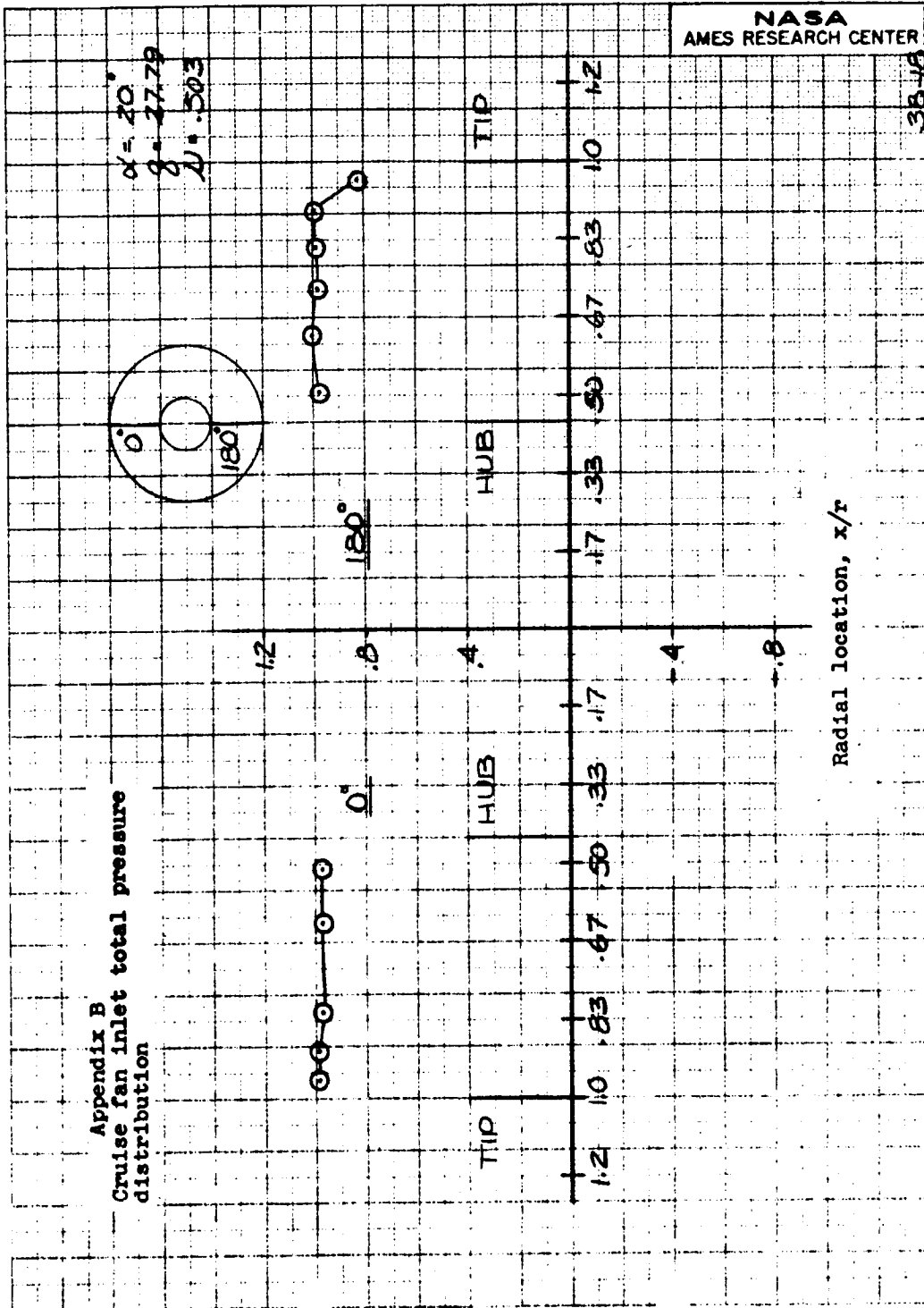


$\alpha = 20^\circ$   
 $\beta = 27.7^\circ$   
 $\lambda = .503$

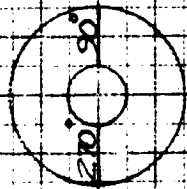


Radial location,  $x/r$

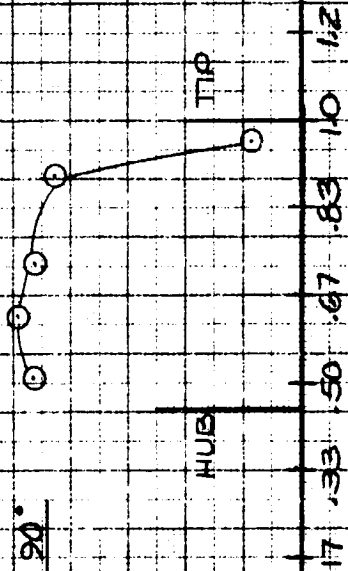
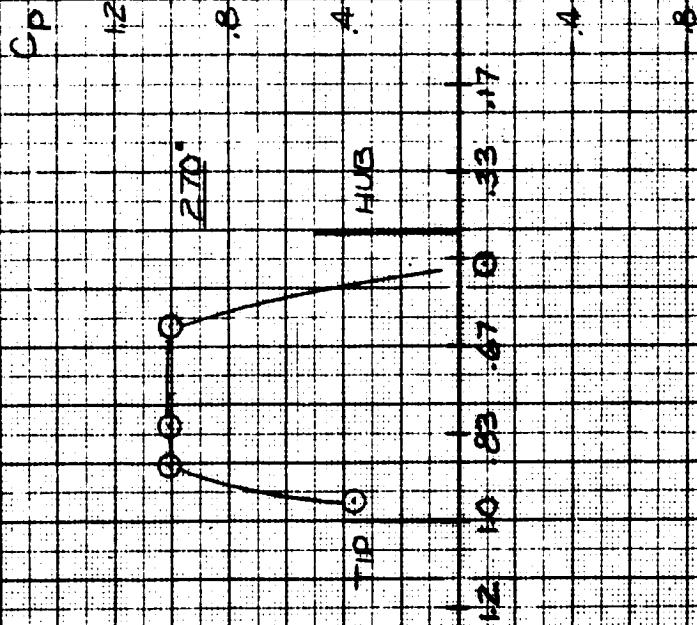
Appendix B  
Cruise fan inlet total pressure  
distribution



Appendix B  
Cruise fan inlet total pressure  
distribution



$\alpha = 22^\circ$   
 $\beta = 27.69$   
 $\Delta = .502$

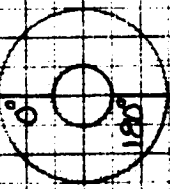


NASA  
AMES RESEARCH CENTER

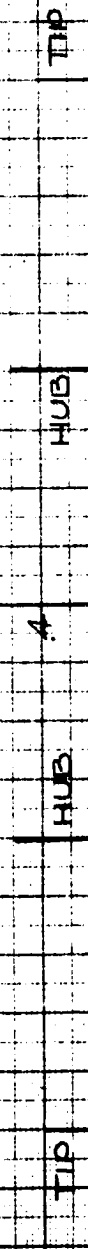
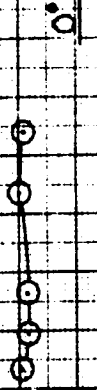
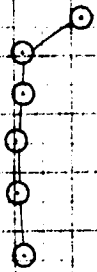
Radial location, x/r

30-FIP

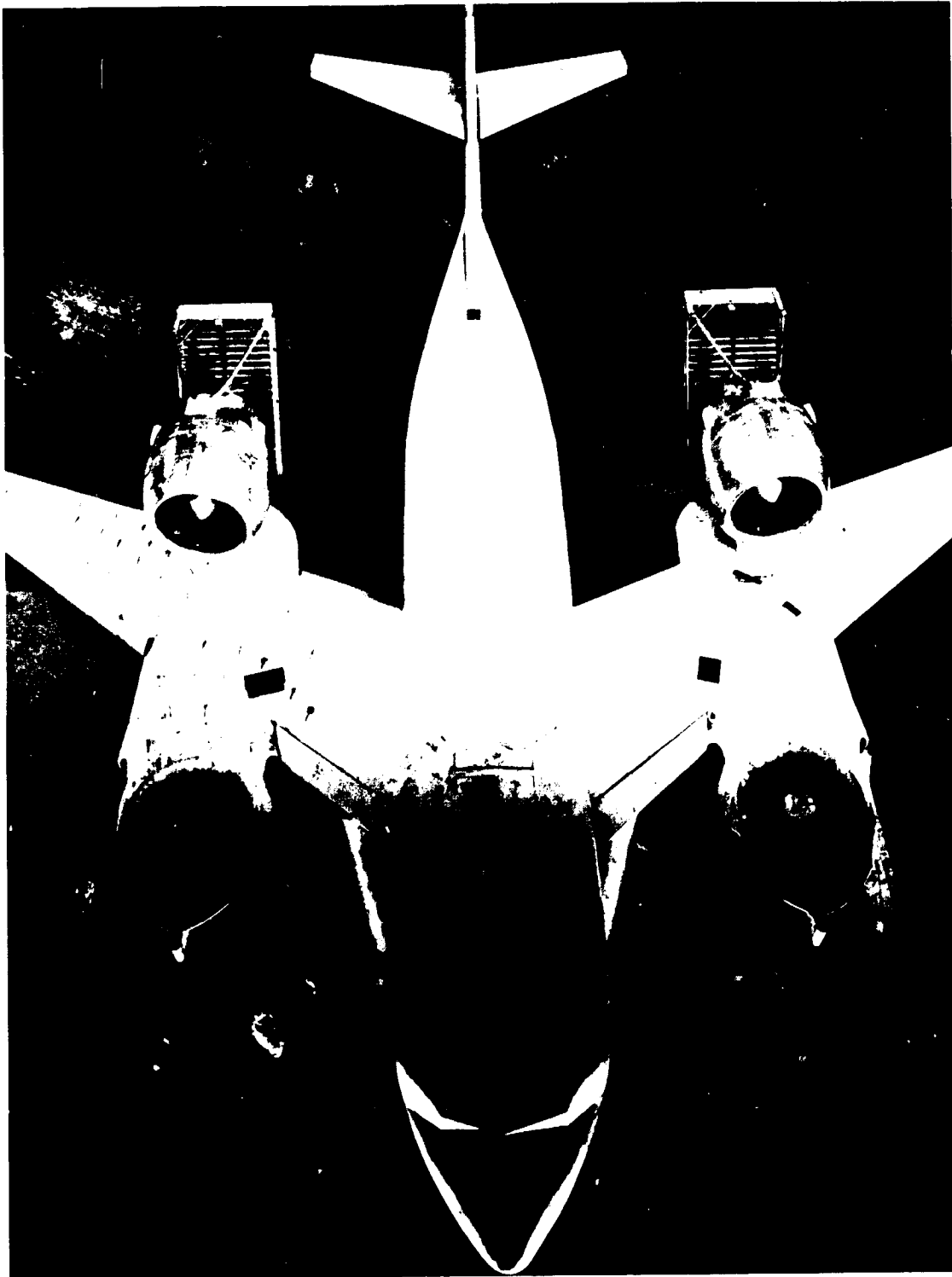
Appendix B  
Cruise fan inlet total pressure  
distribution



$\alpha = 22^\circ$   
 $\rho = 27.69$   
 $\mu = .502$

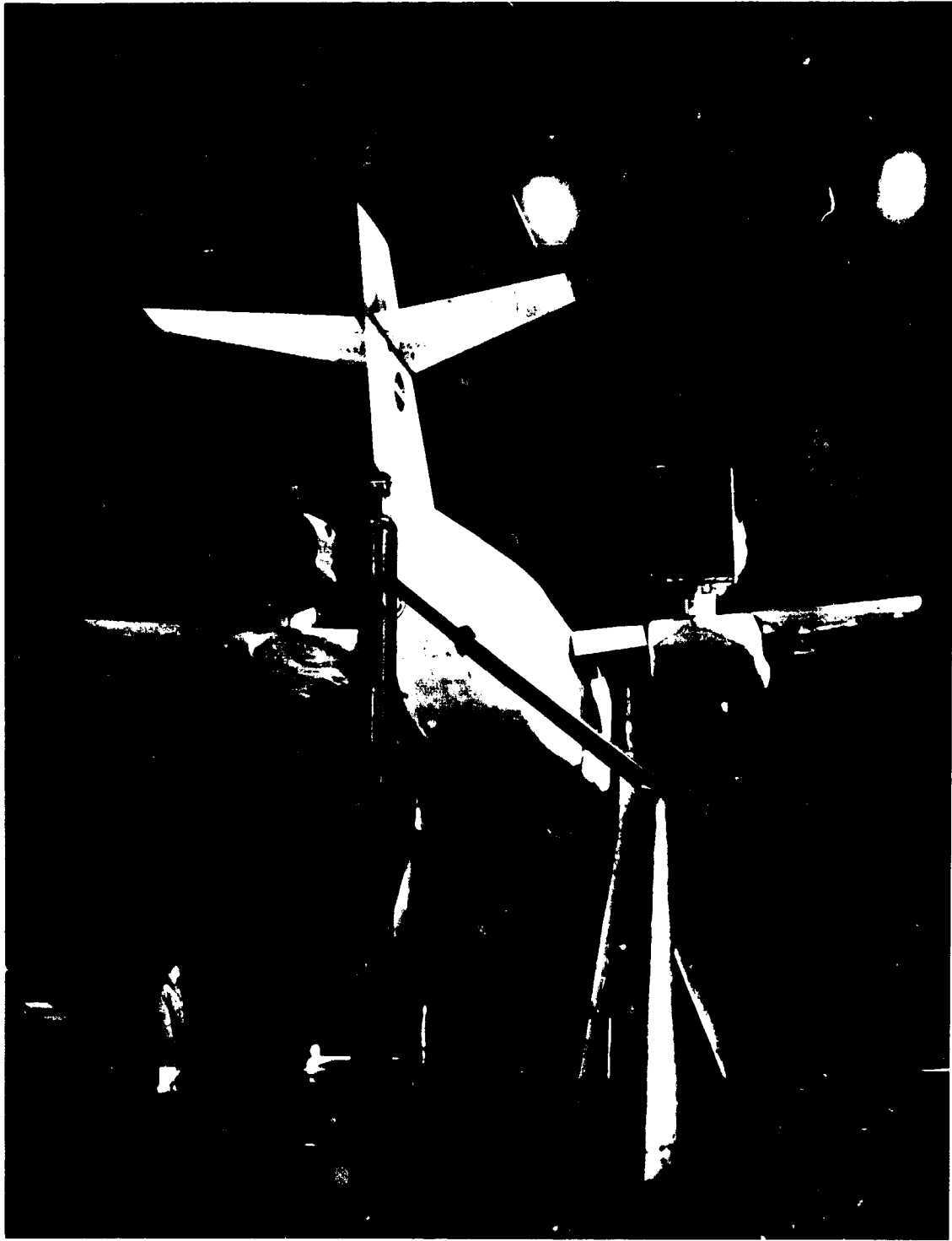


Radial location, x/r



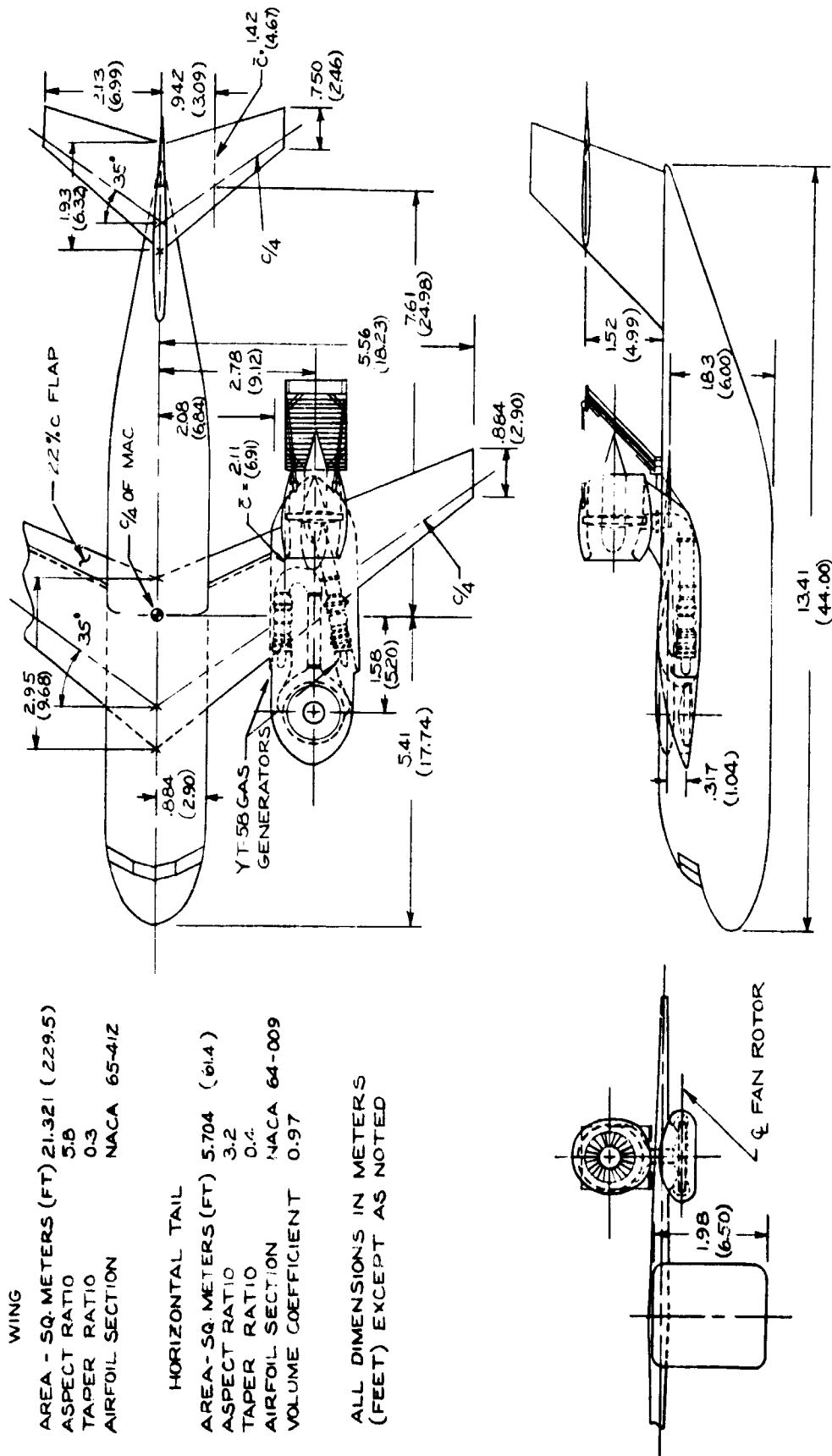
(a) Front view.

Figure 1.- Photographs of the model in the Ames 40- by 80-Foot Wind Tunnel.

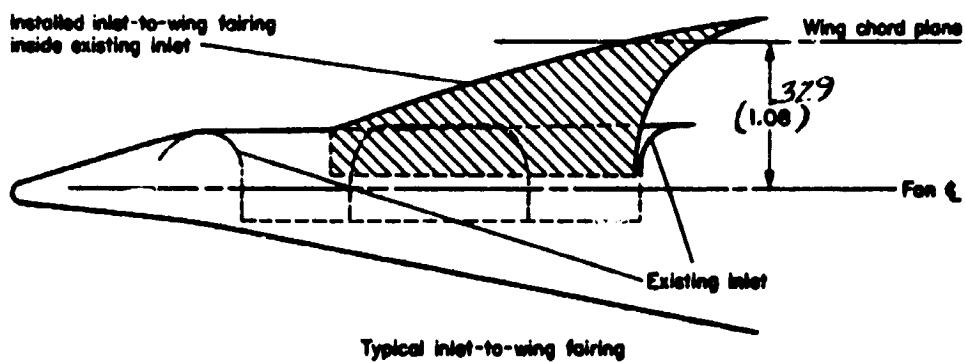
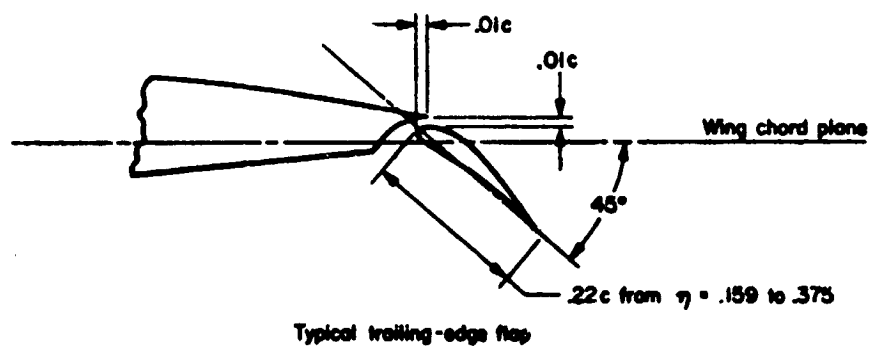
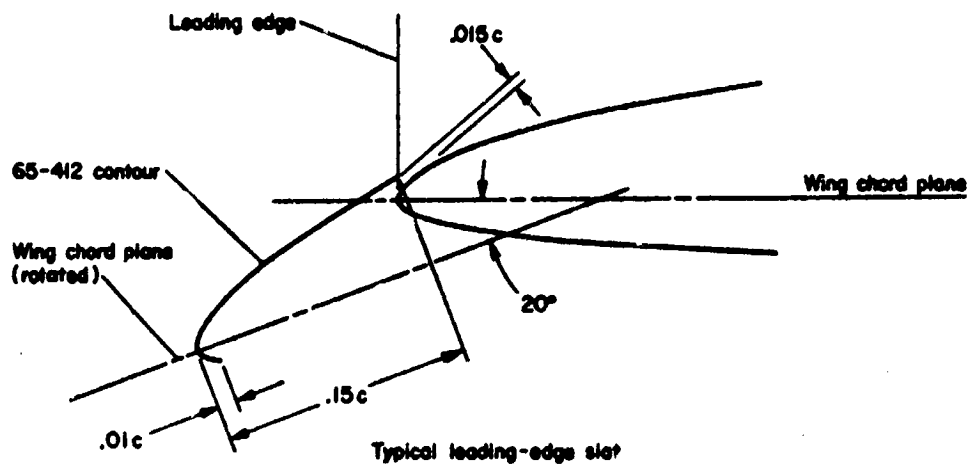


(b) Rear view.

Figure 1.- Concluded.

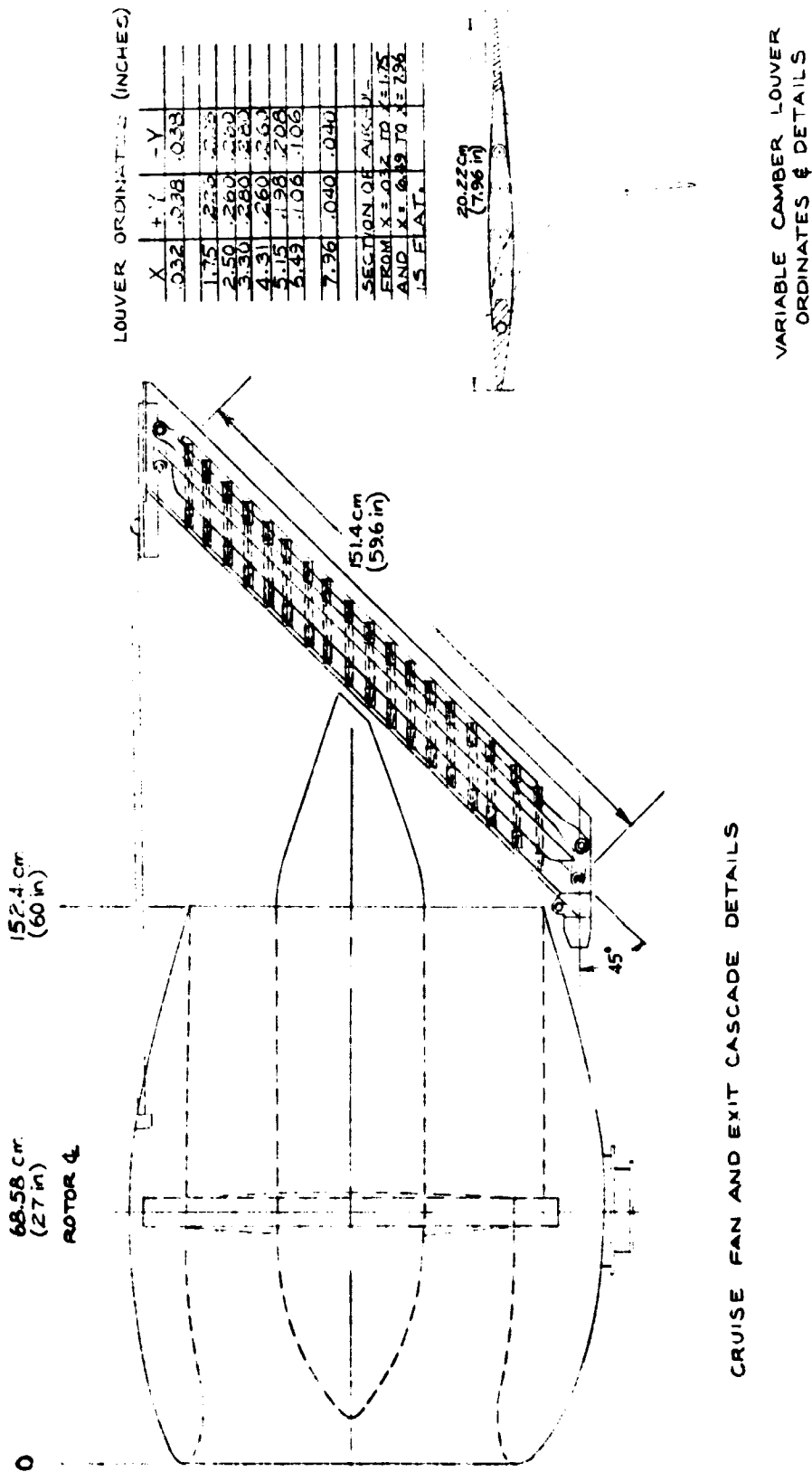






(b) Details of the leading edge slat, trailing edge flap, and forward fan inlet-to-wing fairing.

Figure 2.- Continued.

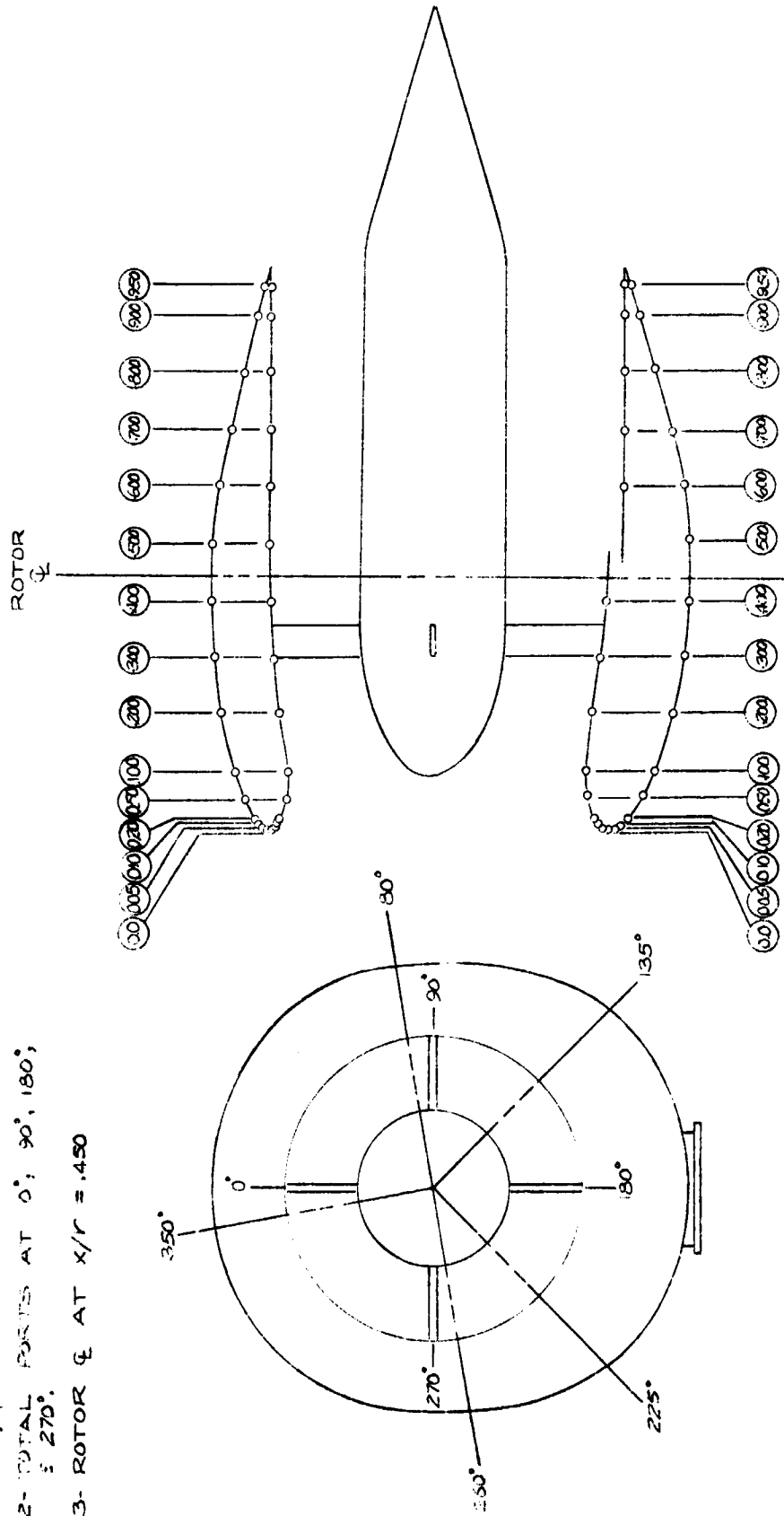


CRUISE FAN AND EXIT CASCADE DETAILS

(c) Aft cruise fan and exit louver geometry.

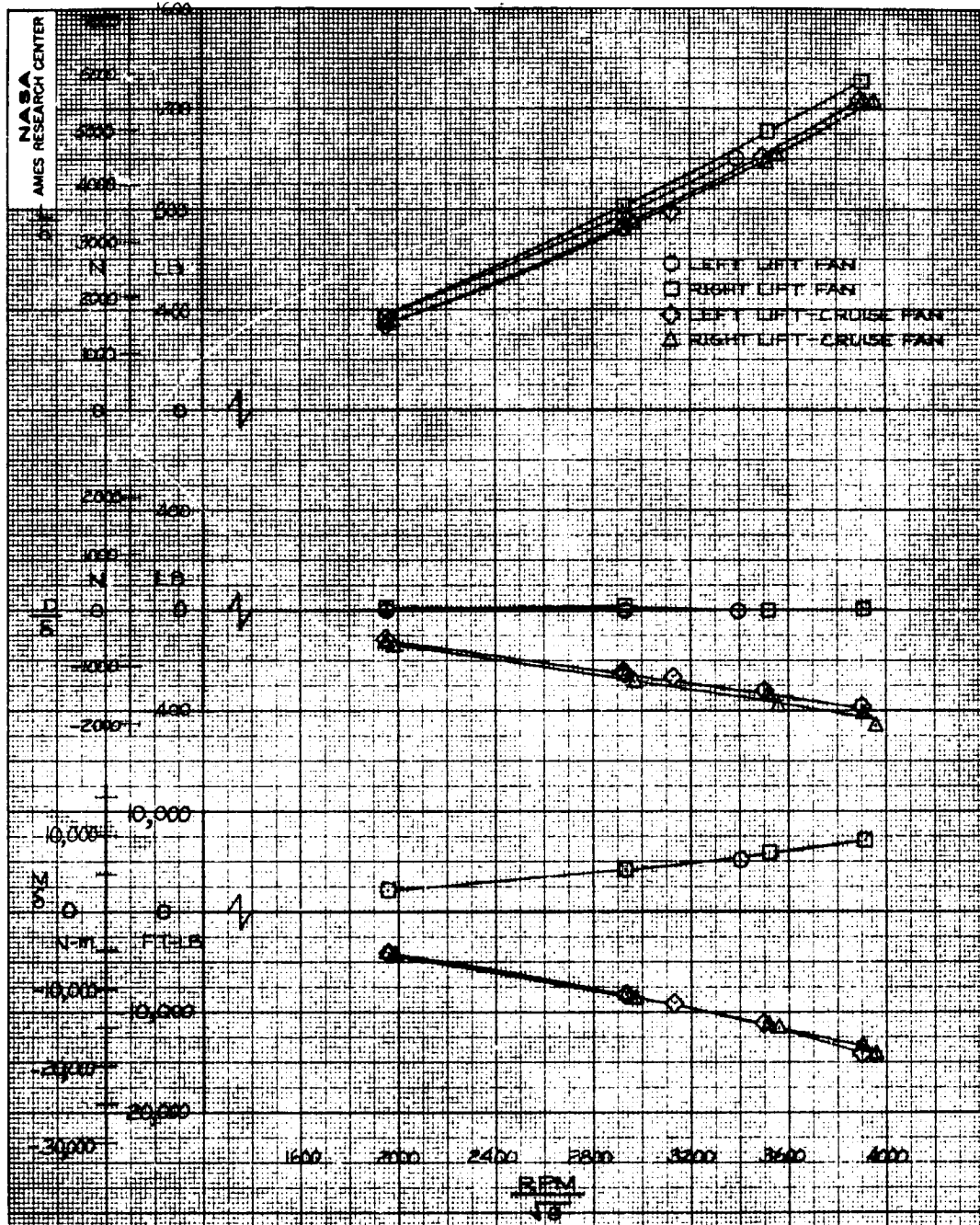
Figure 2.- Continued.

- 1- STATIC PORTS AT  $90^\circ, 135^\circ, 225^\circ, 270^\circ, \& 350^\circ$ .
- 2- TOTAL PORTS AT  $0^\circ, 90^\circ, 180^\circ, \& 270^\circ$ .
- 3- ROTOR  $\phi$  AT  $X/R = 1.450$



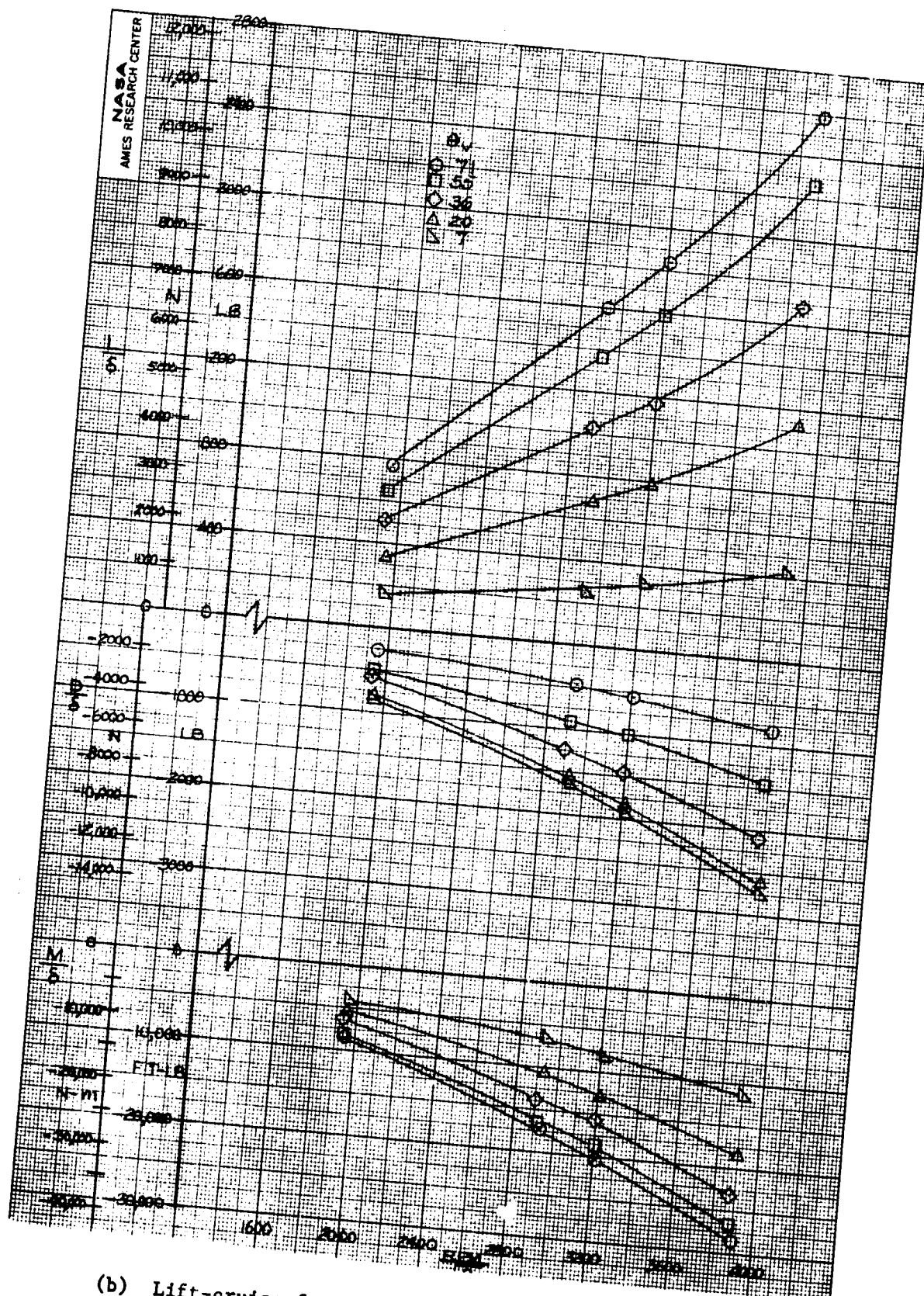
(d) Cruise nacelle pressure instrumentation.

Figure 2.- Concluded.



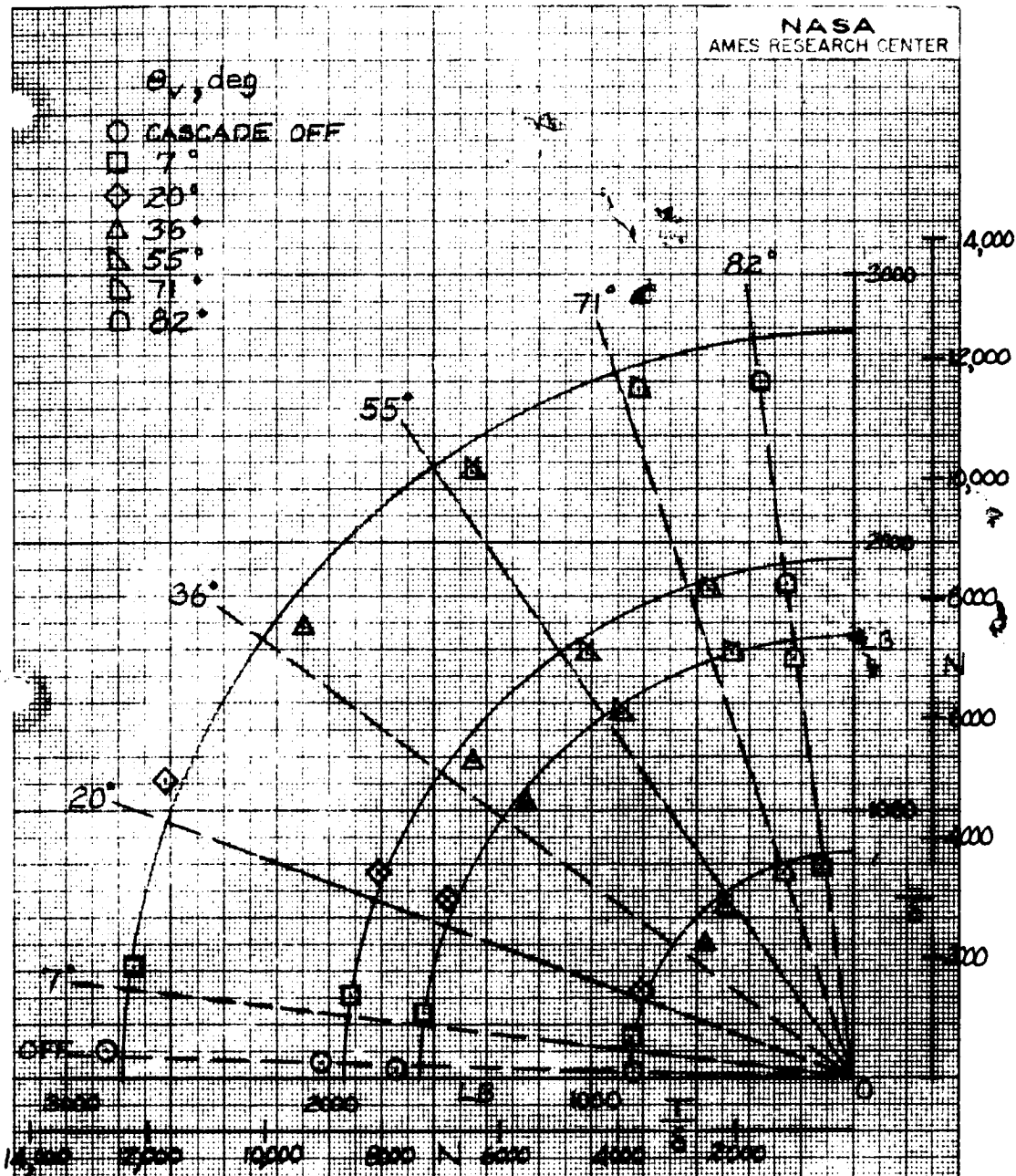
(a) Four fans,  $\beta_v = 0^\circ$ ,  $\theta_v = 71^\circ$ .

Figure 3.- Zero airspeed longitudinal characteristics;  
 $\delta_f = 45^\circ$ , tail on,  $i_t = 0^\circ$ ,  $\alpha = 0^\circ$ .



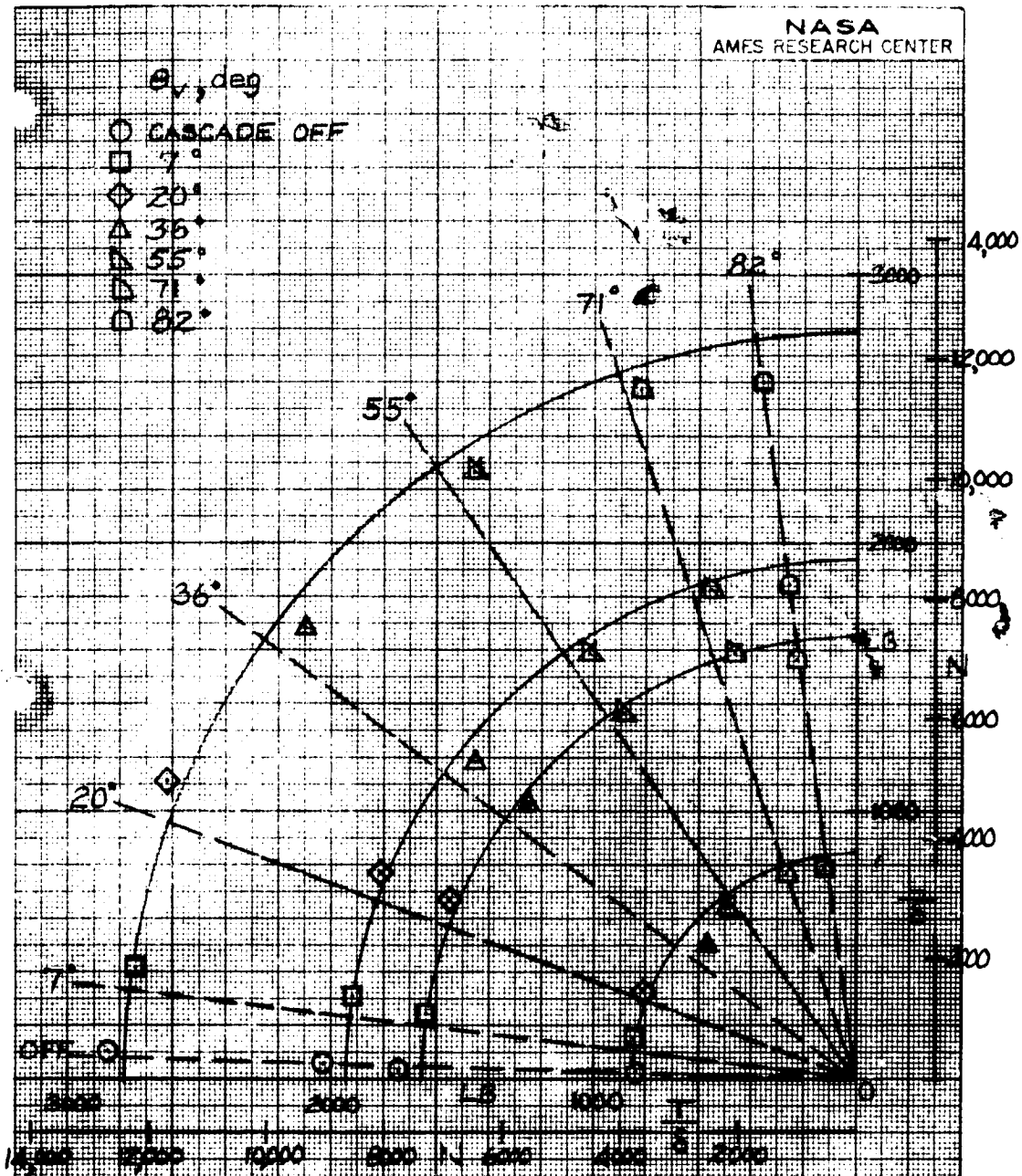
(b) Lift-cruise fans,  $\beta_v = 90^\circ$ , lift fan inlets sealed.

Figure 3.- Concluded.



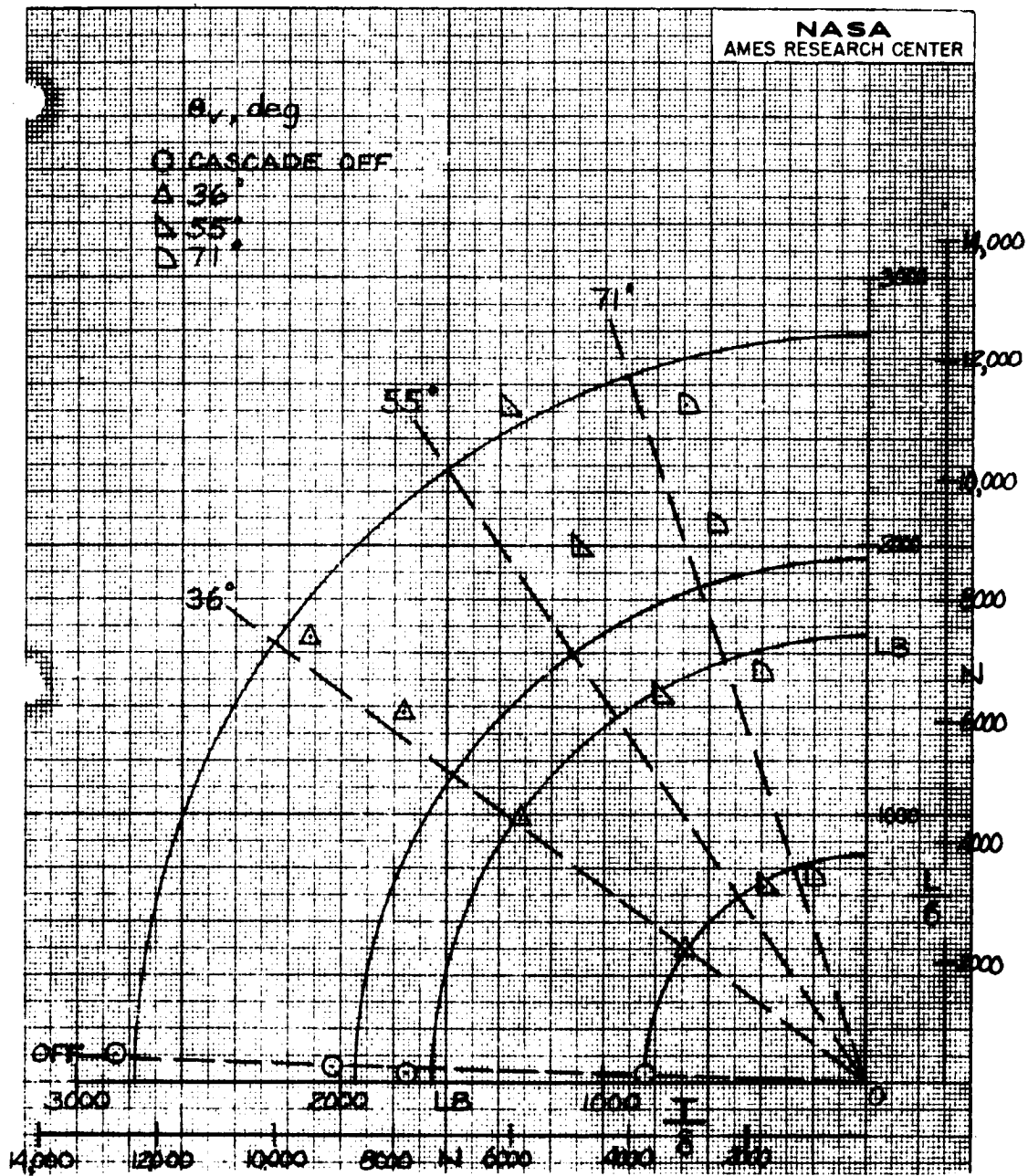
(a) Geometric angle between the fan thrust axis and the cascade carriage = 45°.

Figure 4.- Zero forward speed turning effectiveness of the variable camber exit louver cascade behind the lift-cruise fans.



(a) Geometric angle between the fan thrust axis and the cascade carriage = 45°.

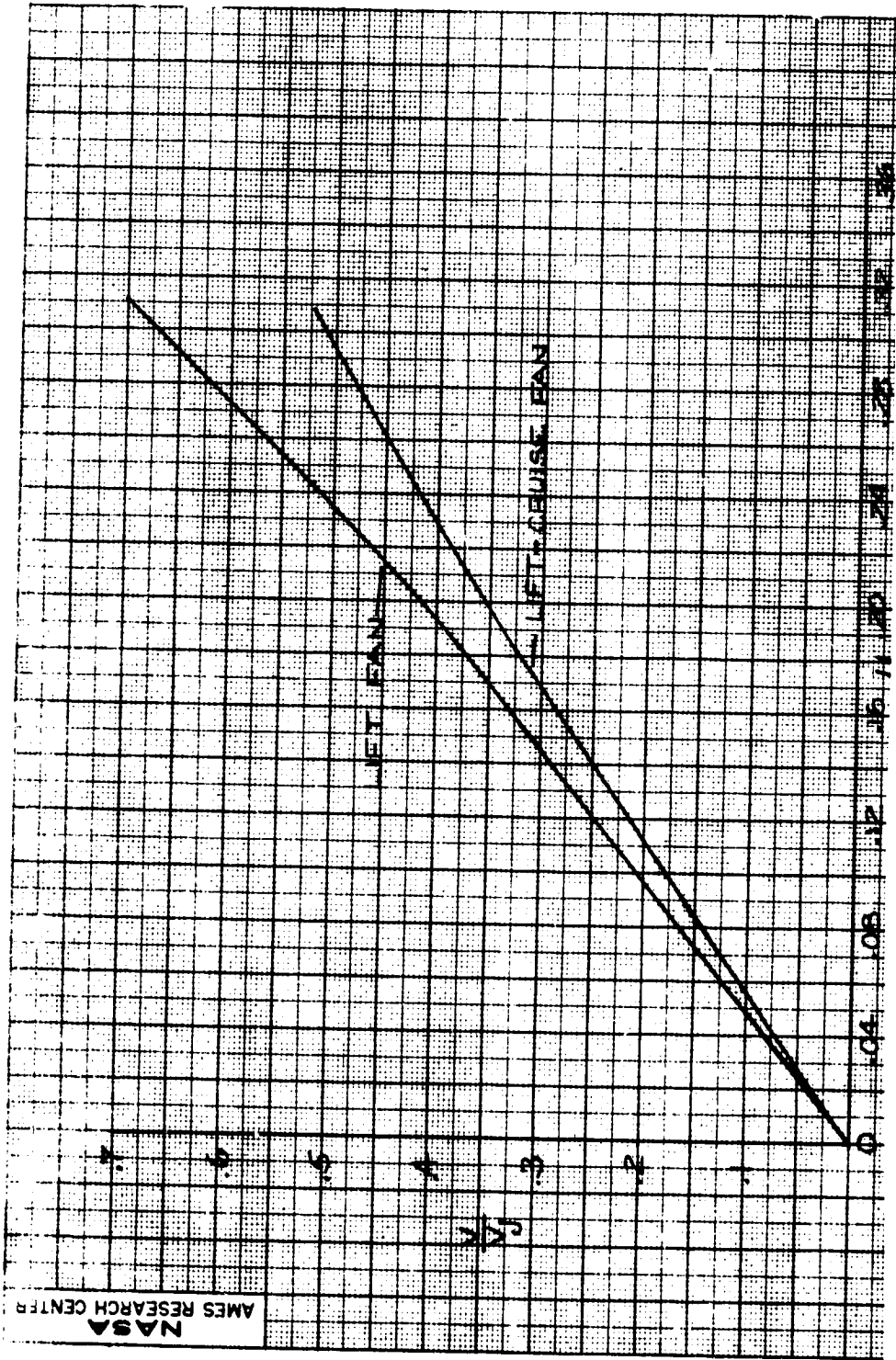
Figure 4.- Zero forward speed turning effectiveness of the variable camber exit louver cascade behind the lift-cruise fans.



(b) Geometric angle between the fan thrust axis and the cascade carriage = 65°.

Figure 4.- Concluded.





NASA  
AMES RESEARCH CENTER

Figure 5.- The relationship between tip-speed ratio and velocity ratio;  $\alpha = 0^\circ$ ,  $\beta_y = 0^\circ$ .

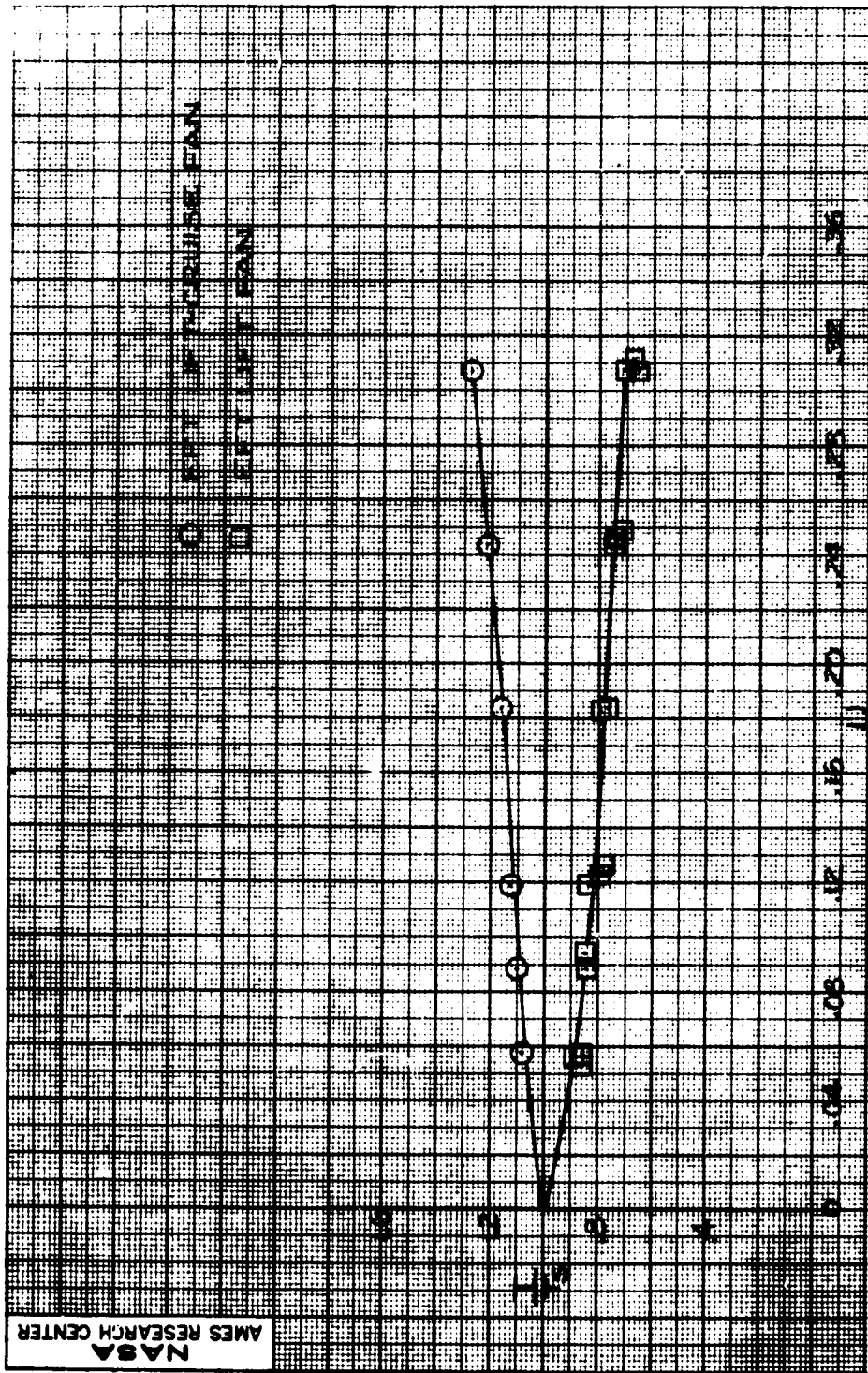
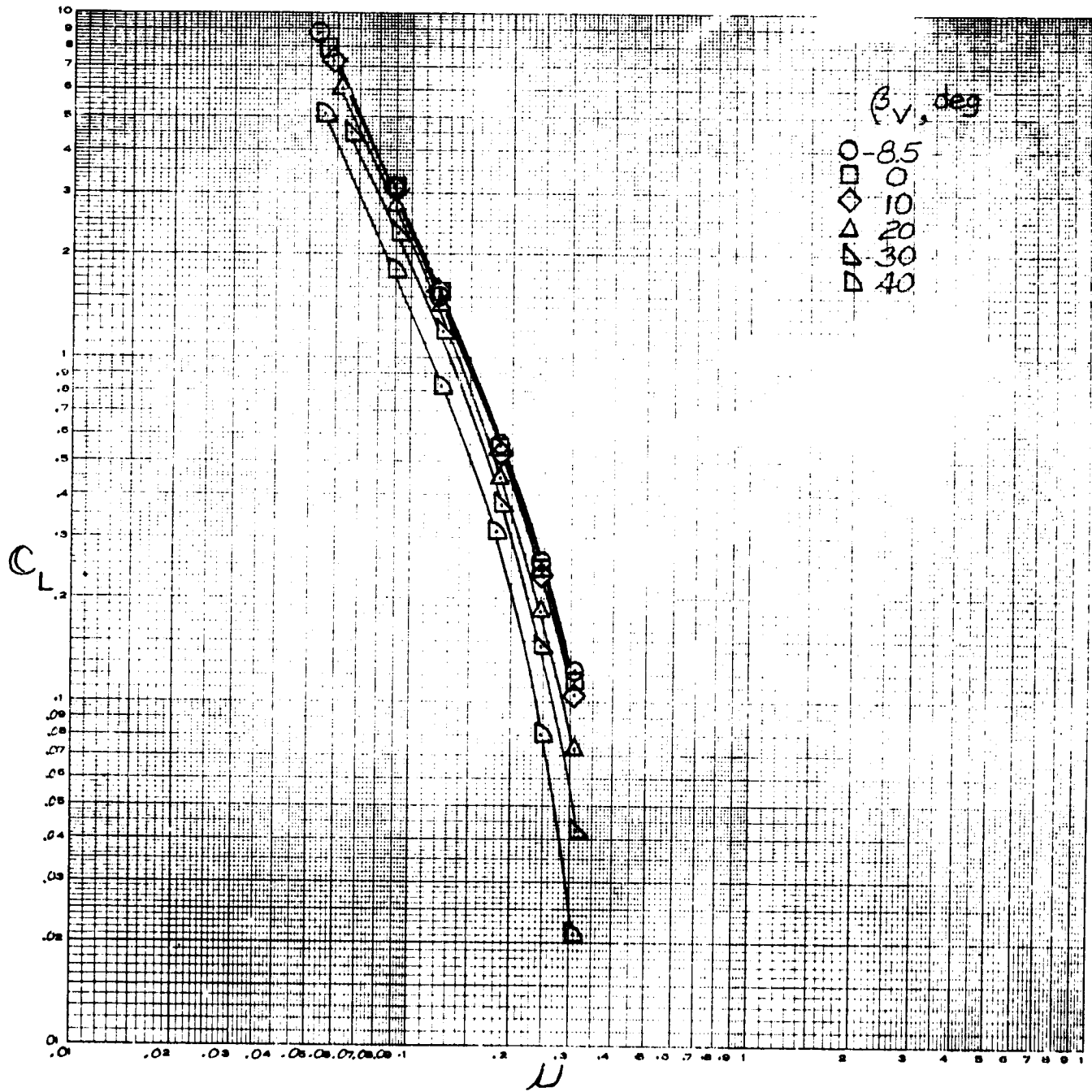
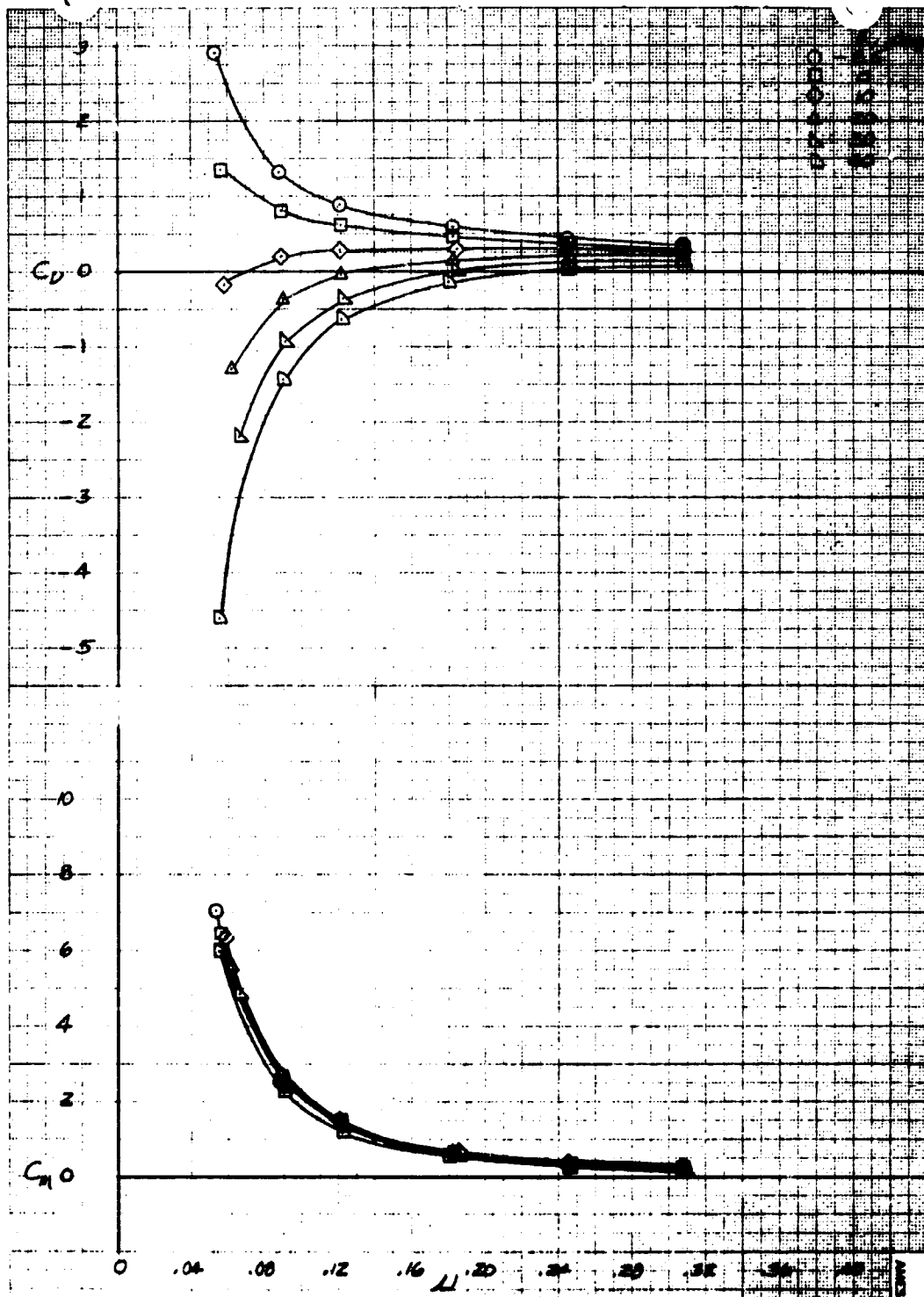


Figure 6.- The variation in fan thrust with tip-speed ratio;  $\alpha = 0^\circ$ .



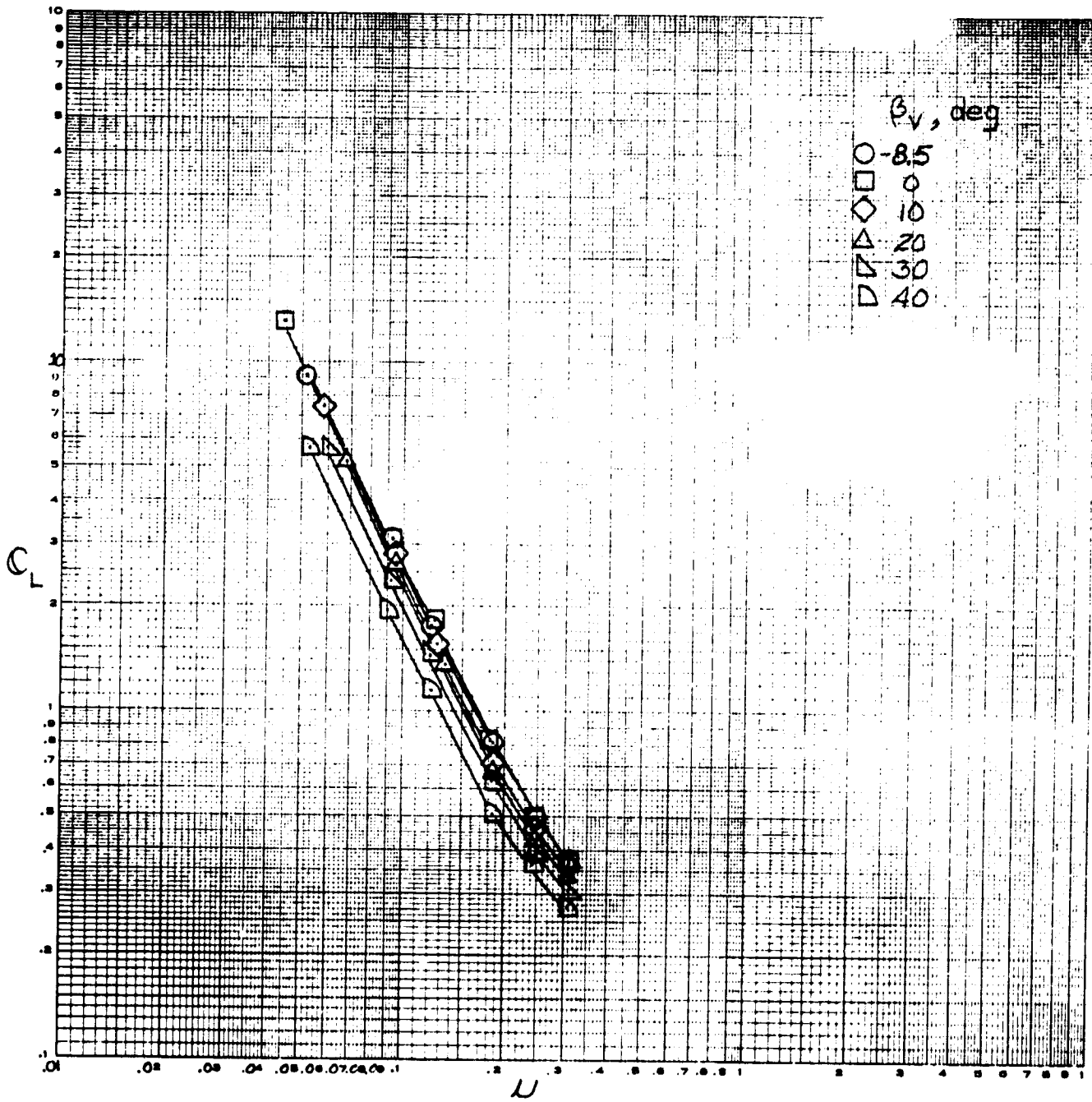
(a)  $C_L$  vs  $\mu$ ,  $\delta_f = 0^\circ$ .

Figure 7.- The effect of tip-speed ratio on longitudinal characteristics; lift fans only, tail on,  $i_t = 0^\circ$ .



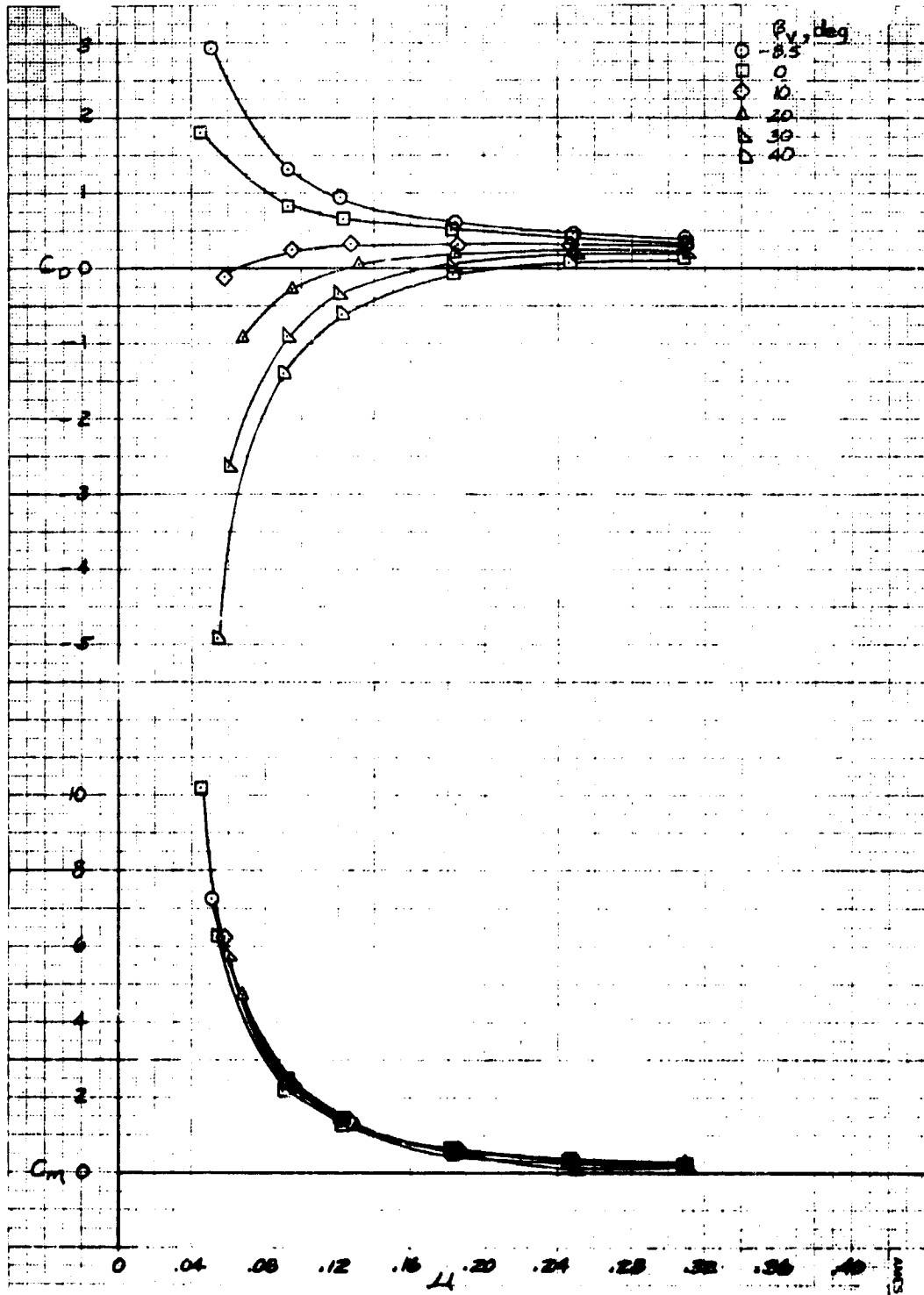
(b)  $C_D, C_m$  vs  $\mu, \delta_f = 0^\circ$ .

Figure 7.- Continued.



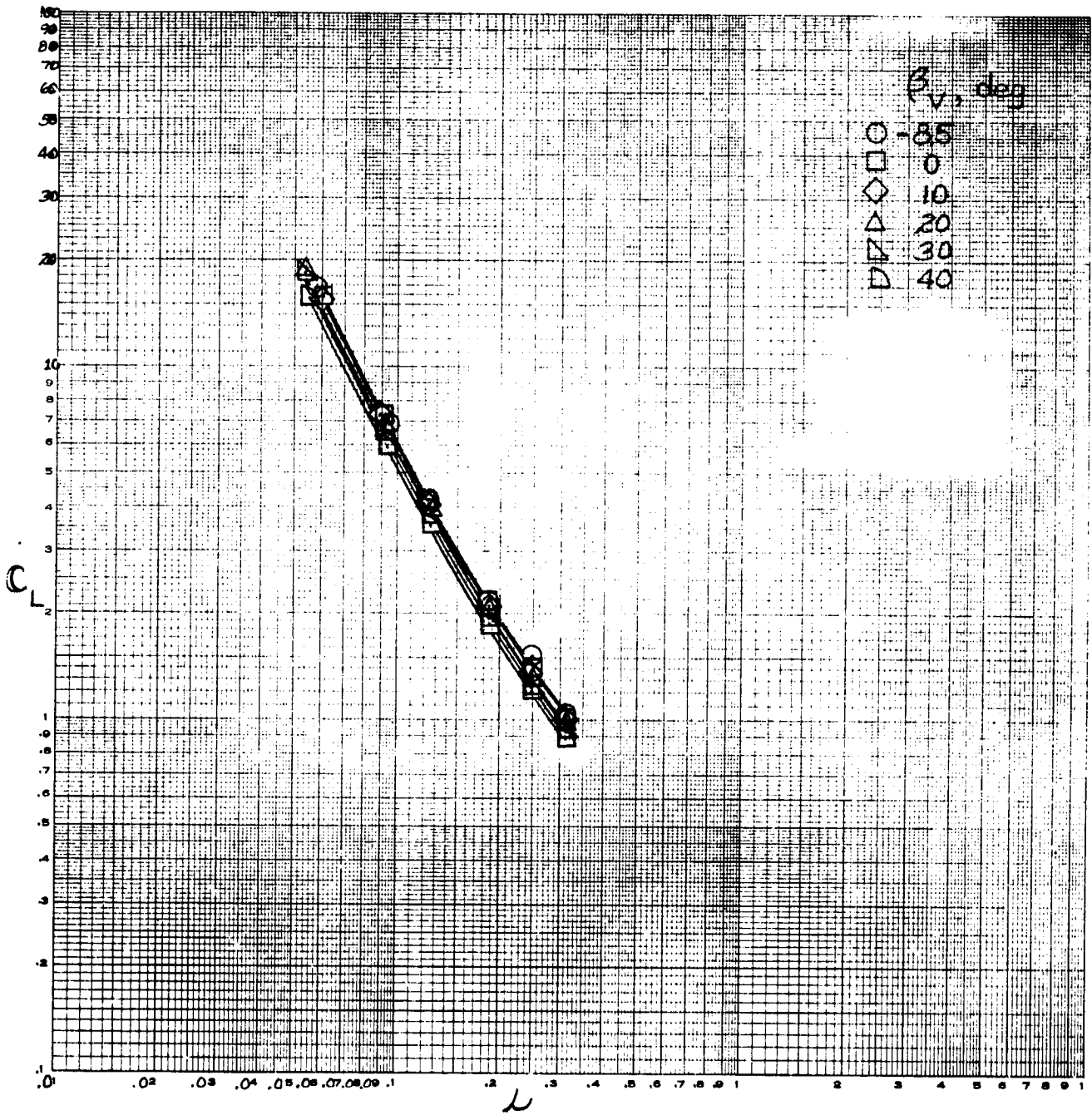
(c)  $C_L$  vs  $\mu$ ,  $\delta_f = 45^\circ$ .

Figure 7.- Continued.



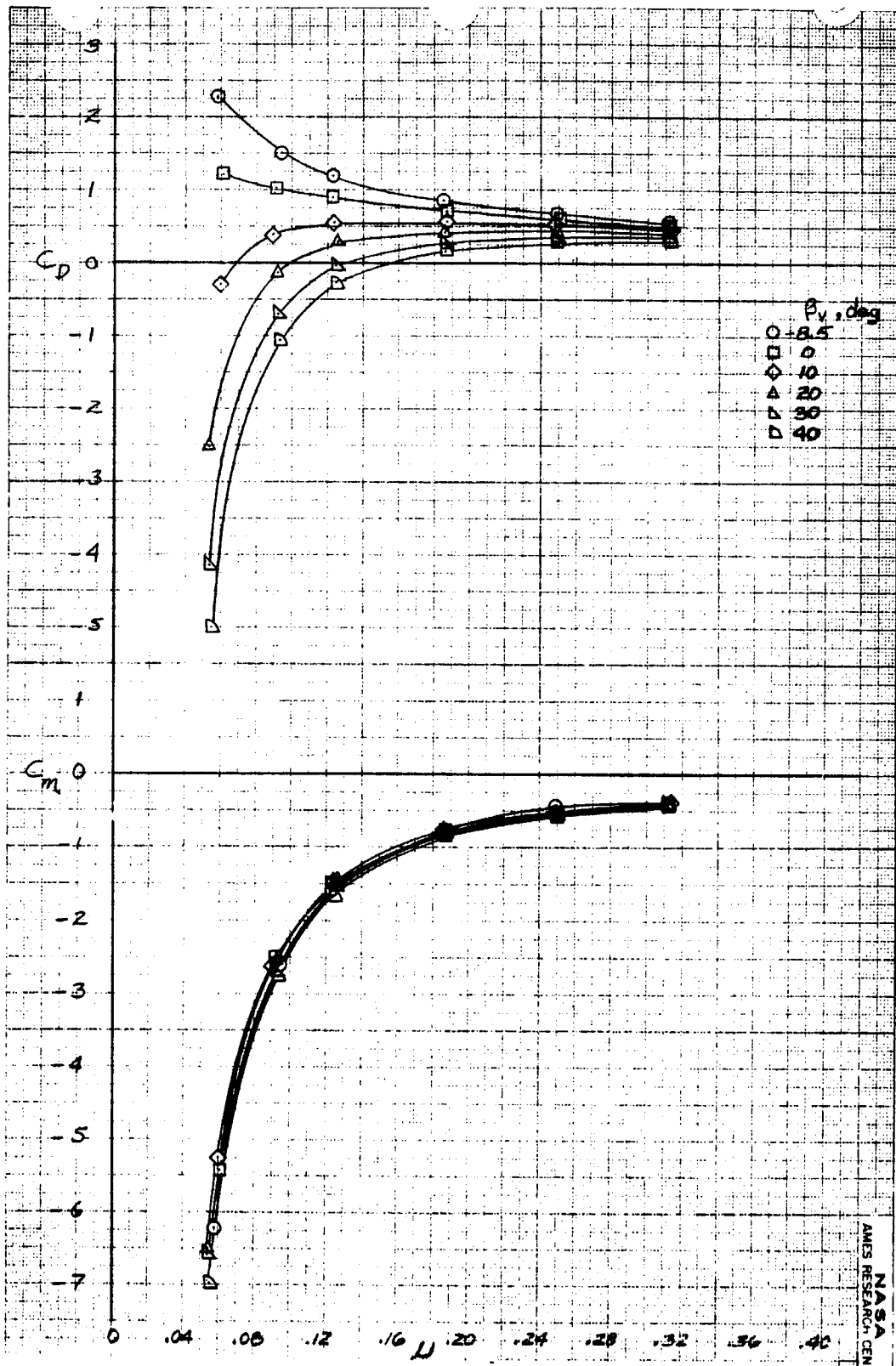
(d)  $C_D, C_M$  vs  $M, \delta_f = 45^\circ$ .

Figure 7.- Concluded.



(a)  $C_L$  vs  $\mu$ ,  $\delta_f = 45^\circ$ .

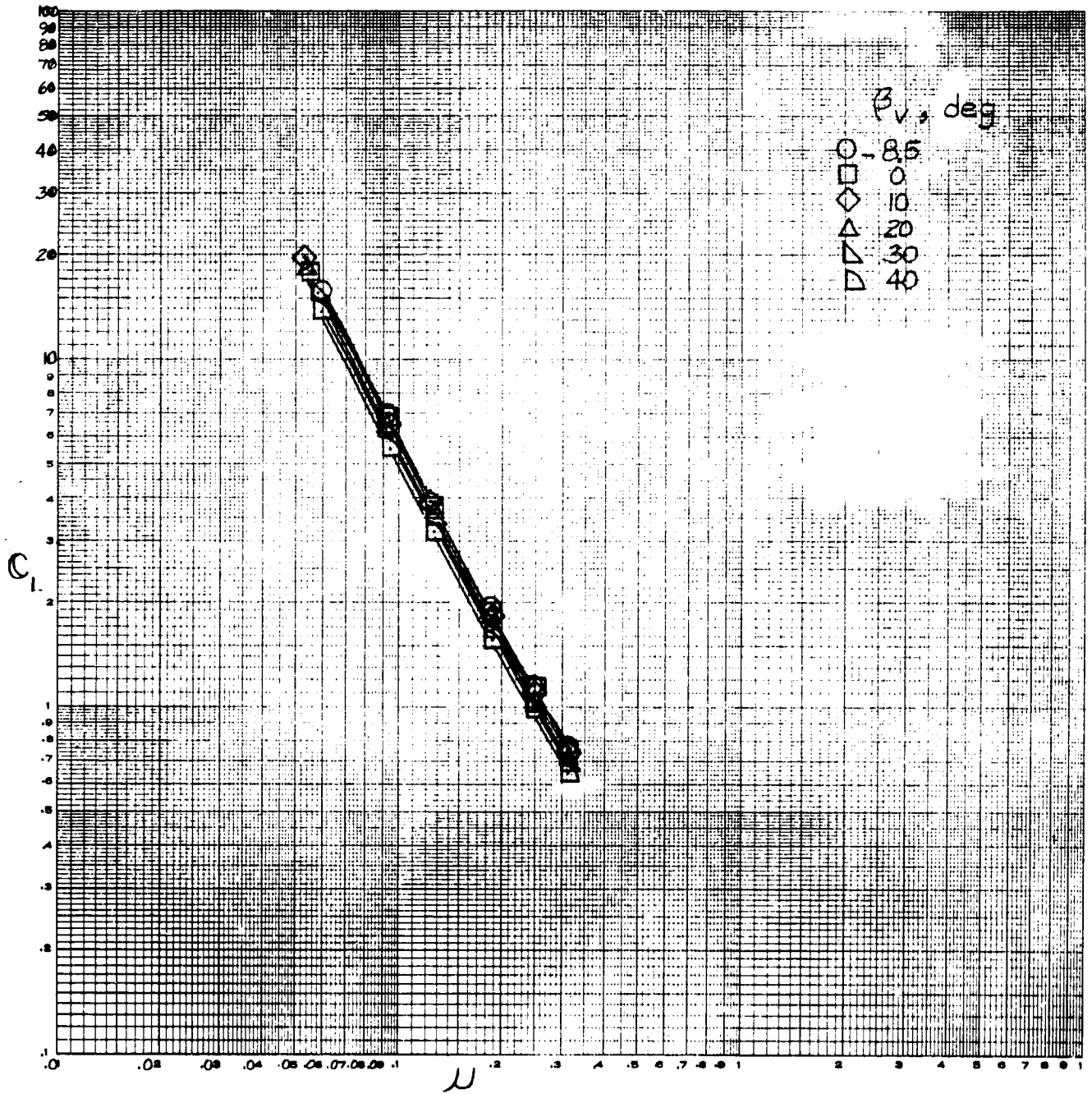
Figure 8.- The effect of tip-speed ratio on longitudinal characteristics; 4 fans,  $\theta_v = 82^\circ$ , tail off.



(b)  $C_D, C_m$  vs  $\mu, \delta_f = 45^\circ$ .

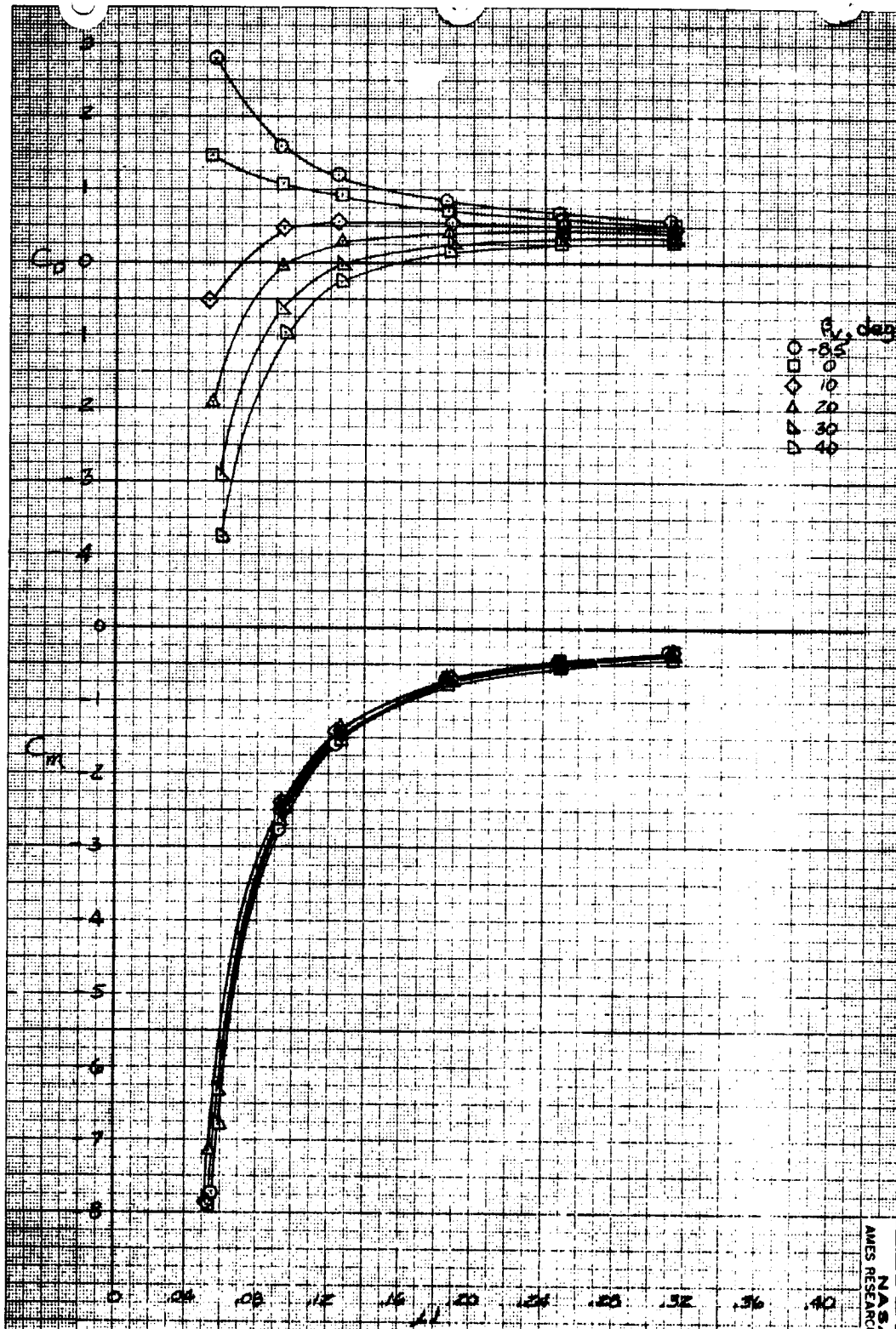
Figure 8.- Continued.





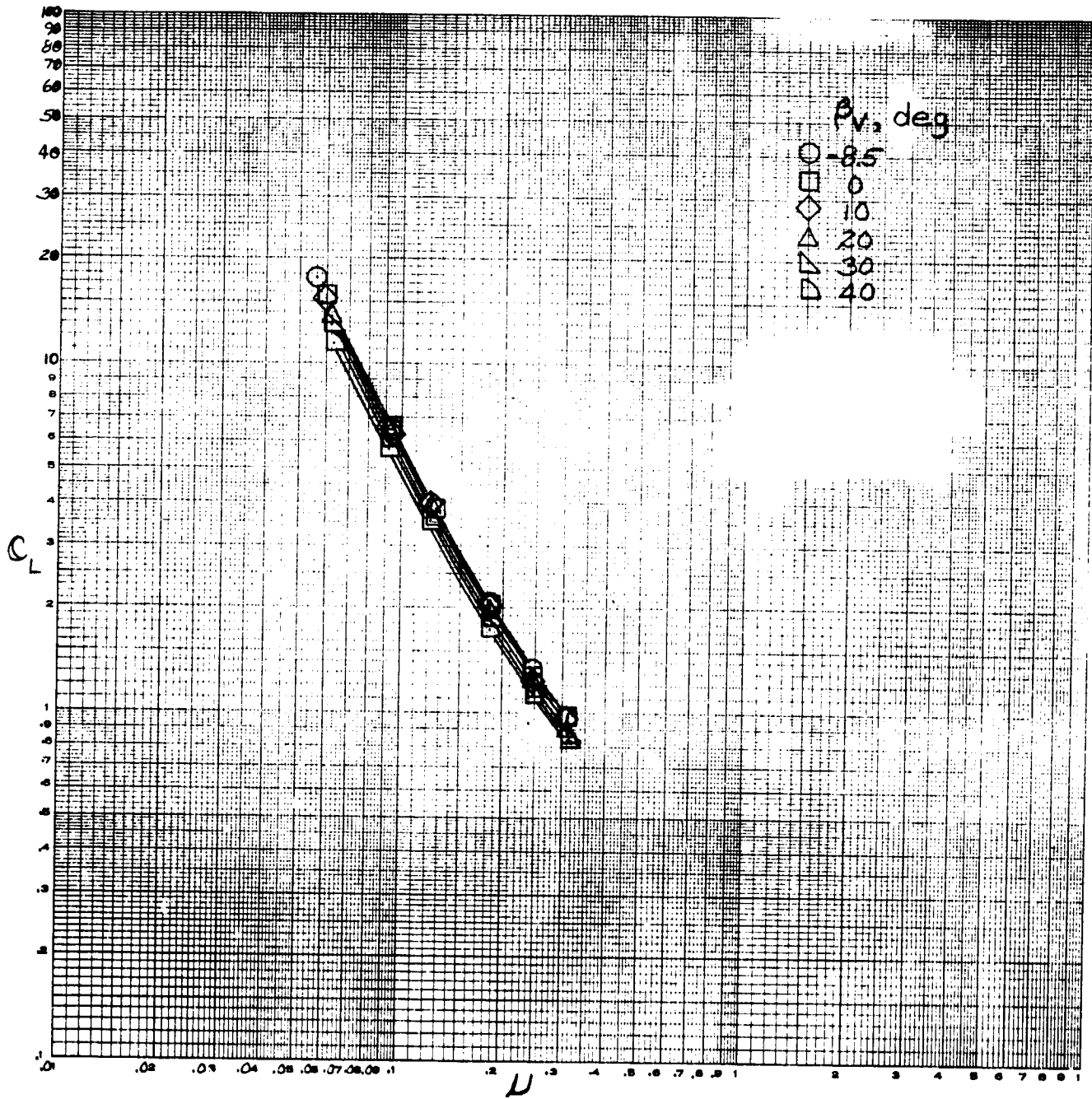
(c)  $C_L$  vs  $\mu$ ,  $\delta_f = 0^\circ$ .

Figure 8.- Continued.



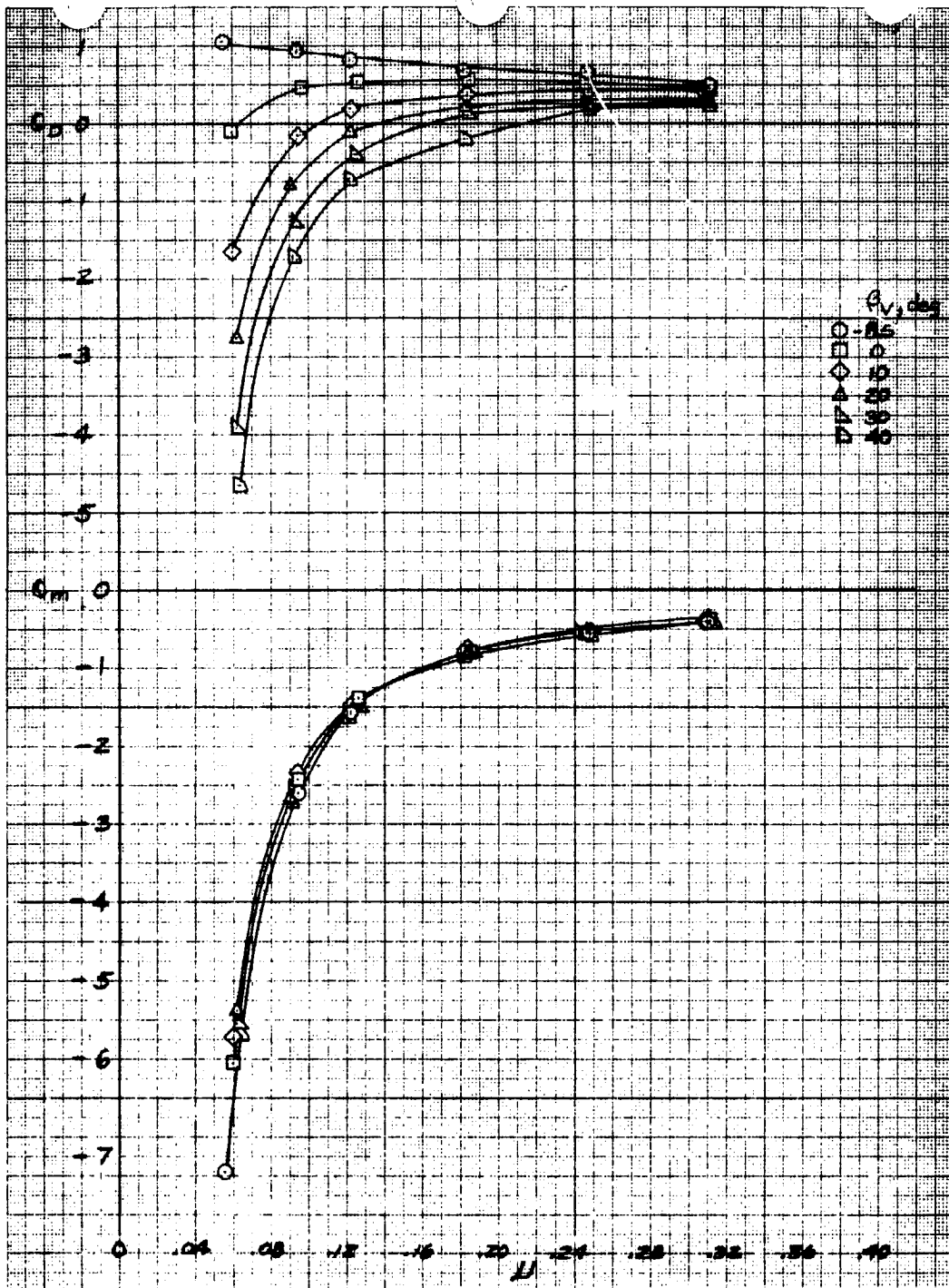
(d)  $C_D, C_M$  vs  $\mu, \delta_f = 0^\circ$ .

Figure 8.- Concluded.



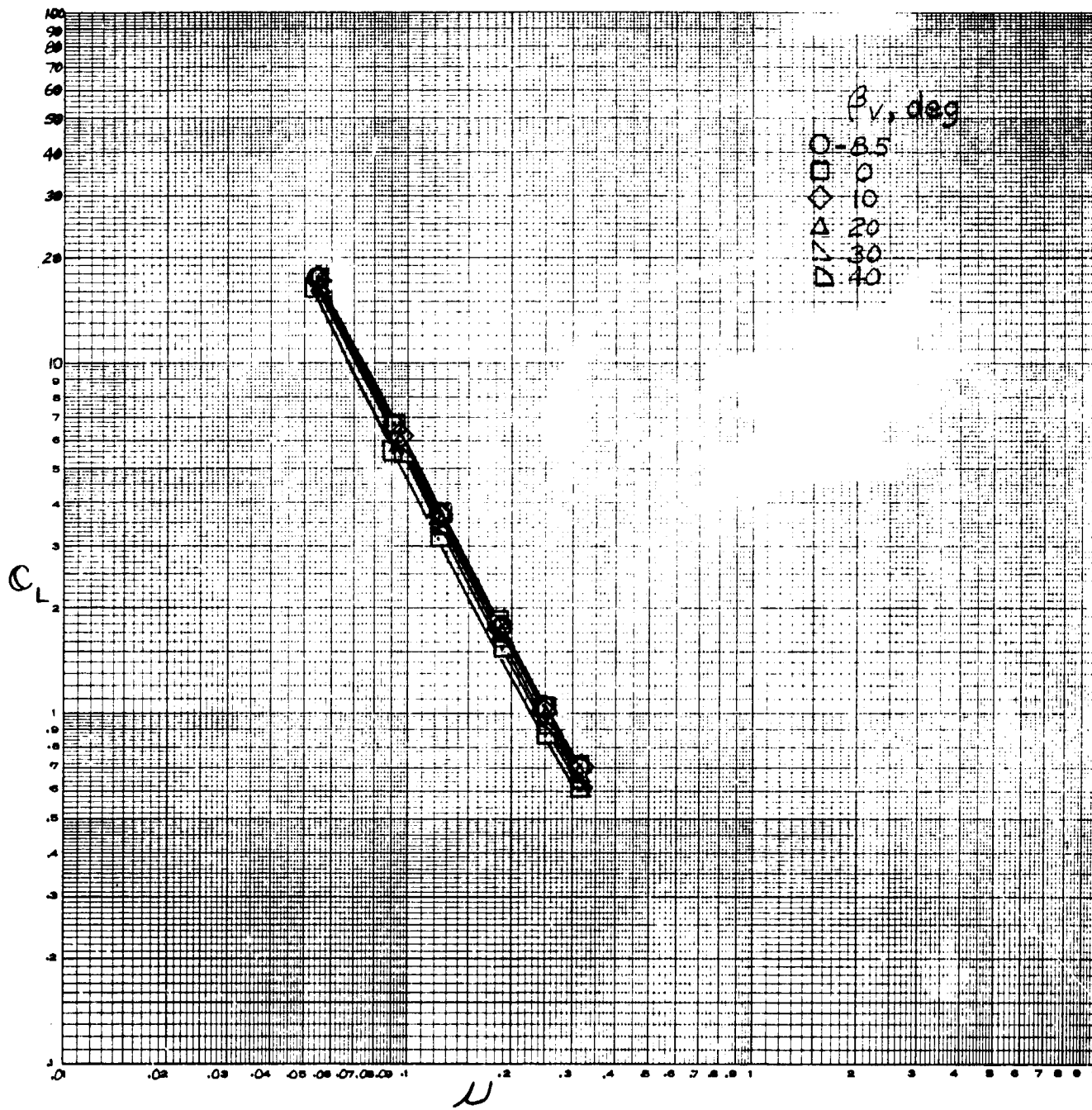
(a)  $C_L$  vs  $\mu$ ,  $\delta_f = 45^\circ$ .

Figure 9.- The effect of tip-speed ratio on longitudinal characteristics; 4 fans,  $\theta_v = 71^\circ$ , tail off.



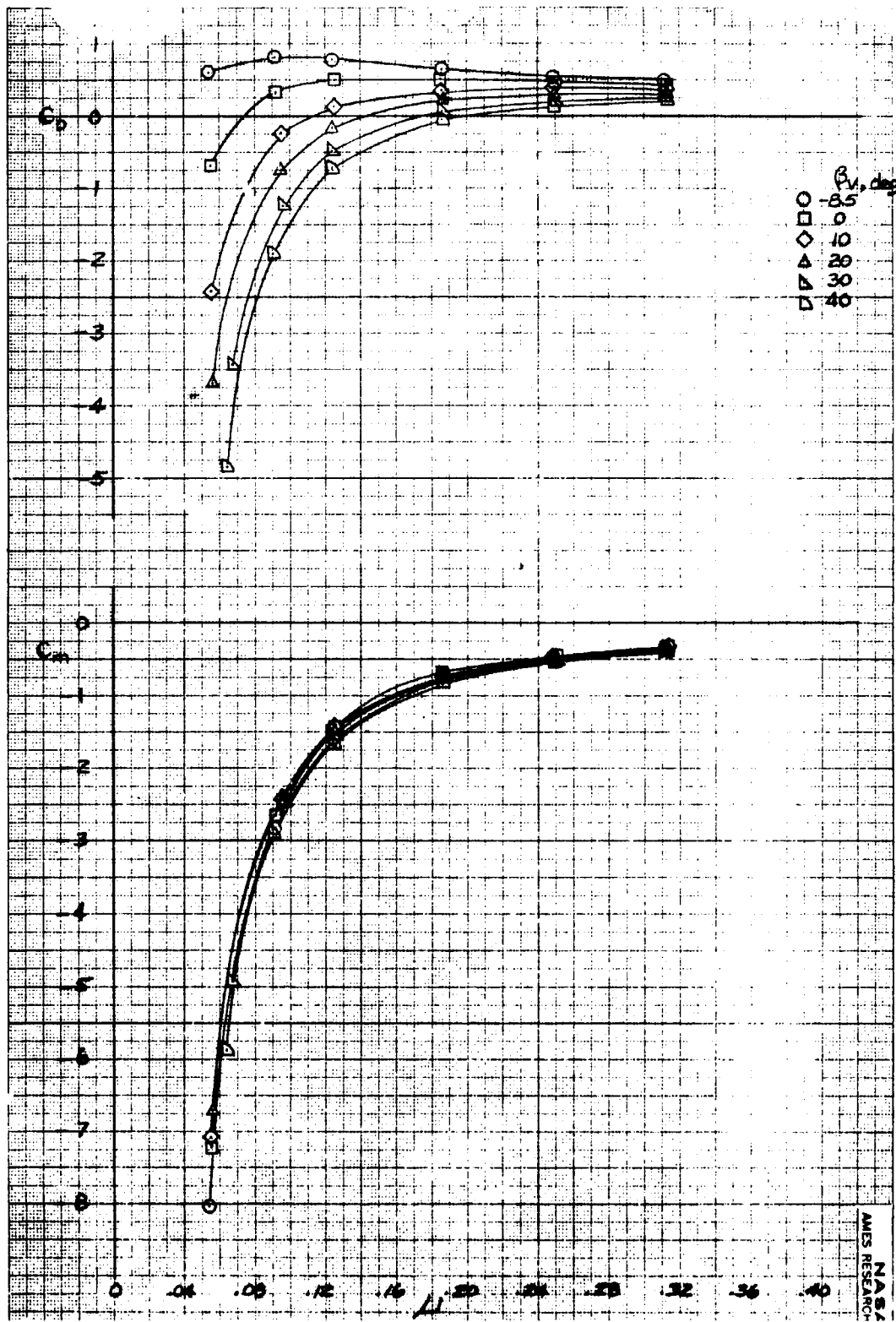
(b)  $C_D, C_m$  vs  $\mu, \delta_f = 45^\circ$ .

Figure 9.- Continued.



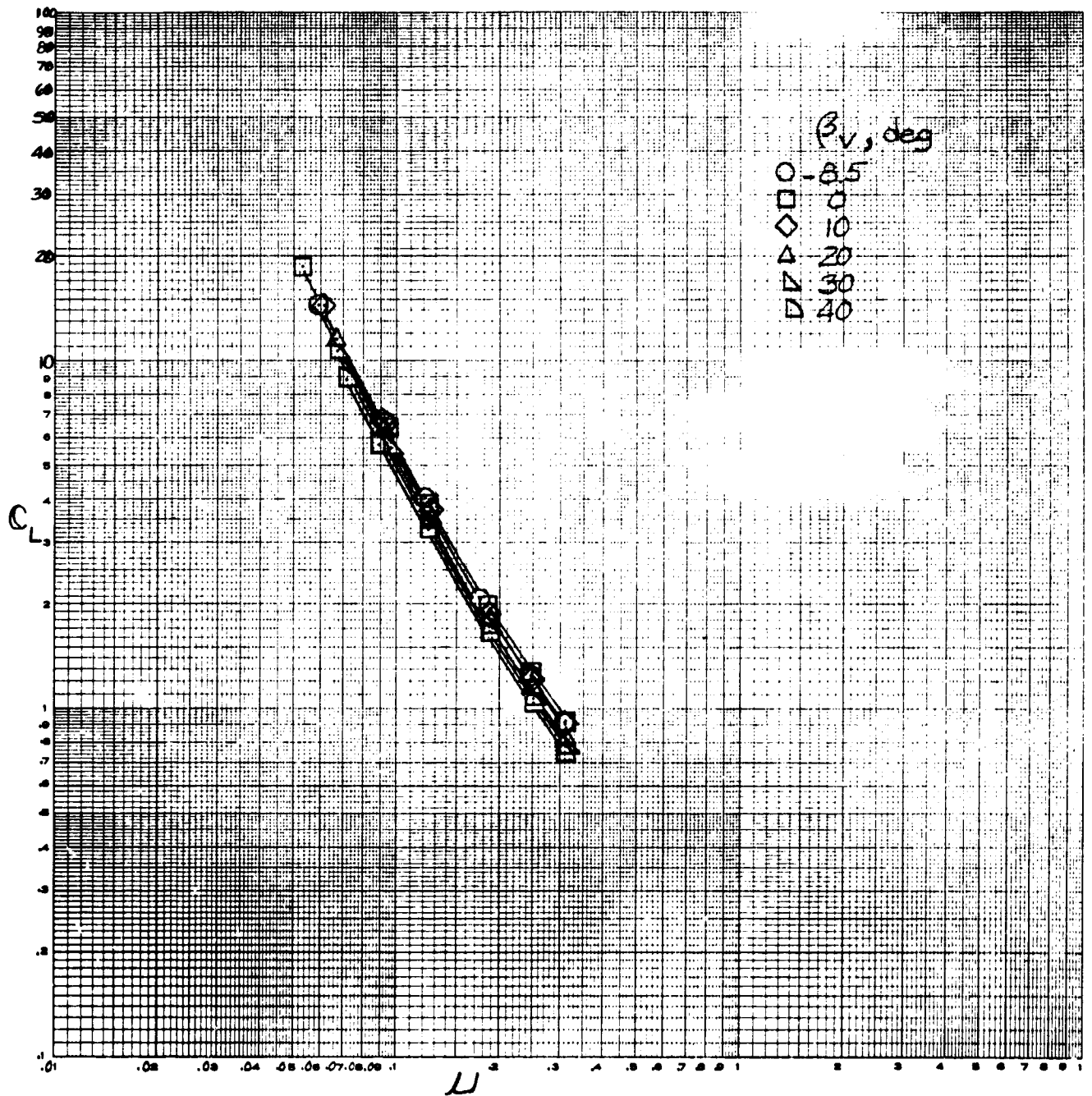
(c)  $C_L$  vs  $\mu$ ,  $\delta_f = 0^\circ$ .

Figure 9.- Continued.



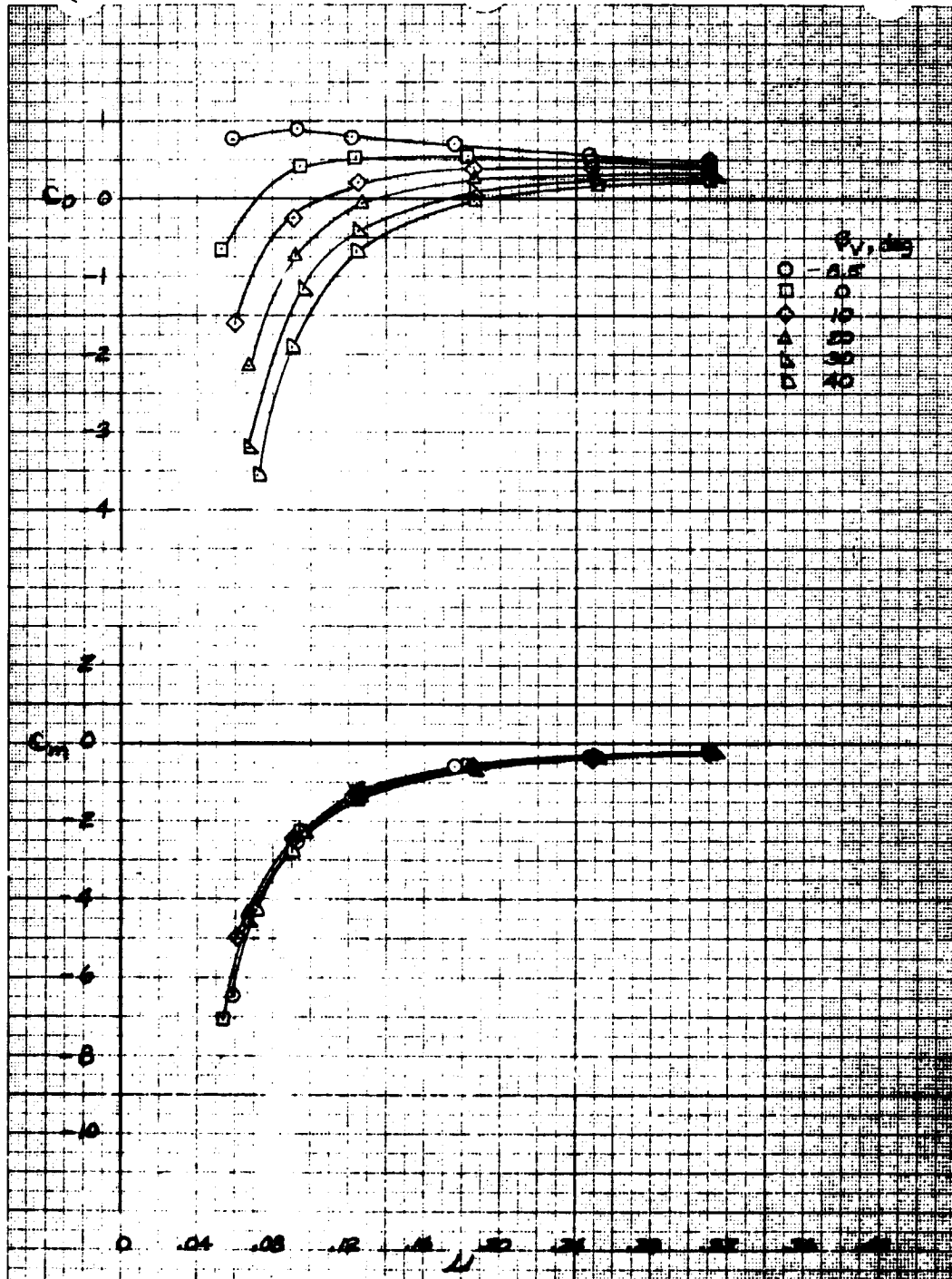
(d)  $C_D, C_m$  vs  $\alpha, \delta_f = 0^\circ$ .

Figure 9.- Concluded.



(a)  $C_L$  vs  $U$ ,  $\delta_f = 45^\circ$ .

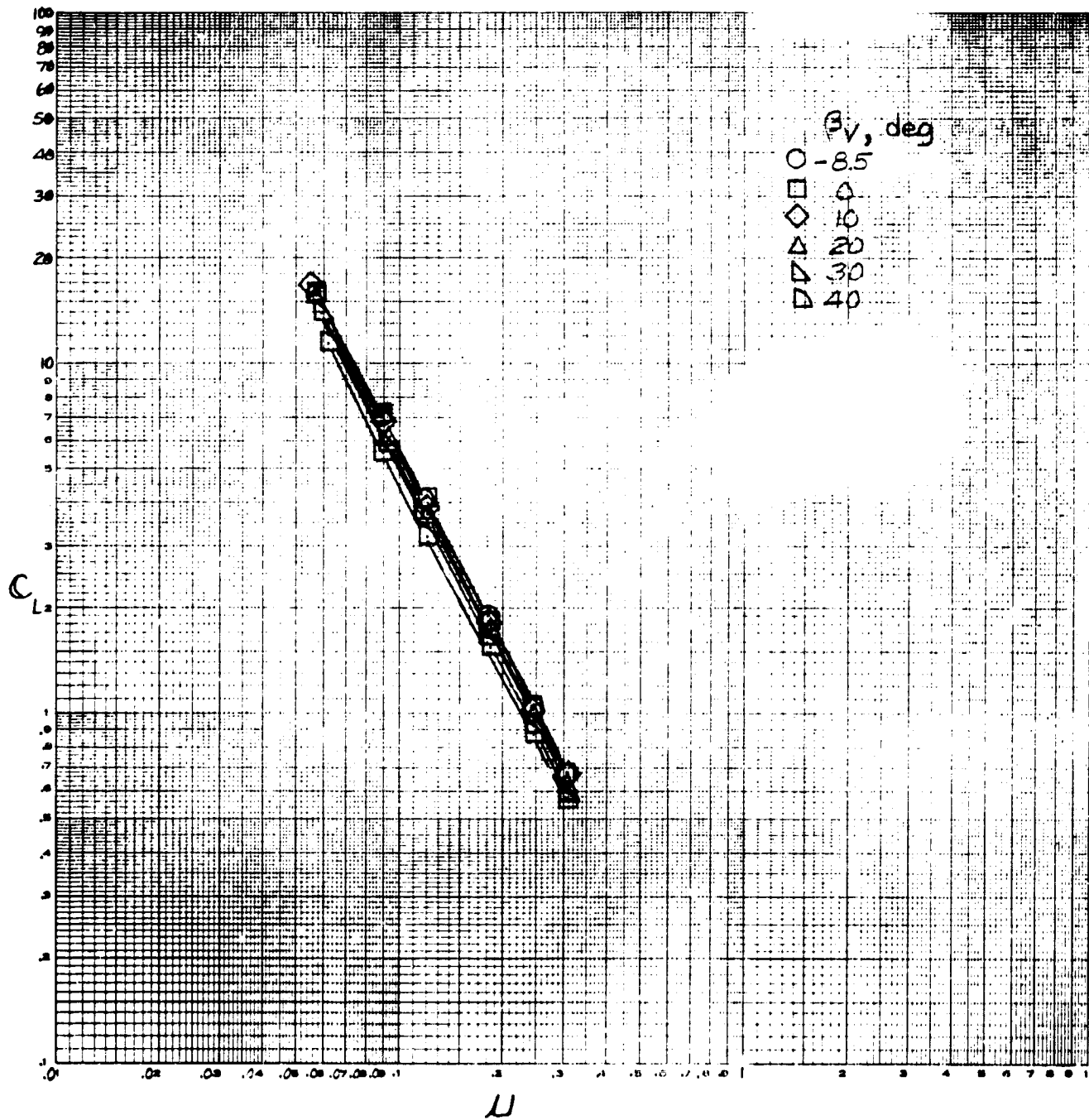
Figure 10.- The effect of tip-speed ratio on longitudinal characteristics; 4 fans,  $\theta_v = 71^\circ$ , tail on,  $i_t = 0^\circ$ .



(b)  $C_D, C_m$  vs  $\mu, \delta_f = 45^\circ$ .

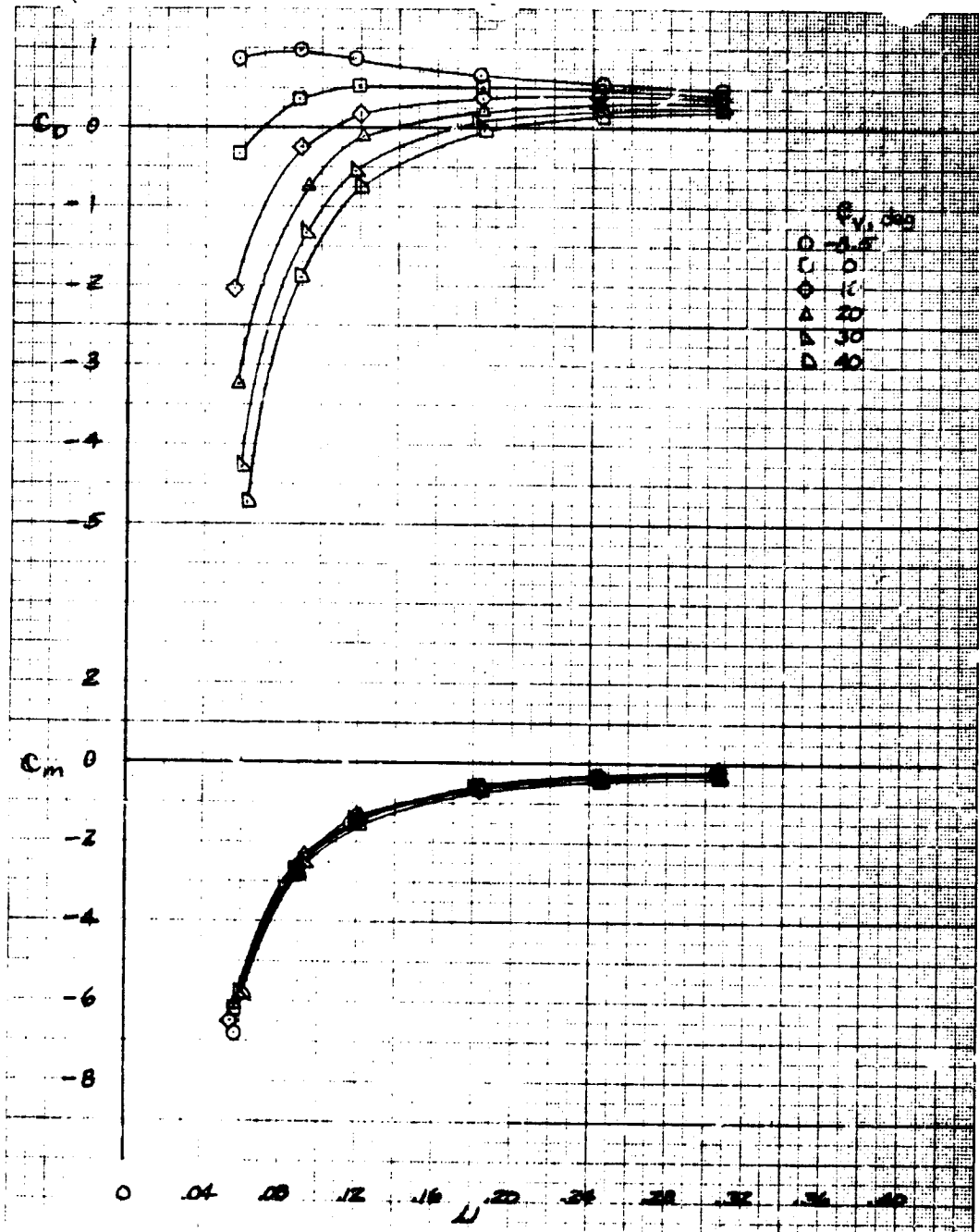
Figure 10.-- Continued.





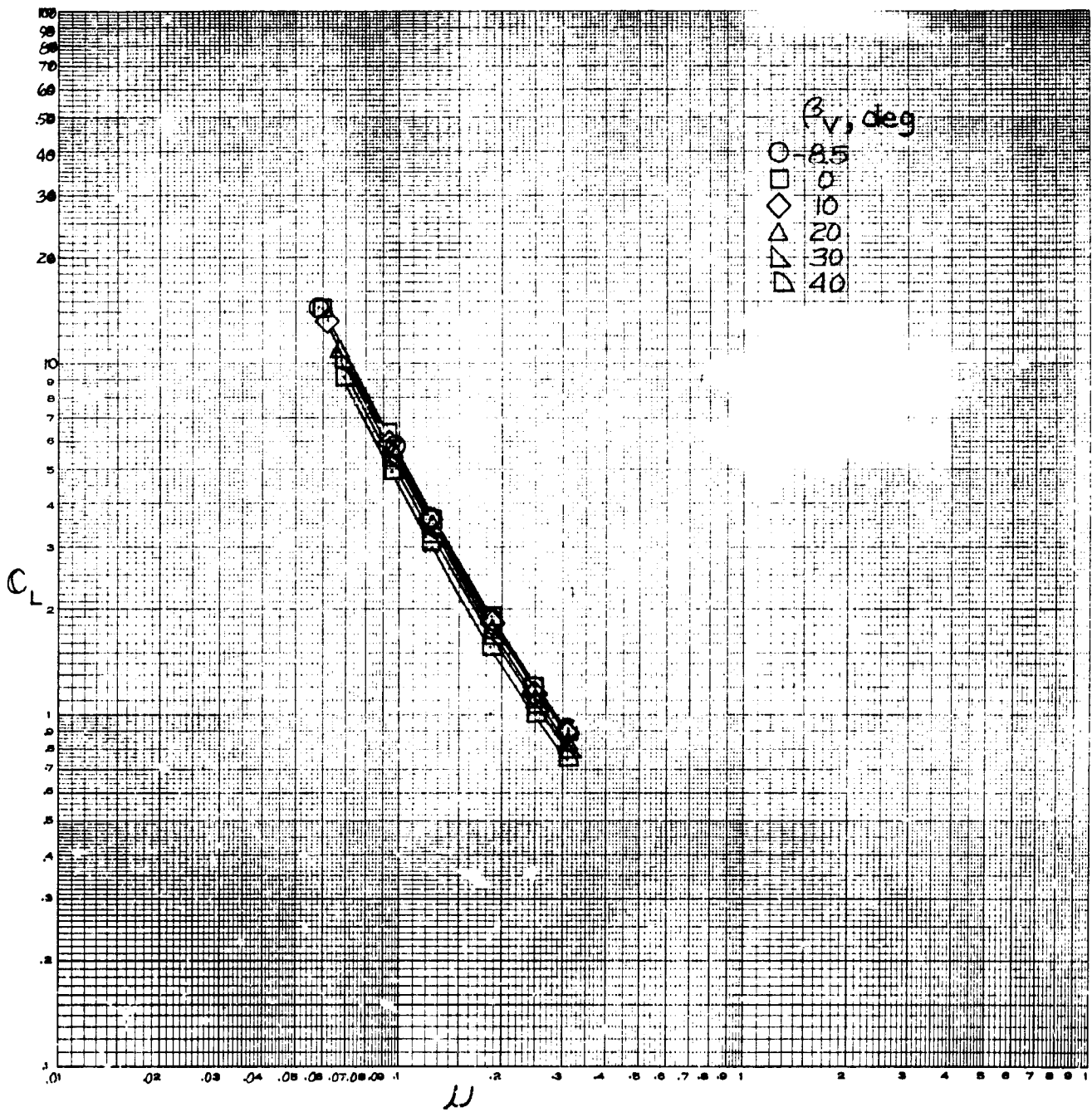
(c)  $C_L$  vs  $M$ ,  $\delta_f = 0^\circ$ .

Figure 10.- Continued.



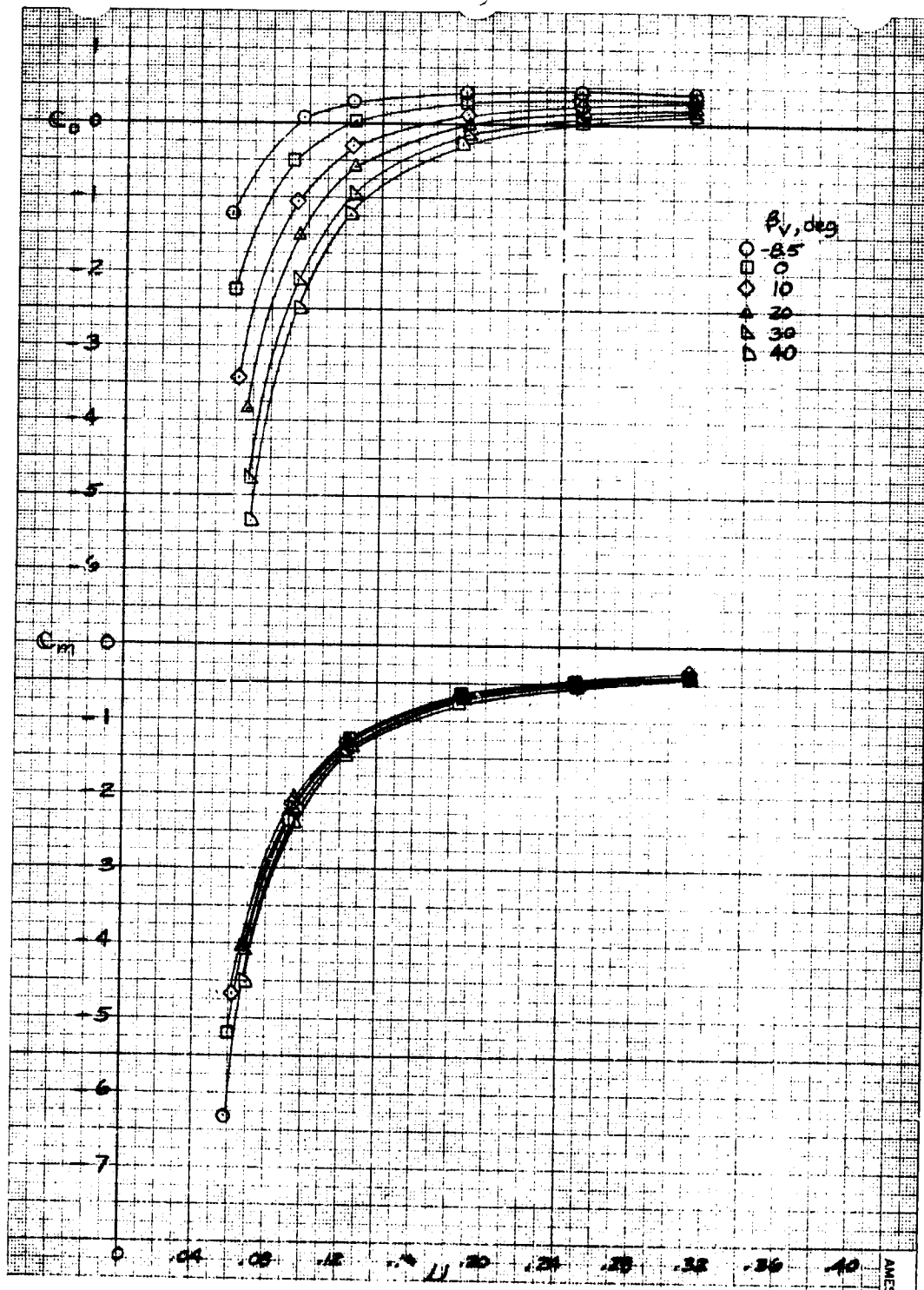
(d)  $C_D, C_m$  vs  $\mu, \delta_f = 0^\circ$ .

Figure 10.- Concluded.



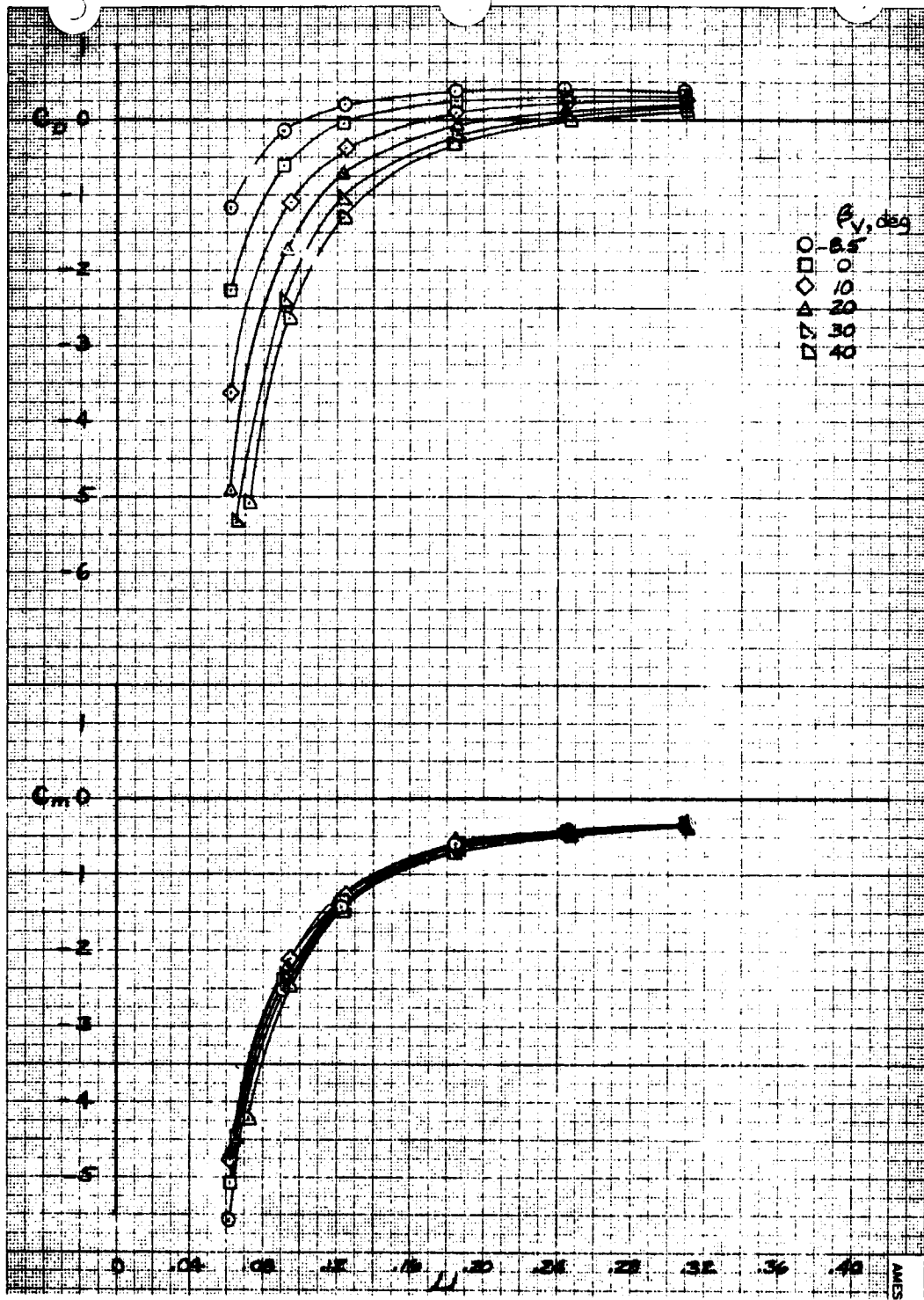
(a)  $C_L$  vs  $\mu$ ,  $\delta_f = 45^\circ$ .

Figure 11.- The effect of tip-speed ratio on longitudinal characteristics; 4 fans,  $\theta_v = 55^\circ$ , tail off.



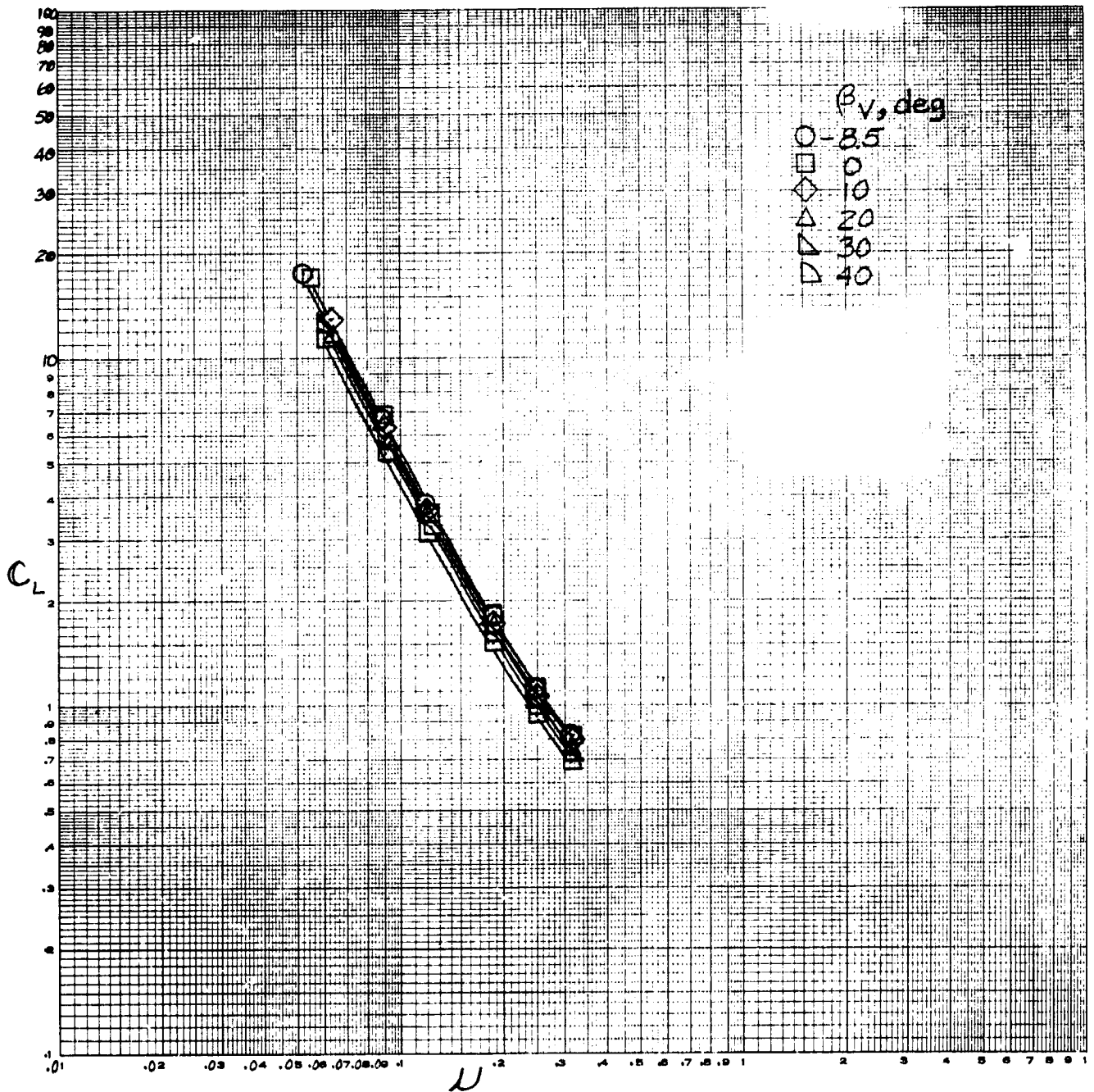
(b)  $C_D, C_M$  vs  $\mu, \delta_f = 45^\circ$ .

Figure 11.- Continued.



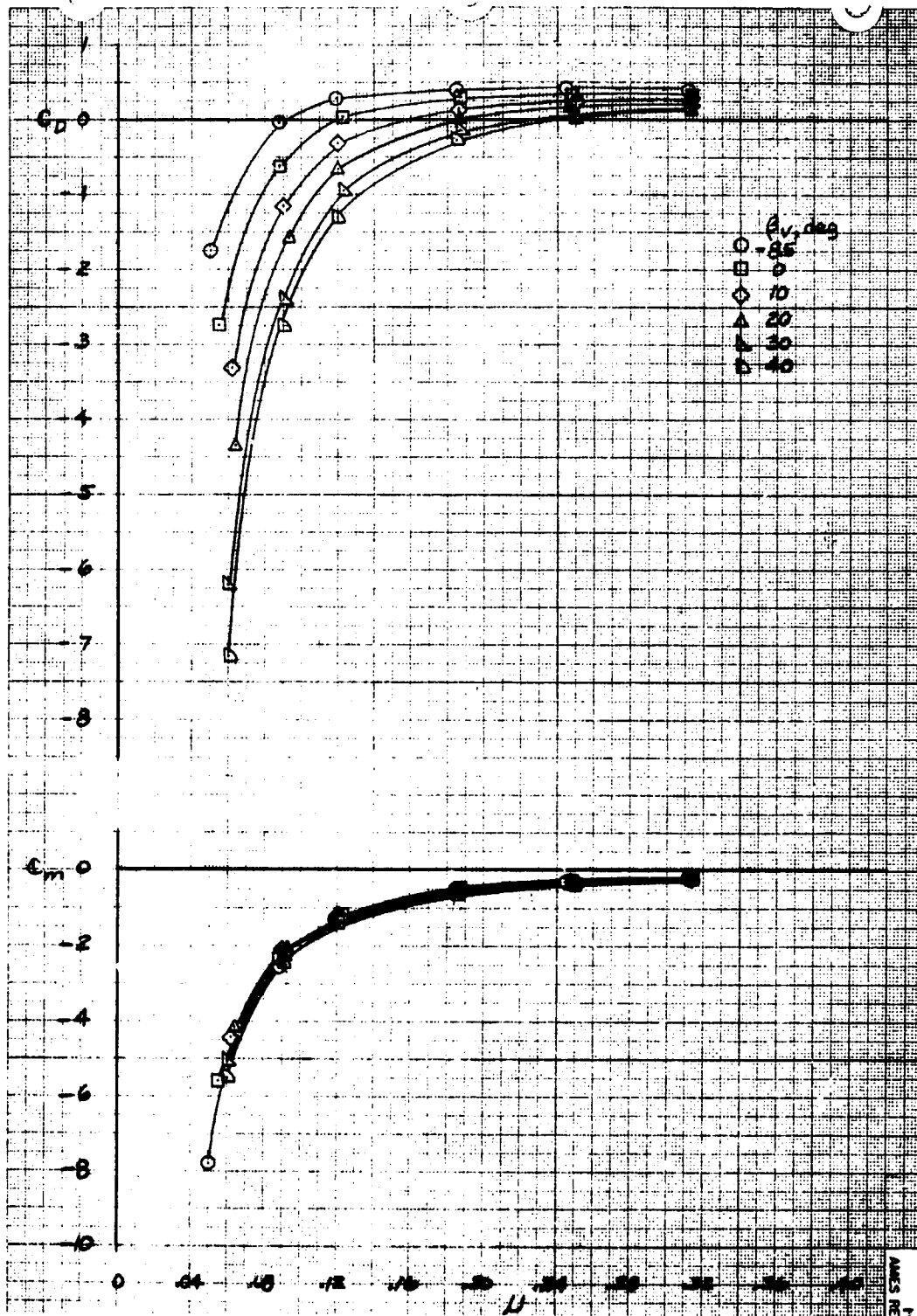
(d)  $C_D, C_m$  vs  $\mu, \delta_f = 0^\circ$ .

Figure 11.- Concluded.



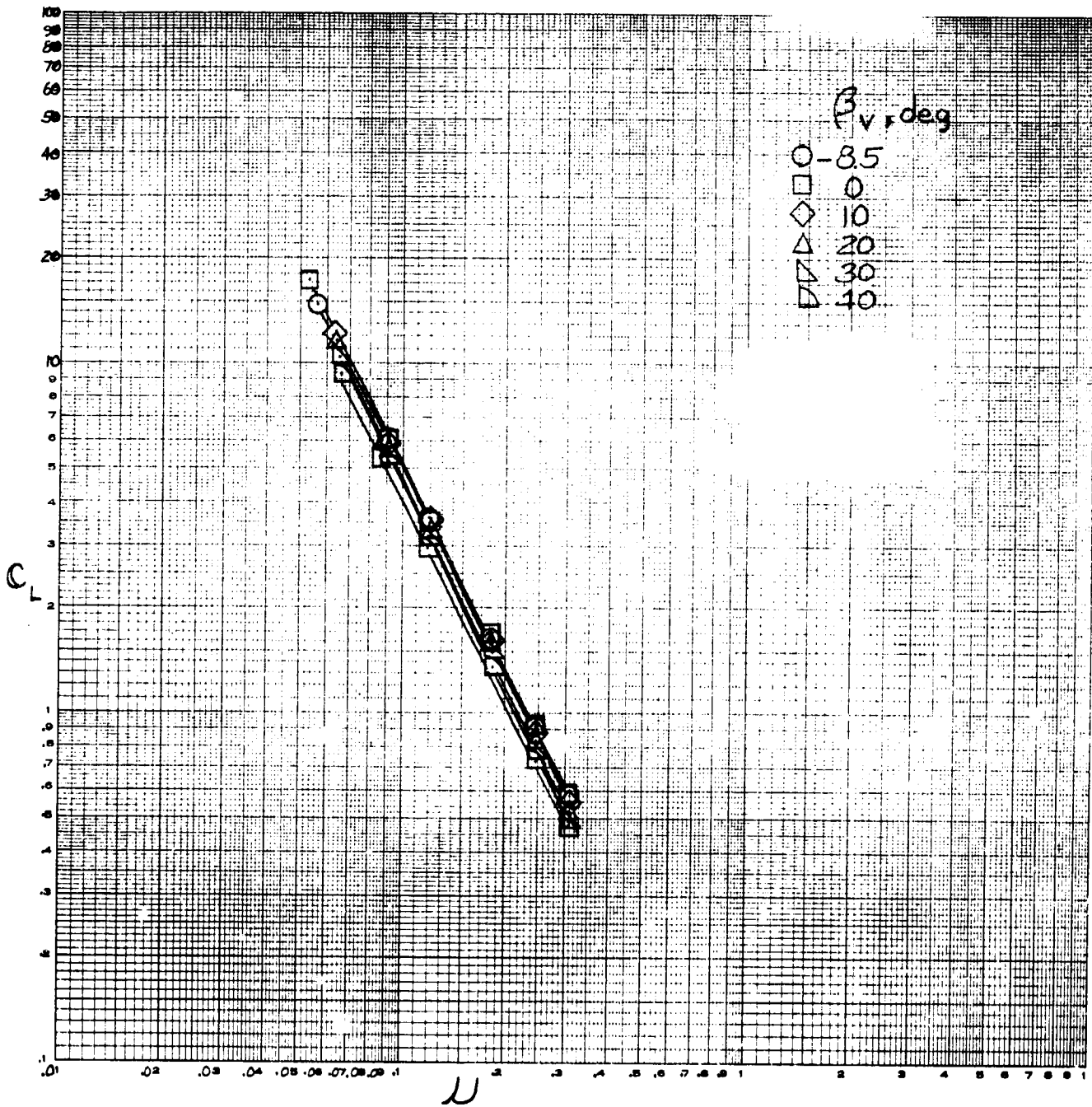
(a)  $C_L$  vs  $U$ ,  $\delta_f = 45^\circ$ .

Figure 12.- The effect of tip-speed ratio on longitudinal characteristics; 4 fans,  $\theta_v = 55^\circ$ , tail on,  $i_t = 0^\circ$ .



(b)  $C_D, C_m$  vs  $\alpha, \delta_f = 45^\circ$ .

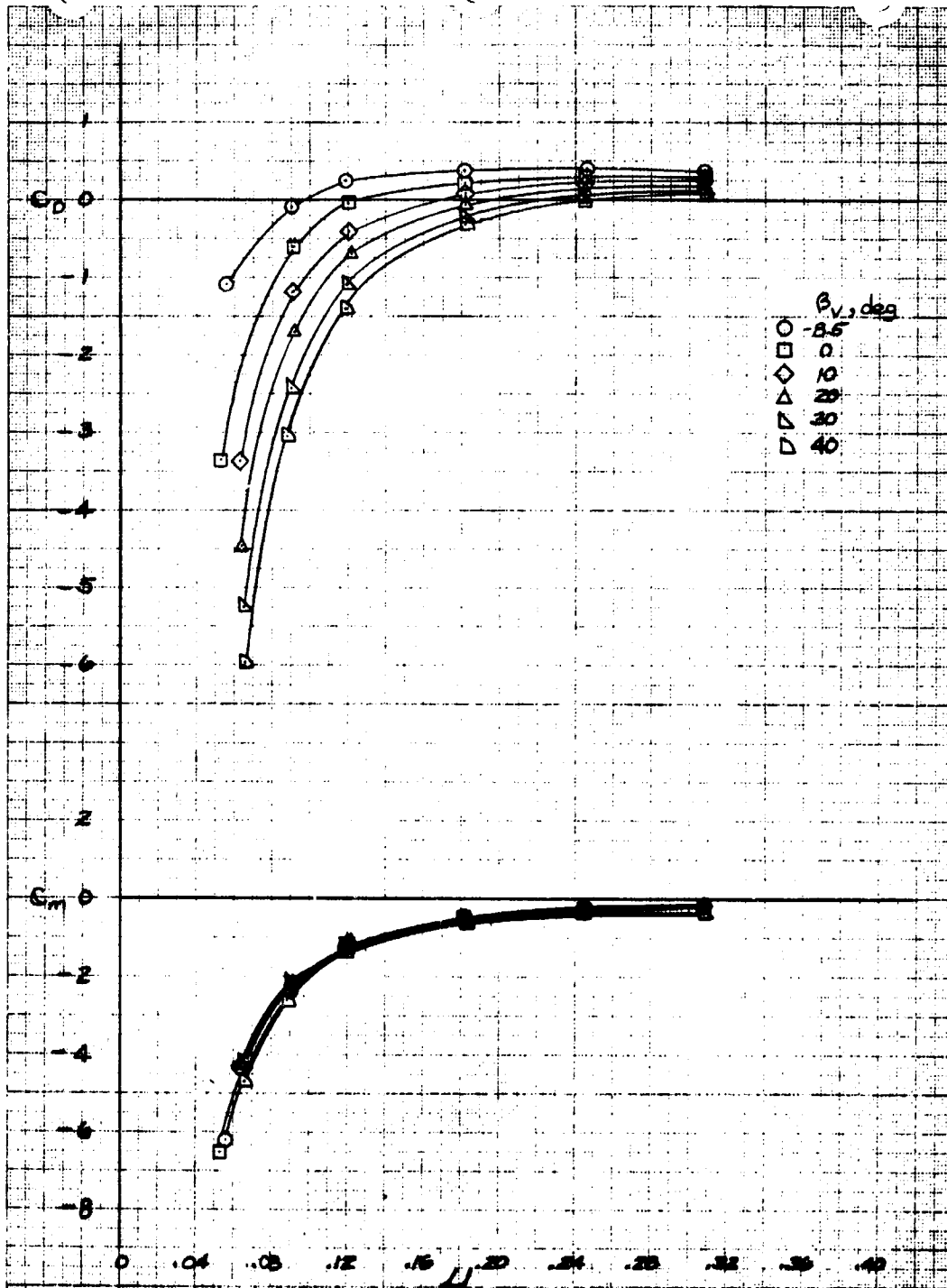
Figure 12.- Continued.



(c)  $C_L$  vs  $\mu$ ,  $\delta_f = 0^\circ$ .

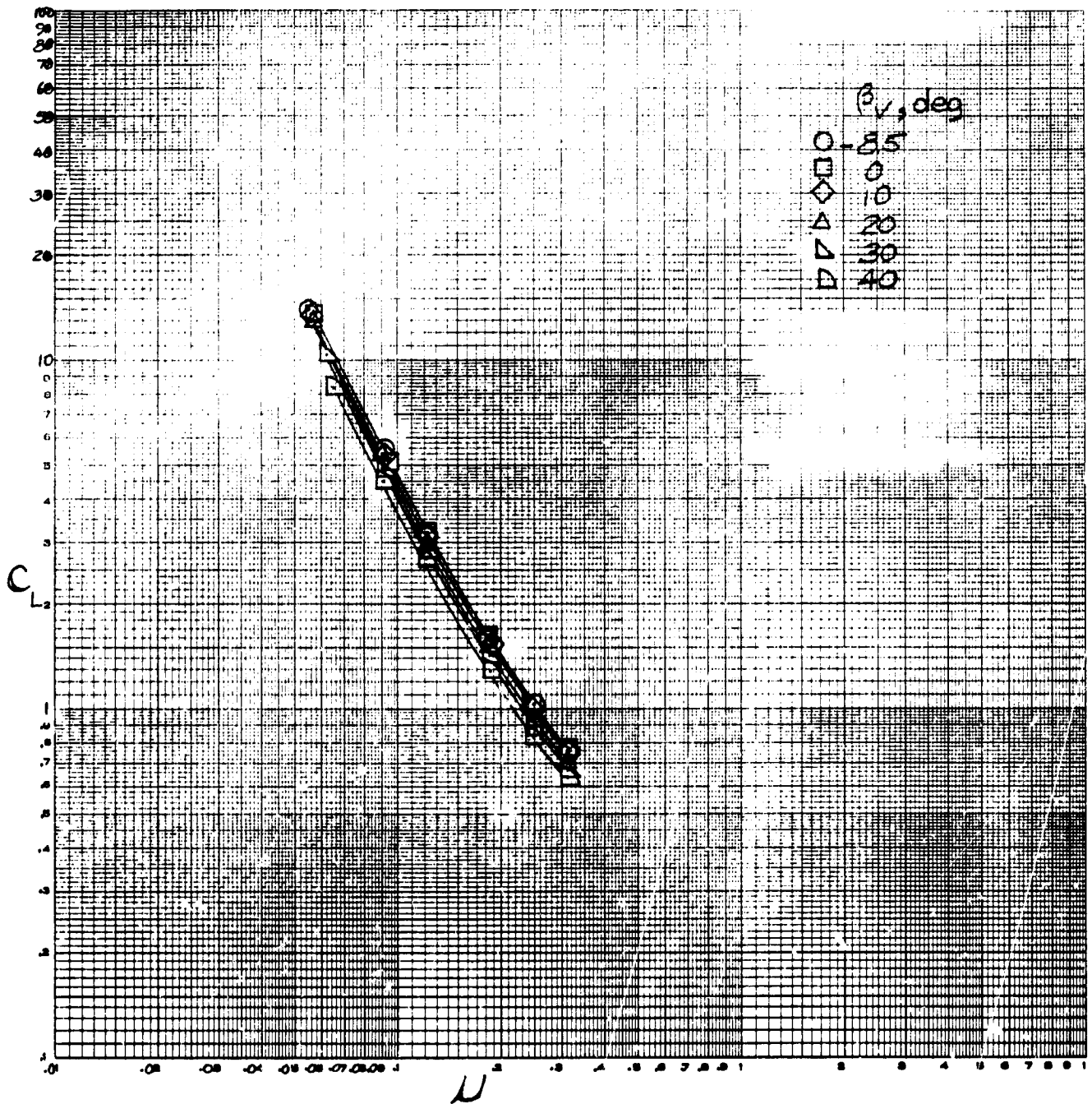
Figure 12.- Continued.





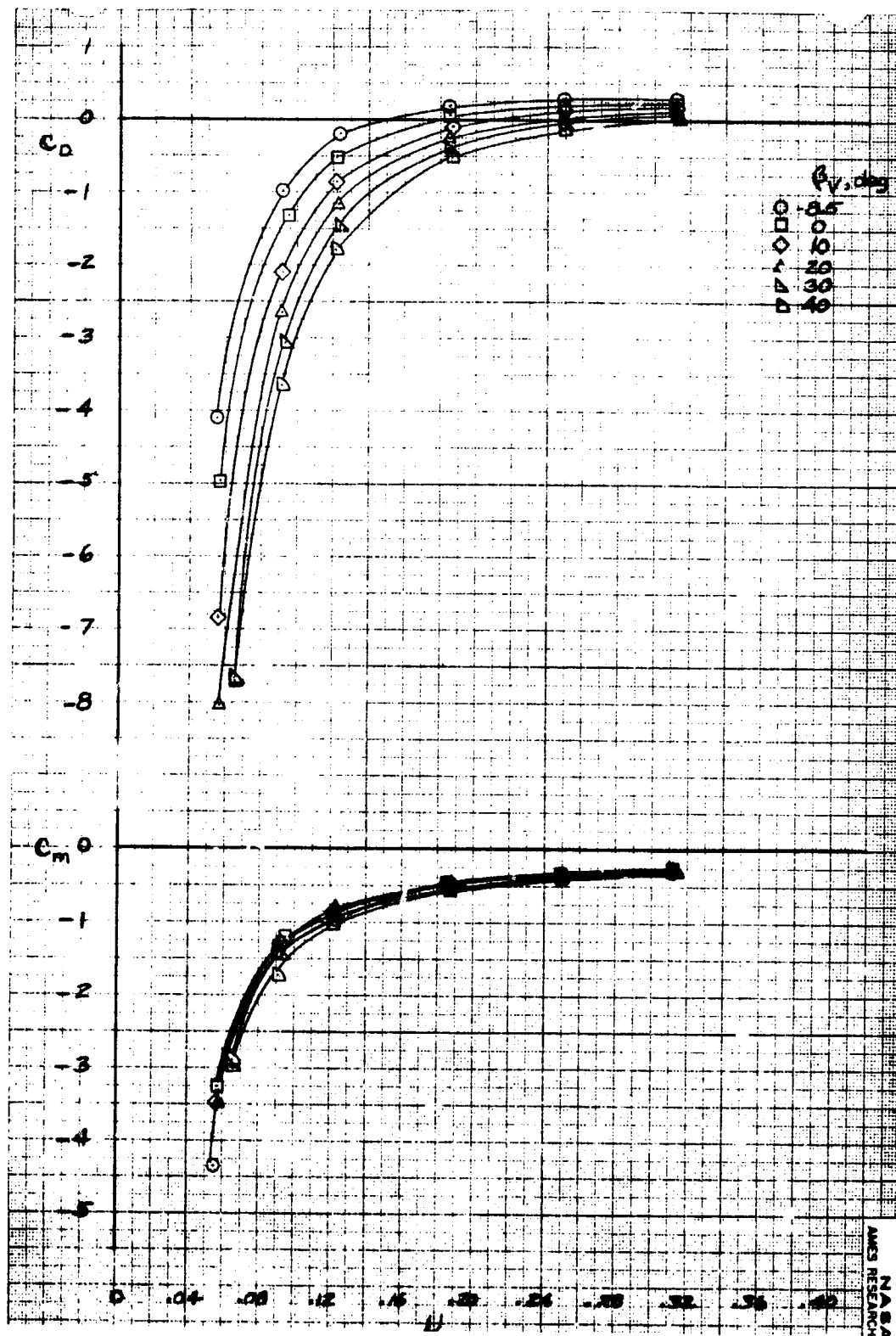
(d)  $C_D, C_M$  vs  $\mu, \delta_f = 0^\circ$ .

Figure 12.- Concluded.



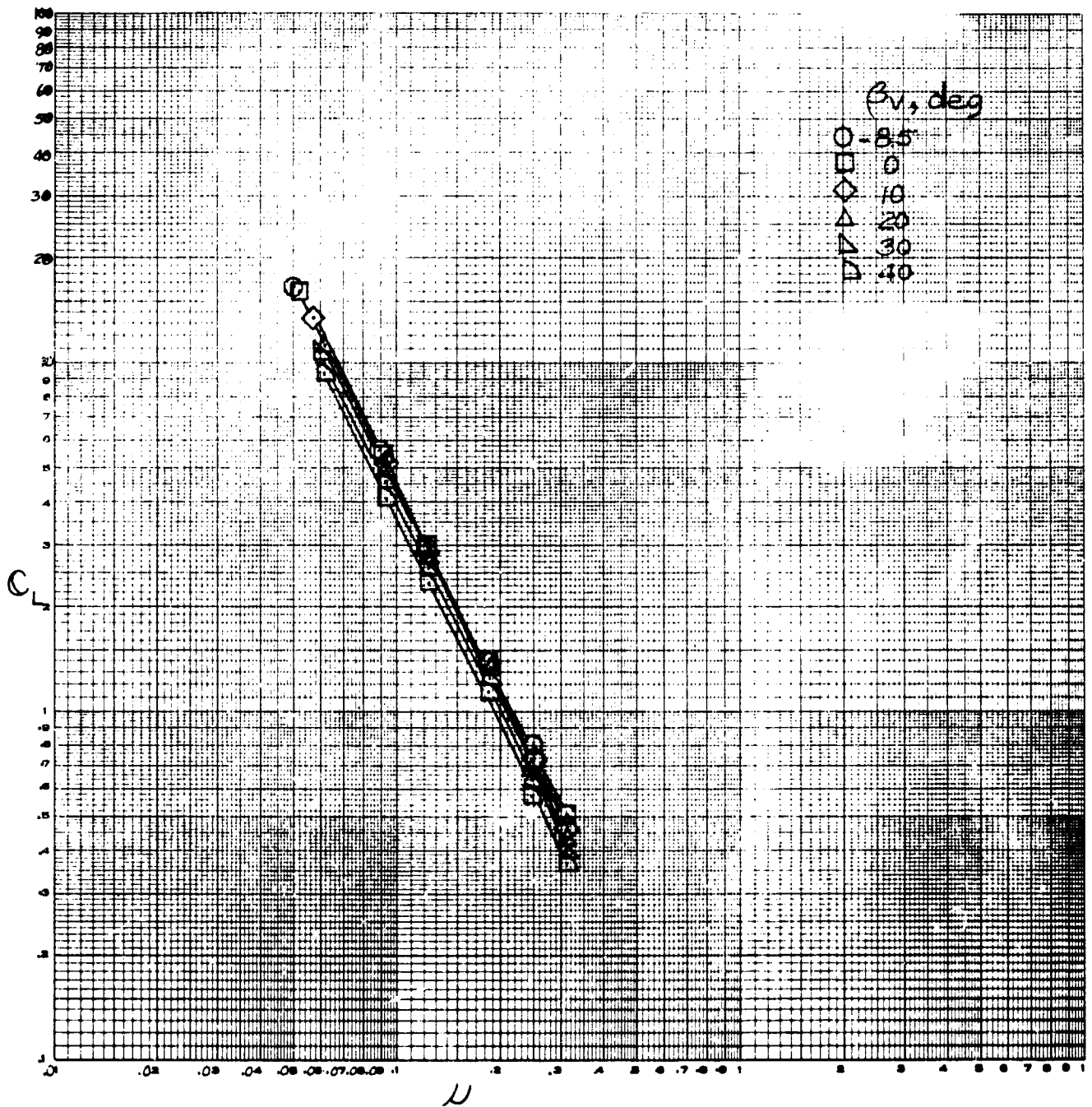
(a)  $C_L$  vs  $\mu$ ,  $\delta_F = 45^\circ$ .

Figure 13.- The effect of tip-speed ratio on longitudinal characteristics; 4 fans,  $\theta_V = 36^\circ$ , tail off.



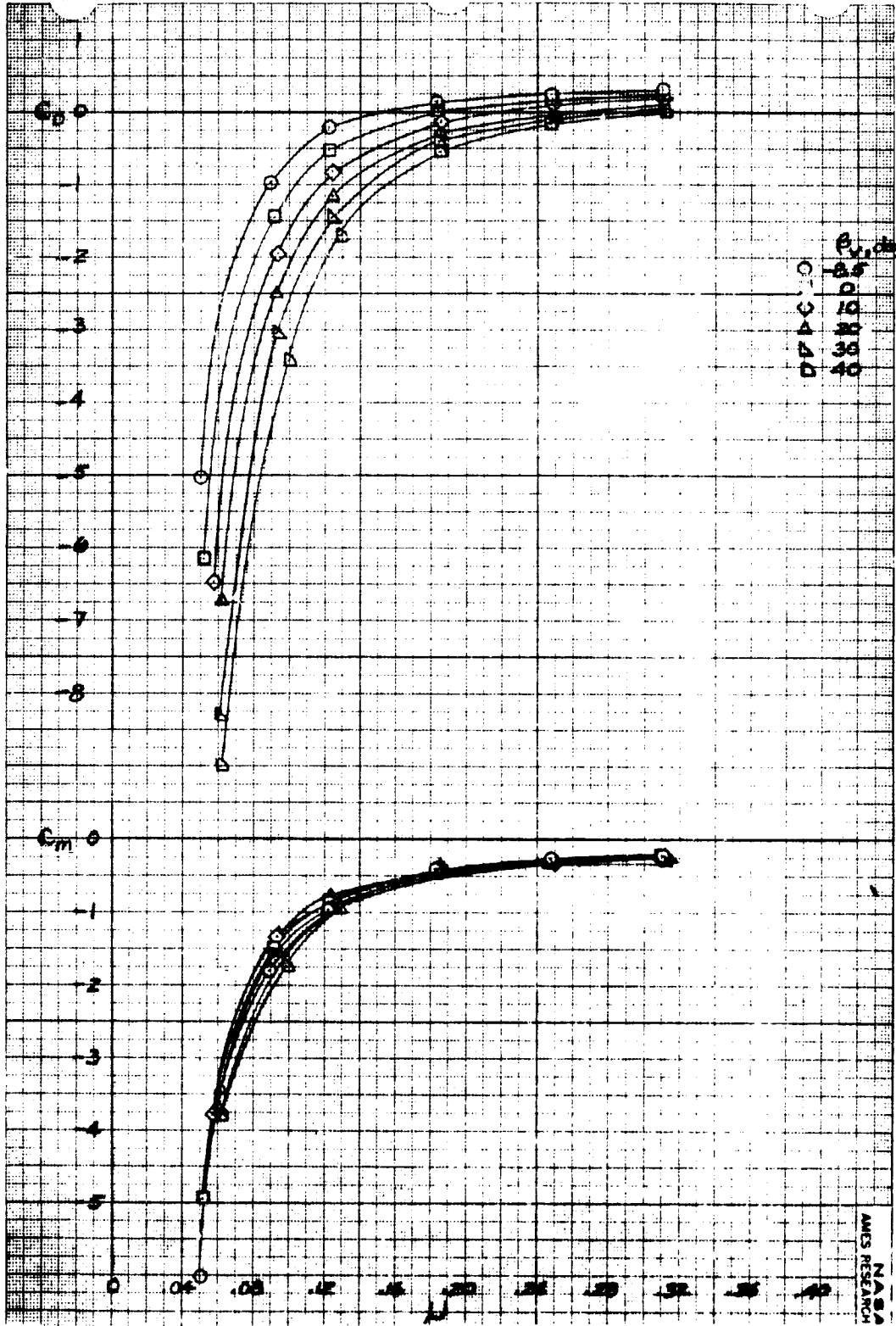
(b)  $C_D, C_m$  vs  $\alpha, \delta \epsilon = 45^\circ$ .

Figure 13.- Continued.



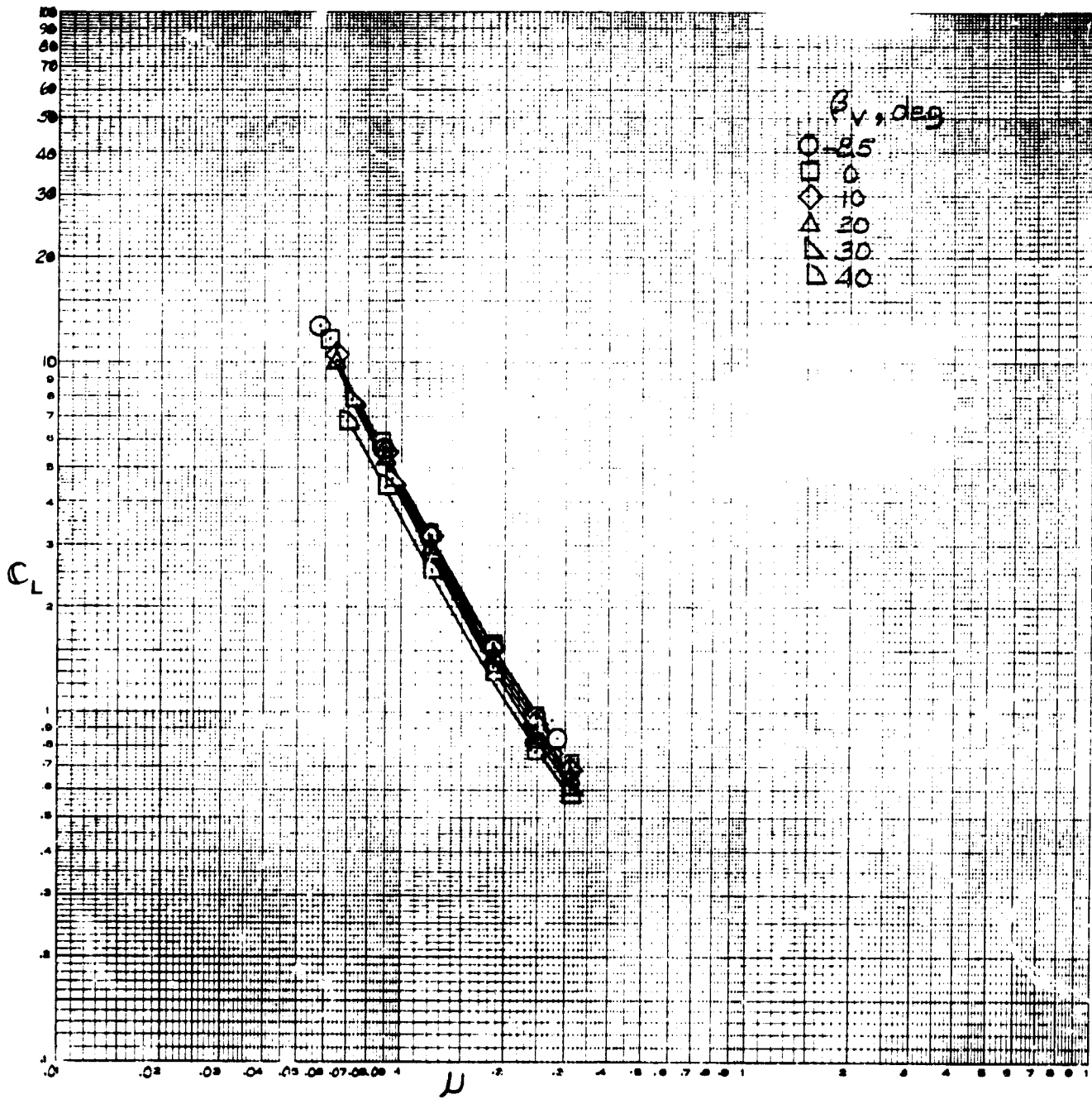
(c)  $C_L$  vs  $\mu$ ,  $\delta_f = 0^\circ$ .

Figure 13.- Continued.



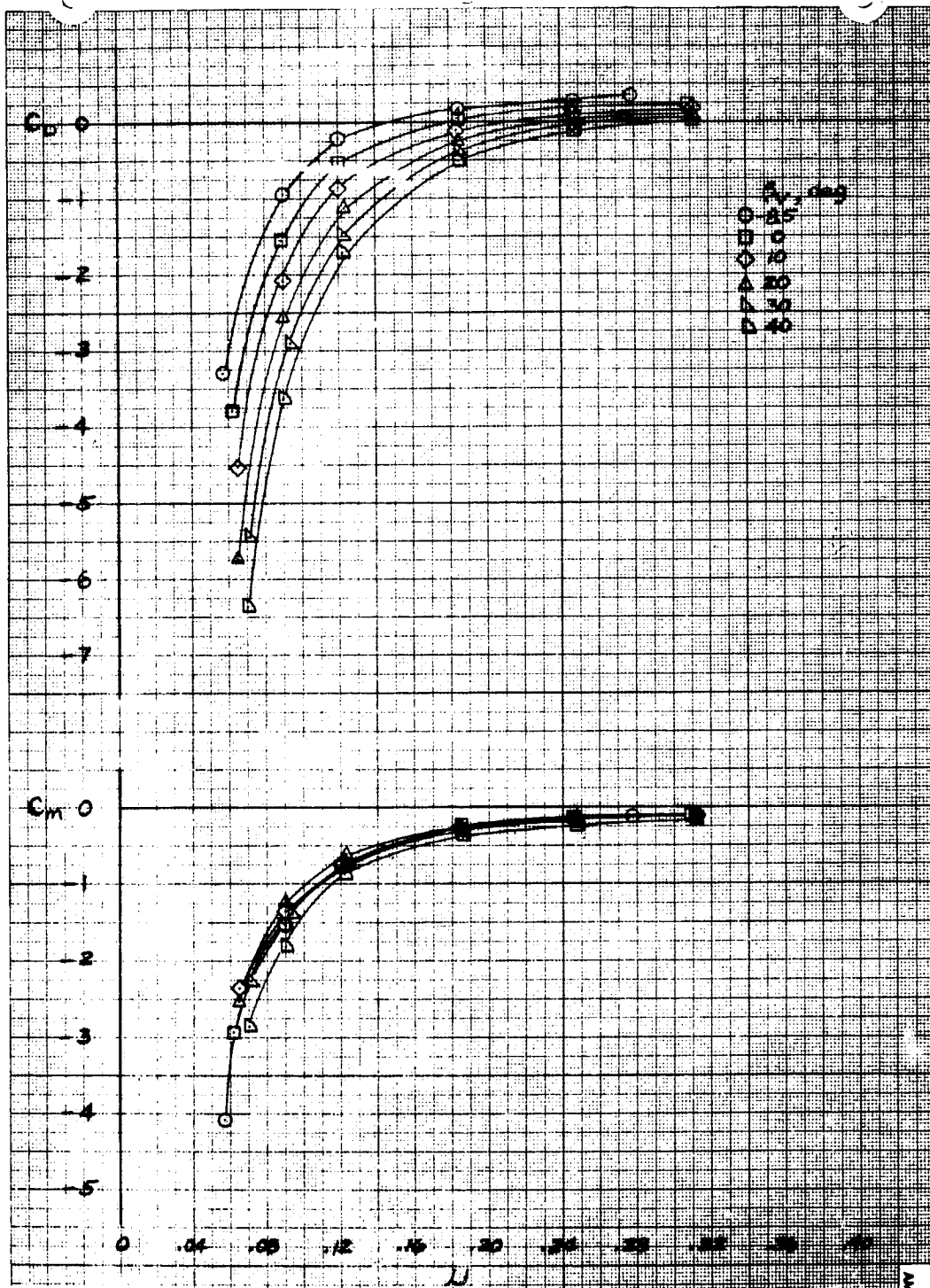
(d)  $C_D, C_m$  vs  $u, \delta_f = 0^\circ$ .

Figure 13.- Concluded.



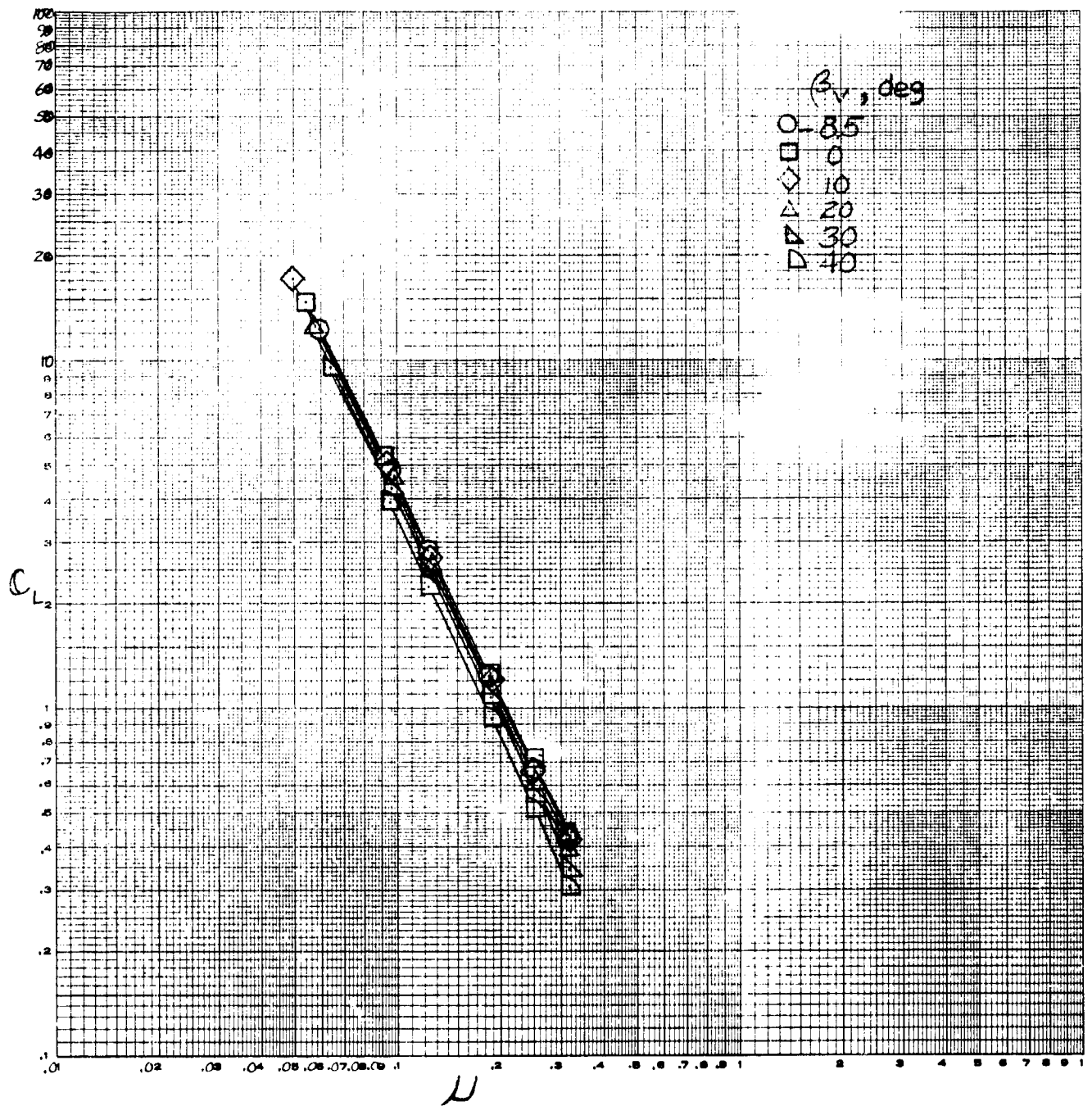
(a)  $C_L$  vs  $\mu$ ,  $\delta_f = 45^\circ$ .

Figure 14.- The effect of tip-speed ratio on longitudinal characteristics; 4 fans,  $\theta_v = 36^\circ$ , tail on,  $i_t = 0^\circ$ .



(b)  $C_D, C_M$  vs  $\alpha, \delta_f = 45^\circ$ .

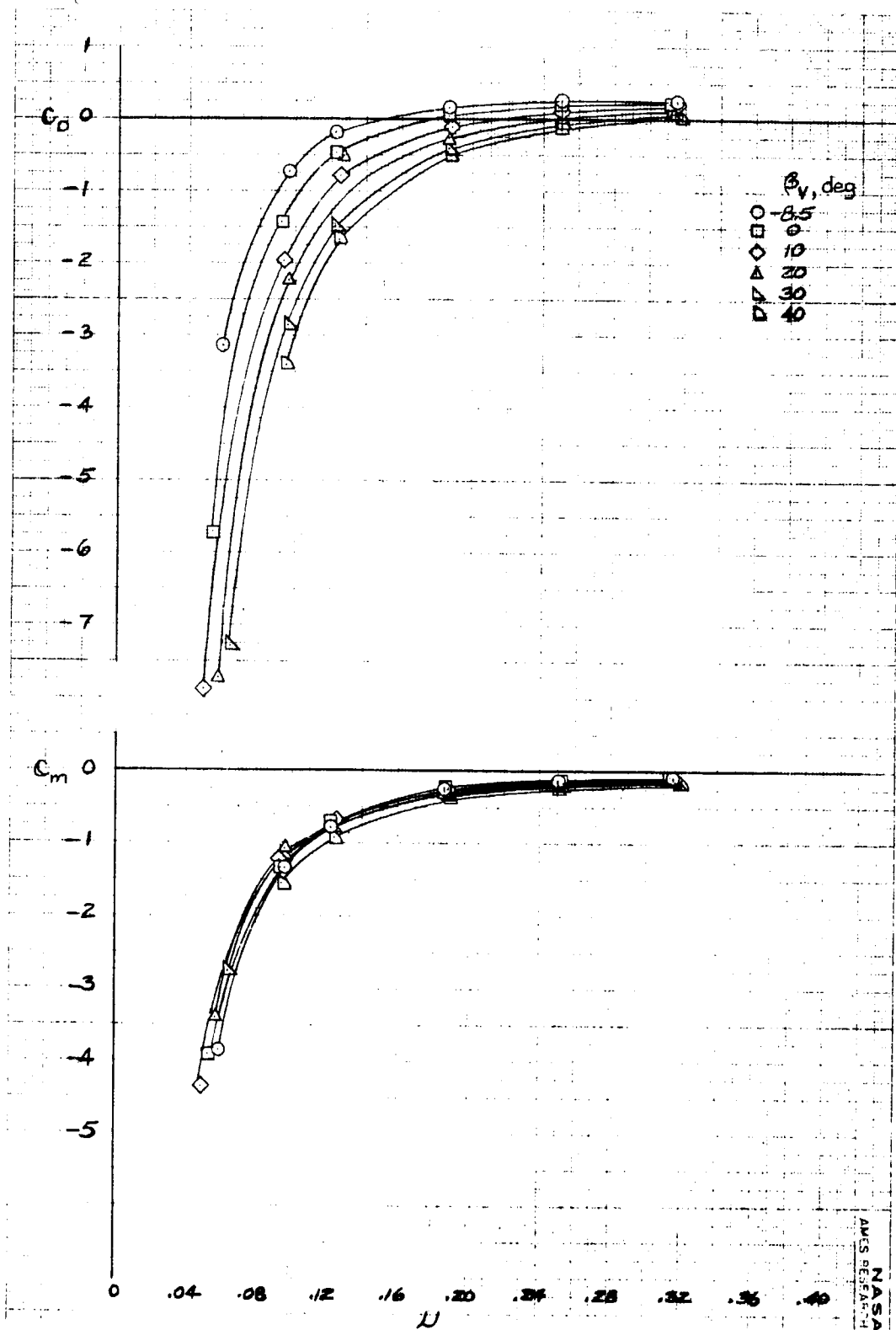
Figure 14.- Continued.



(c)  $C_L$  vs  $M$ ,  $\delta_f = 0^\circ$ .

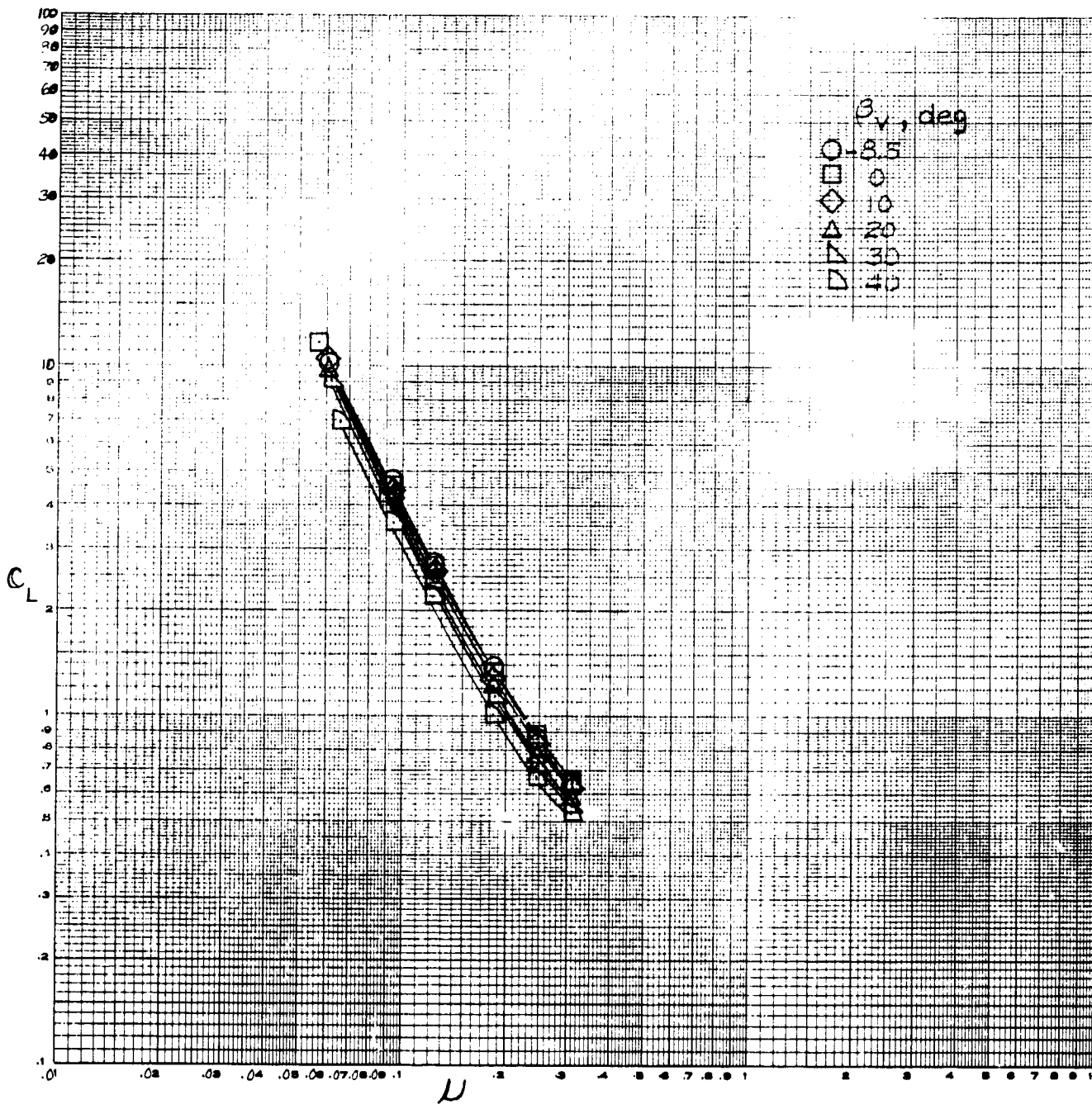
Figure 14.- Continued.





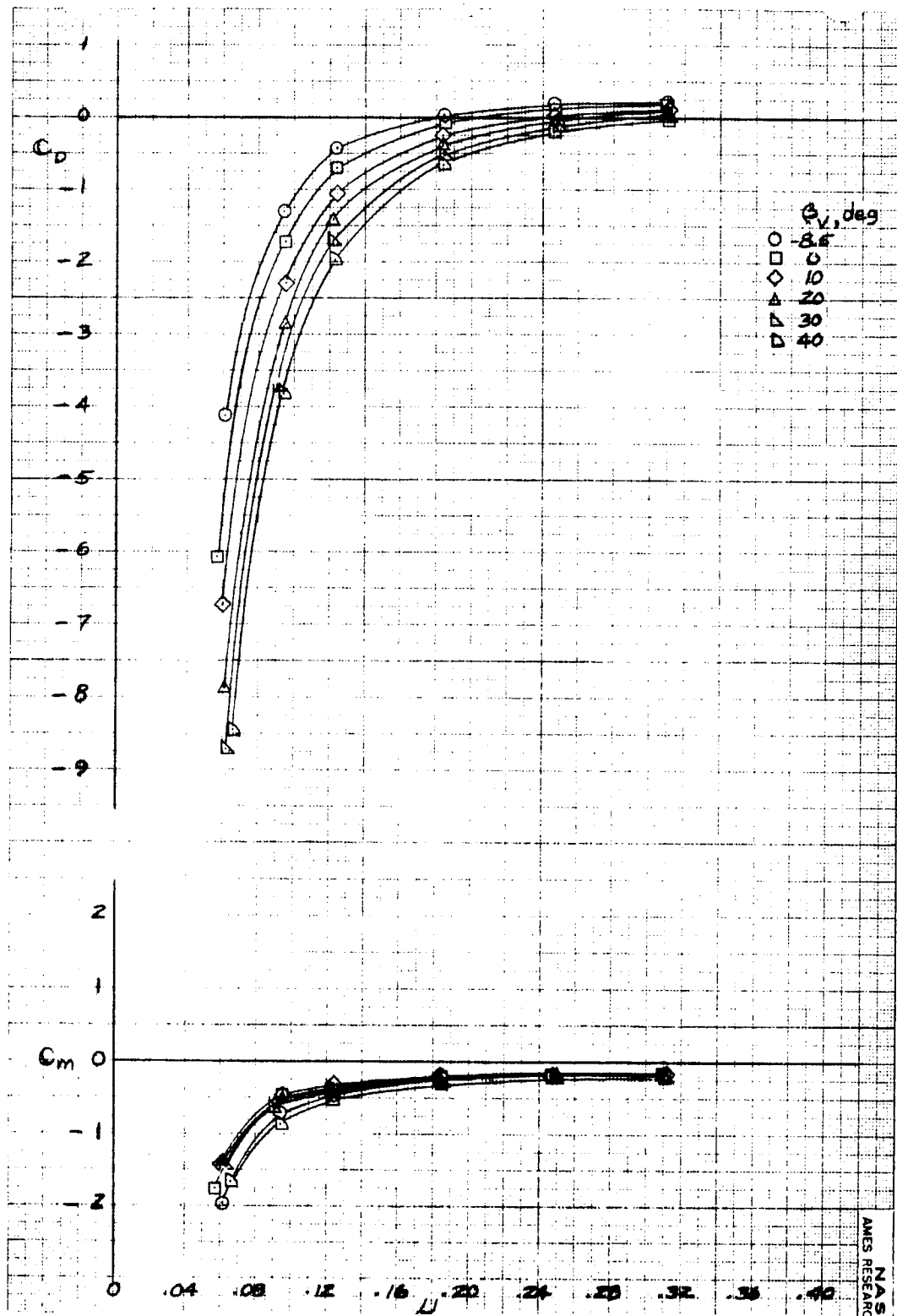
(d)  $C_D, C_m$  vs  $M, \delta_f = 0^\circ$ .

Figure 14.- Concluded.



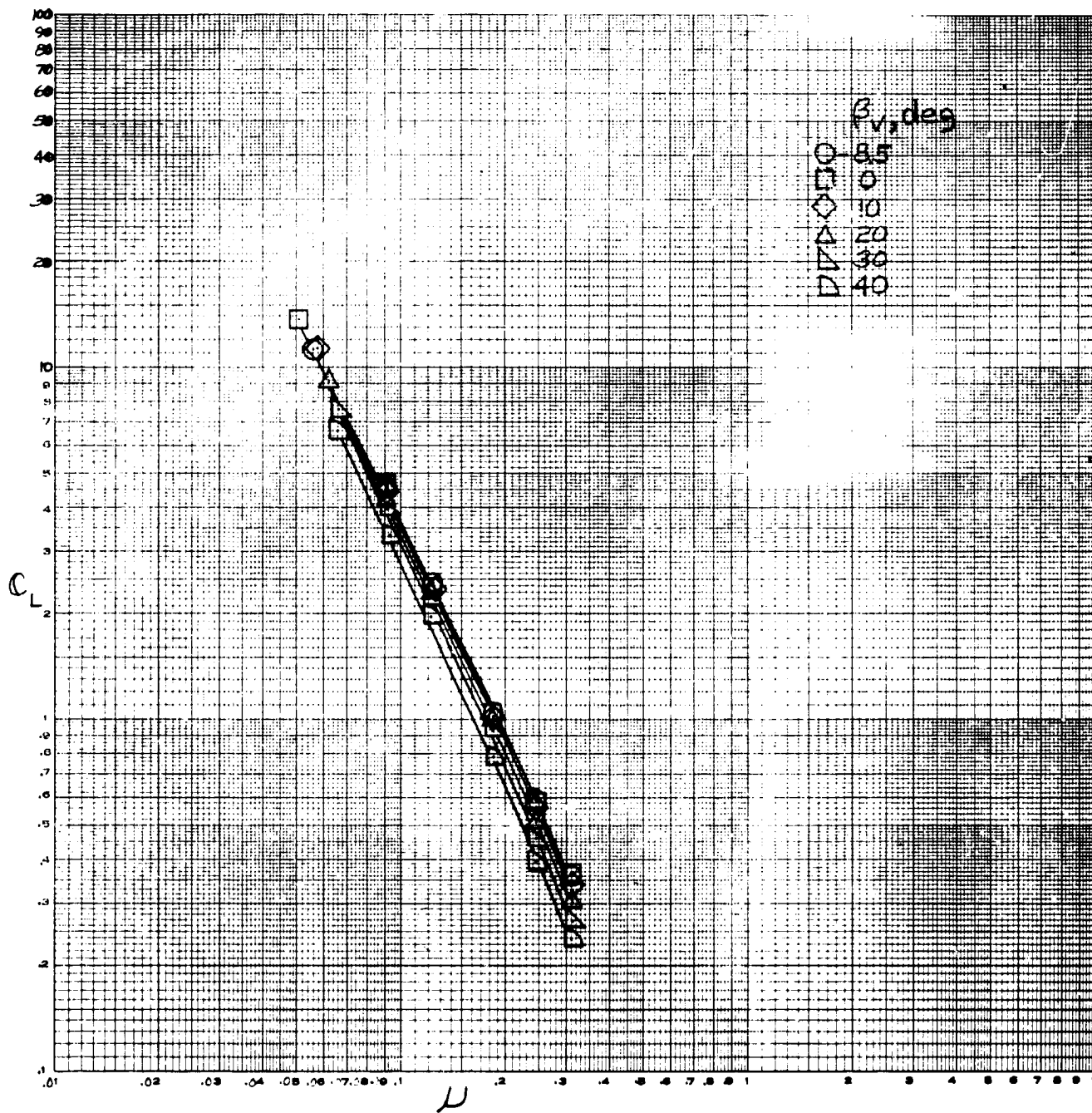
(a)  $C_L$  vs  $\mu$ ,  $\delta_f = 45^\circ$ .

Figure 15.- The effect of tip-speed ratio on longitudinal characteristics; 4 fans,  $\theta_v = 20^\circ$ , tail off.



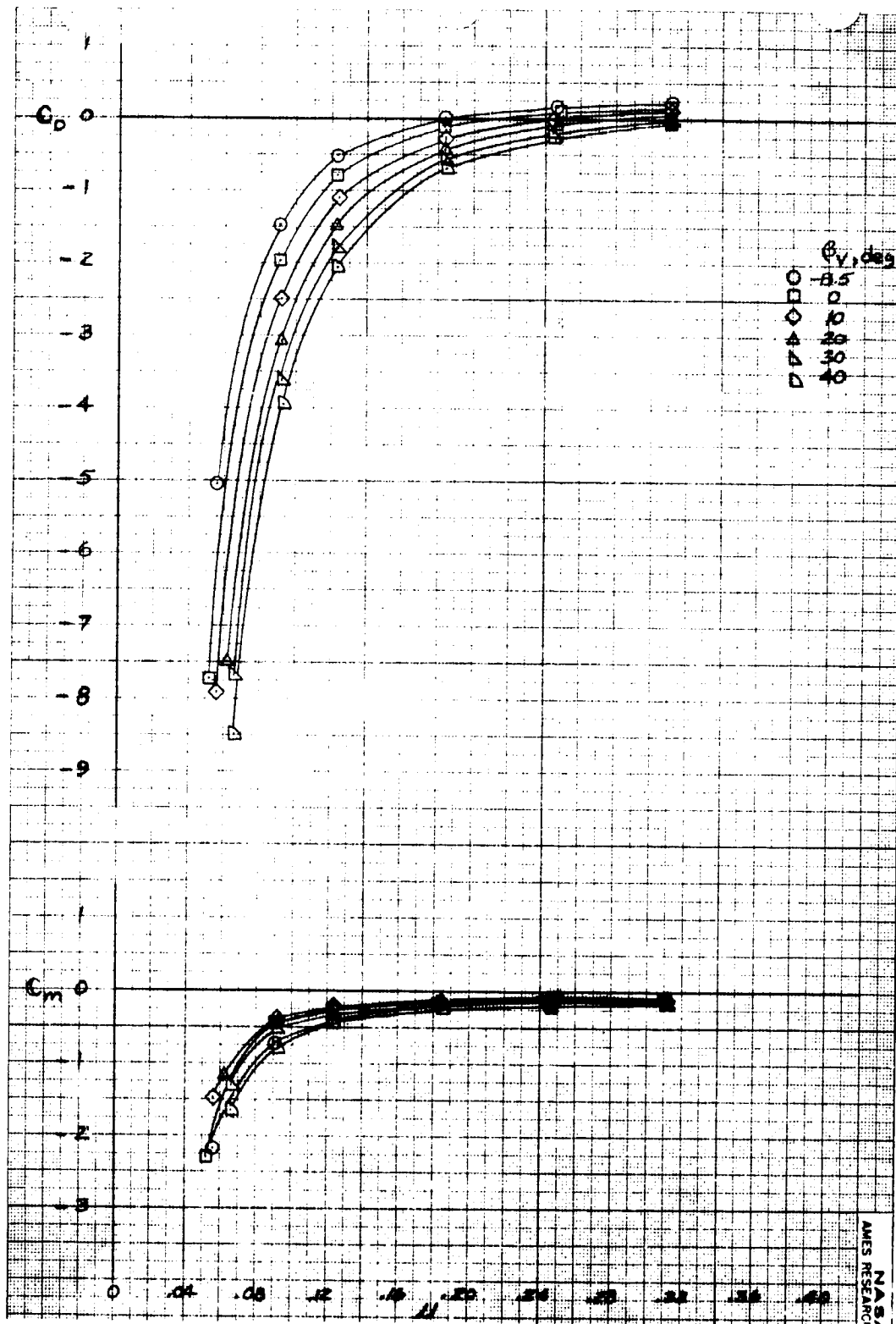
(b)  $C_D, C_m$  vs  $\mu, \delta_f = 45^\circ$ .

Figure 15.- Continued.



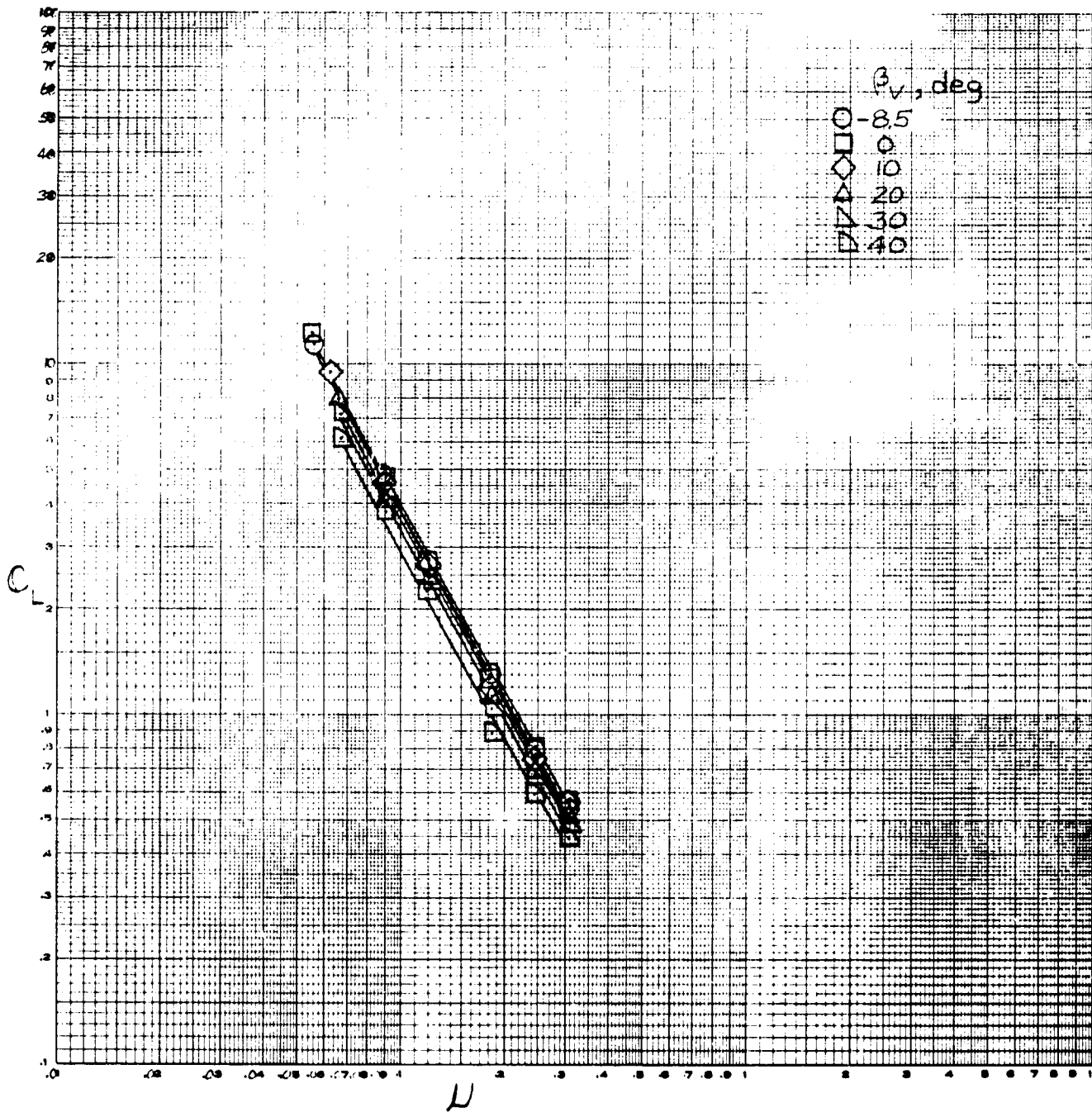
(c)  $C_L$  vs  $\mu$ ,  $\delta_f = 0^\circ$ .

Figure 15.- Continued.



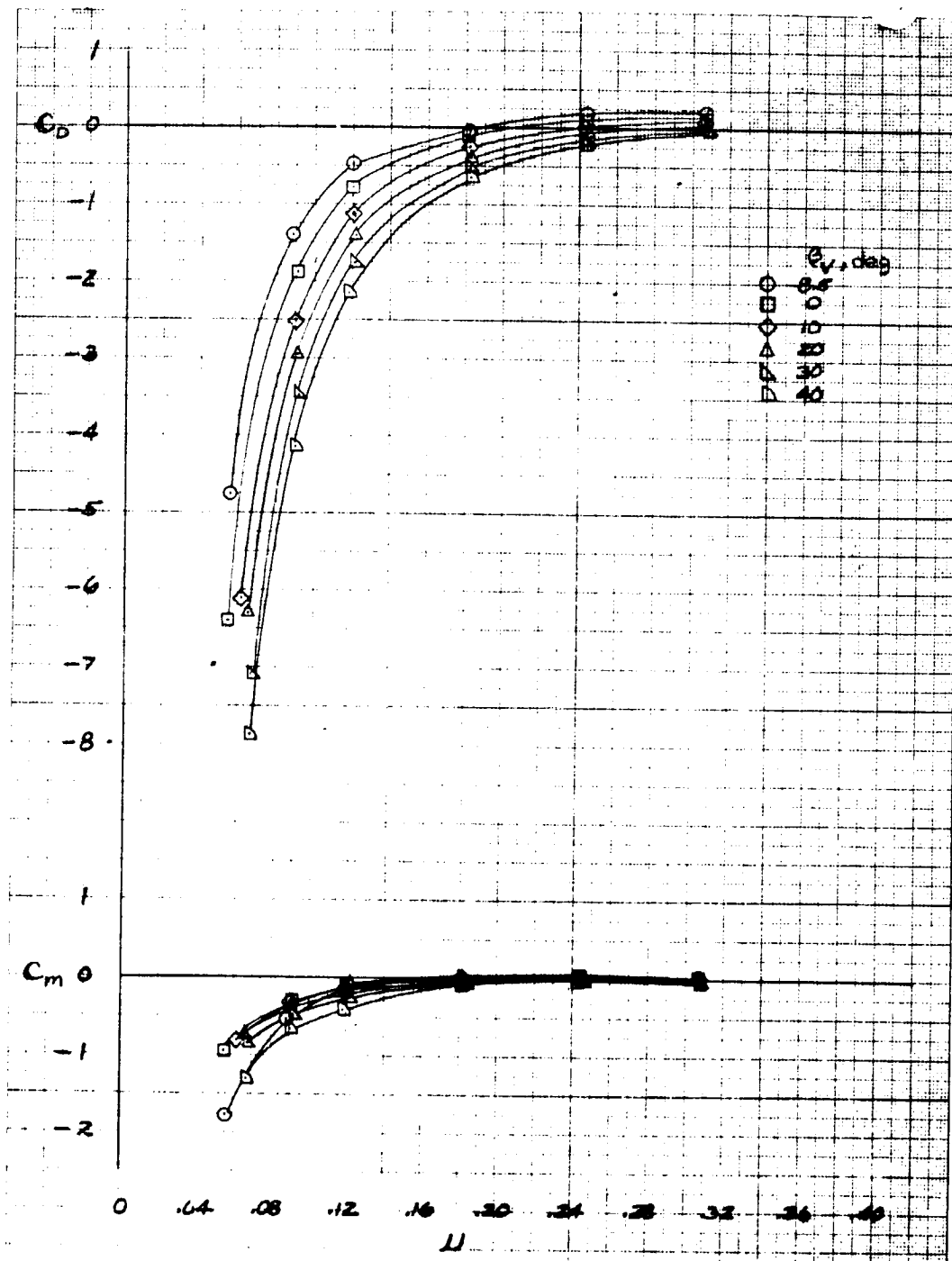
(d)  $C_D, C_m$  vs  $\mu, \delta_f = 0^\circ$ .

Figure 15.- Concluded.



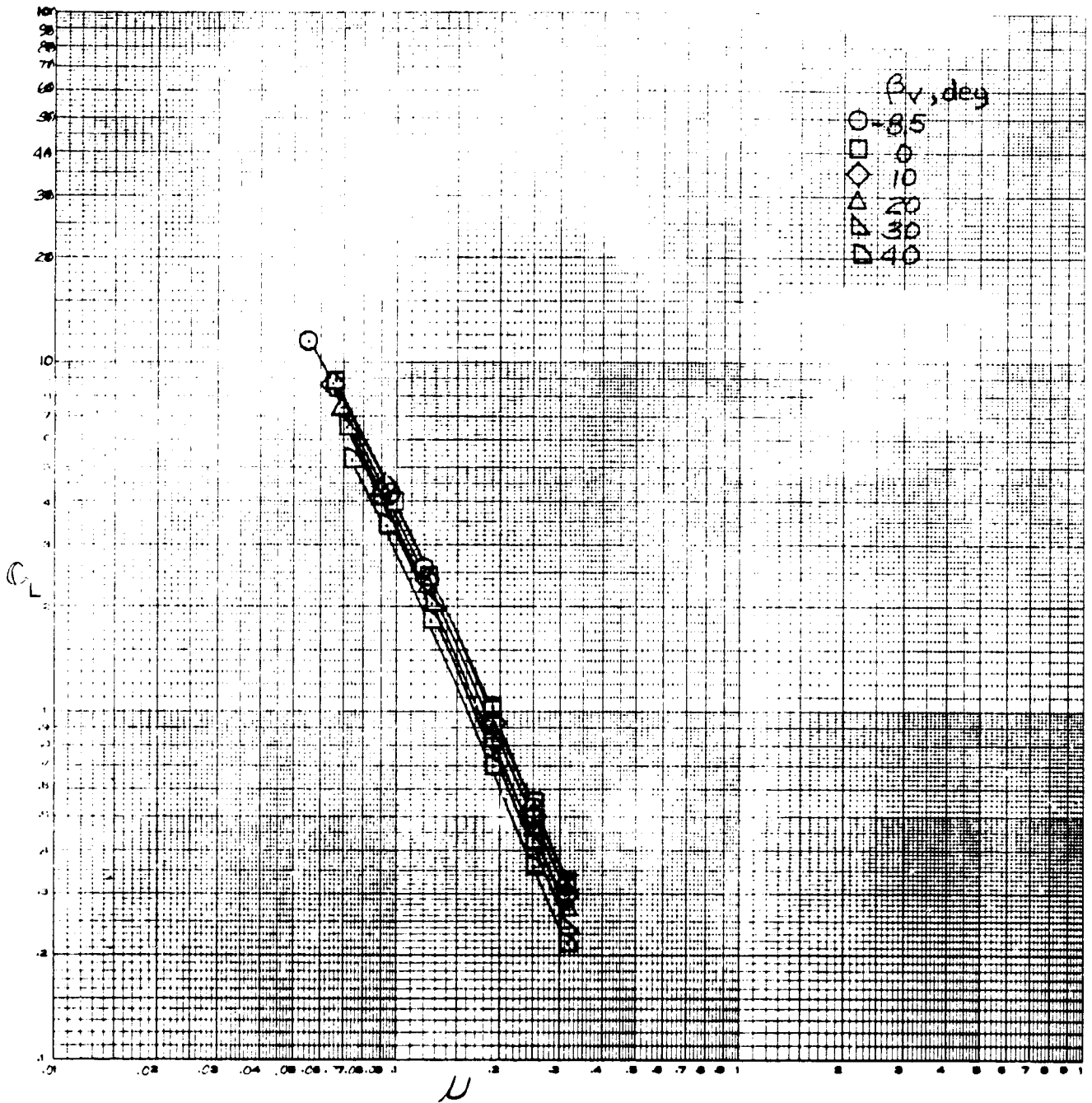
(a)  $C_L$  vs  $\mu$ ,  $\delta_f = 45^\circ$ .

Figure 16.- The effect of tip-speed ratio on longitudinal characteristics; 4 fans,  $\theta_v = 20^\circ$ , tail on,  $i_t = 0^\circ$ .



(b)  $C_D, C_m$  vs  $\mu, \delta_f = 45^\circ$ .

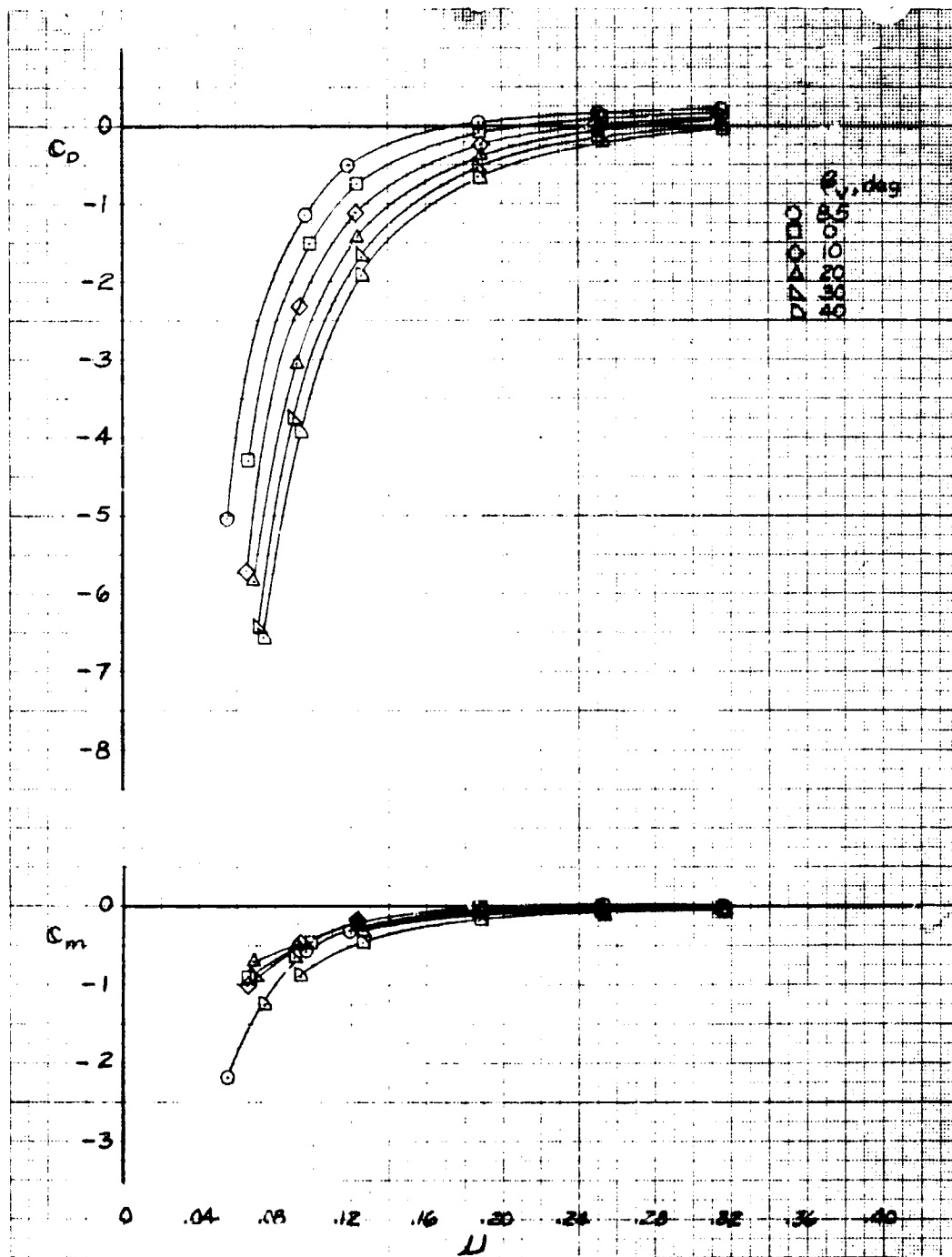
Figure 16.- Continued.



(c)  $C_L$  vs  $\mu$ ,  $\delta_f = 0^\circ$ .

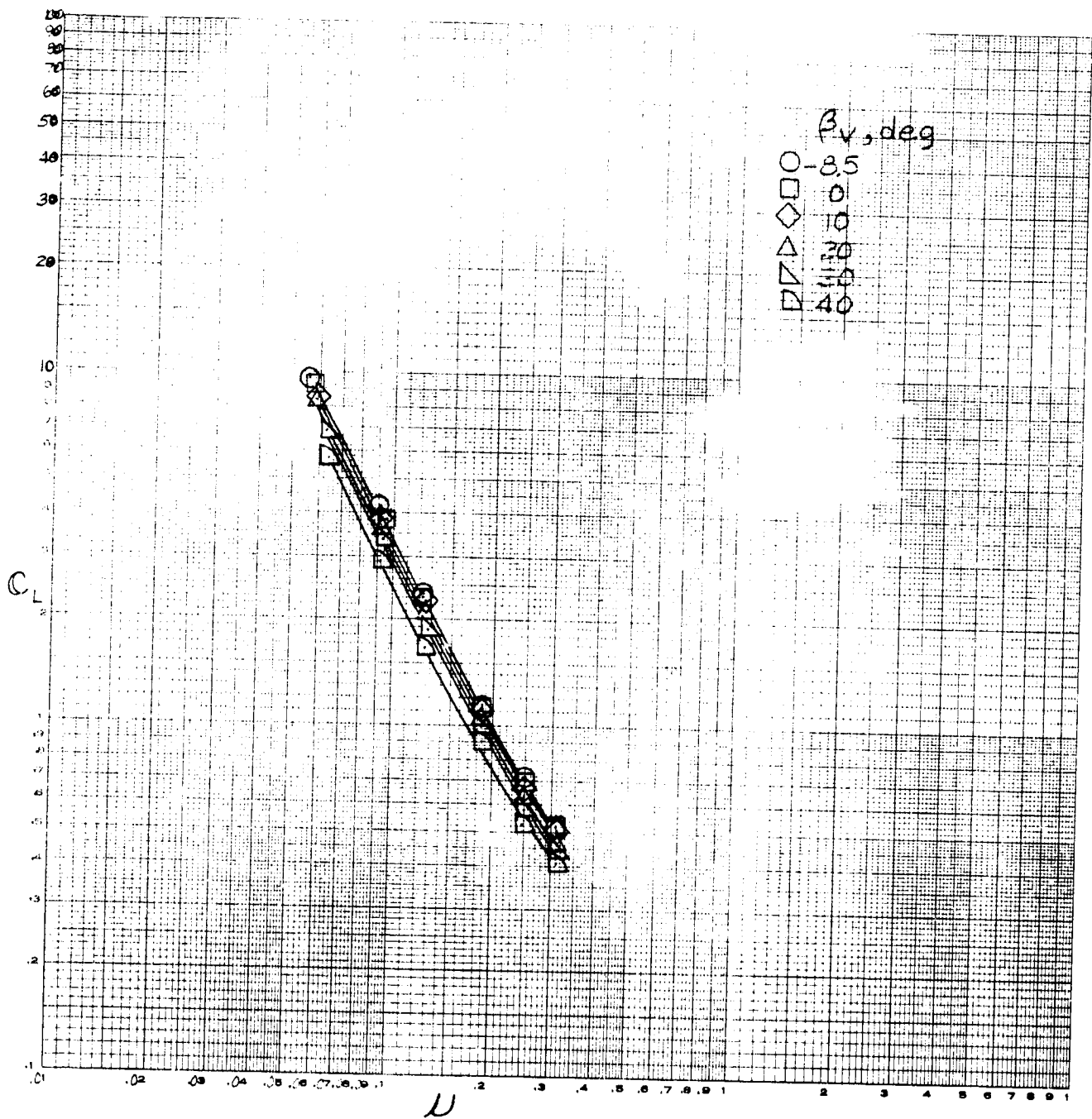
Figure 16.- Continued.





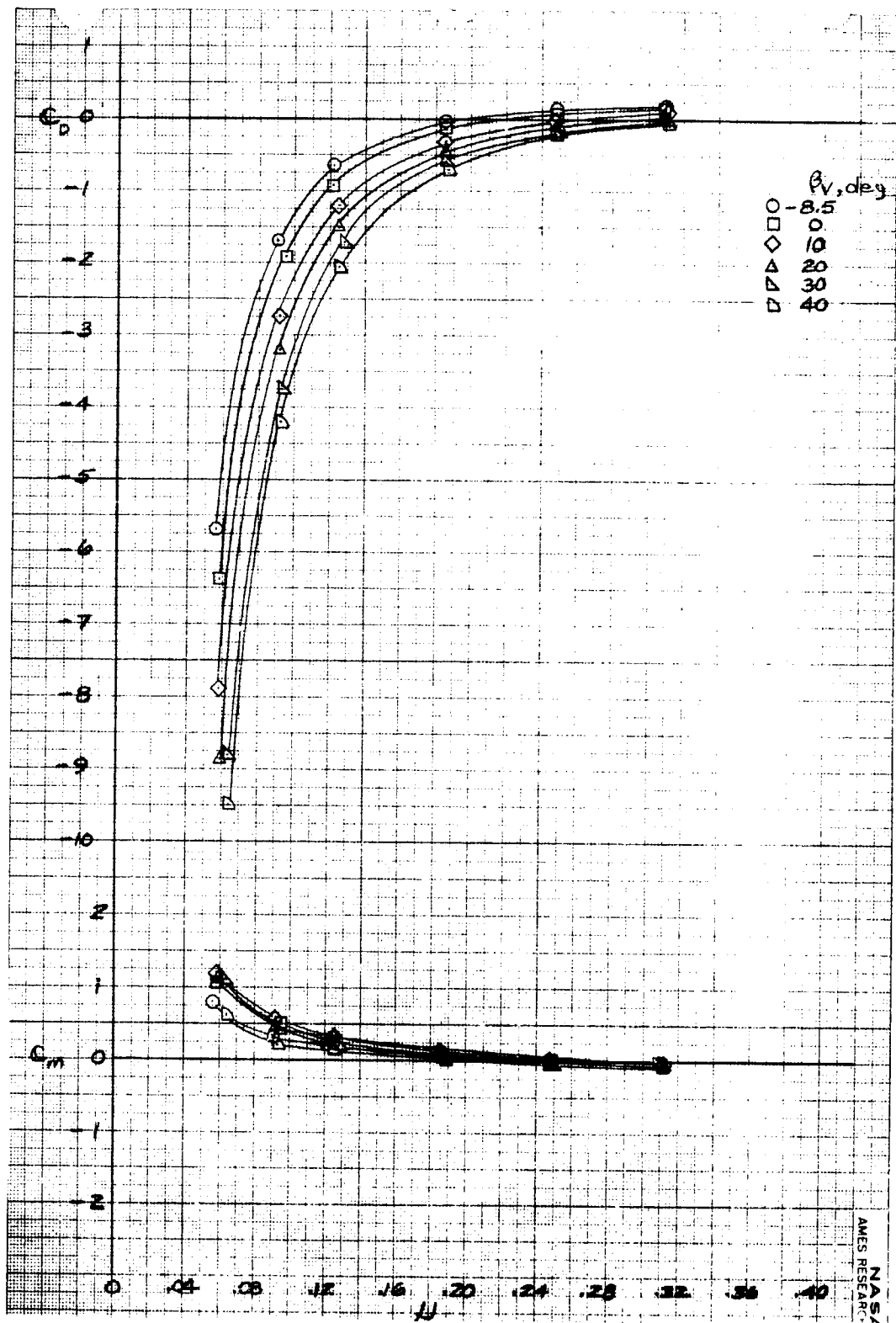
(d)  $C_D, C_m$  vs  $u, \delta_f = 0^\circ$

Figure 16.- Concluded.



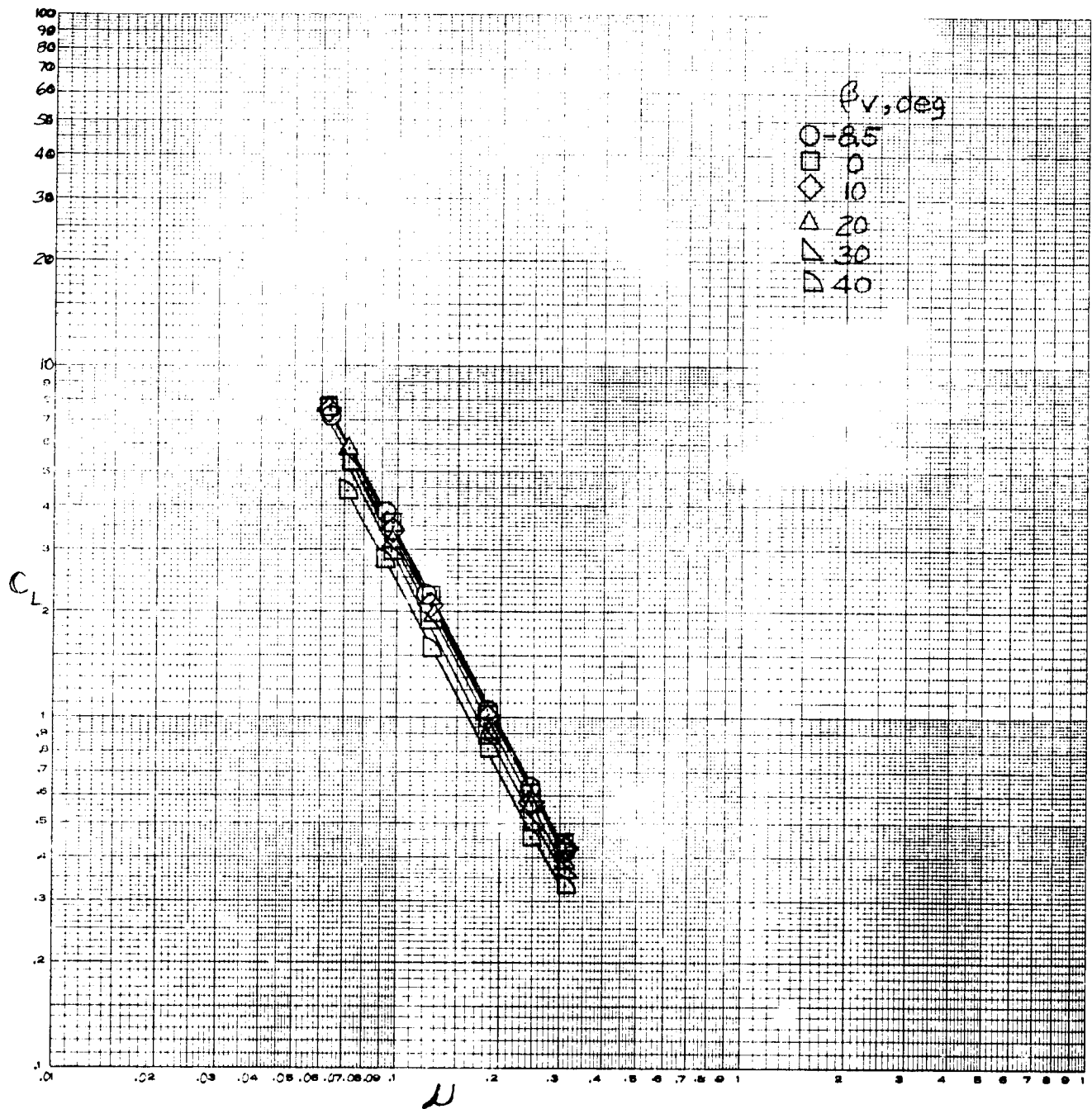
(a)  $C_L$  vs  $\mu$ ,  $\delta_f = 45^\circ$ .

Figure 17.- The effect of tip-speed ratio on longitudinal characteristics; 4 fans,  $\theta_v = 7^\circ$ , tail off.



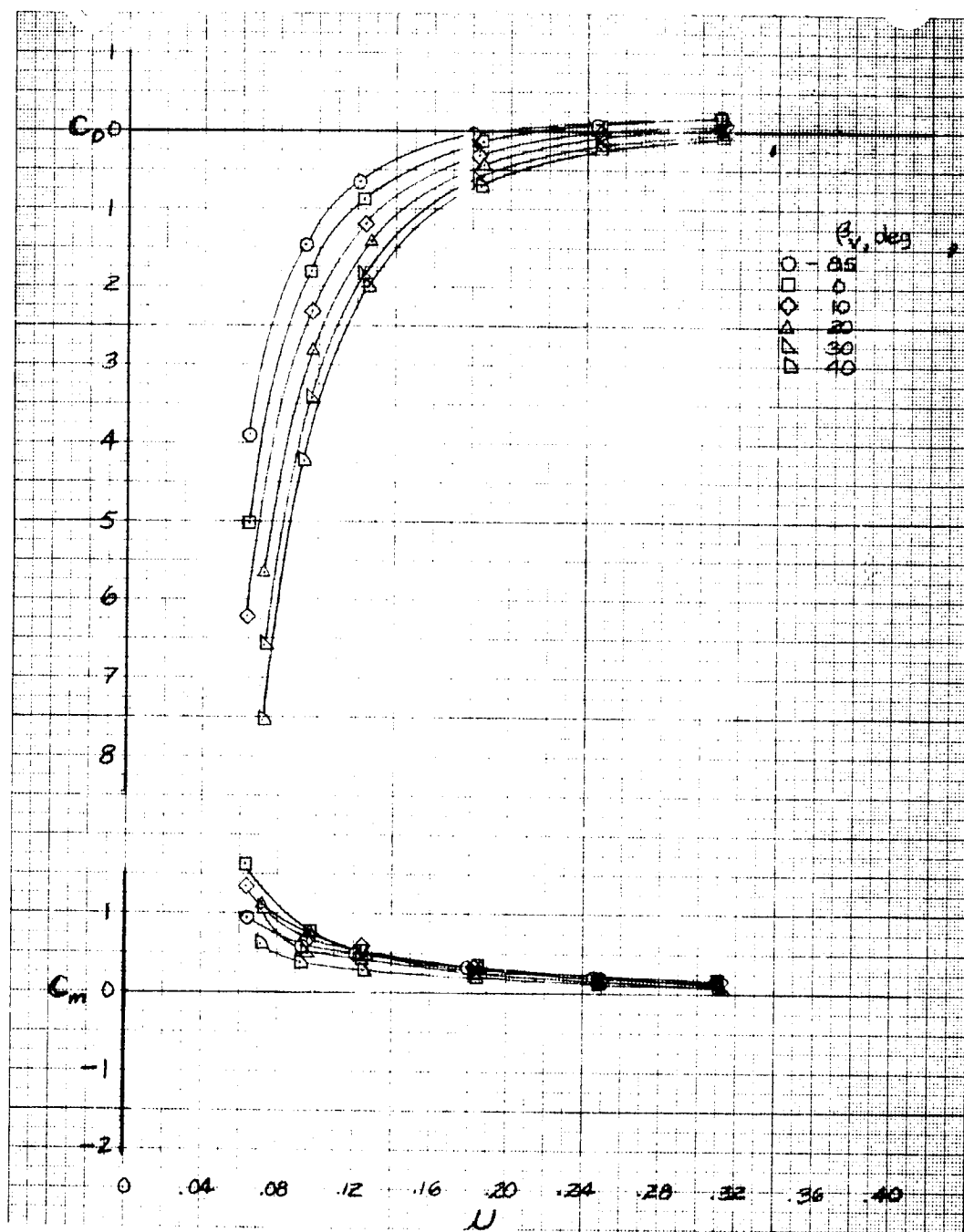
(b)  $C_D, C_m$  vs  $\mu, \delta_f = 45^\circ$ .

Figure 17.- Concluded.



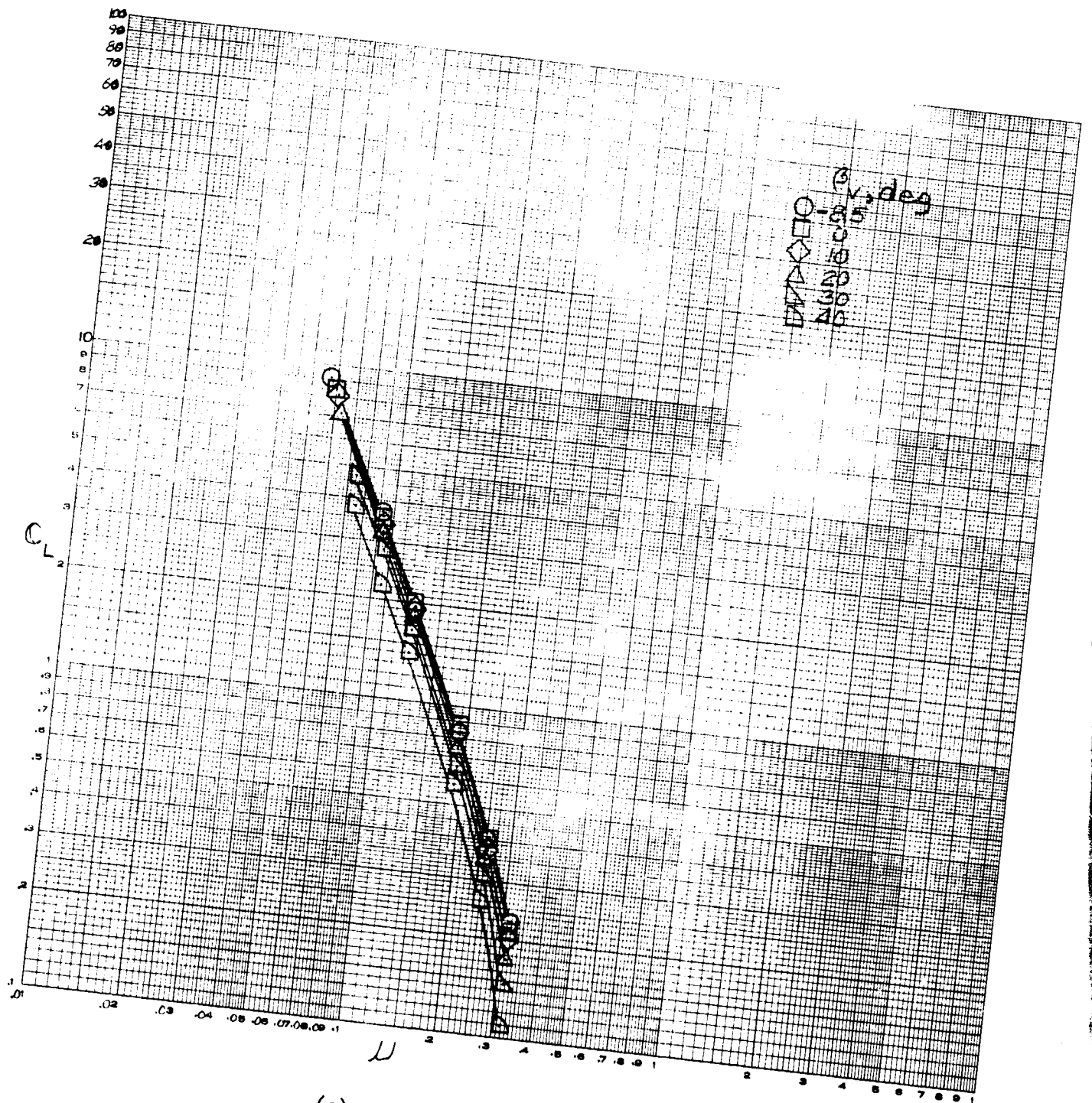
(a)  $C_L$  vs  $\mu$ ,  $\delta_f = 45^\circ$ .

Figure 18.- The effect of tip-speed ratio on longitudinal characteristics; 4 fans,  $\theta_v = 7^\circ$ , tail on,  $i_t = 0^\circ$ .

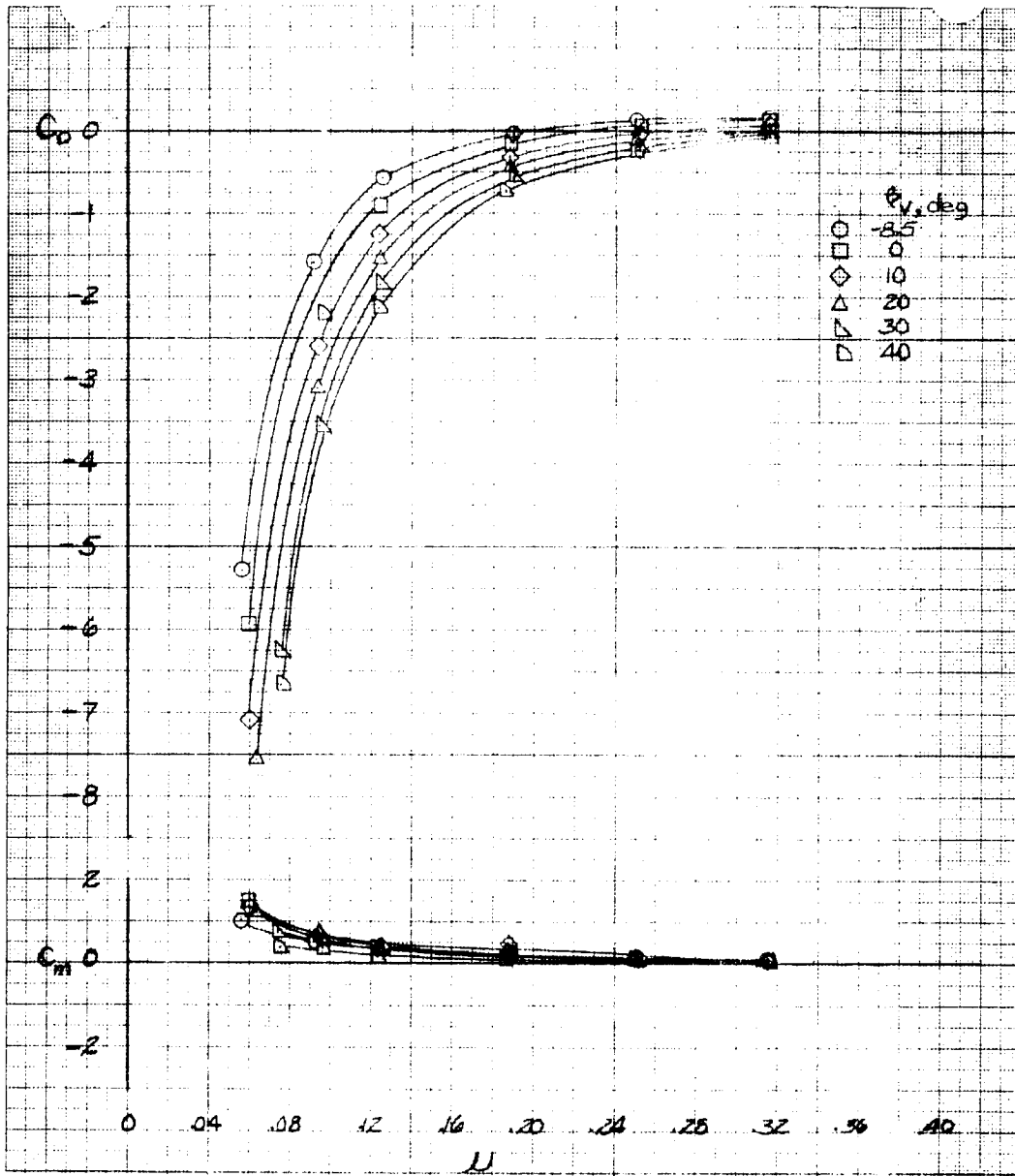


(b)  $C_D, C_m$  vs  $M, \delta_f = 45^\circ$ .

Figure 18.- Continued.

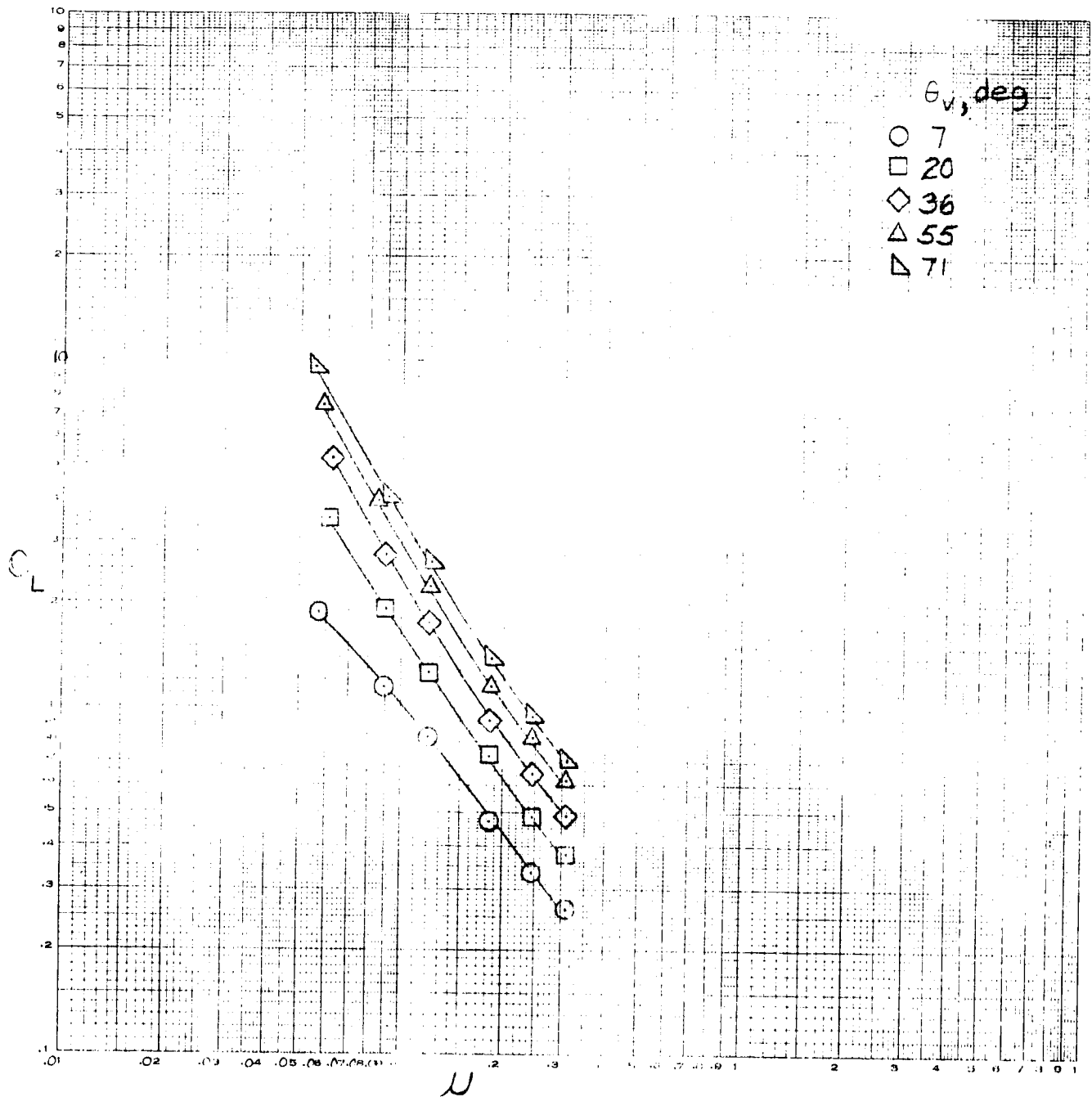


(c)  $C_L$  vs  $M$ ,  $\delta_f = 0^\circ$ .  
 Figure 18.- Continued.



(d)  $C_D, C_m$  vs  $\alpha, \delta_f = 0^\circ$ .

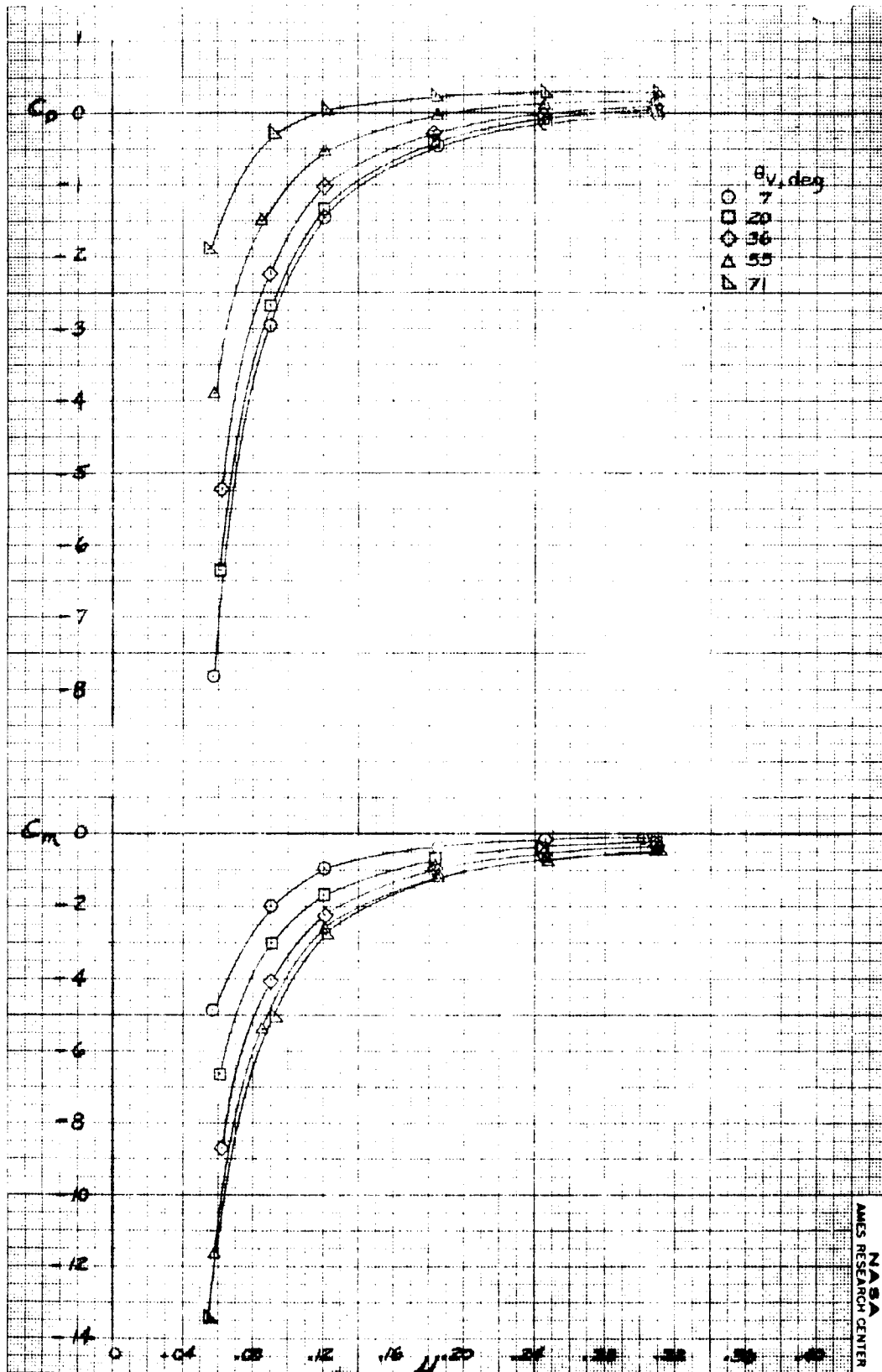
Figure 18.- Concluded.



(a)  $C_L$  vs  $u$

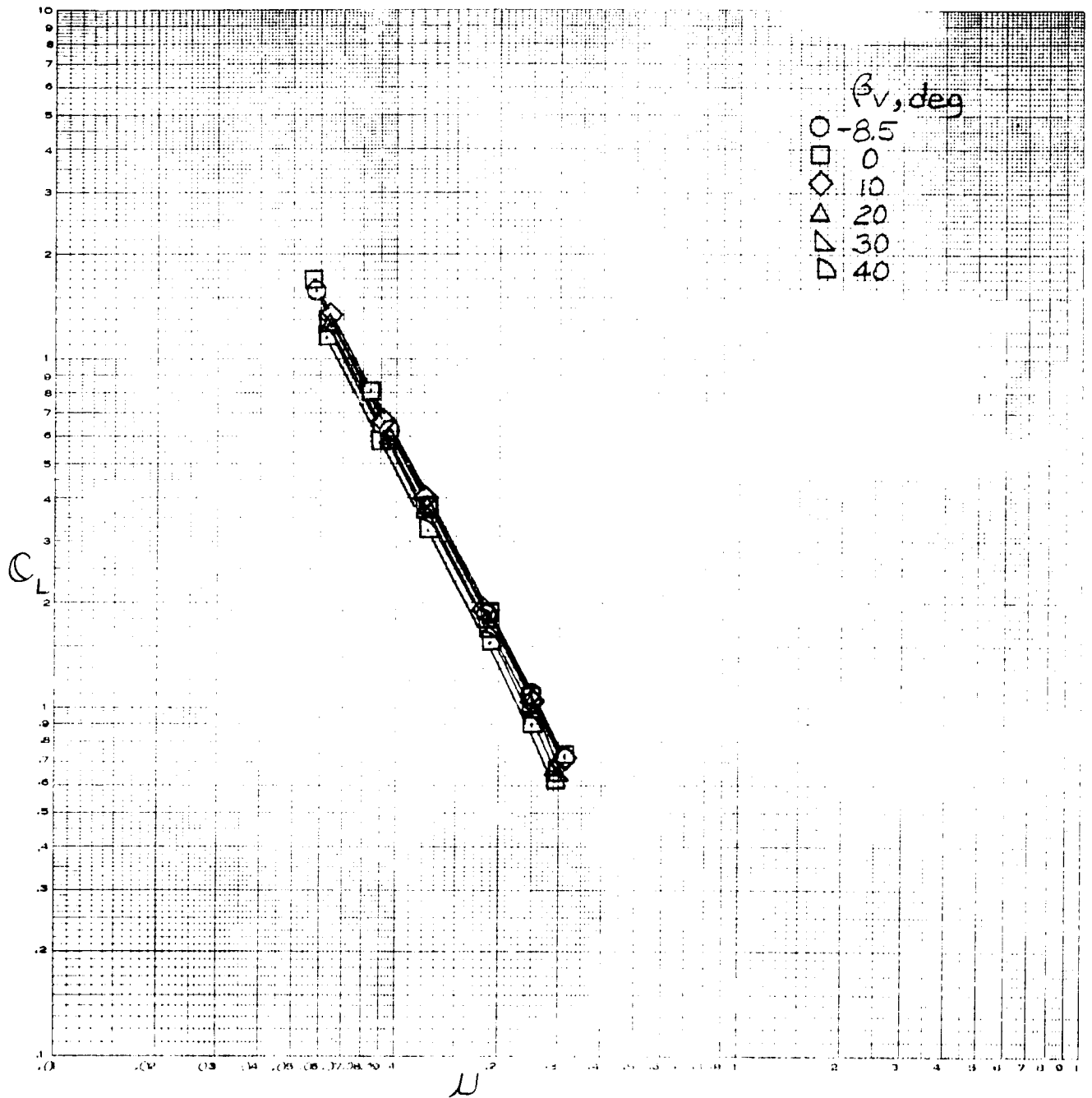
Figure 19.- The effect of tip-speed ratio on longitudinal characteristics; lift-cruise fans only, tail on,  $i_t = 0^\circ$ ,  $\beta_v = 90^\circ$ ,  $\delta_f = 45^\circ$ .





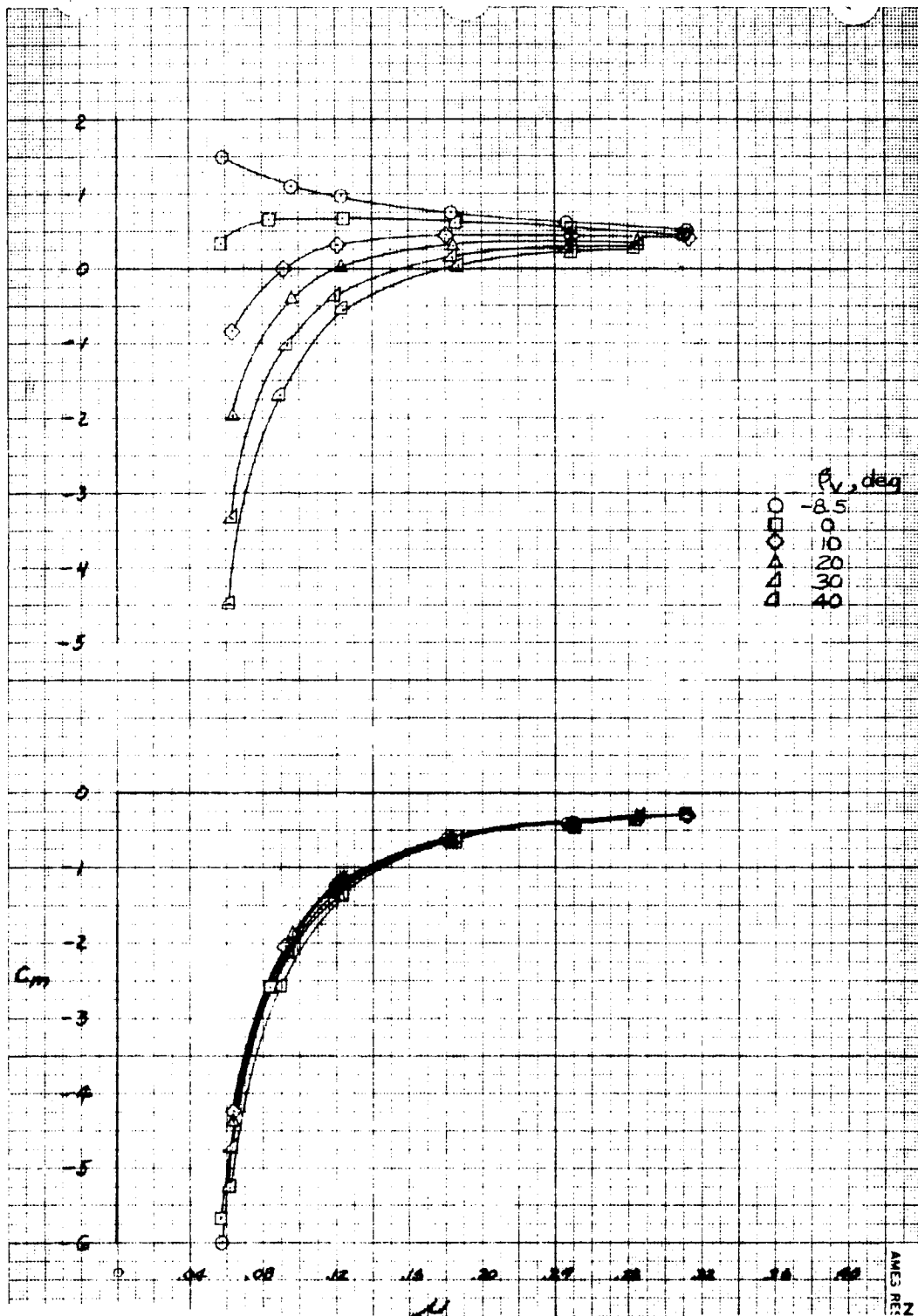
(b)  $C_D, C_m$  vs  $\mu$

Figure 19.- Concluded.



(a)  $C_L$  vs  $\mu$ ,  $\theta_v = 71^\circ$ .

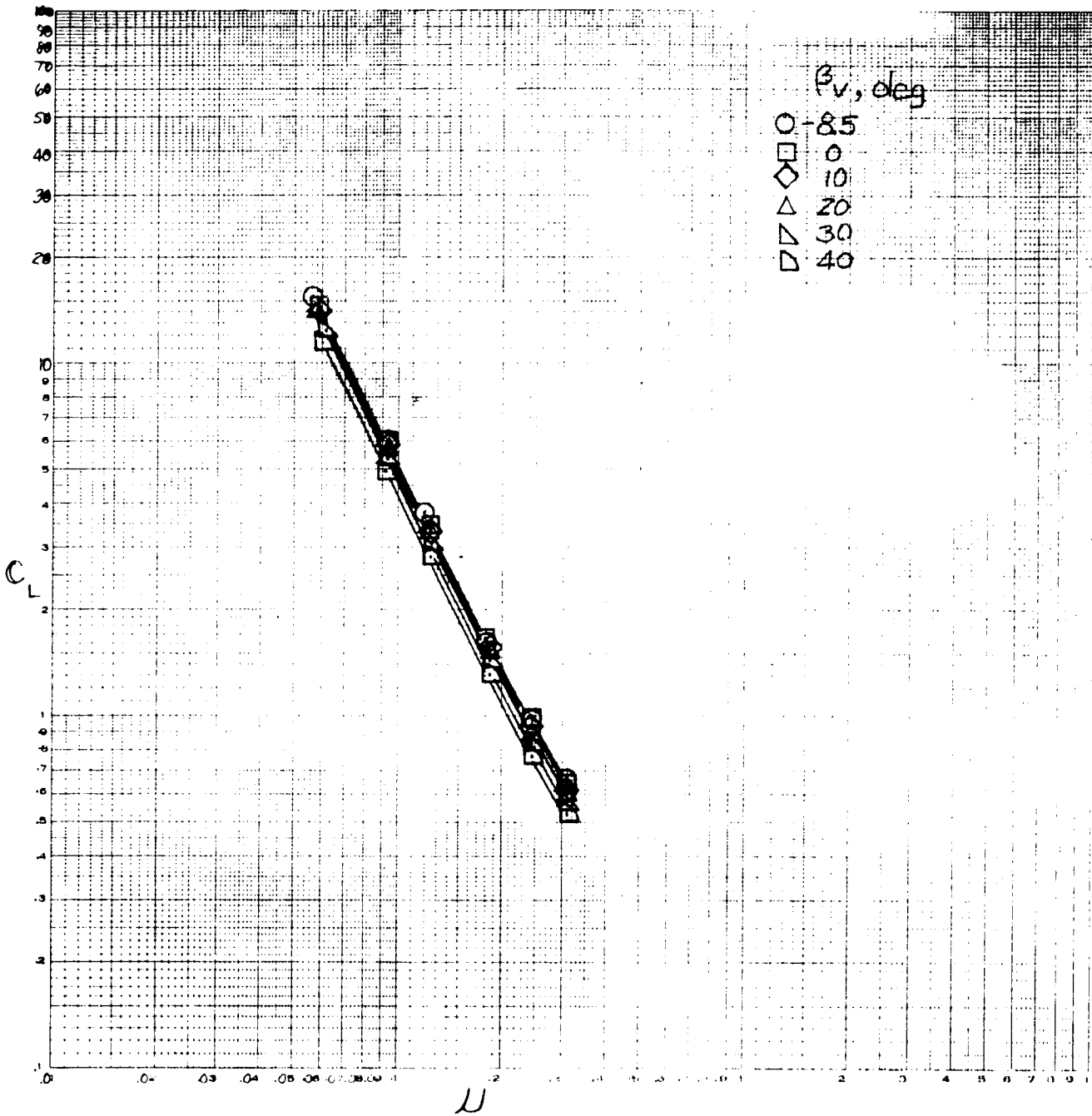
Figure 20.- The effect of tip-speed ratio on longitudinal characteristics; 4 fans, tail off,  $\delta_f = 0^\circ$ , lift-cruise fan exit carriage angle =  $65^\circ$ .



(b)  $C_D, C_m$  vs  $\mu, \theta_v = 71^\circ$ .

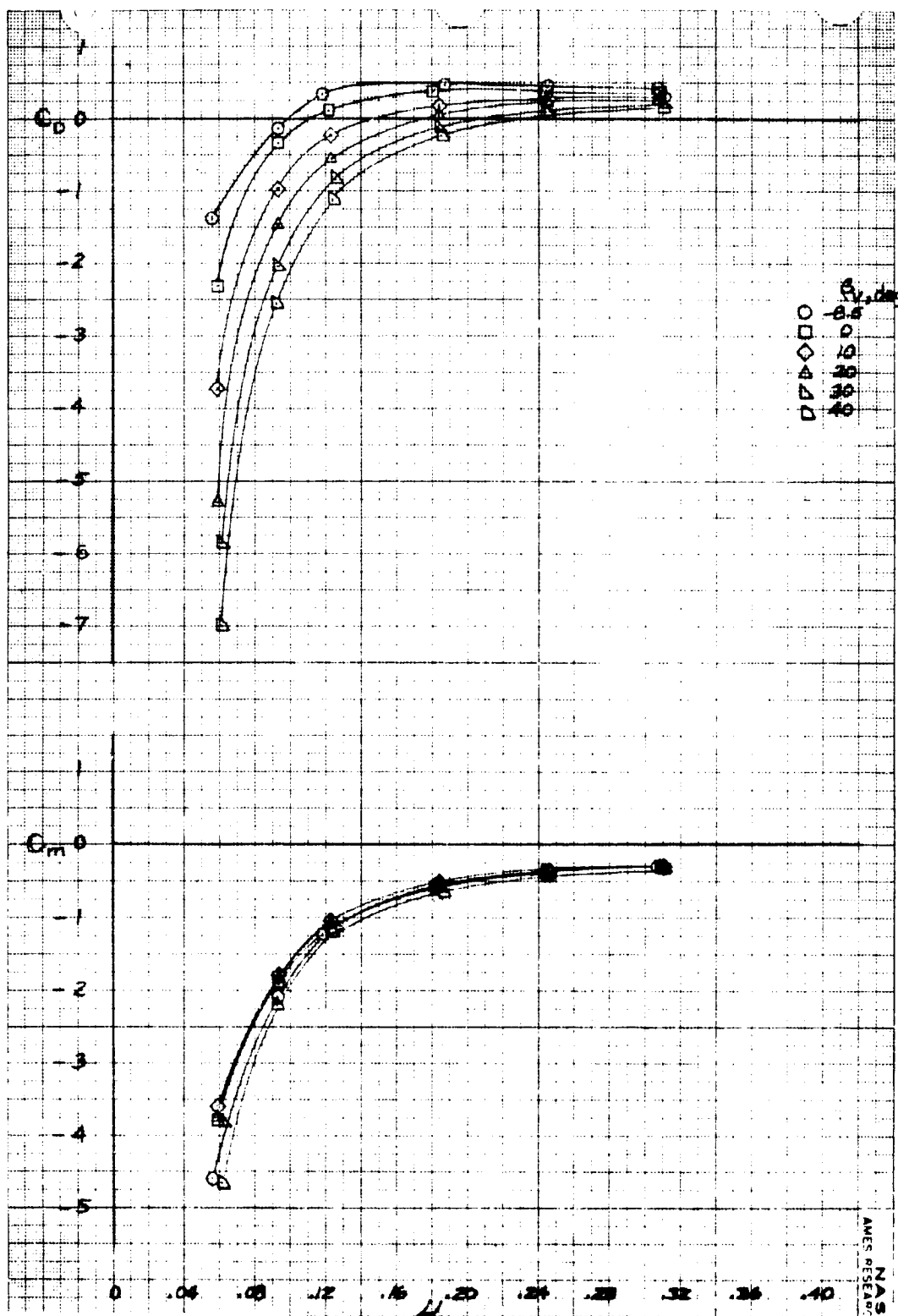
Figure 20.- Continued.

AMES RE  
N2



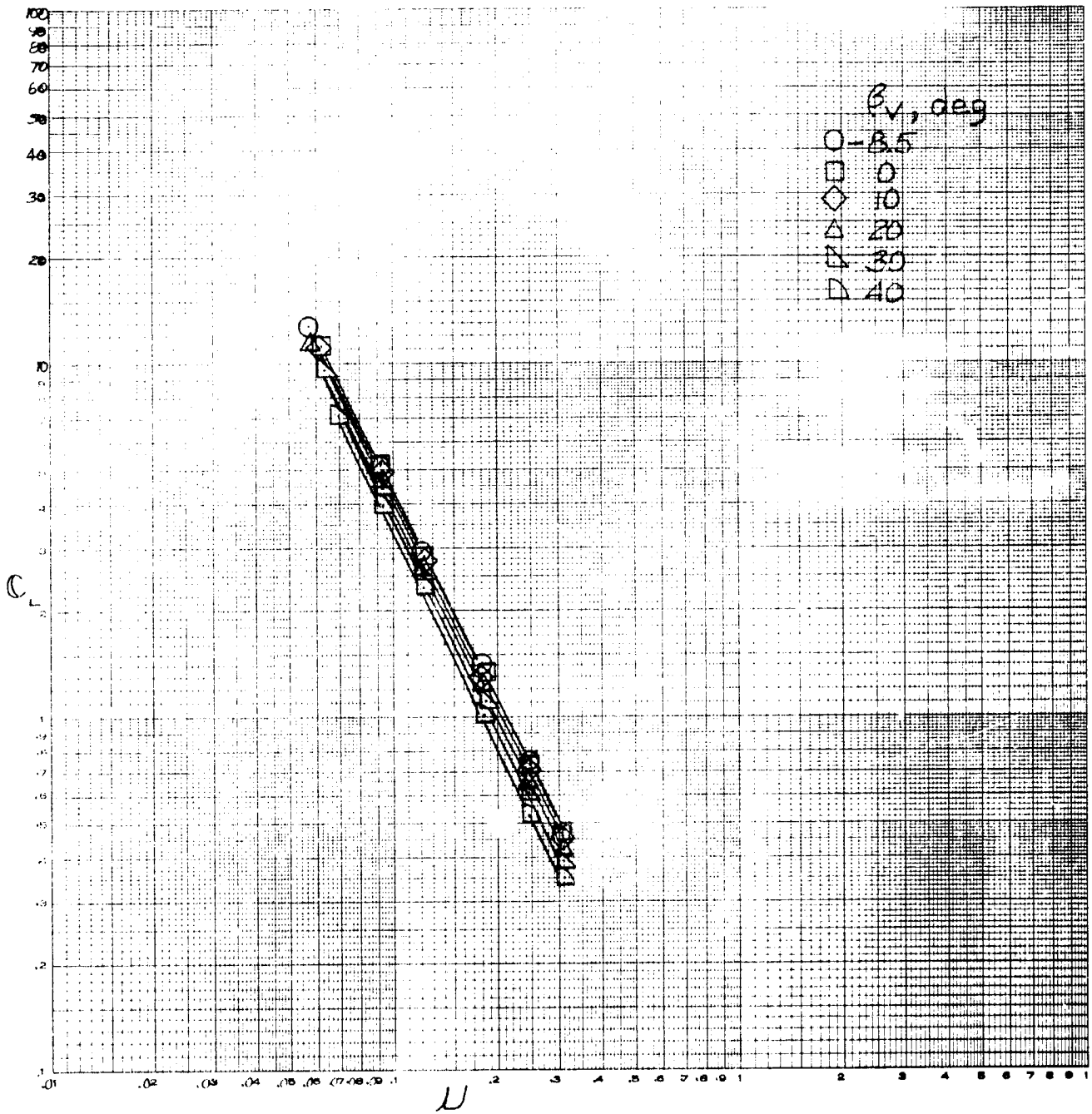
(c)  $C_L$  vs  $\mu$ ,  $\theta_v = 55^\circ$ .

Figure 20.- Continued.



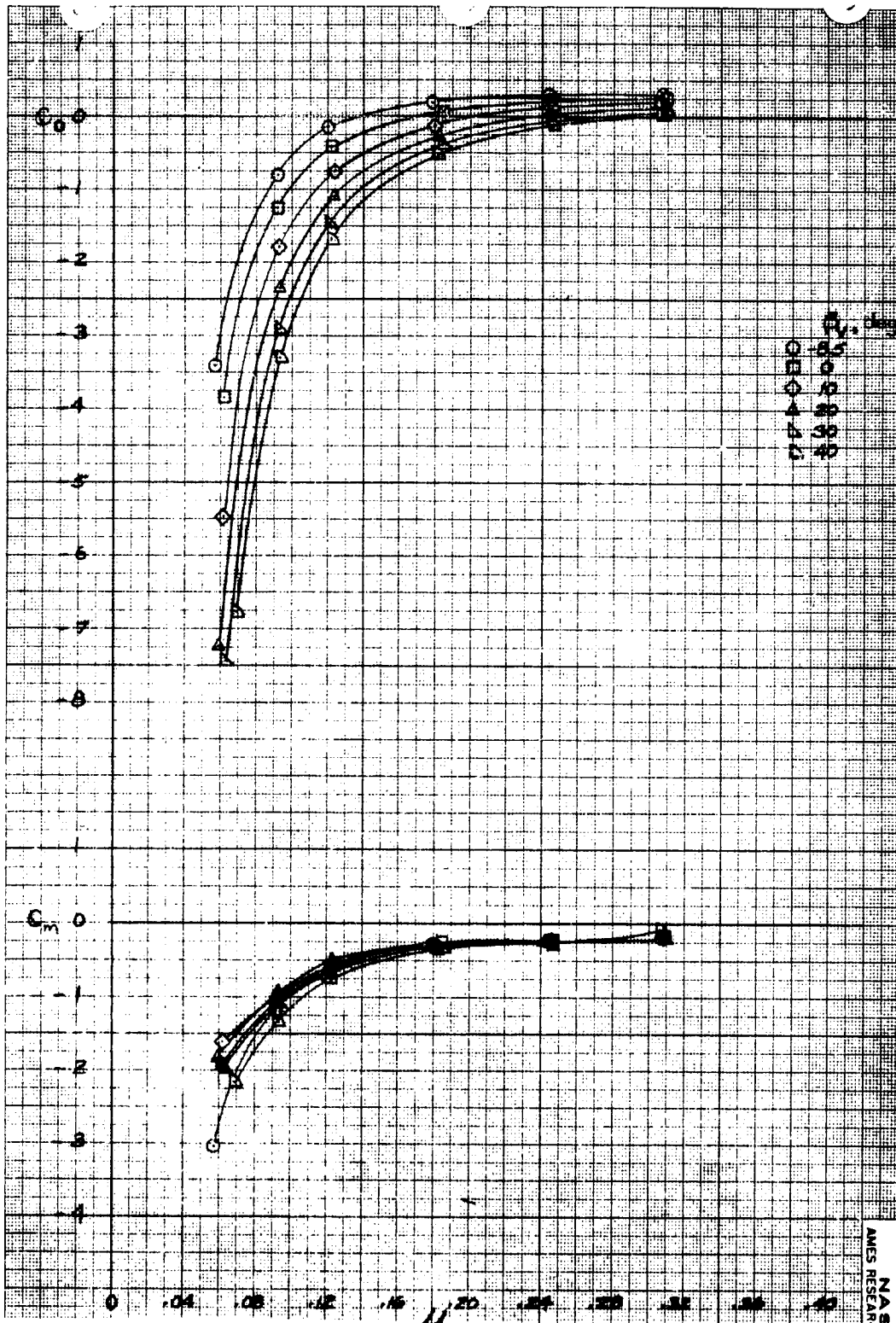
(d)  $C_D, C_m$  vs  $\mu, \theta_w = 55^\circ$ .

Figure 20.- Continued.



(e)  $C_L$  vs  $\mu$ ,  $\theta_v = 36^\circ$ .

Figure 20.- Continued.



(f)  $C_D, C_M$  vs  $\mu, \theta_v = 36^\circ$ .

Figure 20.- Concluded.

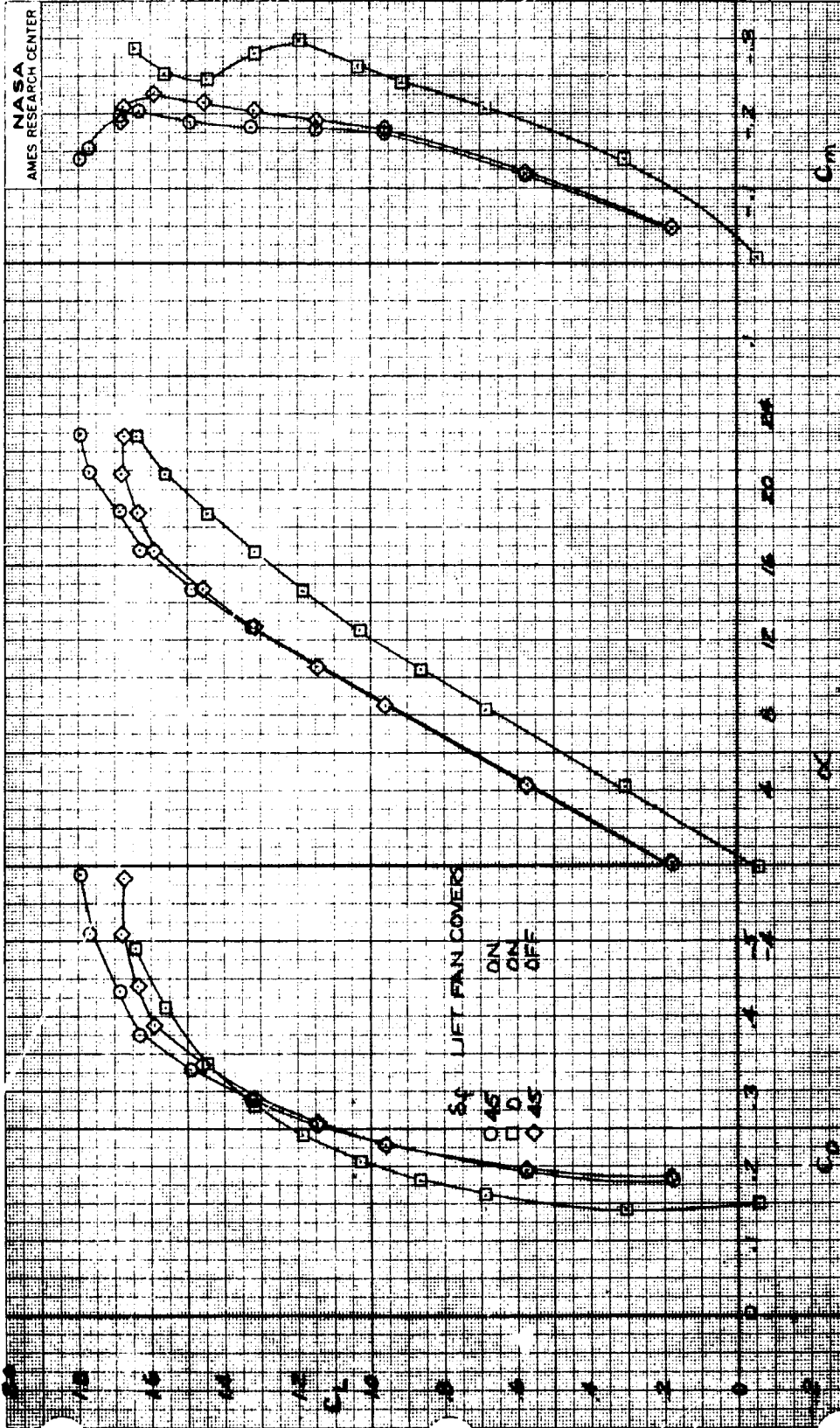


Figure 21.- Longitudinal characteristics with power off;  $\beta_v = 90^\circ$ .  
lift-cruise fans windmilling,  $\theta_v = 7^\circ$ , tail on,  $i_t = 0^\circ$ .



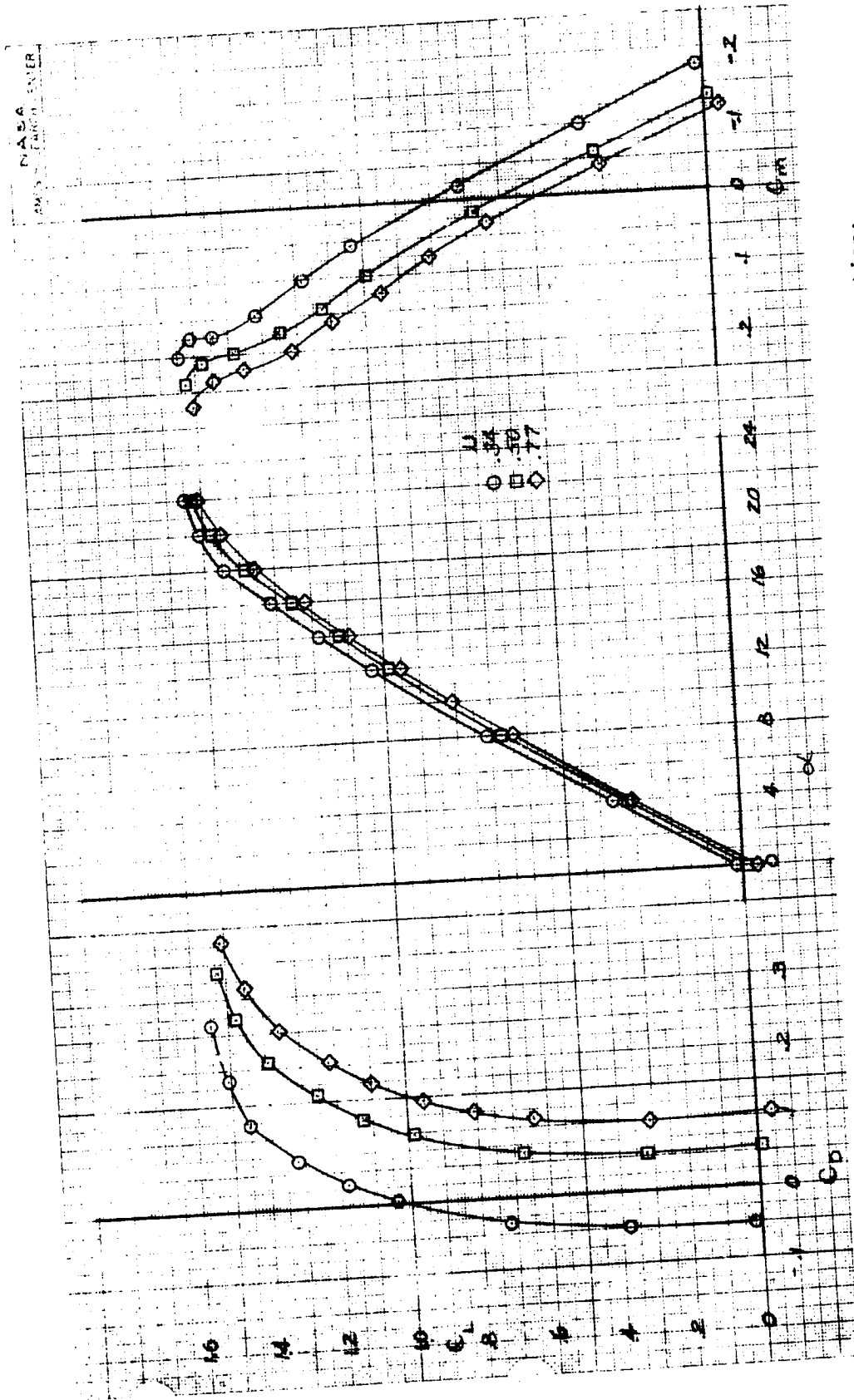


Figure 22.- Longitudinal characteristics with lift-cruise fan operation; exit cascade removed, lift fans covered,  $\beta_v = 90^\circ$ , tail off,  $\delta_f = 0^\circ$ .

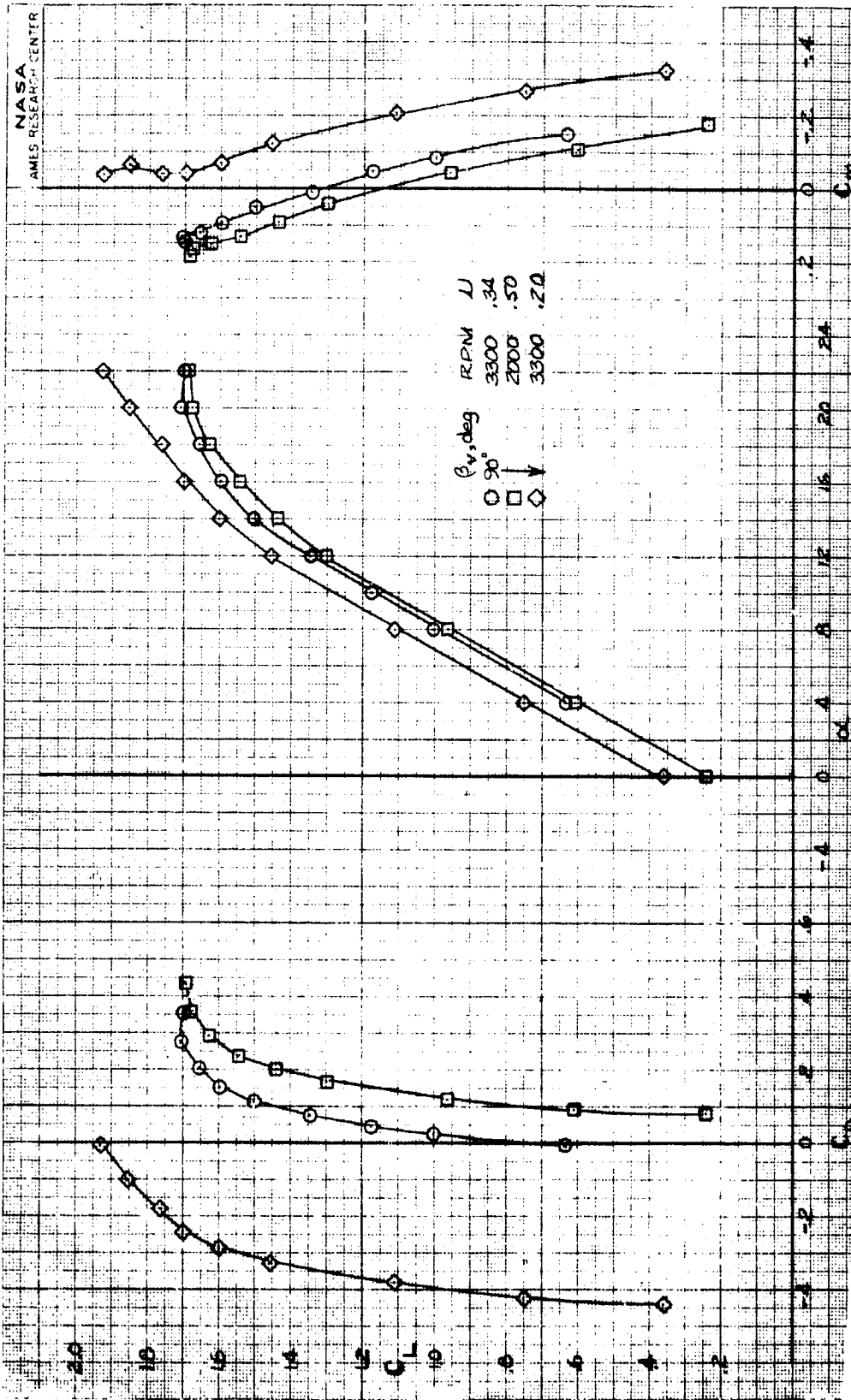


Figure 23.- Longitudinal characteristics with lift-cruise fan operation; exit cascade removed, lift fans covered,  $\beta_v = 90^\circ$ , tail off,  $\delta_f = 45^\circ$ .

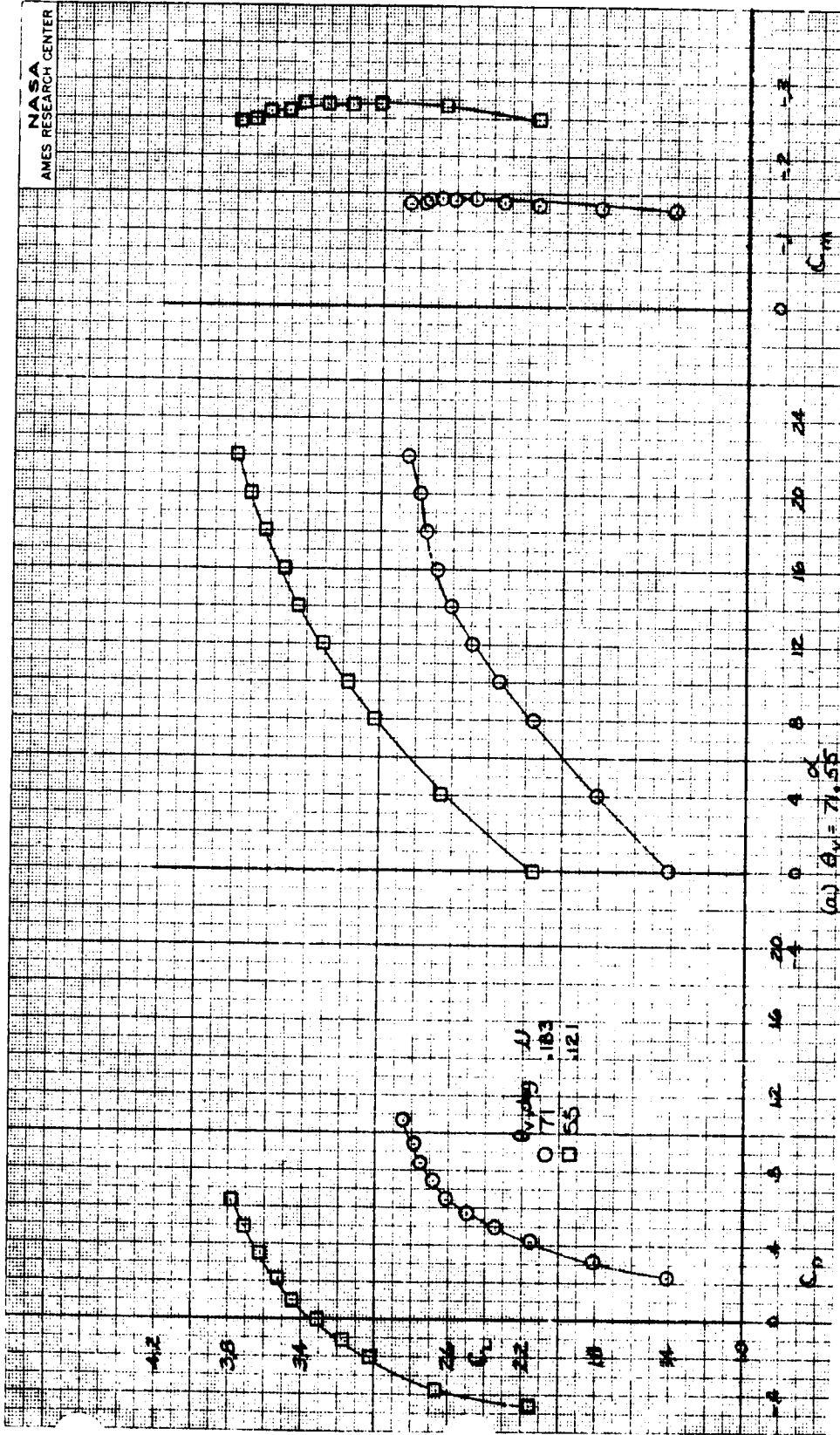
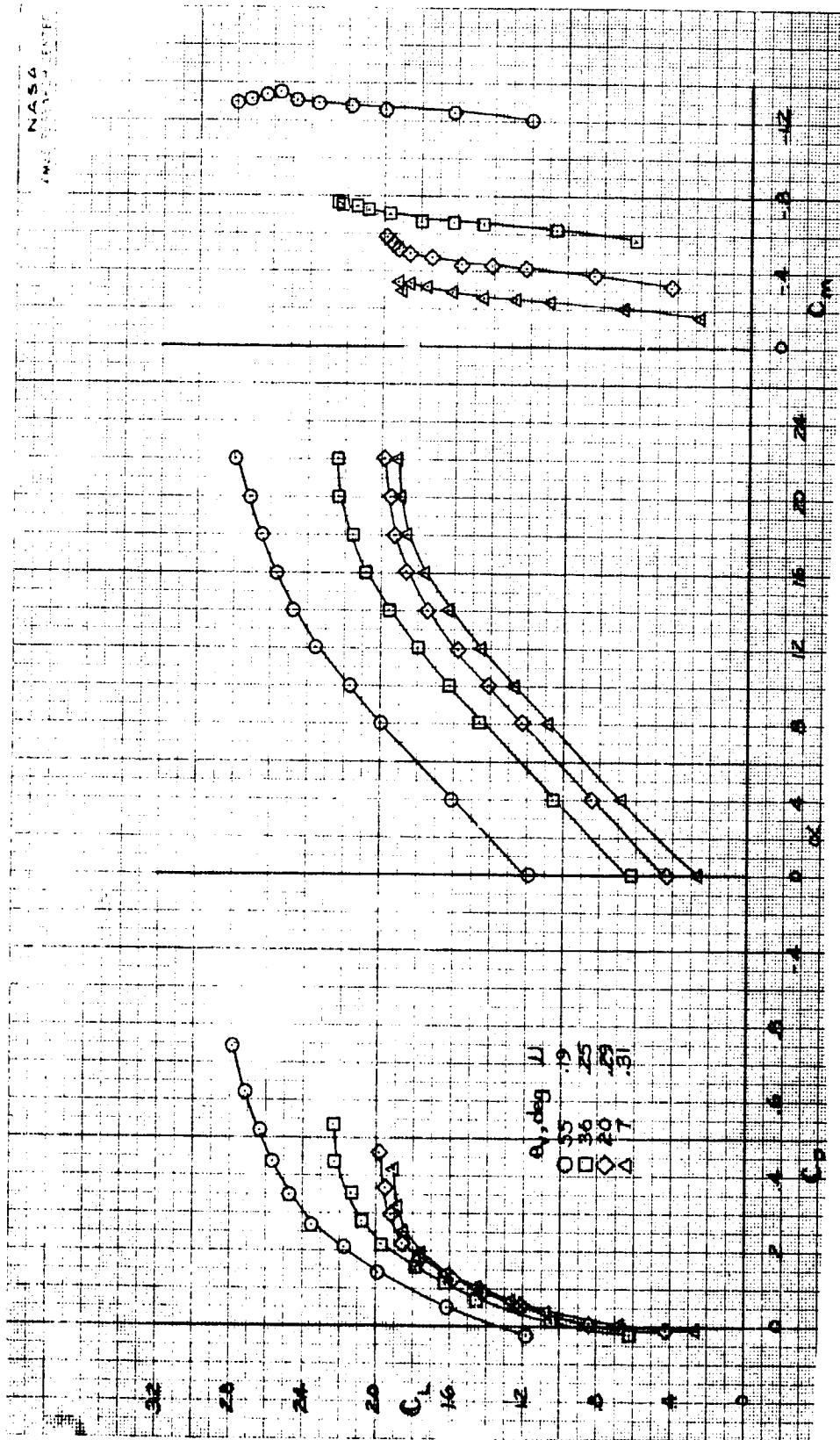
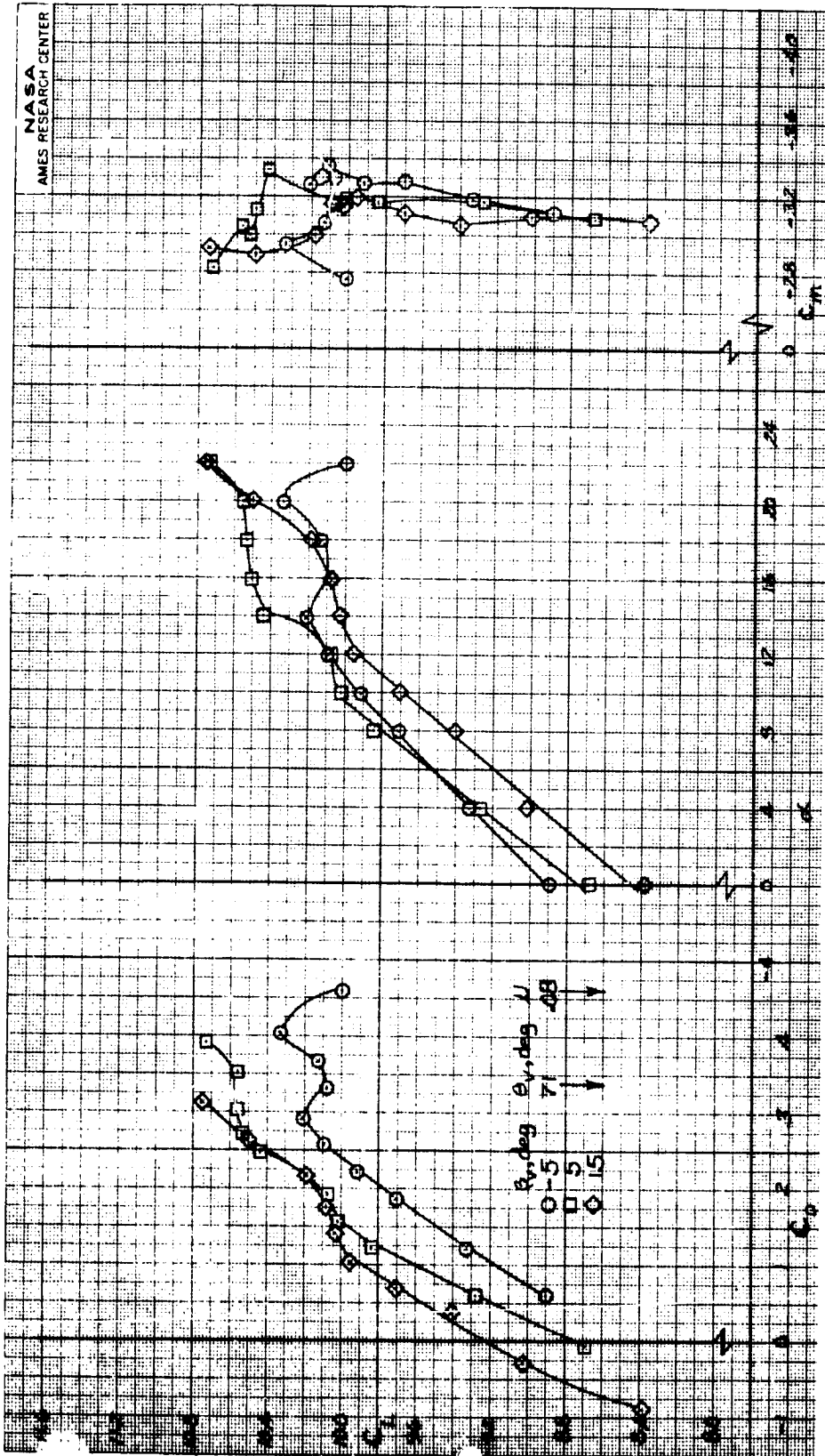


Figure 24.- Longitudinal characteristics with lift-cruise fan operation; lift fans covered,  $\beta_v = 90^\circ$ , tail on,  $i_t = 0^\circ$ ,  $\delta_f = 45^\circ$ .



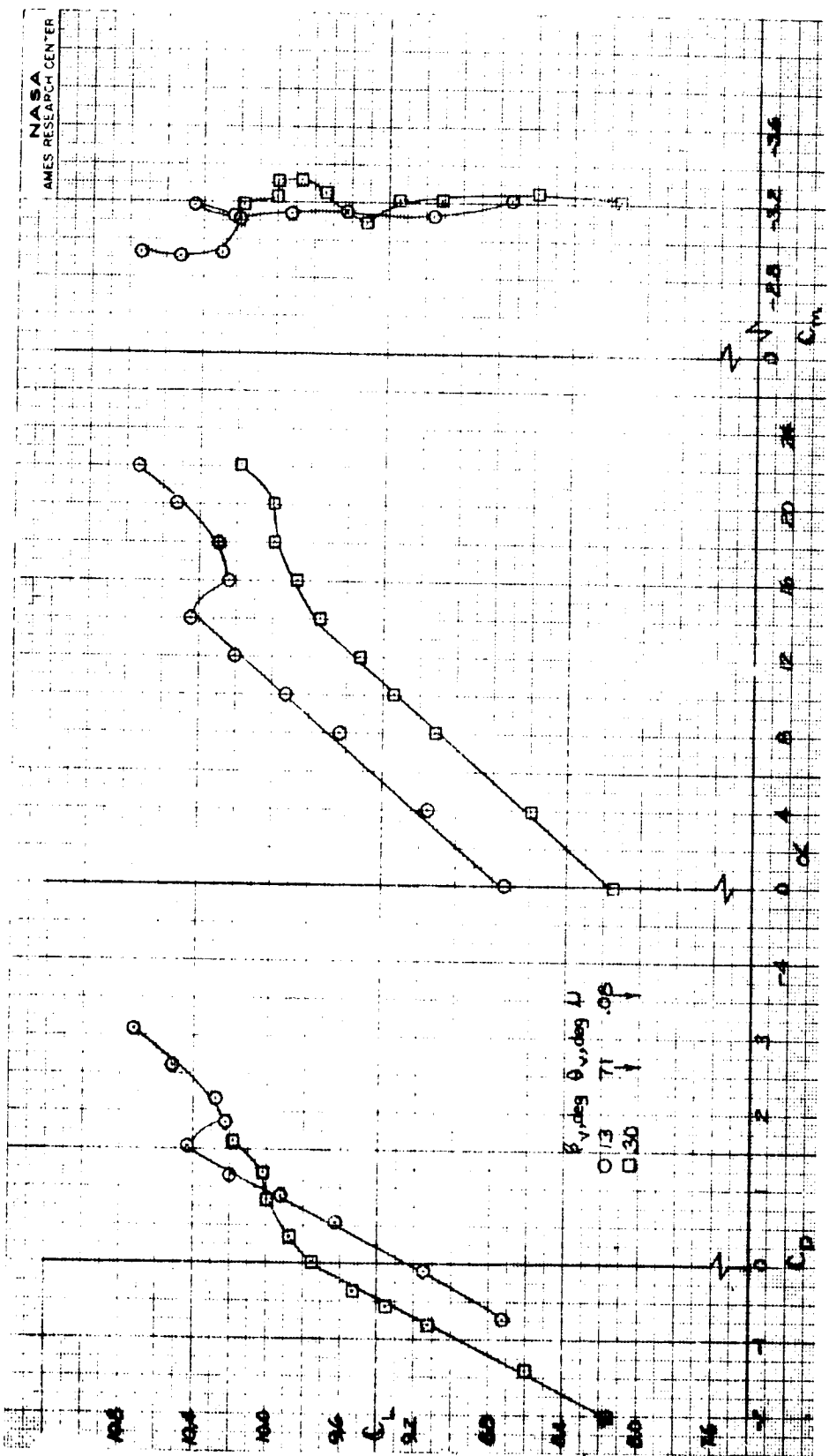
(b)  $\theta_V = 55^\circ, 36^\circ, 20^\circ, 7^\circ$ .

Figure 24.- Concluded.

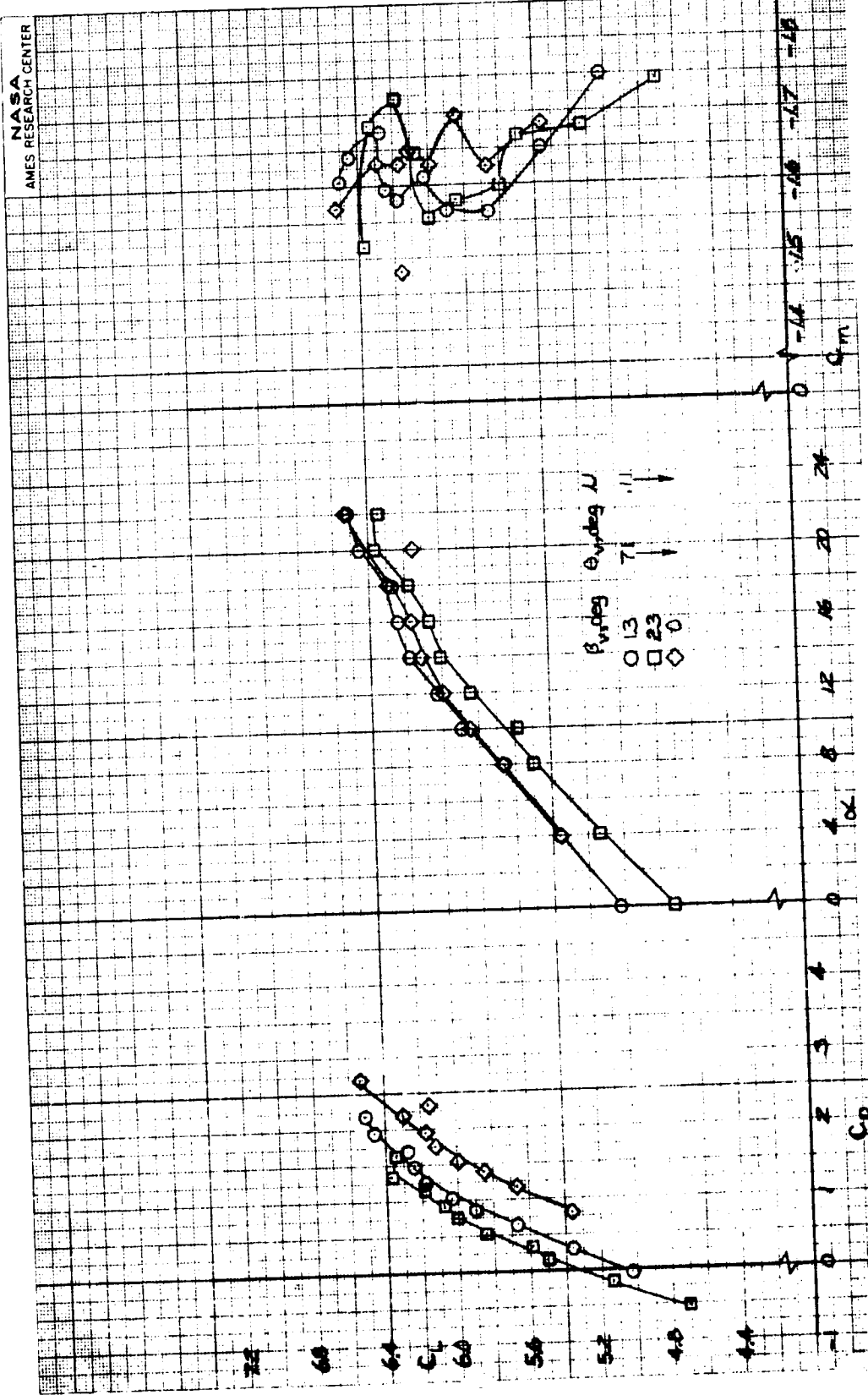


(a)  $\mu = .08$

Figure 25.- Longitudinal characteristics with lift and lift-cruise fan operation; tail on,  $i_t = 0^\circ$ ,  $\delta f = 45^\circ$ .

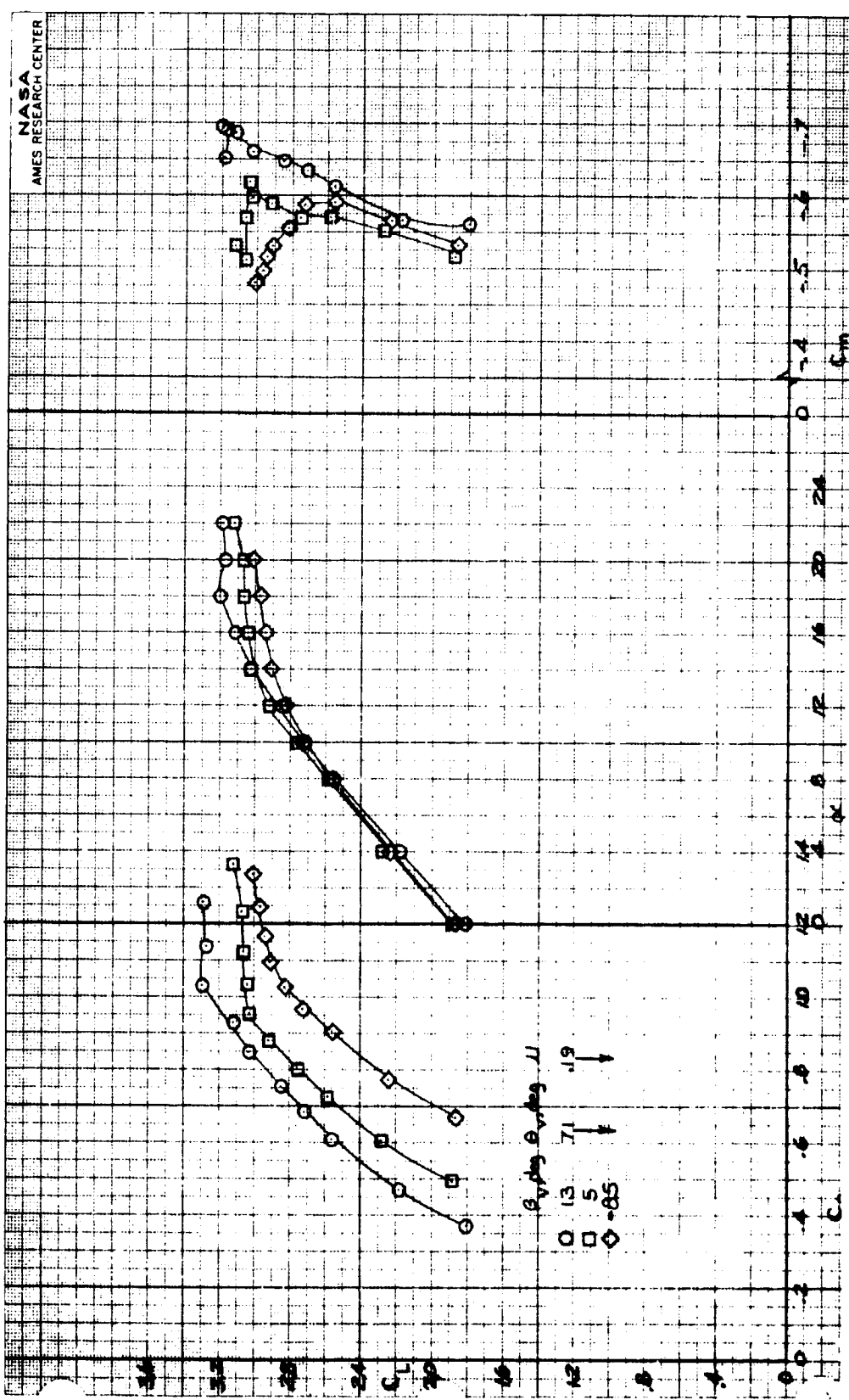


(b)  $\mu = .08$   
Figure 25.- Continued.



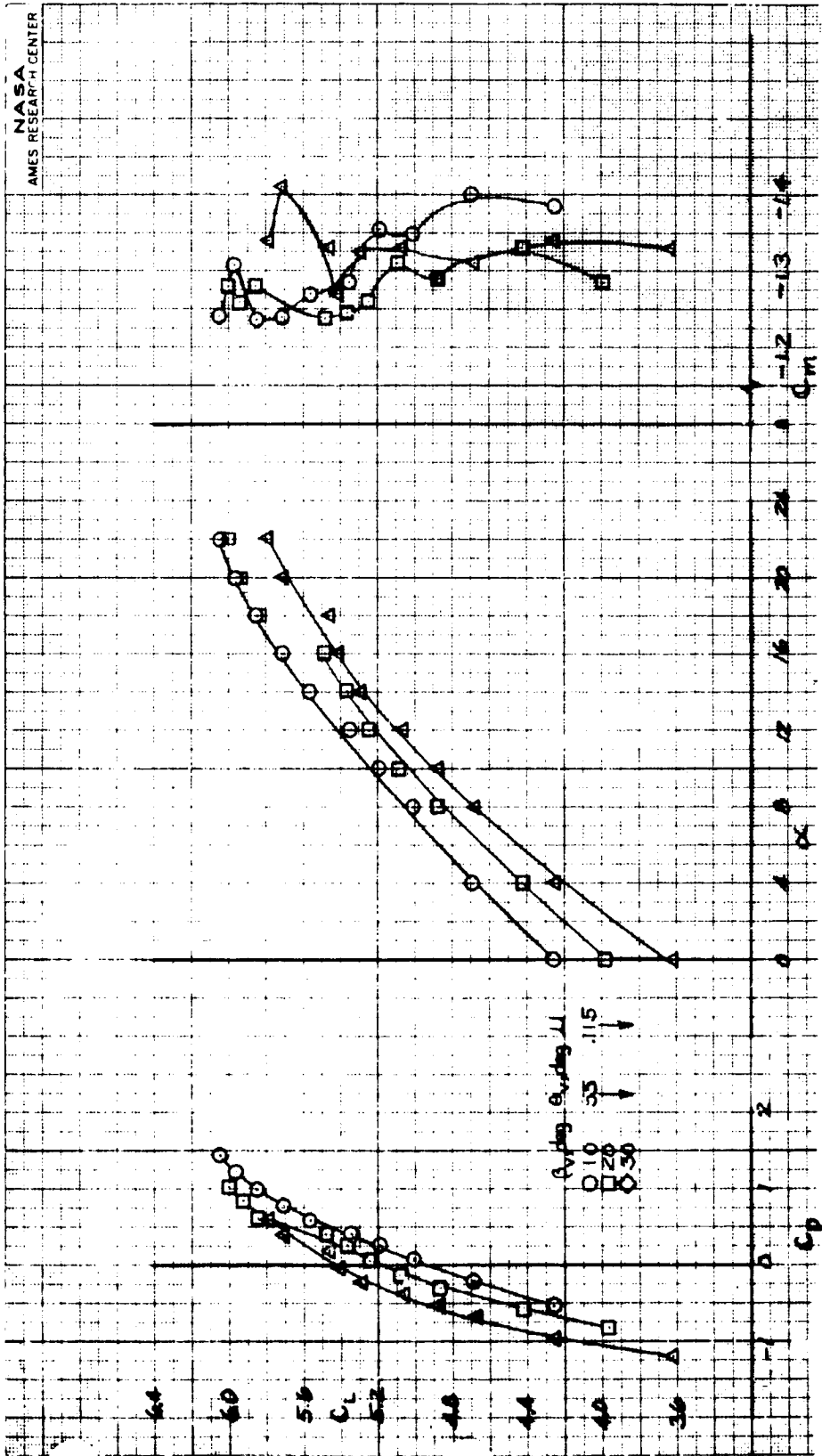
(c)  $\mu = .11$

Figure 25.- Continued.



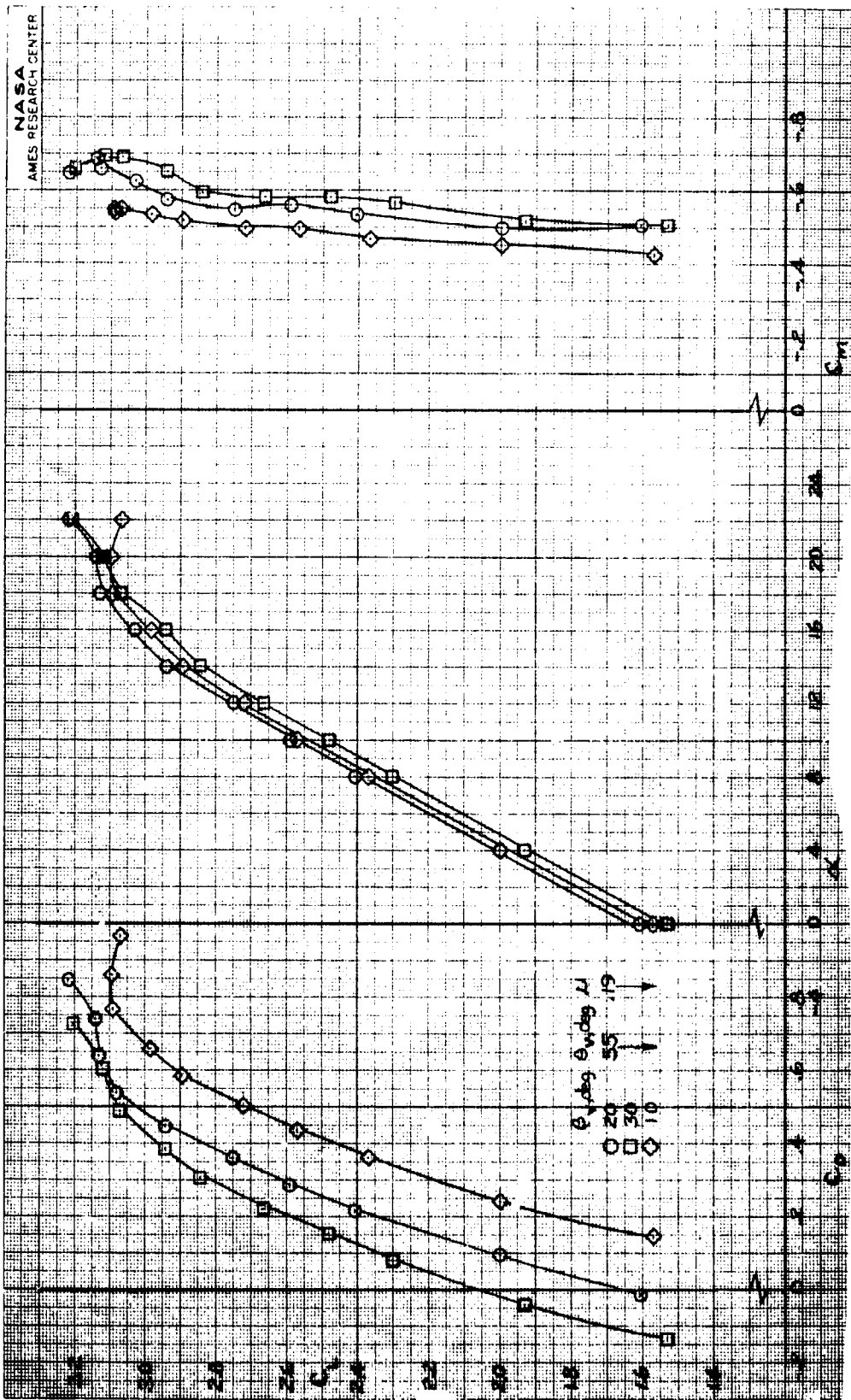
(d)  $\mu = .19$   
 Figure 25.- Concluded.





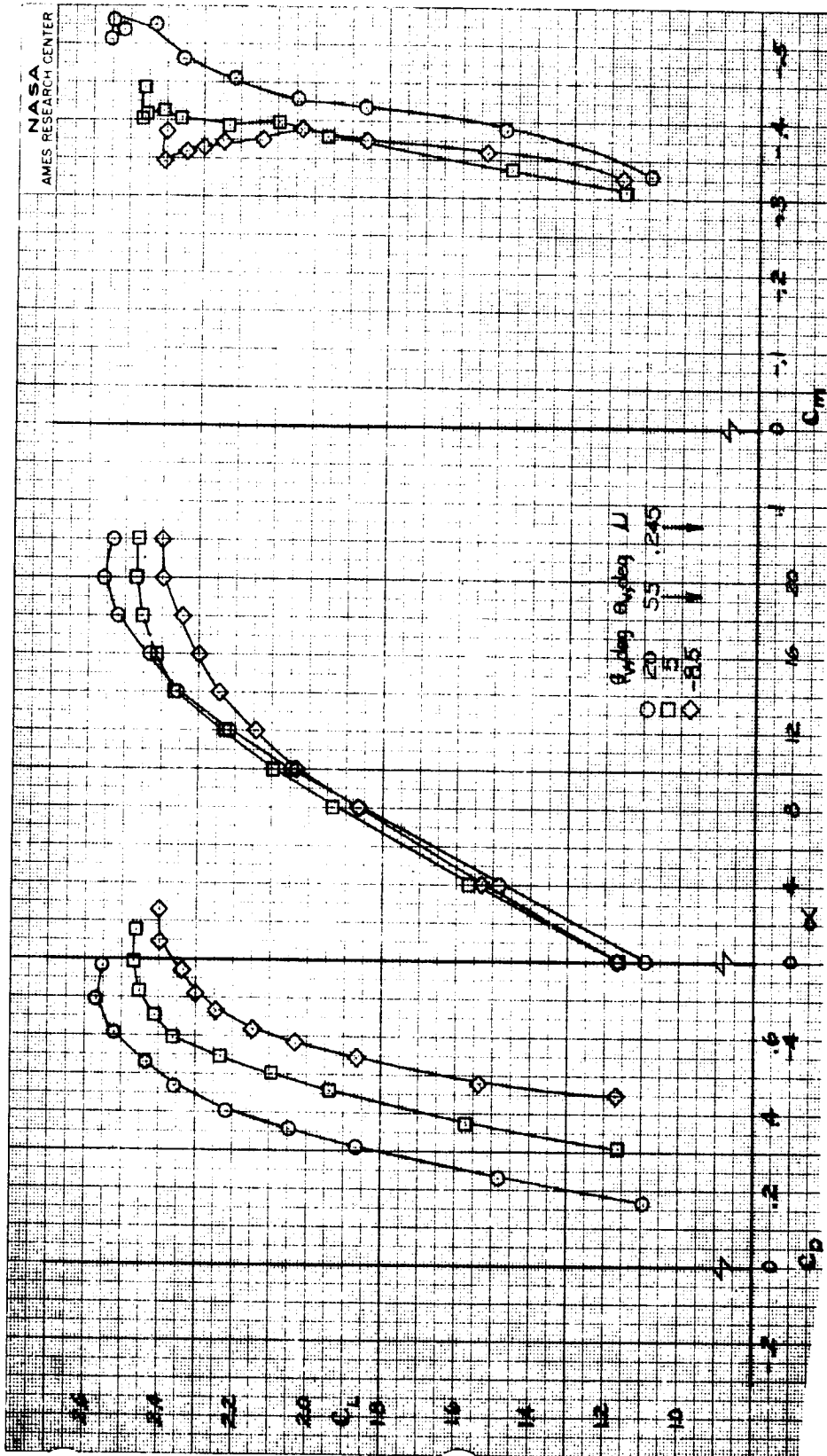
(a)  $\mu = .115$

Figure 26.- Longitudinal characteristics with lift and lift-cruise fan operation; tail on,  $\text{it} = 0^\circ$ ,  $\delta f = 45^\circ$ .



(b)  $\mu = .19$

Figure 26.- Continued.



(c)  $\mu = .245$

Figure 26.- Concluded.

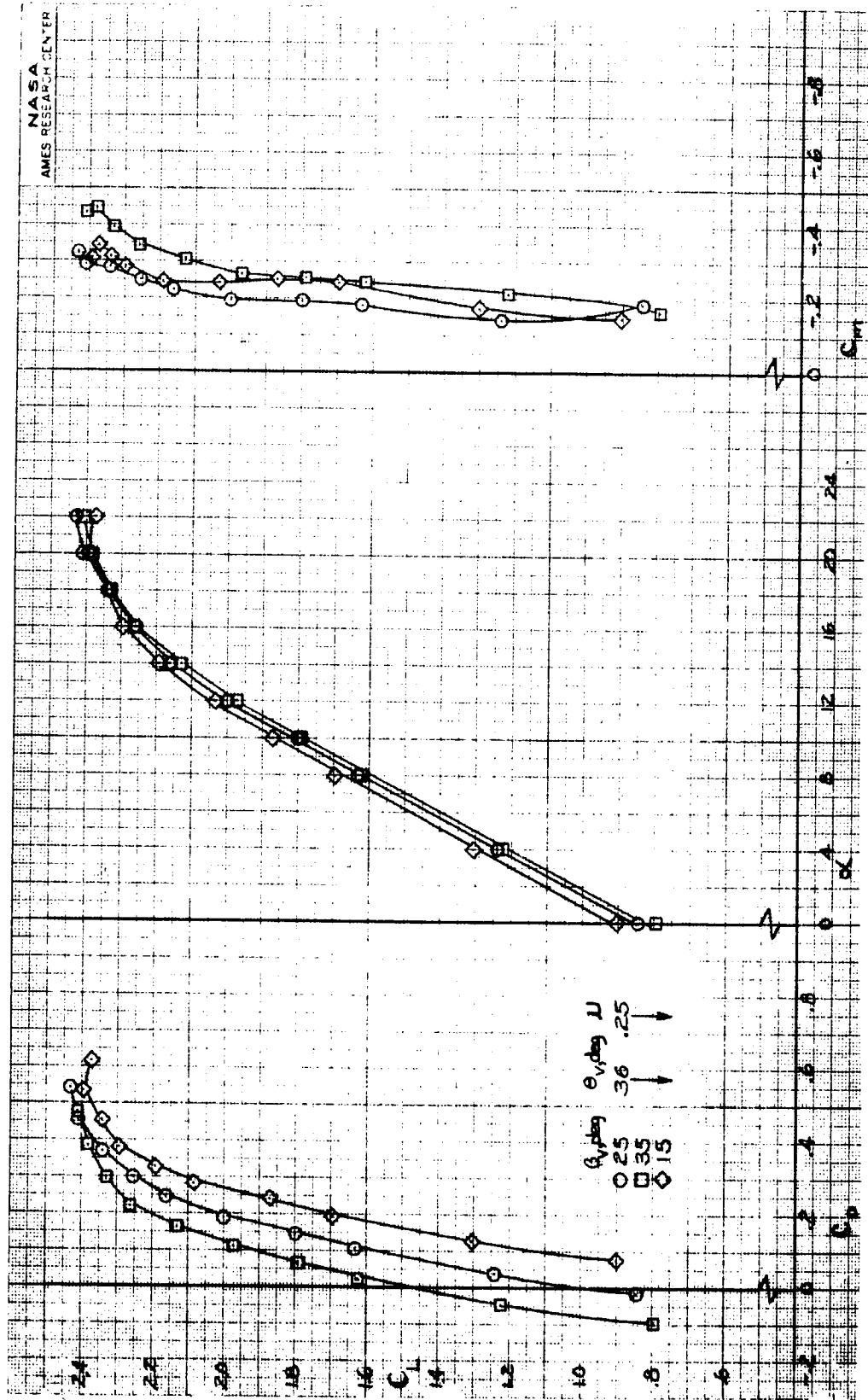


Figure 27.- Longitudinal characteristics with lift and lift-cruise fan operation; tail on,  $i_t = 0^\circ$ ,  $\delta_f = 45^\circ$ .

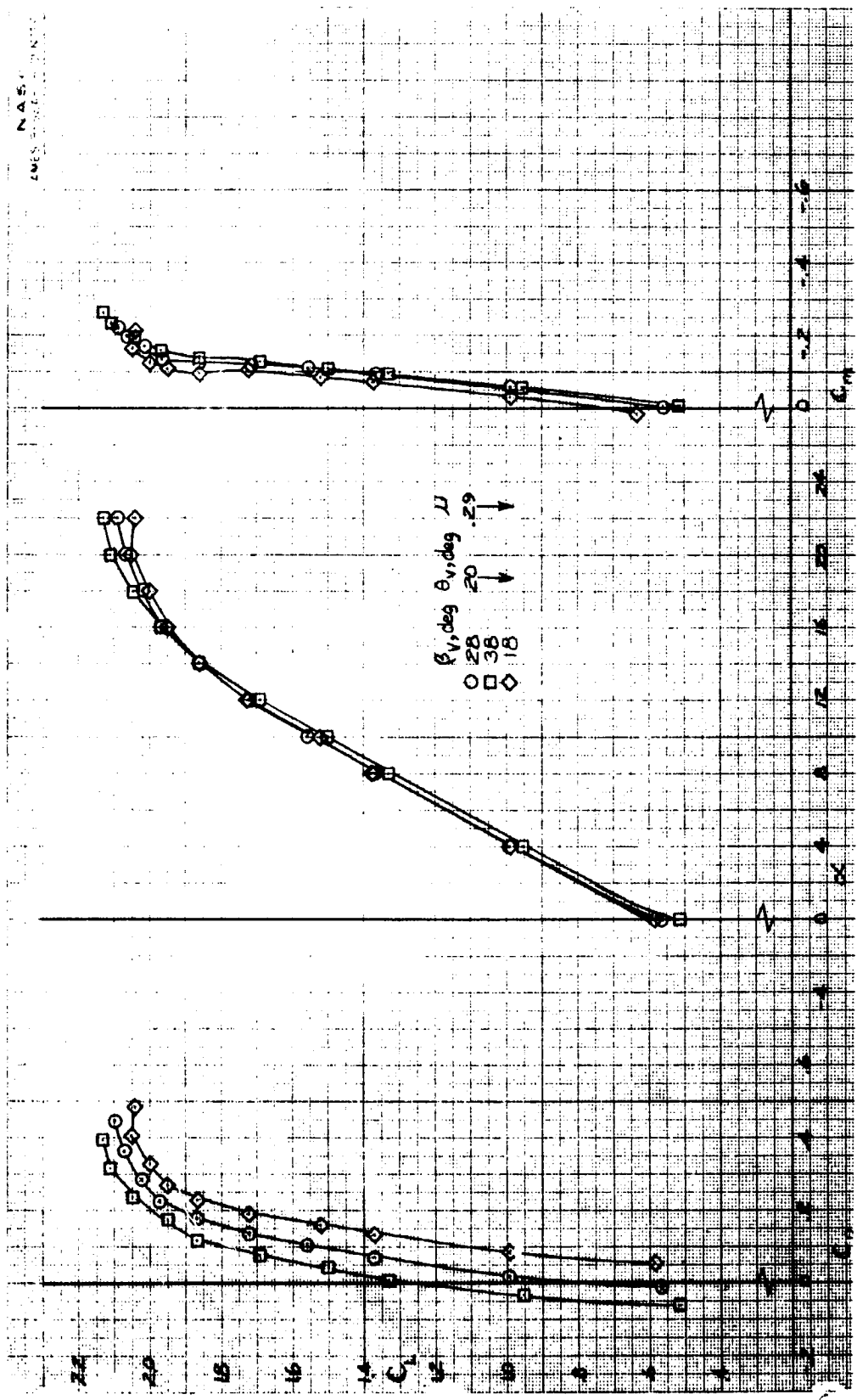


Figure 28.- Longitudinal characteristics with lift and lift-cruise fan operation; tail on,  $i_t = 0^\circ$ ,  $\delta_f = 45^\circ$ .

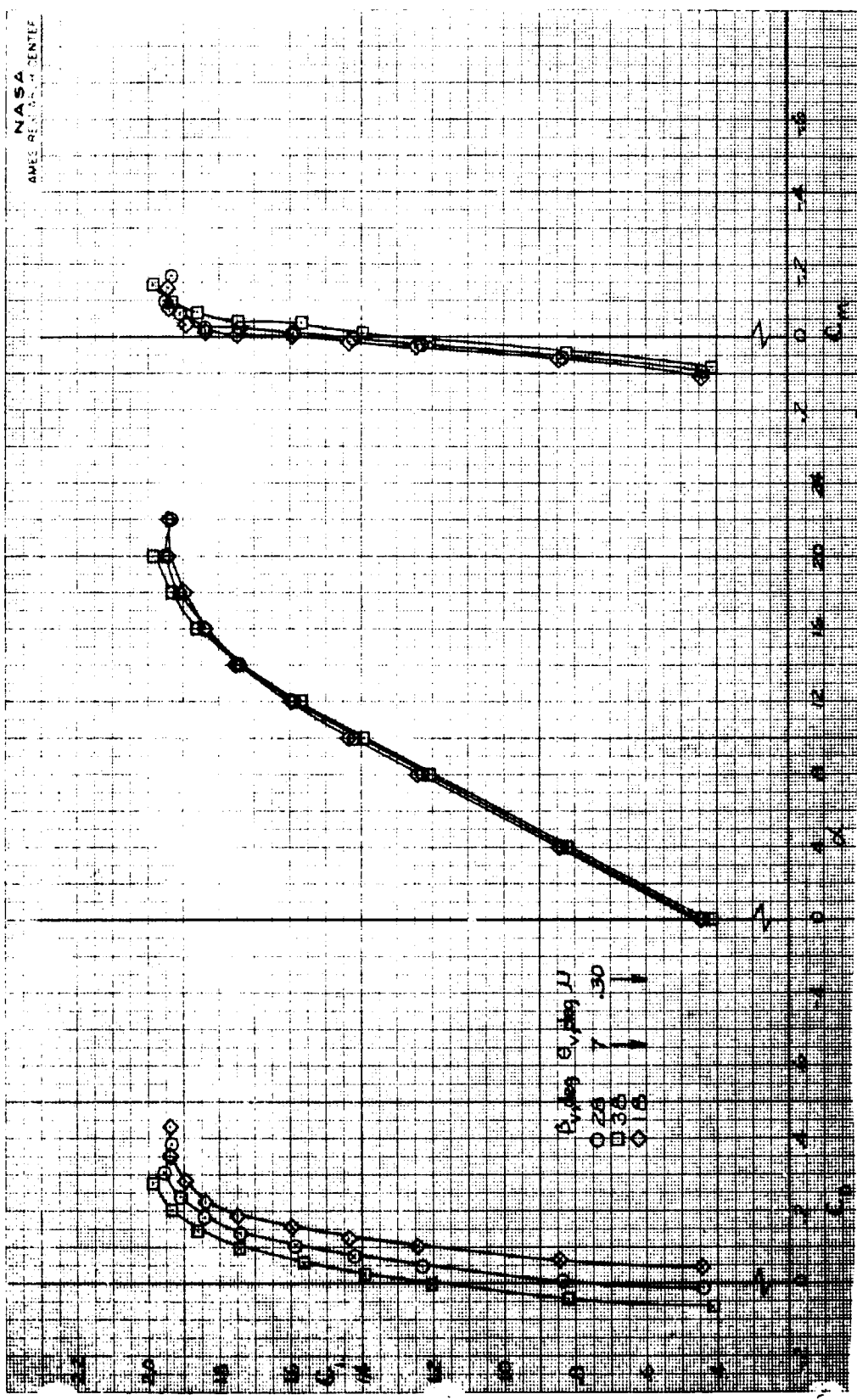


Figure 29.- Longitudinal characteristics with lift and lift-cruise fan operation; tail on,  $i_t = 0^\circ$ ,  $\delta_f = 45^\circ$ .

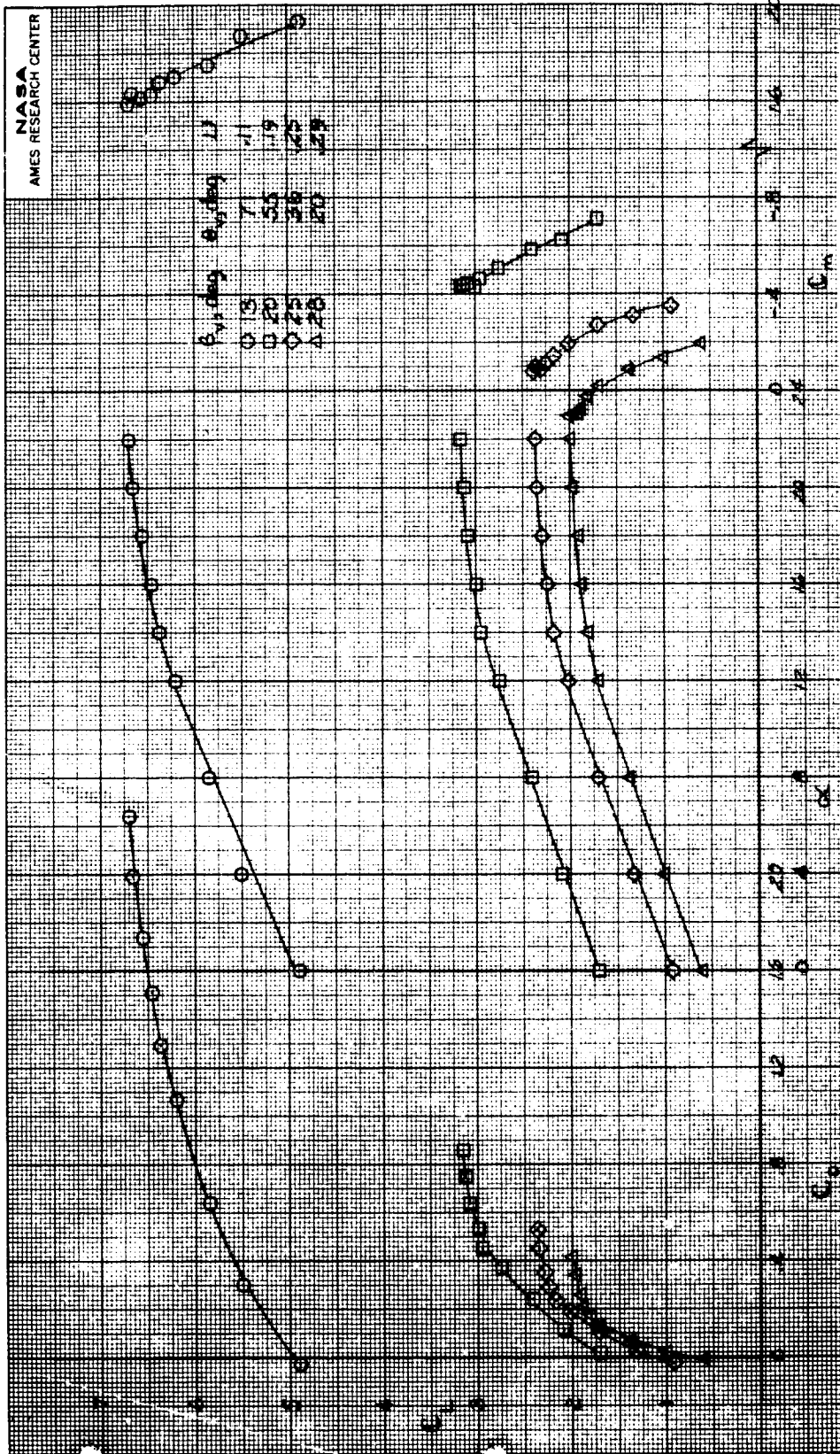


Figure 30.- Longitudinal characteristics with lift and lift-cruise fan operation; tail off,  $\delta_f = 45^\circ$ .

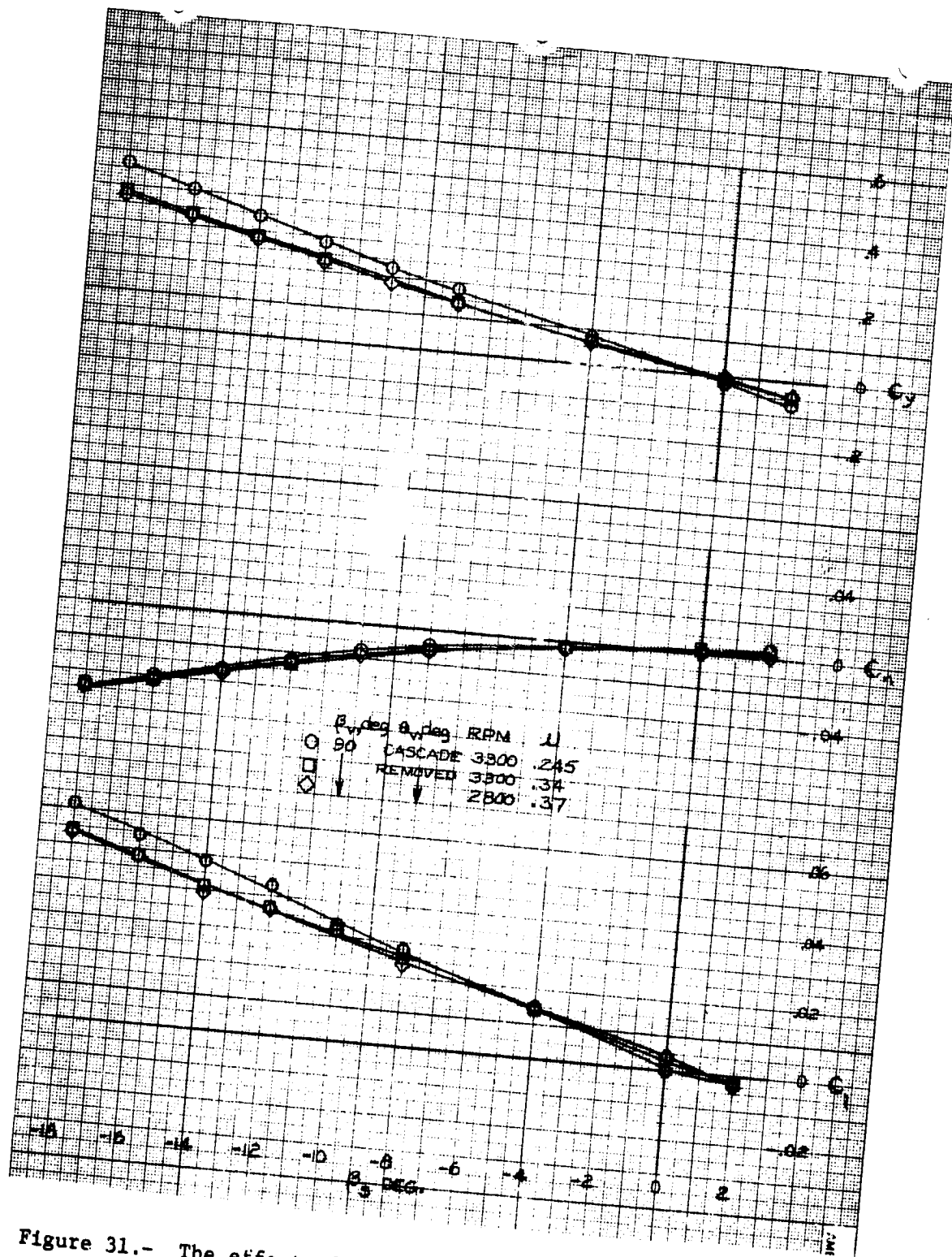


Figure 31.- The effect of tip-speed ratio on lateral-directional characteristics with lift-cruise fan operation; lift fans covered,  $\beta_v = 90^\circ$ , tail off,  $\delta_f = 0^\circ$ ,  $\alpha = 0^\circ$ .



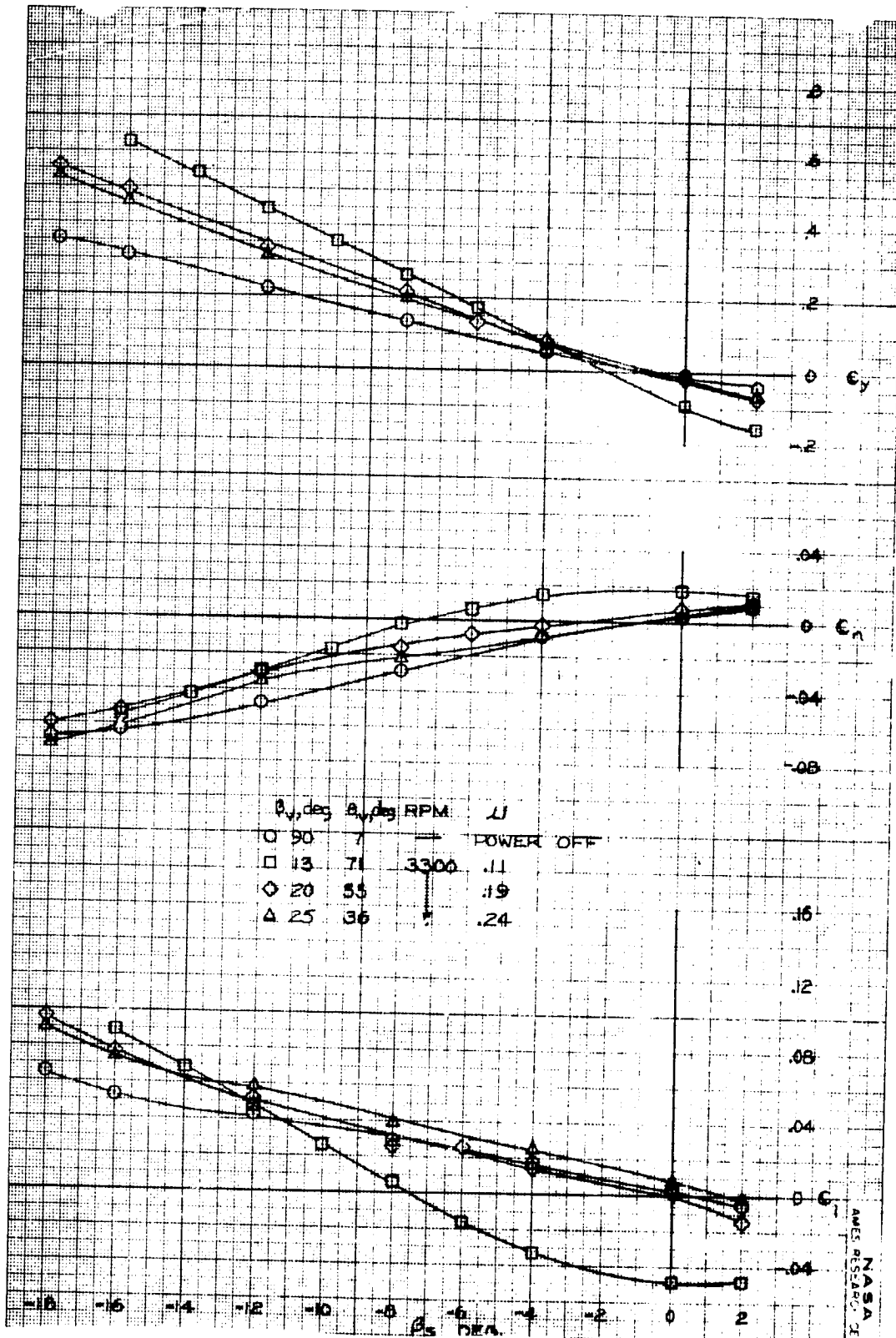


Figure 32.- The effect of tip-speed ratio on lateral-directional characteristics with lift and lift-cruise fan operation, tail off,  $\delta_f = 45^\circ$ ,  $\alpha = 0^\circ$ .

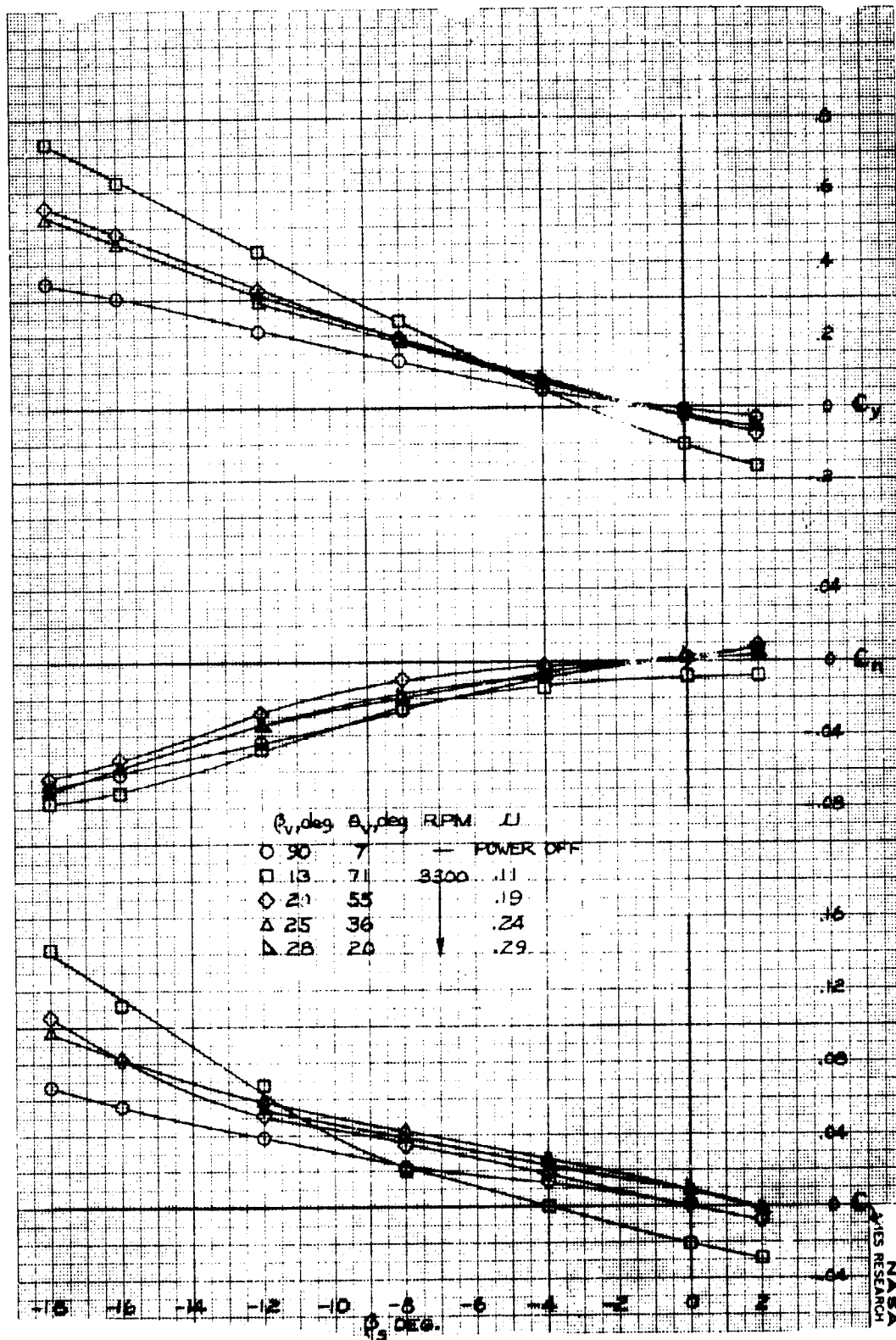


Figure 33.- The effect of tip-speed ratio on lateral-directional characteristics with lift and lift-cruise fan operation; tail on,  $i_t = 0^\circ$ ,  $\delta_f = 45^\circ$ ,  $\alpha = 0^\circ$ .

NASA  
AMES RESEARCH

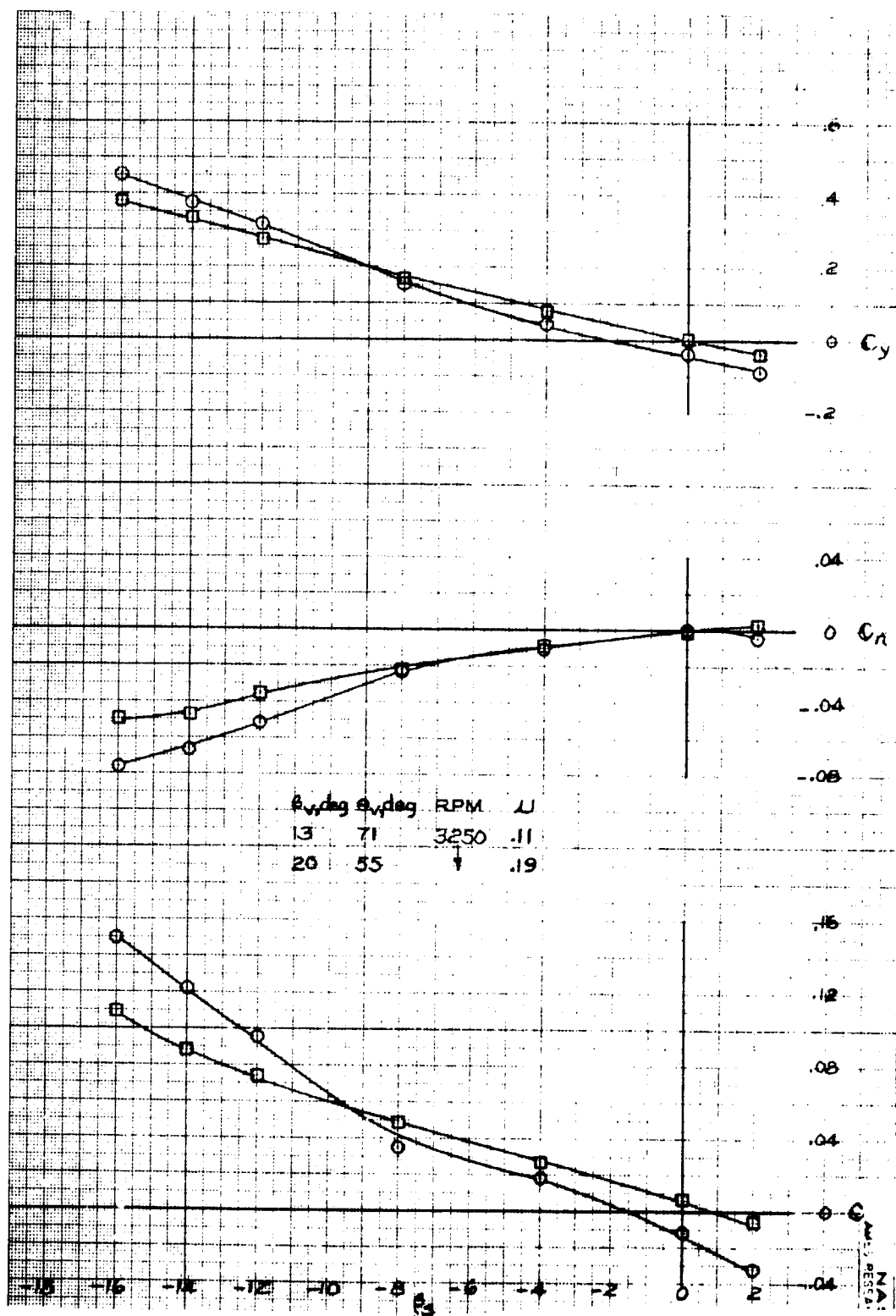


Figure 34.- The effect of tip-speed ratio on lateral-directional characteristics with lift and lift-cruise fan operation; tail on,  $i_t = 0^\circ$ ,  $\delta_f = 45^\circ$ ,  $\alpha = 8^\circ$ .